

Cooperative Marine Science Program

**AD-A261 638 for the Black Sea
(CoMSBlack)**



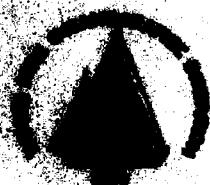
**CoMSBlack 92-010
Technical Report
September, 1992**

**The Black Sea General Circulation
and Climatic Temperature and Salinity Fields**

Dimitur Ivanov Trulchev, Ph. D.,
Institute of Oceanology
Bulgarian Academy of Sciences
Varna, Bulgaria

Yuri Leonidovich Demin, Prof., Sc. D.
Institute of Numerical Mathematics,
Russian Academy of Sciences
Moscow, Russia

**DTIC
ELECTE
MAR 02 1993
S E D**



**CRC-92-02
Coastal Research Center
Woods Hole Oceanographic Institution**



93-04227



1358

**STATEMENT
Approved for public release
Distribution Unlimited**

98 3 1 009

WHOI-92-34
CRC-92-02

The Black Sea General Circulation and Climatic Temperature and Salinity Fields

Dimitur Ivanov Trukhchev, Ph. D.,
Institute of Oceanology
Bulgarian Academy of Sciences
Varna, Bulgaria

Yurii Leonidovich Demin, Prof., Sc. D.
Institute of Numerical Mathematics,
Russian Academy of Sciences
Moscow, Russia


September, 1992

Technical Report

Reproduction in whole or in part is permitted for any purpose of the
United States Government. This report should be cited as:
Woods Hole Oceanog. Inst. Tech. Rept., WHOI-92-34, CRC-92-02.

Approved for publication; distribution unlimited.

Approved for Distribution:


G. Michael Purdy, Chairman
Department of Geology and Geophysics


Robert C. Beardsley, Director
Coastal Research Center


David G. Aubrey, Chairman
ComsBlack

Accession For	
NTIS CRA&I	<input checked="" type="checkbox"/>
DTIC TAB	<input checked="" type="checkbox"/>
Unannounced	<input type="checkbox"/>
Justification	
By	
Distribution /	
Availability Codes	
Dist	Avail and/or Special
A-1	

EXCLUDED 1

TABLE OF CONTENTS

	Page
I. Numerical Modelling of Climatic Water Mass Dynamics in the Black Sea	1
II. References	12
III. Appendix: Climatic Atlas of the Black Sea	15

LIST OF FIGURES

	Page
Figure 1. Average kinetic energy (a) and enstrophy (b) versus time on the surface and for levels of 30 m, 100 m, 1000 m, and for the whole volume.	3
Figure 2. Diagnostic (a) and adaptive (b) climatic currents at a depth of 100 m.	8
Figure 3. Climatic salinity distributions (‰) at the sea surface in February (a), May (b), August (c) and November (d) (from ^[18]).	9
Figure 4. Climatic salinity distributions (‰) at the sea surface for different seasons.	10

THE BLACK SEA GENERAL CIRCULATION AND CLIMATIC TEMPERATURE AND SALINITY FIELDS

Dimitur Ivanov Trukhchev, Ph. D.,
Institute of Oceanology, Bulgarian Academy of Sciences
Varna, Bulgaria

Yurii Leonidovich Demin, Prof., Sc. D.,
Institute of Numerical Mathematics,
Russian Academy of Sciences
Moscow, RUSSIA

I. NUMERICAL MODELLING OF CLIMATIC WATER MASS DYNAMICS IN THE BLACK SEA

It is a pity that the experimental investigations of the currents in the Black Sea are limited in scope and too non-systematic. In general, we at present know only the basic rules governing the large-scale circulation^[1, 2]. Numerical modelling is therefore the only possible way to reconstruct the steady circulation features in the Black Sea. The main problem solved so far, using diagnostic and adaptive models of the Black Sea, is the calculation of currents from experimental observations of the hydrological fields. These models can be interpreted as methods for hydrodynamic analysis of the experimental observations.

The dynamic method (a simple geostrophic model) developed by Sandstrom and Halland-Hansen^[3] at the start of this century has long been the only practical method for calculation of the currents. This method has some important shortcomings, but due to its simple implementation is widely used in oceanological work. A. Sarkisyan developed the first diagnostic model in the sixties, used to perform diagnostic calculations of the large-scale currents in the North Atlantic. Numerical modelling of water mass dynamics in the Black Sea was first performed in the former USSR at the beginning of the seventies. Since then numerous diagnostic (and prognostic) investigations of the currents in this basin have been performed. New and more accurate models have been developed, and the methods of the diagnostic calculations have been improved. The main results of these investigations of the Black Sea are published in various monographs^[4, 5, 6, 7]. Some results, obtained at the Computational Center of the Siberian Branch of the USSR Academy of Sciences, under the guidance of academician G. Marchuk, are published in^[5] as well.

The first step in the diagnostic investigations of the Black Sea has included diagnostic current calculations, using experimental data on sea water density distribution, and based on simple models and sparse grids. These investigations have proven the realistic character of the dynamic approach (especially if the dynamic heights are referenced to the bottom). They have shown that the homogeneous ocean models are groundless and have confirmed the main features of the large-scale water circulation in the sea, obtained using the dynamic method. At the same time however, these investigations have demonstrated some important shortcomings of the dynamic method. Additionally, the calculations have provided the first substantiated 3D fields of vertical velocity^[8].

The next logical step has been to perform diagnostic calculations of the currents, using small-interval grids and higher-level models. The 1° or 0.5° grids, used earlier for the diagnostic calculations of the currents in the Black Sea, make it possible to describe (with significant approximations) only the most general features of the circulation. At these sparse grids even the most important dynamic features - including the General Black Sea Current (GBSC) - are often lost. The various simplifying assumptions used in the earlier models have been the cause of significant inaccuracies. To overcome these shortcomings, new and more accurate diagnostic models have been developed and tested, and the methods of performing diagnostic calculations

have been improved. The high resolution grids and more accurate models used allow study of not only the circulation of the sea as a whole, but also investigations of smaller regions, characterized by complex dynamic processes and strong spatial variability of the currents.

Use of high resolution grids is a common trend for all numerical models of ocean dynamics. Besides the evident advantages, the increased resolution causes some new problems to appear. For instance, when diagnostic calculations are performed on small-interval grids, the quality of the input data is an important problem. Significant errors are caused by the insufficient statistical reliability of the climatic distributions of temperature and salinity, the lack of synchronization in the "quasi-synchronous" hydrological surveys, the experimental measurement errors, and the inconsistency of the input fields of density, winds and bottom relief. It's clear that the use of the traditional data filtration procedures can not solve these problems, because:

- (a) filtration smooths down both the high-frequency noise, and the real large-scale features of the fields, e.g. streams;
- (b) the numerous types of filters used, although always claimed to be unbiased, are in fact a source of subjective and formal data modifications, not reflecting the thermo- and hydrodynamical features of the real fields;
- (c) the problem of hydrodynamical adjustment of the fields isn't being solved at all.

The "defects" of the input data and the shortcomings of the methods used for processing hydrological information have stimulated the development of new, more general hydrodynamic methods of experimental data filtration and adjustment^[9]. For the Black Sea these investigations have been initiated by Sarkisyan, Demin and Trukhchev^[10] and have been performed under the Intergovernmental program "Sections" and the topic "World Ocean"^[4, 5, 6, 11].

The main feature of this new approach is that it combines the most important practical advantages of the diagnostic models (being of practical significance due to the use of experimental data) and of the prognostic models (producing hydrodynamical adjustment and filtered fields). At the same time the new approach doesn't have the shortcomings of the older models - inconsistency of the fields and the presence of noise in them (for the diagnostic models), and idealization and smoothing down of the large gradients (for the prognostic models). The new approach is based on the successive application of both diagnostic and prognostic models. The temperature and salinity fields, obtained from the observations, and the currents, obtained from the diagnostic models, are used as the initial approximation of the prognostic model. The time integration process in the latter isn't performed until a fully stationary solution is obtained, as is usually done in the prognostic models. The integration is performed only until the completion of the basic reconstruction of the fields. This process takes place at the adjustment stage of the integration (semidiagnostic calculations) due to the high-speed wave processes, and results in hydrodynamic noise filtration. If the integration process is continued longer, the solution gets worse, its correlation with the initial data is lost, and the final result is close to that of the ordinary prognostic models. This is the reason for limiting the integration time in the adaptive method. The "worsening" of the solution can be expressed by excessive smoothing of the structures, and even loss of some qualitative features, present in the input data. The adaptation process is monitored through the kinetic energy variations versus time, and by test calculations. The time dependence of kinetic energy shows the transition from the stage of fast distribution adjustment due to wave processes (expressed by oscillations of kinetic energy) to the stage of slow, smooth changes (Figure 1).

This problem is similar to the initiation problem in meteorology, but it has some additional complexity due to the fact that one of the fields (the currents) isn't measured and has to be reconstructed by calculations. The initiation of the hydrological fields requires reconstruction of the current distribution from the given fields of temperature and salinity, with some adaptation of all three fields to the equations and boundary conditions used by the model, and to the shape of the

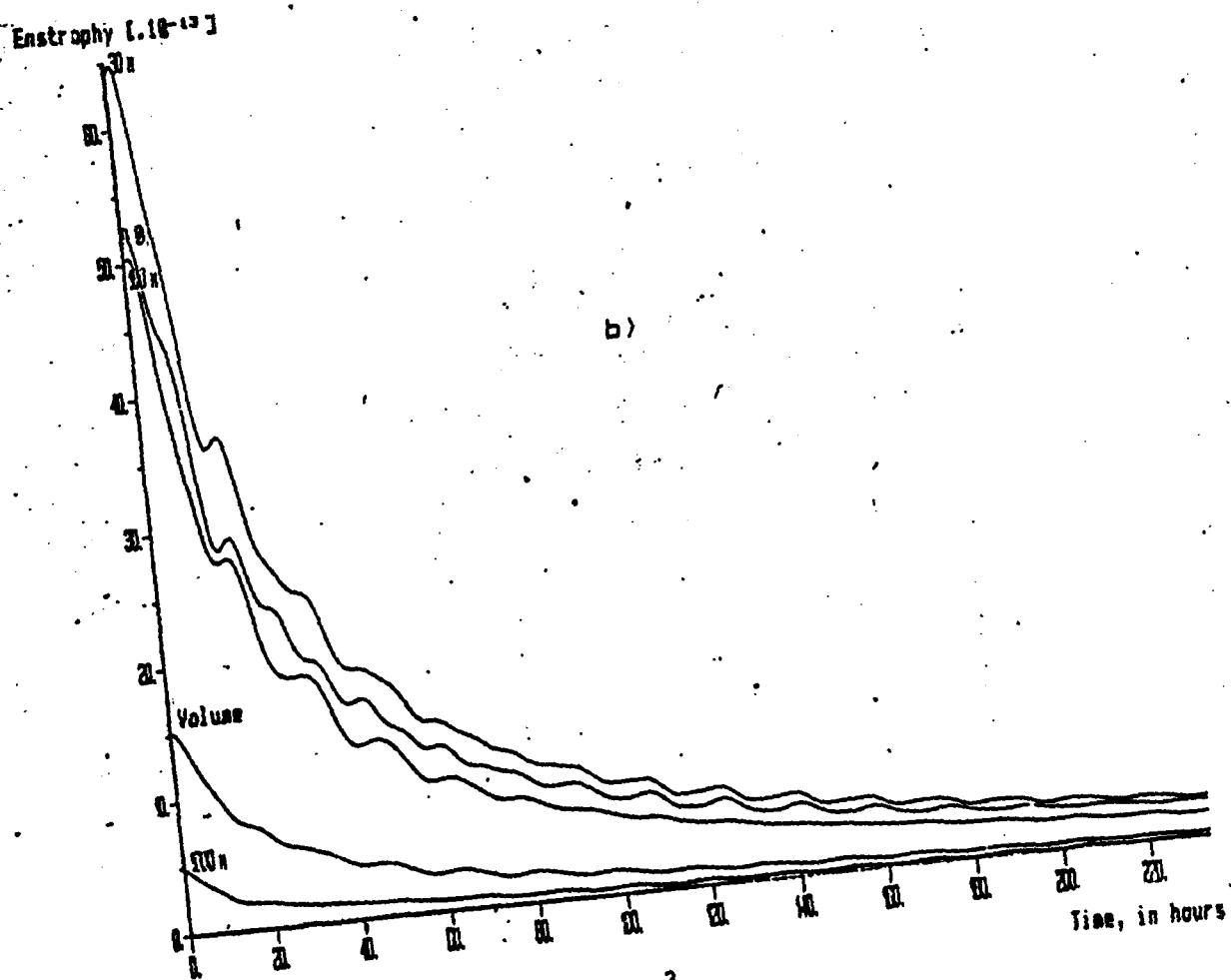
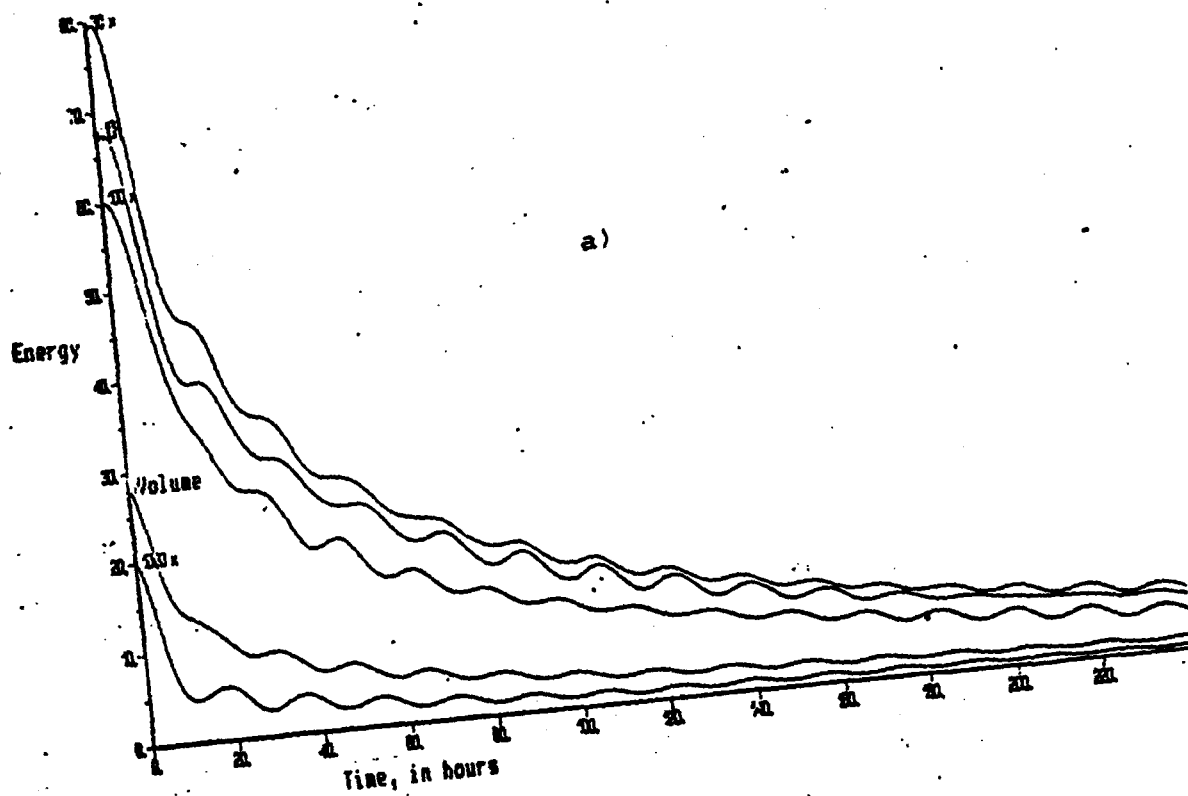


Figure. 1. Average kinetic energy (a) and enstrophy (b) versus time on the surface and for levels of 30 m, 100 m, 1000m, and for the whole volume.

sea basin. The experience gained up to now shows that the typical model time for adaptation for the Black Sea is approximately several days. The main adaptation mechanism is by inertial-gravity waves. As a result of this adaptation, "instantaneous" or "frozen" hydrological fields are obtained, corresponding to the temporal characteristics of the input temperature and salinity information (annual, seasonal, monthly, or simply reflecting one specific condition in time).

References^[4, 5, 6] contain the results of numerical experiments on the adaptation of main hydrological fields at the western part of the Black Sea. They have been performed by 3D-models of varying complexity, using grids with a horizontal step of 5 miles. Several interesting features of the eddy circulation in this region have been obtained, describing its synoptic character and the seasonal variations. In the present work we discuss only the results, obtained by a model, using the full equations of ocean thermo- and hydrodynamics, and intended for adaptation of temperature, salinity (i.e., density) and current fields. This model has been used earlier for calculations at the western regions of the sea^[6, 12]. The aim of the investigations is to build the climatic (seasonal and annual) distributions of these fields for the whole sea basin. The horizontal grid steps are 0.25° and 0.5° along the parallels and the meridians respectively. Twenty five levels (0, 5, 10, 15, 20, 25, 30, 50, 75, 100, 125, 150, 200, 250, 300, 400, 500, 600, 800, 1000, 1200, 1400, 1600, 1800, 2000 m) have been investigated in the calculations. The input temperature and salinity fields are built using about 50,000 observations, covering a period of approximately 100 years. This information has been prepared by Dr. G. S. Dvoryaninov and his colleagues from the Marine Hydrophysical Institute in Sevastopol--the T-S data have been seasonally and annually averaged at the centers of rectangular cells of 0.5° by 0.5° . The spring season includes March, April and May, the summer season - June, July and August, etc. To improve the resolution we have additionally interpolated the source fields along the parallels. No preliminary filtration of the data has been performed.

The numerical model is based on the complete system of nonsimplified geophysical hydrodynamics with the approximations commonly used in oceanology (in β -plane):

MODEL EQUATIONS

$$(1) \quad \frac{du}{dt} + \frac{\partial}{\partial x} A_1 \frac{\partial u}{\partial x} + \frac{\partial}{\partial y} A_1 \frac{\partial u}{\partial y} + \frac{\partial}{\partial z} v \frac{\partial u}{\partial z} = g \frac{\partial \zeta}{\partial x} + \frac{g}{\rho_0} \int_0^z \frac{\partial \rho}{\partial x} d\zeta - fv.$$

$$(2) \quad \frac{dv}{dt} + \frac{\partial}{\partial x} A_1 \frac{\partial v}{\partial x} + \frac{\partial}{\partial y} A_1 \frac{\partial v}{\partial y} + \frac{\partial}{\partial z} u \frac{\partial v}{\partial z} = g \frac{\partial \zeta}{\partial y} + \frac{g}{\rho_0} \int_0^z \frac{\partial \rho}{\partial y} d\zeta + fu,$$

$$(3) \quad \Delta \zeta + \frac{1}{H} \frac{\partial H}{\partial x} \frac{\partial \zeta}{\partial x} + \frac{1}{H} \frac{\partial H}{\partial y} \frac{\partial \zeta}{\partial y} =$$

$$= -\frac{1}{\rho_0 H} \int_0^H (H-z) \Delta \rho d\eta - \frac{1}{\rho_0 H} \left[\frac{\partial H}{\partial x} \int_0^H \frac{\partial \rho}{\partial x} dz + \frac{\partial H}{\partial y} \int_0^H \frac{\partial \rho}{\partial y} dz \right] -$$

$$-\frac{\beta}{H} \int_0^H u dz + \frac{f}{gH} \int_0^H \left(\frac{\partial v}{\partial x} - \frac{\partial u}{\partial y} \right) dz - \frac{1}{gH} \int_0^H \left(\frac{\partial A_1}{\partial x} - \frac{\partial B_1}{\partial y} \right) dz +$$

$$+ \frac{1}{\rho g H} \left[\left(\frac{\partial \tau_x}{\partial x} + \frac{\partial \tau_y}{\partial y} \right) + \left(\frac{\partial \tau_x^H}{\partial x} + \frac{\partial \tau_y^H}{\partial y} \right) \right] +$$

$$+ \frac{1}{gH} \left[\frac{\partial}{\partial x} \int_0^H \left(\frac{\partial}{\partial x} A_1 \frac{\partial u}{\partial x} + \frac{\partial}{\partial y} A_1 \frac{\partial u}{\partial y} \right) dx + \frac{\partial}{\partial y} \int_0^H \left(\frac{\partial}{\partial x} A_1 \frac{\partial v}{\partial x} + \frac{\partial}{\partial y} A_1 \frac{\partial v}{\partial y} \right) dz \right],$$

$$\text{where } \frac{d}{dt} = \frac{\partial}{\partial t} + u \frac{\partial}{\partial x} + v \frac{\partial}{\partial y} + w \frac{\partial}{\partial z},$$

$$\tau_x^H = \left(\rho_0 v \frac{\partial u}{\partial z} \right)_{z=H} \quad \tau_y^H = \left(\rho_0 v \frac{\partial v}{\partial z} \right)_{z=H}$$

$$A_1' = \frac{\partial u^2}{\partial x} + \frac{\partial uv}{\partial y}, \quad B_1' = \frac{\partial v^2}{\partial y} + \frac{\partial uv}{\partial x}$$

$$(4) \quad \frac{\partial u}{\partial x} + \frac{\partial v}{\partial y} + \frac{\partial w}{\partial z} = 0,$$

$$(5) \quad \frac{dT}{dt} = \frac{\partial}{\partial x} A_T \frac{\partial T}{\partial x} + \frac{\partial}{\partial y} A_T \frac{\partial T}{\partial y} + \frac{\partial}{\partial z} \chi_T \frac{\partial T}{\partial z},$$

$$(6) \quad \frac{dS}{dt} = \frac{\partial}{\partial x} A_S \frac{\partial S}{\partial x} + \frac{\partial}{\partial y} A_S \frac{\partial S}{\partial y} + \frac{\partial}{\partial z} \chi_S \frac{\partial S}{\partial z},$$

$$(7) \quad \rho = a_{1k} T + a_{2k} S + a_{3k} T^2 + a_{4k} S^2 + a_{5k} TS + a_{6k} T^3 + a_{7k} S^2 T + \\ + a_{8k} T^2 S + a_{9k} S^3 + \dots \quad [13]$$

All designations are generally accepted [4, 5].

There is one important feature of this model. In contrast to other numerical models of ocean circulation (where the total mass transport function is used as the integral function), in this case an equation of surface level is considered. A similar integral function is applied rarely as a rule, in diagnostic calculations. The approximation of the input equations by Fiadeiro and Veronis numerical scheme [14] (of the second order accuracy on the grid A) and the numerical algorithms are described in detail in the publications listed above. The Neumann boundary problem and the overrelaxation method for computation of the sea surface topography has been used. Here we'll only describe the main features of the basic model and shall list the parameters used, without details or discussion of the specific calculations. For horizontal velocity components, the boundary condition of zero velocity on the bottom and on the vertical walls has been used; for T&S - the isolation condition on all boundaries; for w - the "rigid lid" condition at the undisturbed upper boundary, and w=0 on the bottom have been accepted as well:

$$(8) \quad \begin{aligned} & - \text{for } \zeta: \\ & \frac{\partial \zeta}{\partial x} = - \frac{1}{\rho_0 H} \int_0^H (H-z) \frac{\partial \rho}{\partial x} dz + \frac{\tau_x + \tau_x^H}{\rho_0 g H} + \frac{f}{g H} \int_0^H v dz + \end{aligned}$$

$$+ \frac{1}{gH} \left[\int_0^H \left(\frac{\partial}{\partial x} A_1 \frac{\partial u}{\partial x} + \frac{\partial}{\partial y} A_1 \frac{\partial u}{\partial y} \right) dz - \int_0^H A_1' dz \right],$$

$$(9) \quad \frac{\partial \zeta}{\partial y} + - \frac{1}{\rho_0 H} \int_0^H (H-z) \frac{\partial p}{\partial y} dz + \frac{\tau_y + \tau_y^H}{\rho_0 g H} + \frac{f}{gH} \int_0^H u dz +$$

$$+ \frac{1}{gH} \left[\int_0^H \left(\frac{\partial}{\partial x} A_1 \frac{\partial v}{\partial x} + \frac{\partial}{\partial y} A_1 \frac{\partial v}{\partial y} \right) dz - \int_0^H B_1' dz \right];$$

– on the sea surface:

$$(10) \quad \rho_0 v \frac{\partial u}{\partial z} = -\tau_x, \quad \rho_0 v \frac{\partial v}{\partial z} = -\tau_y,$$

$$(11) \quad w = 0,$$

$$(12) \quad \frac{\partial T}{\partial z} = 0,$$

$$(13) \quad \frac{\partial S}{\partial z} = 0;$$

– on the bottom

$$(14) \quad u = v = w = 0,$$

$$(15) \quad \frac{\partial T}{\partial n} = \frac{\partial S}{\partial n} = 0;$$

– on the vertical walls:

$$(16) \quad u = v = 0,$$

$$(17) \quad \frac{\partial T}{\partial n} = \frac{\partial S}{\partial n} = 0.$$

The wind stress has been chosen according to the data of Hellerman^[15]. The time step has been selected to be 20 min. and the values of the coefficients of the vertical turbulent exchange and vertical heat and salt diffusion have been determined as 1 cm²/sec. The horizontal turbulent diffusion coefficient has been chosen to be 0.0264 h^{4/3} cm²/sec and the horizontal coefficient of eddy viscosity has been calculated using the Smagorinsky formula^[16].

The adaptation calculation process has been completed after 2 or 3 days of model time (see Figure 1), i.e. the adjustment time is relatively fast (with respect to the prediction period). In this way the main advantages of the adaptive models have been realized: using a short integration period good diagnostic results have been obtained (adequate to the experimental data) and at the

same time some of the errors in the T-S fields, leading to meso- and small-scale perturbations, have been removed. The hydrological adjustment of the fields results mainly in hydrodynamic filtration of the noise (with respect to the model) - Figures 2, 4. The basic mechanisms of the adaptation are the "scattering" and the dissipation of the inertial gravity waves. These aren't physical, but model waves. Their amplitude exceeds the amplitude of the real waves, and their wavelength depends on the grid interval. These waves are initiated by the "noise" in the input data (by their incompatibility with the model), and they are typical of the models, based on "primitive" equations of motion, describing them (in contrast to the filtered, quasigeostrophic model^[17]). Figure 1 shows that the oscillations of energy and enstrophy disappear after 2 or 3 days of integration. If the integration process is continued further, the fields are slowly smoothed down and modified towards the model solution. There are no significant differences between the results, obtained after 3 and after 10 days of integration--the differences are much smaller than those observed at this stage of semidiagnostic calculations.

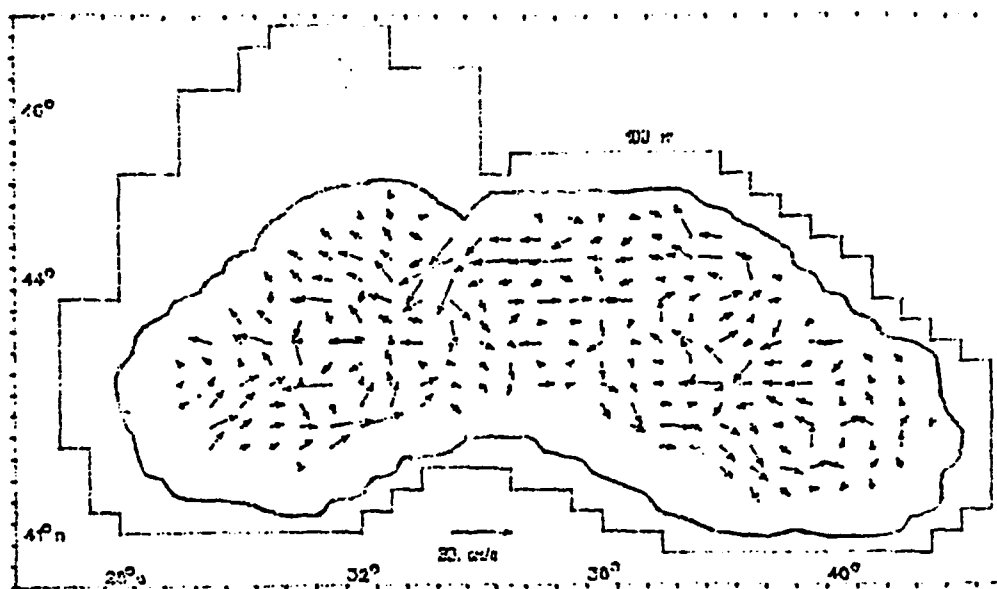
The process of adaptation removes the small-scale structures (eddies and meanders), and causes undesirable broadening and weakening of the GBSC. This effect is much weaker than the influence of the traditional filtration procedures, but is nevertheless observable. For some regions of the GBSC (for instance, near Cape Kaliakra), the grid step is too large, leading to "loss" of the current jet. We'll list some characteristic features of the solution obtained:

(1) the distributions obtained after the adaptation are of regular and "legible" character; at the same time all large-scale features of the initial data have been preserved (Figure 2);

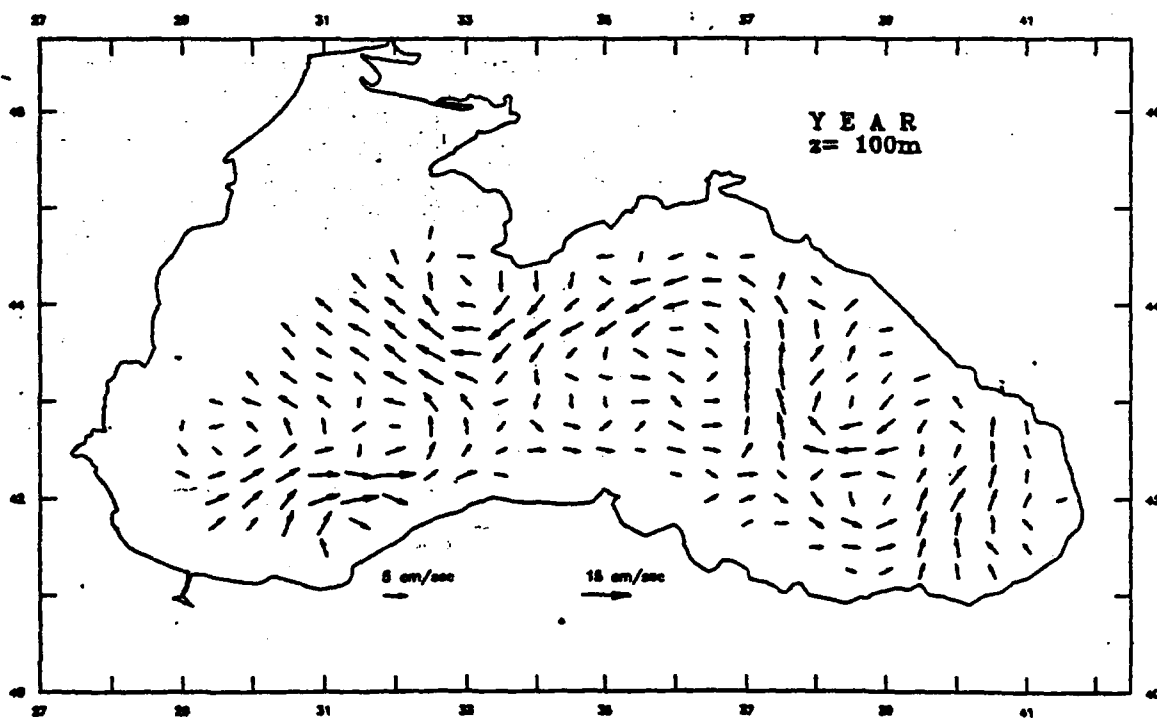
(2) the adaptation method gives better results than the traditional filtration procedures, used for instance by the authors of^[18]; the charts there show that the GBSC has been significantly broadened and weakened by the filtration (Figures 3 and 4), which is too high a price for the regularity obtained.

* * *

Annual current fields at a depth of 100 m are shown in Figure 2. They have been obtained by diagnostic and adaptive calculations. It can be clearly seen that all basic structures of circulation are more distinct after the adjustment process. The GBSC, the basic dynamic feature of the Black Sea, encircles the whole sea within one cyclonic circular stream. It can be considered as a frontal current, which generates eddies. Its structure, however, is quite different from the common concept of a smooth, symmetrical stream with two gyres at the western and eastern parts of the sea. The presence of these two gyres in the results of model calculations is usually considered to be a sufficient proof that the model is satisfactorily describing the real circulation. The structure of the currents is much more complex - the stream meanders, the gyres are elongated and change their positions seasonally. The number of cores at the center of the cyclonic gyres can exceed two. On the background of the general cyclonic rotation a series of anticyclonic eddies develops close to the shore. Some of them are present on the charts for all four seasons. Another important feature, different from the common circulation representations, is the fact that the current isn't always close to the continental shelf slope. Sometimes (especially in regions with eddies and meanders) the current detaches from the shore. It's evident that the GBSC is subject to significant seasonal variations (see Appendix), though its general circulation structure is qualitatively constant. The structure of the surface currents is preserved quite well down to large depths, with decreasing velocity modulus only. Gradually the GBSC loses its jet character. A significant change is observed at depths below 800 m. For instance, at the center of the sea at a depth of ~1000 m, the direction of the main stream is opposite to that at the upper layer. This strong (relatively! - with respect to the other currents at the periphery) stream to the east is observed in all seasons and for all other levels to the bottom, which suggests that it is a stable feature of the circulation at large depths. This result confirms the hypothesis of Neumann^[19] that at 1000 m depths a current exists, flowing in the direction opposite that of the surface current.

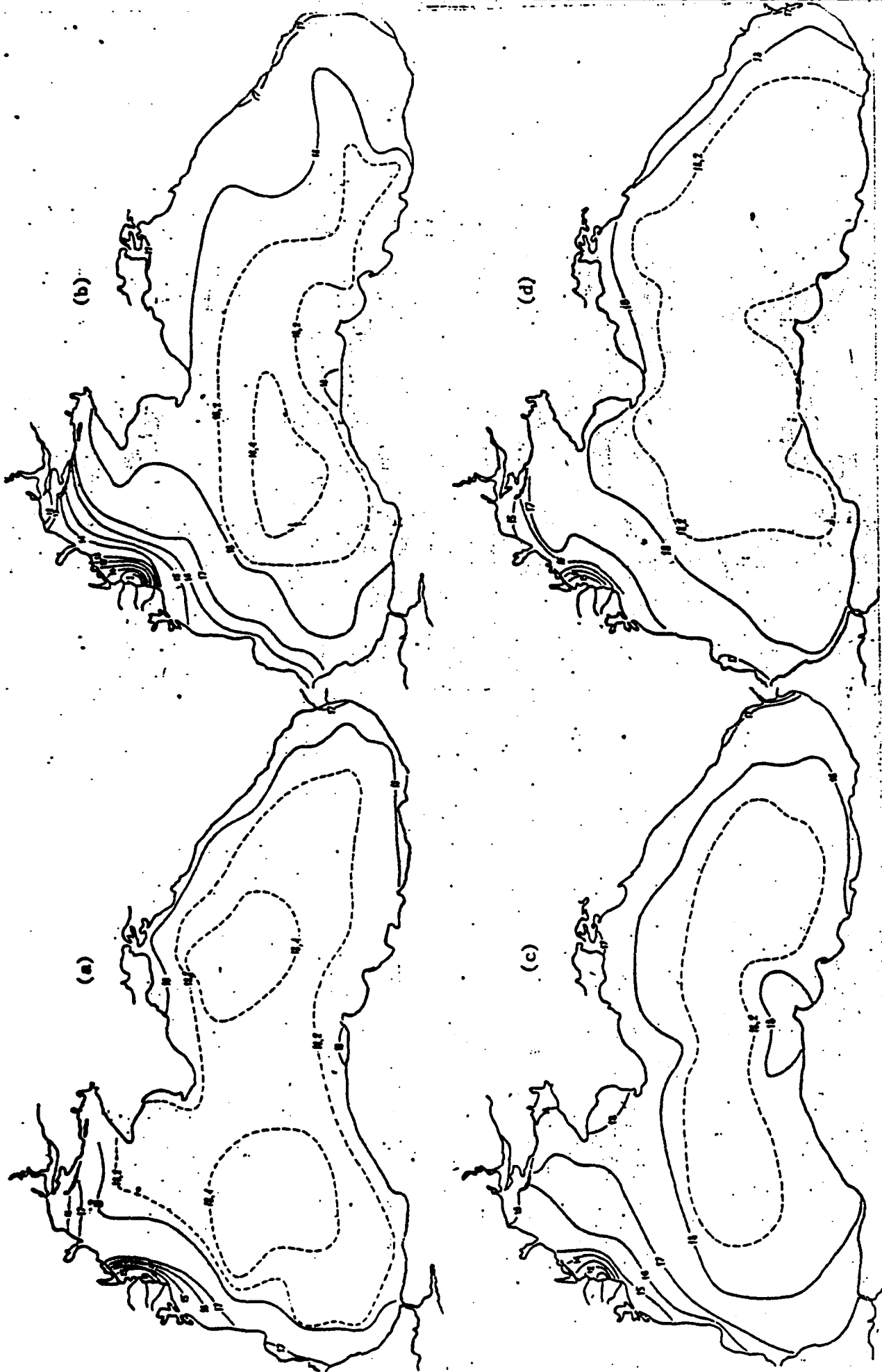


(a)

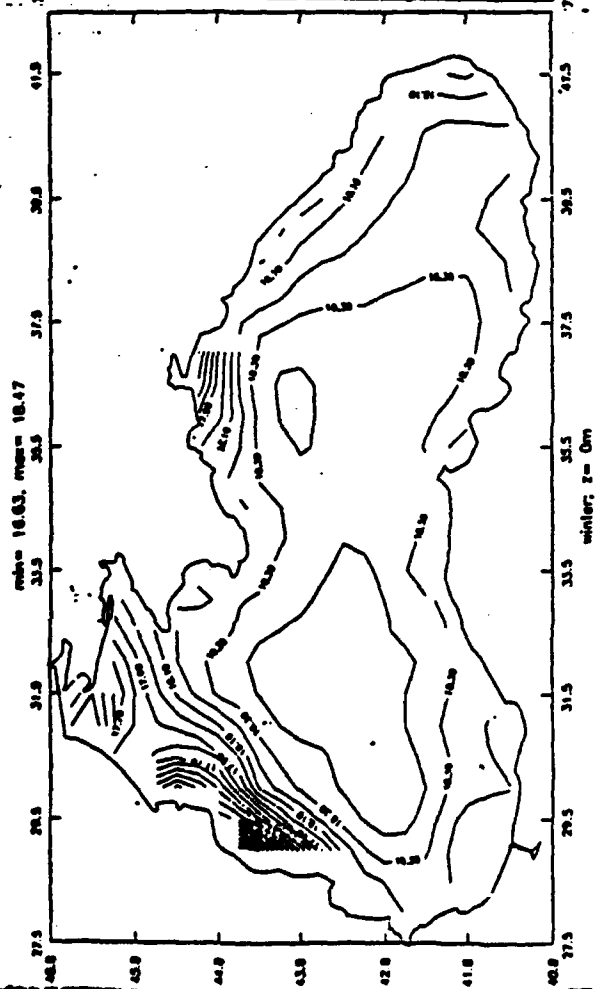


(b)

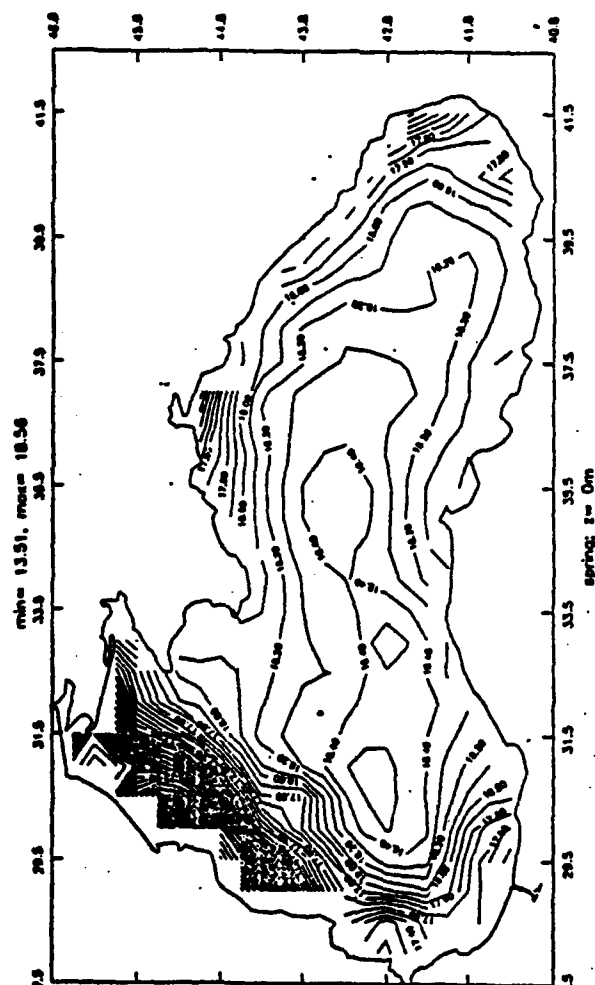
Figure 2. Diagnostic (a) and adaptive (b) climatic currents at a depth of 100 m.



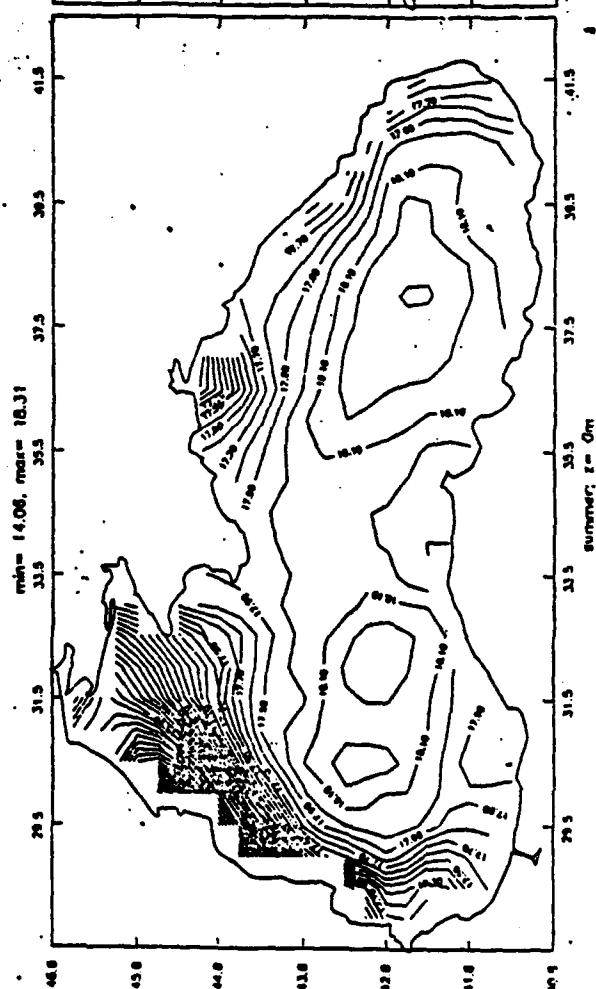
The Black sea climate salinity



The Black sea climate salinity



The Black sea climate salinity



The Black sea climate salinity

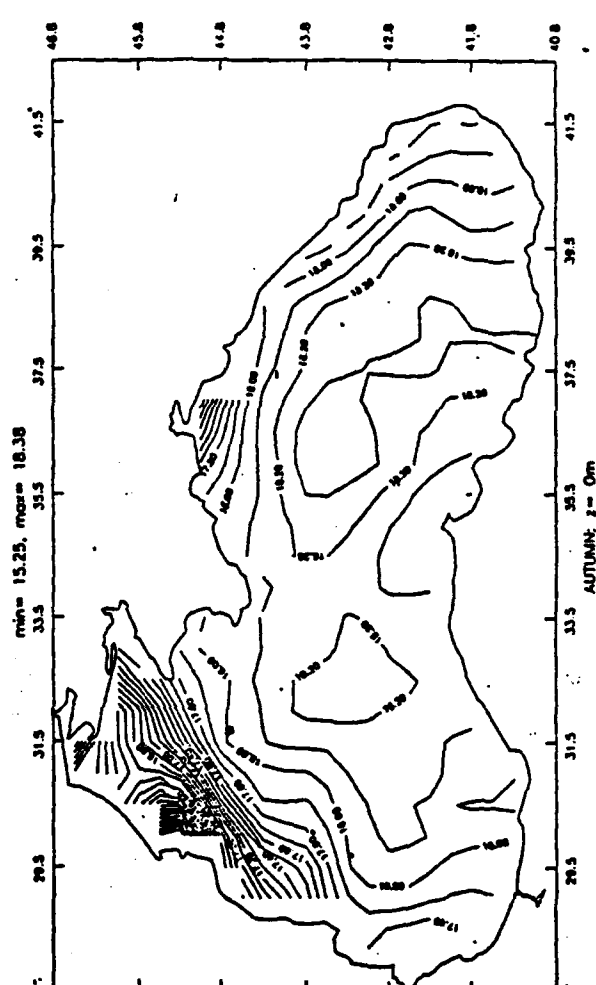


Figure 4. Climatic salinity distributions (‰) at the sea surface for different seasons.

The results described in the present work show that the method proposed can be used to perform hydrodynamic analysis of the main hydrological fields in the Black Sea. Our experience proves that the 3D current fields obtained by hydrodynamical adjustment are a reliable basis for numerical investigations of a wide variety of applied problems, connected with sea pollution modelling, using, for instance, the direct and conjugated diffusion problems and obtaining a number of integral characteristics (balance approach)^[20]. The climate data produced from a given experiment should be taken as a starting point for obtaining information from the existing arrays of hydrological data. To further develop and complement this information, some requirements have to be met by the future surveys. It's important to increase significantly the statistical reliability of the data for large depths. The result will be a more reliable description of the deep water dynamics. It's also necessary to provide information about the wind stress and the atmospheric pressure above the water surface of the Black Sea. The data of Hellerman^[15], which are widely used in numerical calculations, are too generalized, and are quite different from the real wind characteristics of the Black sea. The distribution of surface temperature in winter turned out to be the "noisiest" of all fields used. This is easily explained by the dynamic character of the processes, taking place on the surface in this season, and by the insufficient survey activity in winter. It's possible that for future investigations, information will be obtained from satellites and from ship weather stations as well.

* * *

When the results of numerical experiments are discussed, comparisons of the type "practically coinciding", "qualitatively similar", etc. are often used^[4, 5, 6]. The quantitative evaluations like "decrease by 10 to 20 percent" are implicitly understood as similarity of the results as well. The imperfections of the models used and the lack of sufficient quantitative (and often - qualitative as well) understanding about the investigated processes are the reason why 10% to 20% variations in the results cannot be regarded as sufficiently reliable. With the future development of new and more adequate models and broadening of our knowledge about the investigated processes, the importance of these conclusions will increase (this is the case for example with weather forecasts).

ACKNOWLEDGMENTS

This work has been thought and realized together with my best friend, colleague and teacher Yu. Demin, who died suddenly quite young in the prime of his abilities. I worked with QG-models to numerical nonlinear models with his help, as well as using the general Knipovich scheme for the complex eddy structure of hydrological fields in the Black Sea.

The present results have become possible due to Dr. G. Dvoryaninov's help (from MHI in Sevastopol, Ukraine) in systematizing the existing hydrological data. Pr. Sarkisyan was our best supporter and consultant. The whole research work had been financially helped and computer provided by the Intergovernmental program "Sections" under the leadership of Acad. G. Marchuk and by the topic "World Ocean". We were able to publish this Atlas due to Dr. D. Aubrey from WHOI, who was greatly interested in the results. I appreciate greatly their help and sincerely thank all of them.

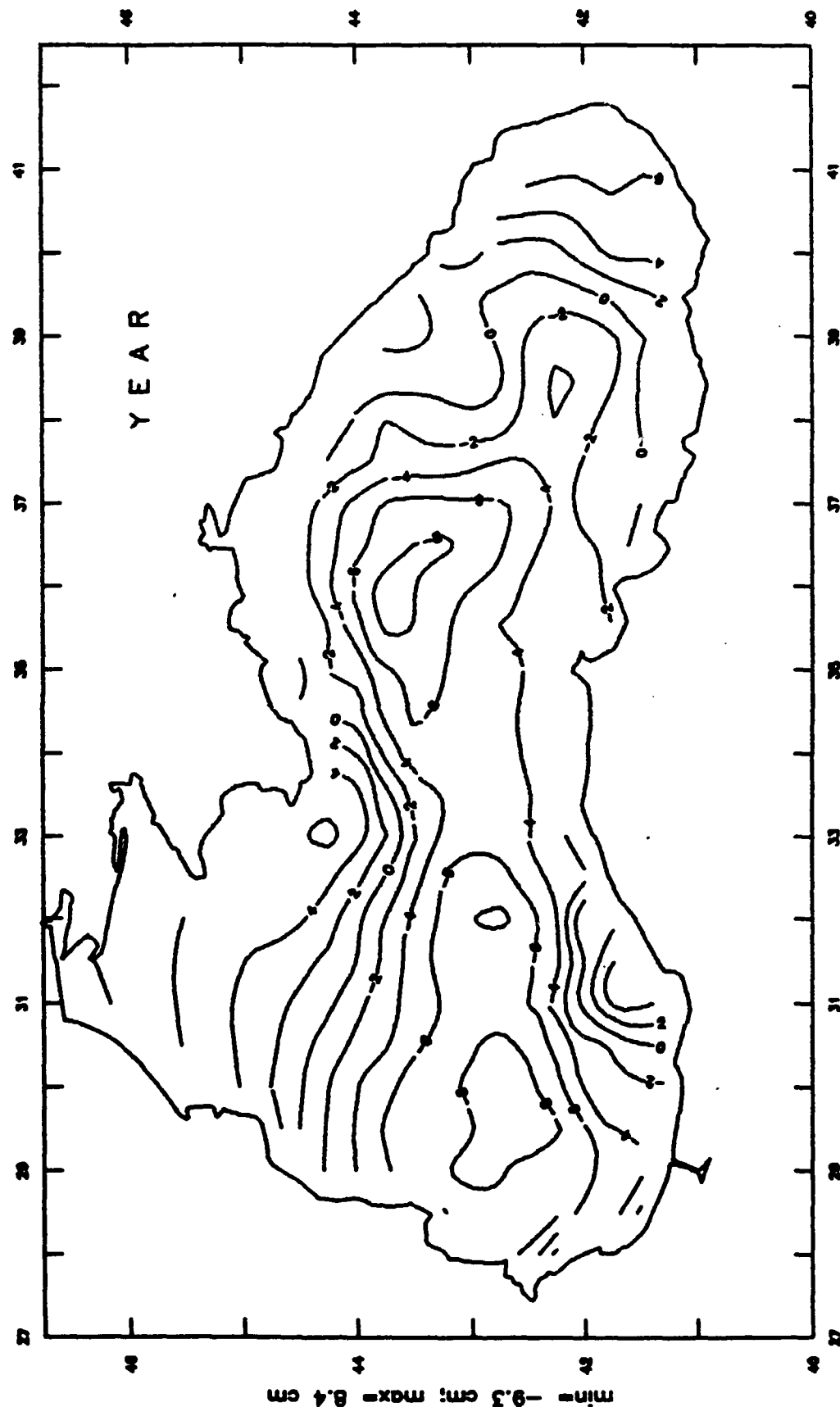
II. REFERENCES

1. Blatov, Ç., N. Bulgakov, V. Ivanov et al., 1984. Variability of hydrophysical fields of the Black Sea. Leningrad, *Gidrometeoizdat*. 240 pp., (in Russian).
2. Bogatko, O., S. Boguslavskii, Yu. Belyakov, 1979. Surface currents in the Black Sea. In: *Kompleksnie issledovaniya Chernogo morya*. Sevastopol, MGI AN USSR, p. 25-33, (in Russian).
3. Sandstrom, J. and B. Halland-Hansen, 1903. Über die Berechnung vor Meeresströmungen. *Rept. Norway Fish and Marine Investig.*, v. 2, N 4 (in German).
4. Sarkisyan, A., Yu. Demin., A. Brekhovskikh and T. Shakhanova, 1986. Methods and results of calculation of the World Ocean circulation. Leningrad, *Gidrometeoizdat*. 181 pp., (in Russian).
5. Stanev, E., D. Truhchev and V. Roussenov, 1988. The Black sea circulation and its numerical modelling. *Kliment Ohridski University Press*, Sofia. 222 pp., (in Bulgarian).
6. Demin, Yu. and D. Trukhchev, 1989. Hydrodynamical diagnosis of the currents in marine basins. In: *Modelirovanie gidrofizicheskikh processov v zamknutih vodoemah i moryah*. Moscow, Nauka, p. 6-31, (in Russian).
7. Stanev, E., 1988. Numerical study of the Black Sea circulation. *Mitteilungen des Instituts für Meereskunde der Universität Hamburg*, No. 28. 232 pp.
8. Sarkisyan, A., Yu. Demin and D. Trukhchev, 1983. On calculation of vertical velocity in models of sea currents. *Atmosp. and Ocean Physics*, v. 19, p. 730-740.
9. Sarkisyan, A. and Yu. Demin, 1983. A semidiagnostic method of sea currents calculation. In: *Large-scale oceanographic experiments in the WCRP*, WCRP Publications Series, Tokyo, v. 2, p. 201-214.
10. Sarkisyan, A., Yu. Demin and D. Trukhchev, 1983. Hydrodynamical model of currents and density field at the sea coast zone. *C. R. Bulg. Acad. Sci.*, Sofia, v. 36, p. 341-344 (in Russian).
11. Trukhchev, D., 1985. On the results of numerical modelling of currents in the west part of the Black Sea. In: *Integrated global ocean monitoring*, v. 3, Leningrad, *Gidrometeoizdat*, p. 129-140.
12. Sarkisyan, A., Yu. Demin and D. Trukhchev, 1987. A model of hydrodynamical adjustment of temperature, salinity and current fields. *Atmosp. and Ocean Physics*, v. 23, p. 45-51.
13. UNESCO, 1976. Seventh report of the joint panel on oceanographic tables and standards. UNESCO Techn. Papers. Mar. Sci., v. 24, Appendix 1, p. 39-54.
14. Fiadeiro, M. and G. Veronis, 1977. On the weighted-mean schemes for the finite-difference approximation to the advection-diffusion equation. *Tellus*, v. 29, p. 512-522.
15. Hellerman, S., 1967. An updated estimate of the wind stress on the world ocean. *Month. Weath. Rev.*, v. 95, p. 607-626.

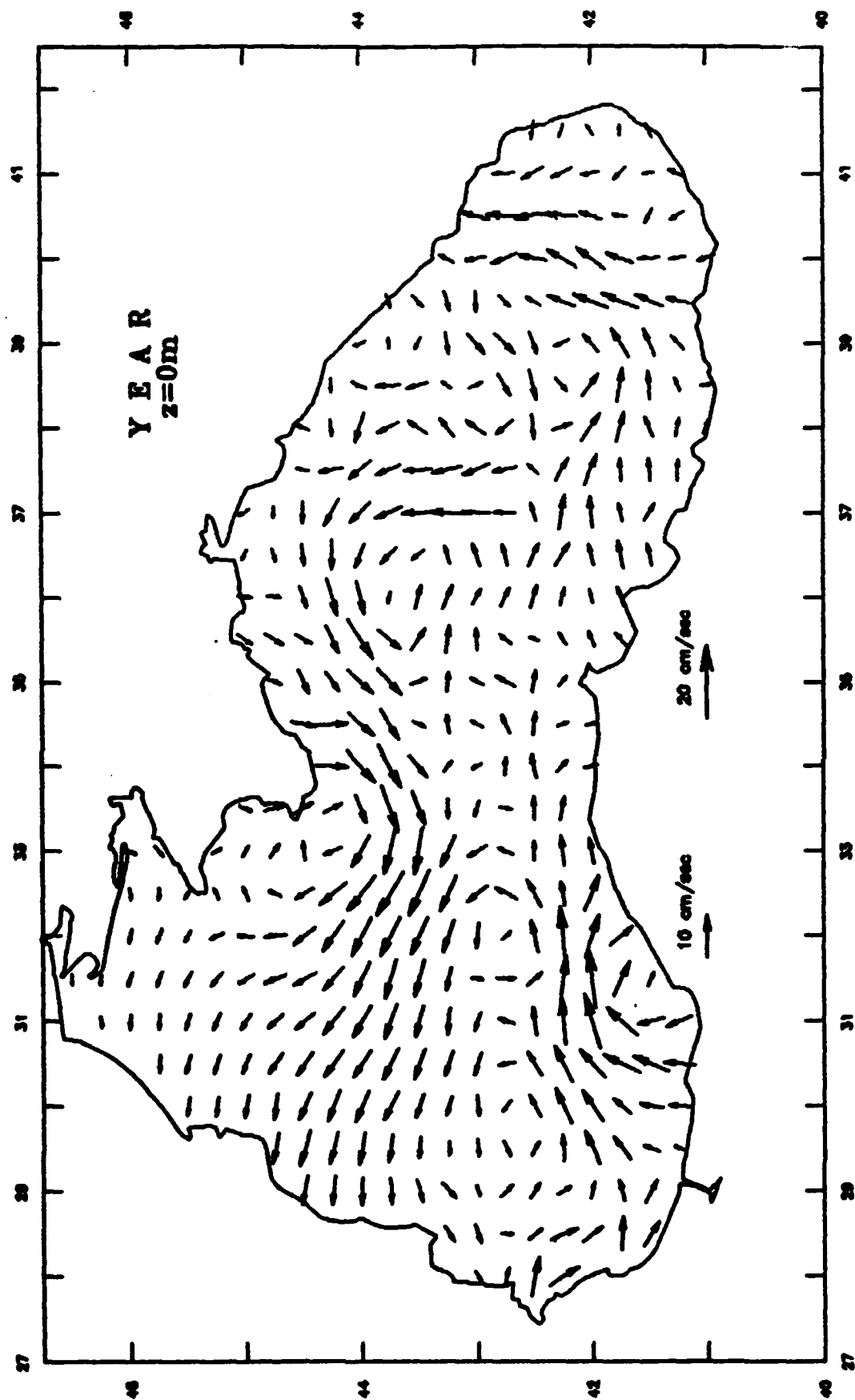
16. Smagorinsky, J., S. Manabe and J. Holloway, 1965. Numerical results from a nine-level general circulation model of the atmosphere. *Month. Weath. Rev.*, v. 93, p. 727-768.
17. Sarkisyan, A., 1977. The diagnostic calculations of a large-scale oceanic circulation. In: *The Sea. Marine Modelling*, J. Wiley & Sons, New York-London-Sidney-Toronto, v. 6, p. 363-458.
18. Al'tman, E., I. Gertman and Z. Golubeva, 1987. Climatic fields of salinity and temperature of the Black Sea. *GOIN*, Sevastopol. 108 pp. (in Russian).
19. Neumann, G., 1943. Über den Aufbau und die Frage der Tiefenzirkulation des Schwarzen Meers. *Ann. D. Hydr. und Marit Meteorol.*, v. 71, 4/6, p. 1-20 (in German).
20. Godev, N., E. Syrakov, K. Ganey and D. Trukhchev, 1984. Comprehensive approach to the study of diffusion of sea pollutants. *C. R. Bulg. Acad. Sci.*, Sofia, v. 37, p. 1323-1326.

III. APPENDIX
CLIMATIC ATLAS OF THE BLACK SEA
SEA LEVEL TOPOGRAPHY, CURRENTS, SALINITY, TEMPERATURE

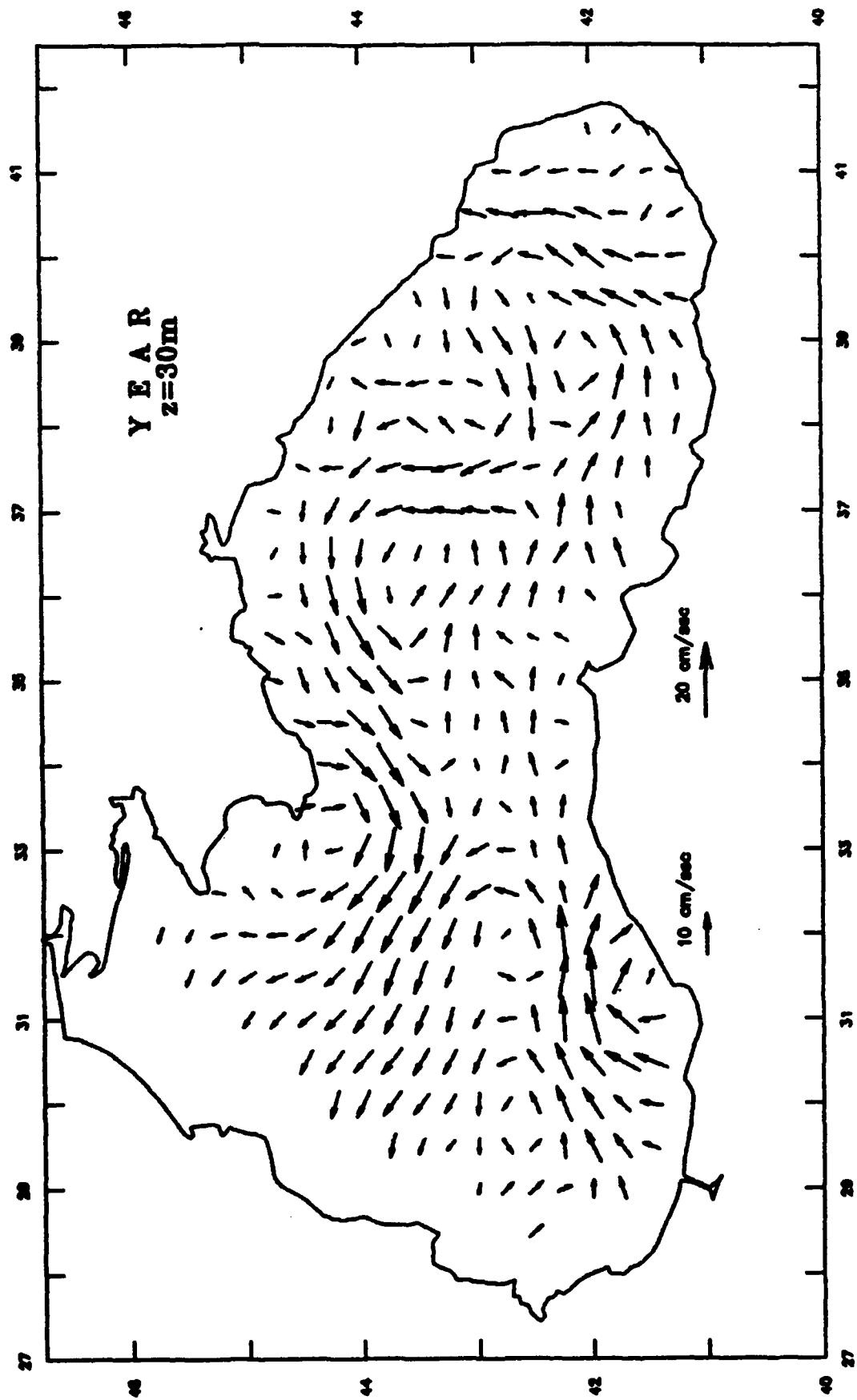
The Black Sea Climate Surface



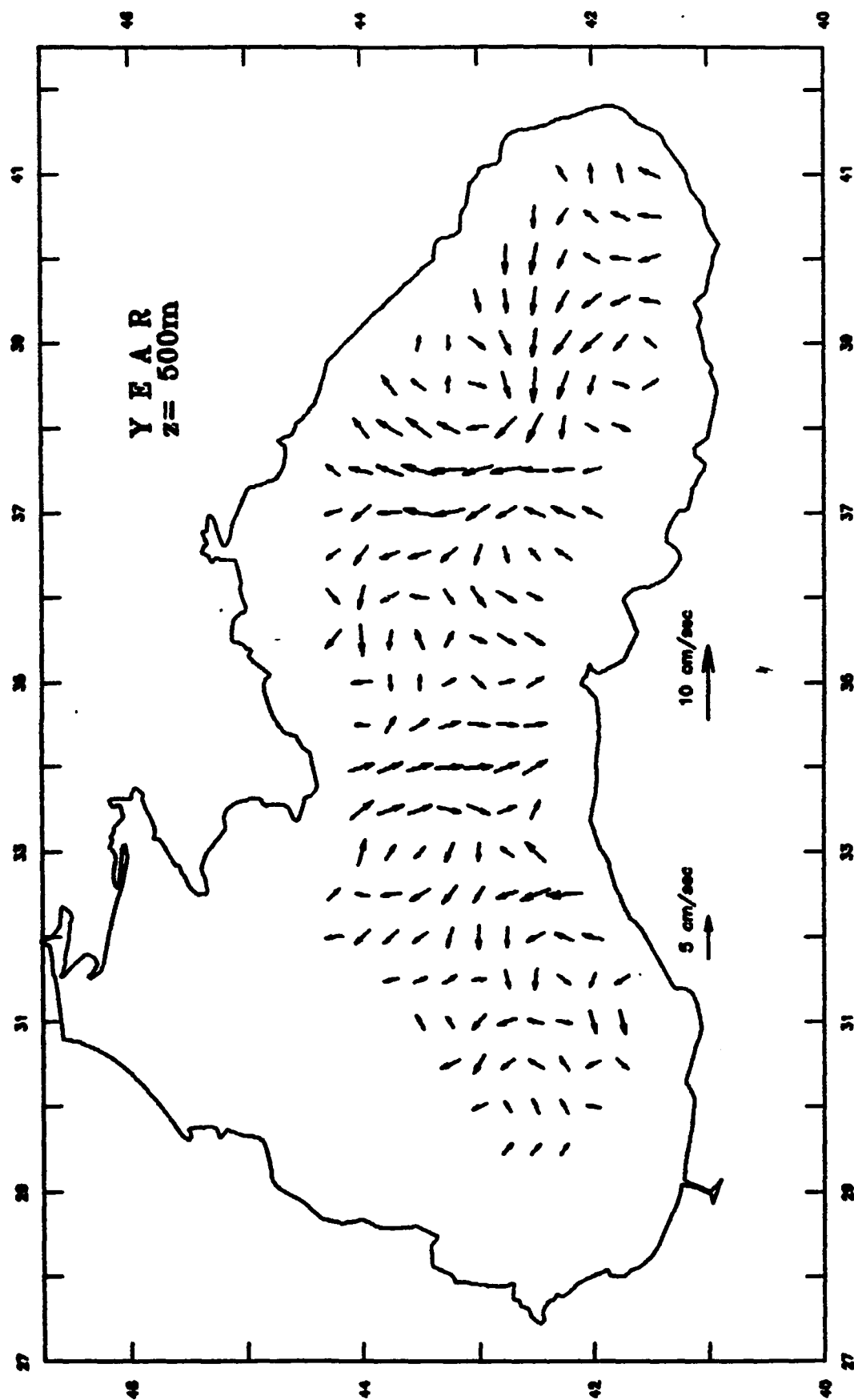
The Black Sea Climate Velocity



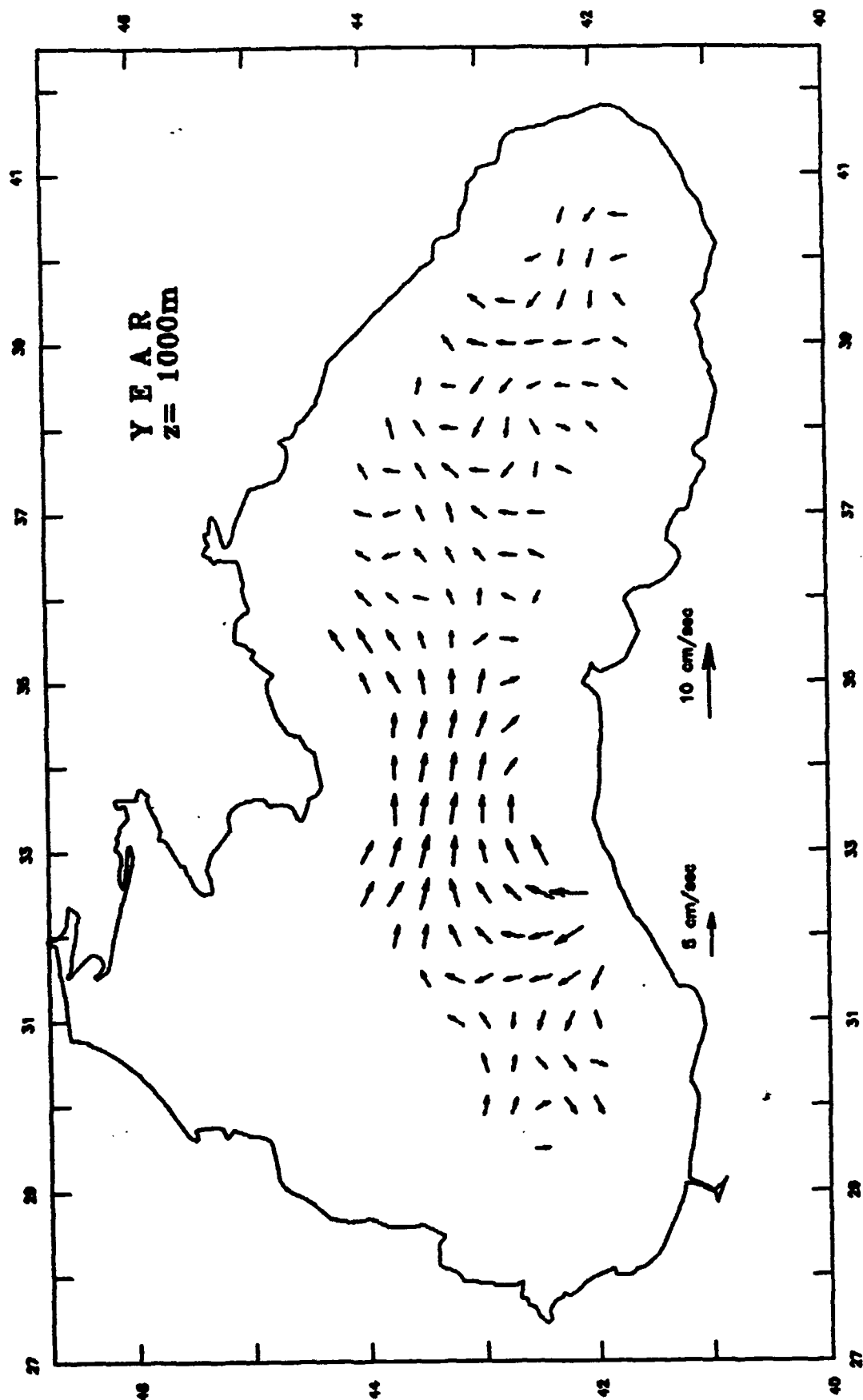
The Black Sea Climate Velocity



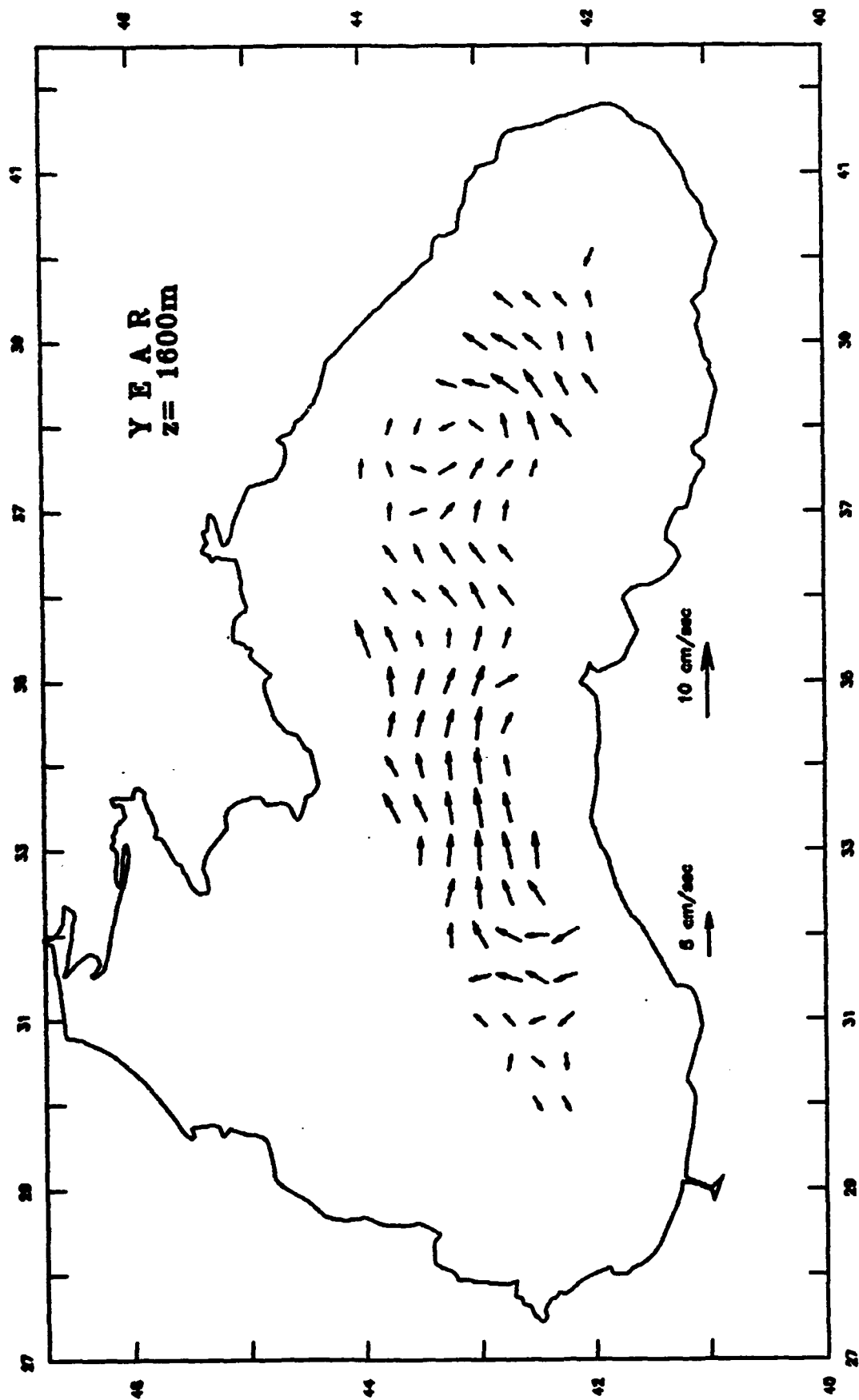
The Black Sea Climate Velocity



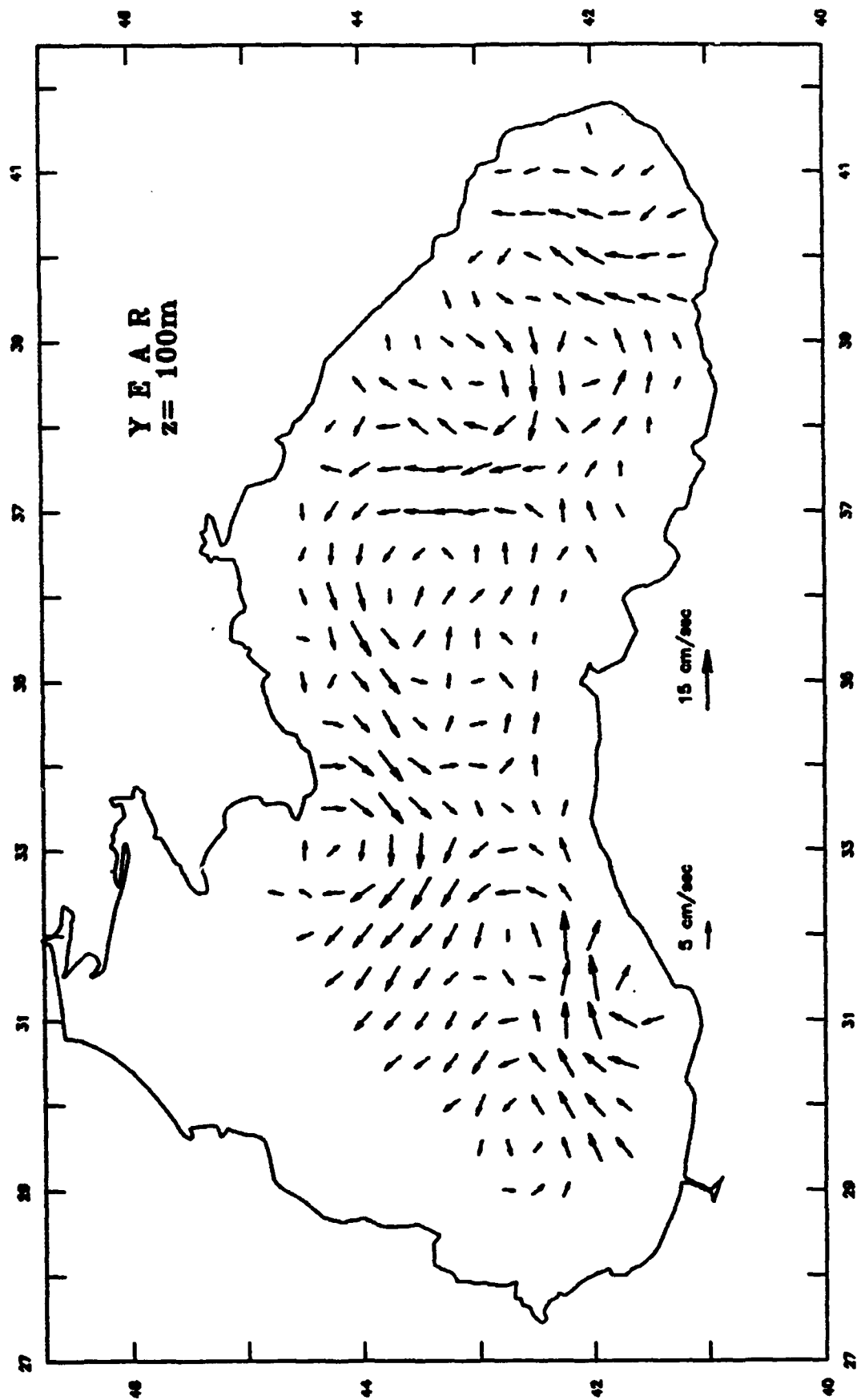
The Black Sea Climate Velocity



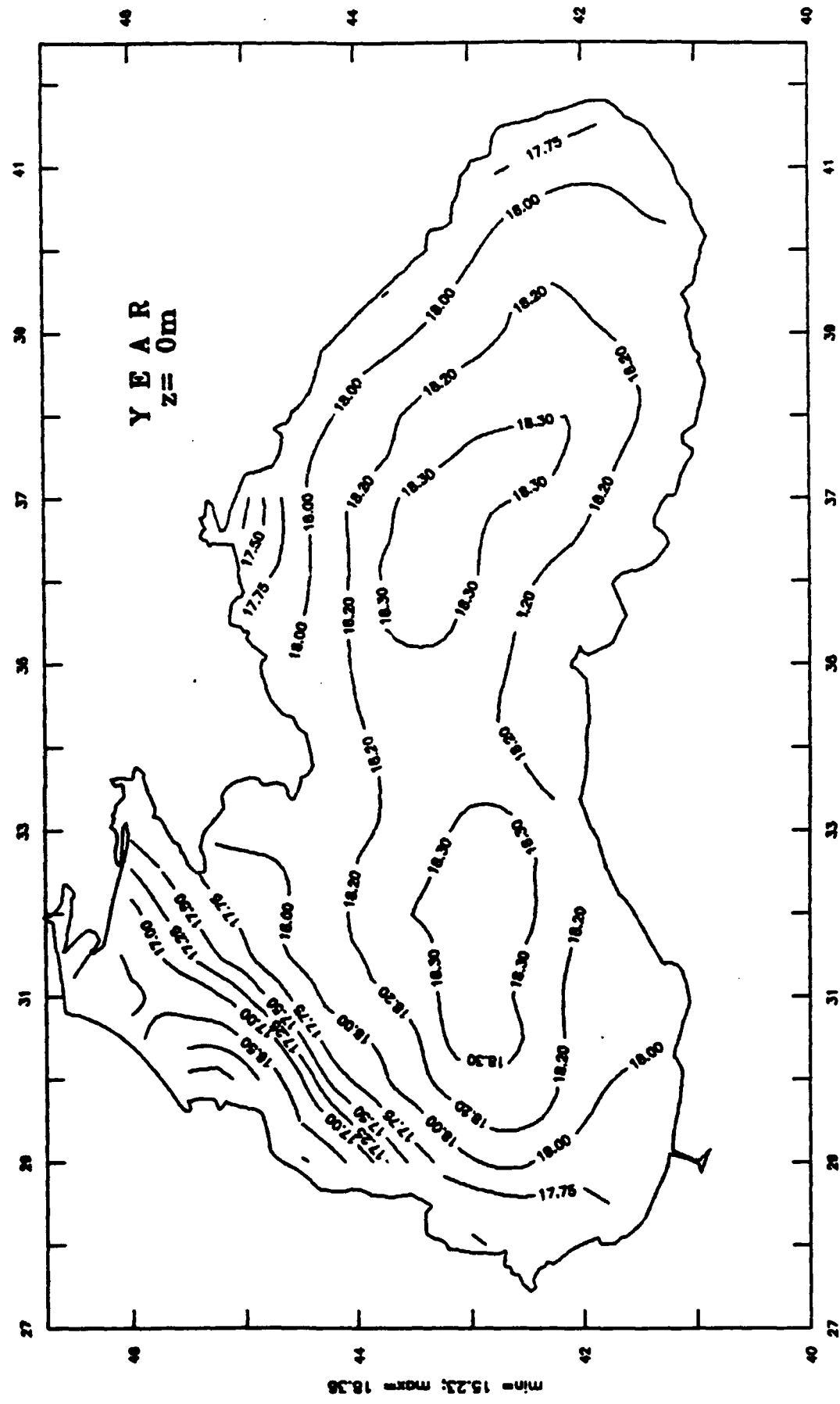
The Black Sea Climate Velocity



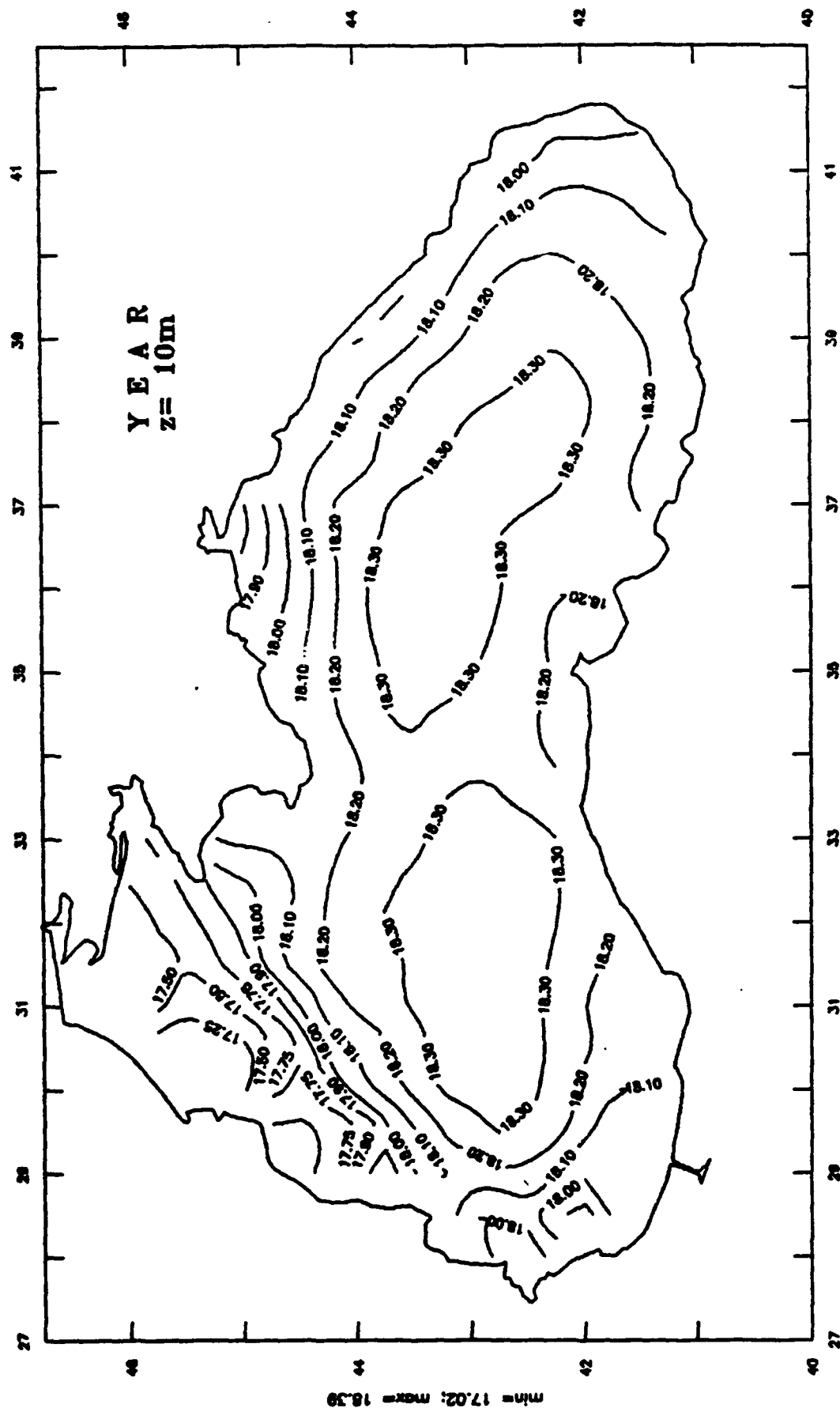
The Black Sea Climate Velocity



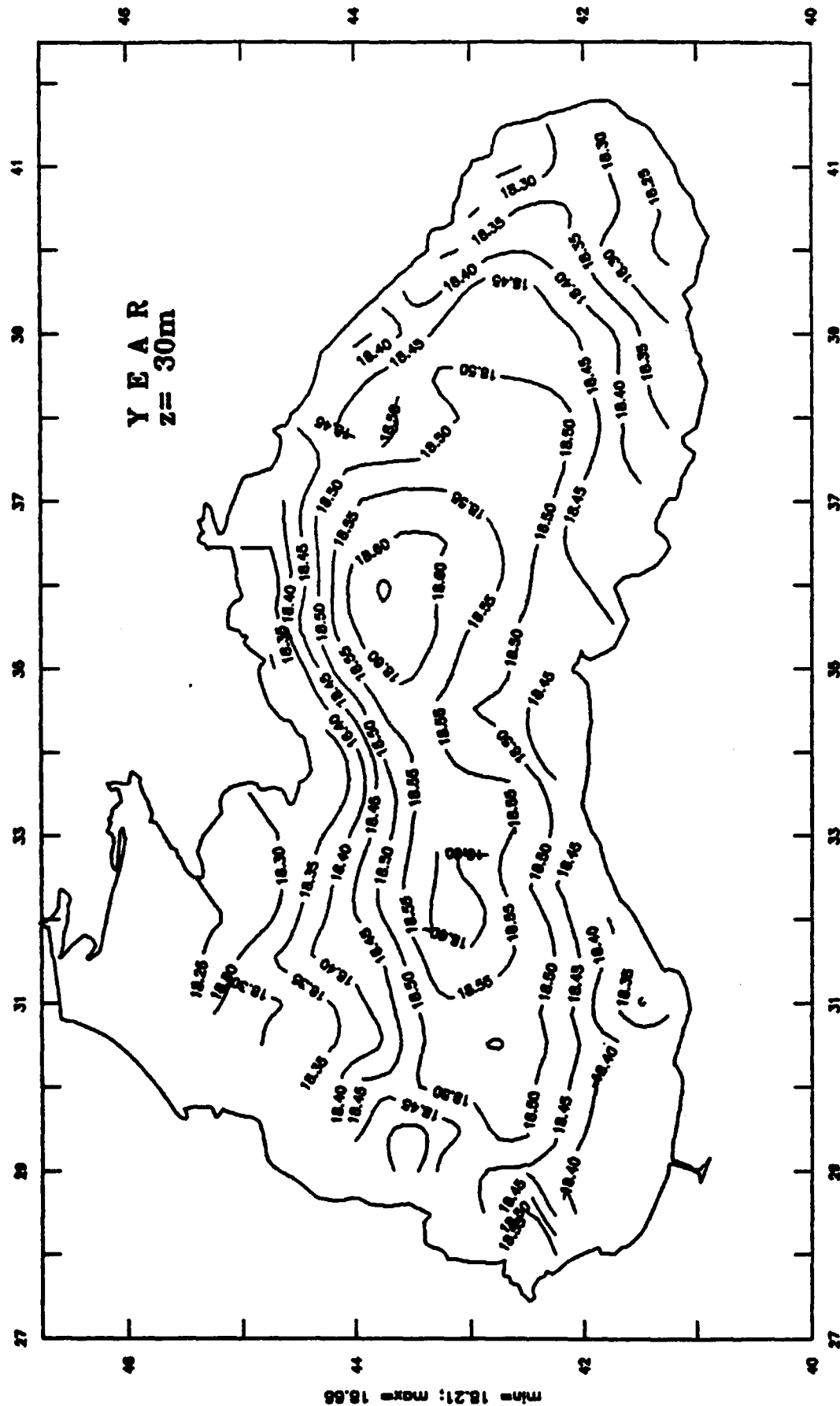
The Black Sea Climate Salinity



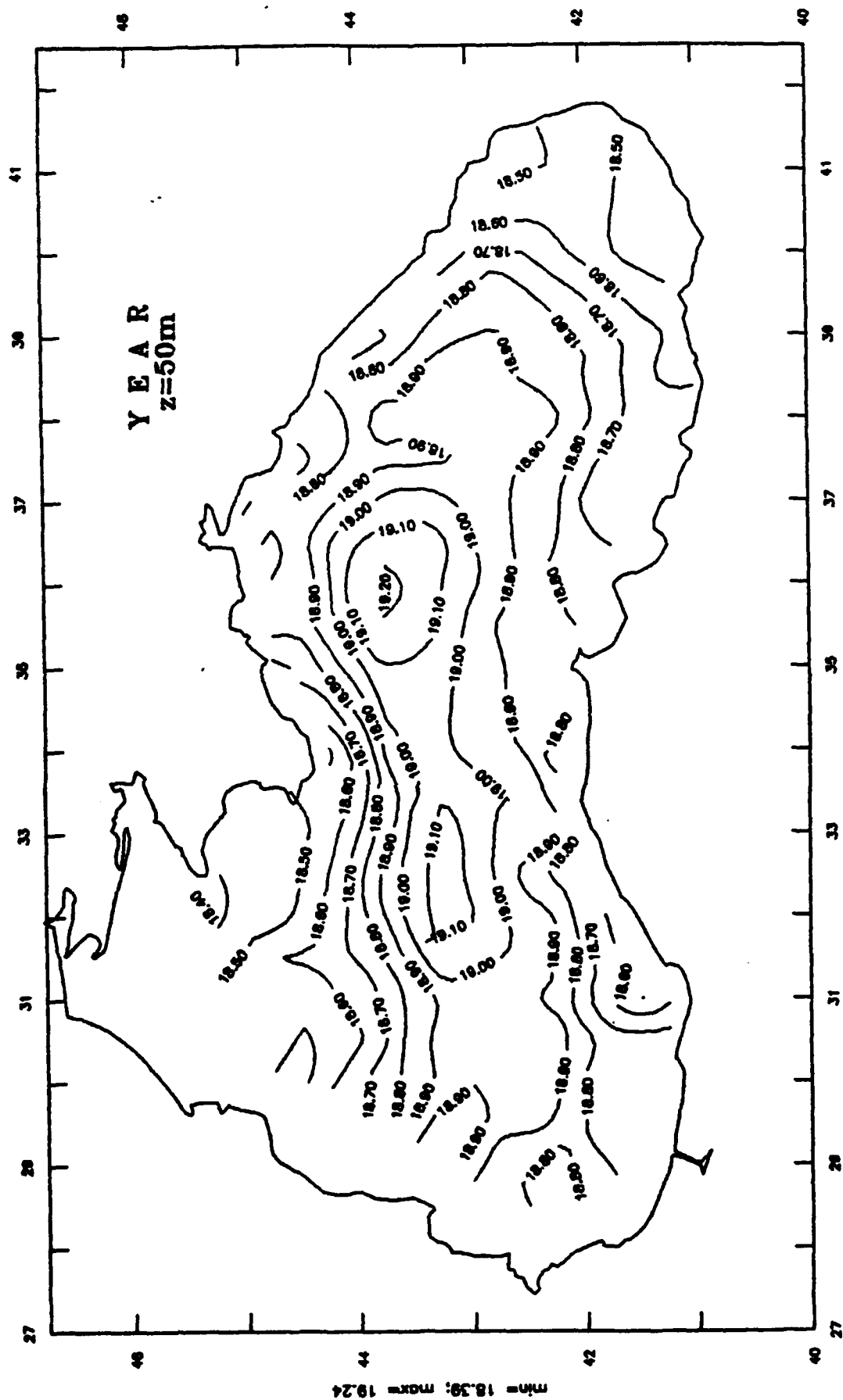
The Black Sea Climate Salinity



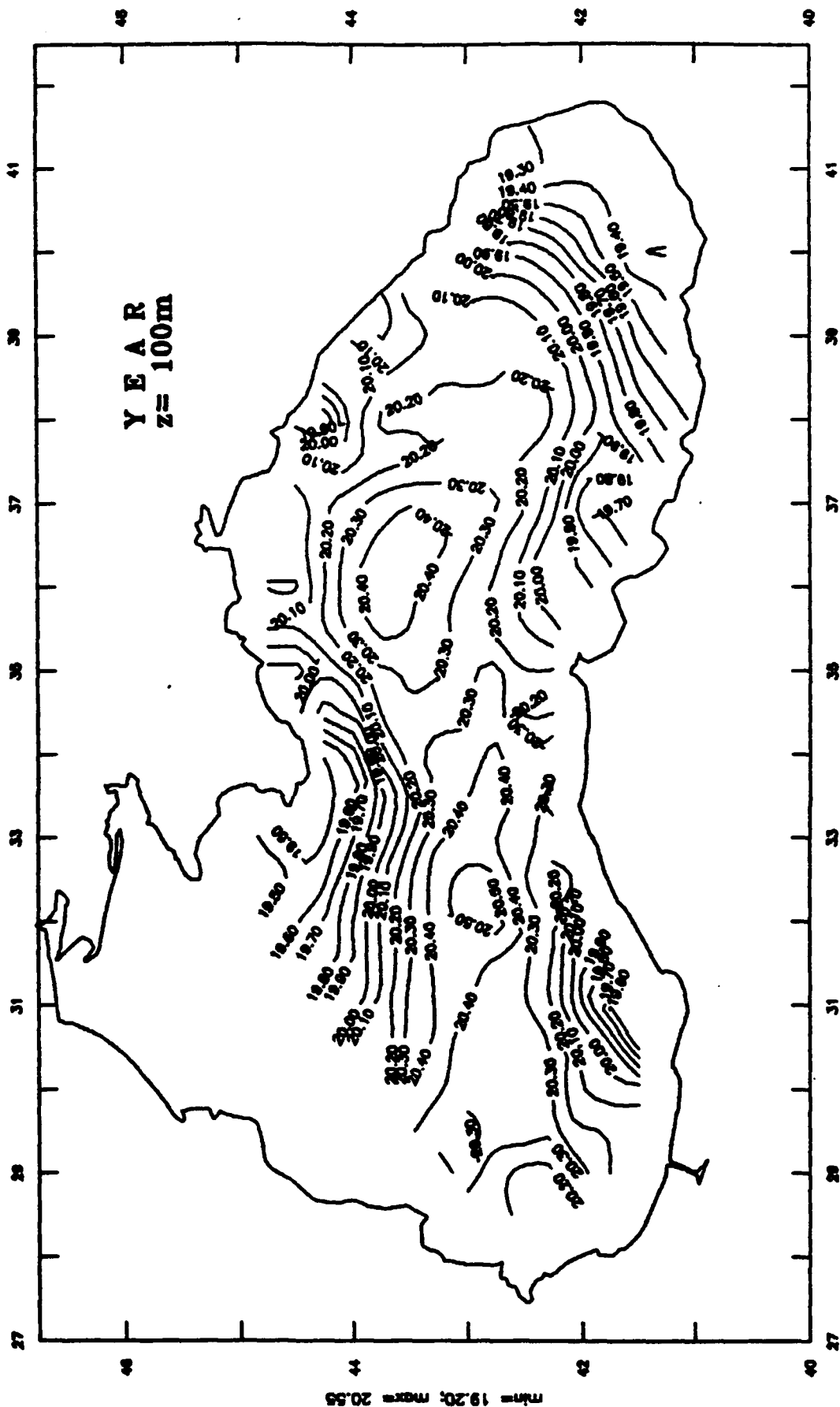
The Black Sea Climate Salinity



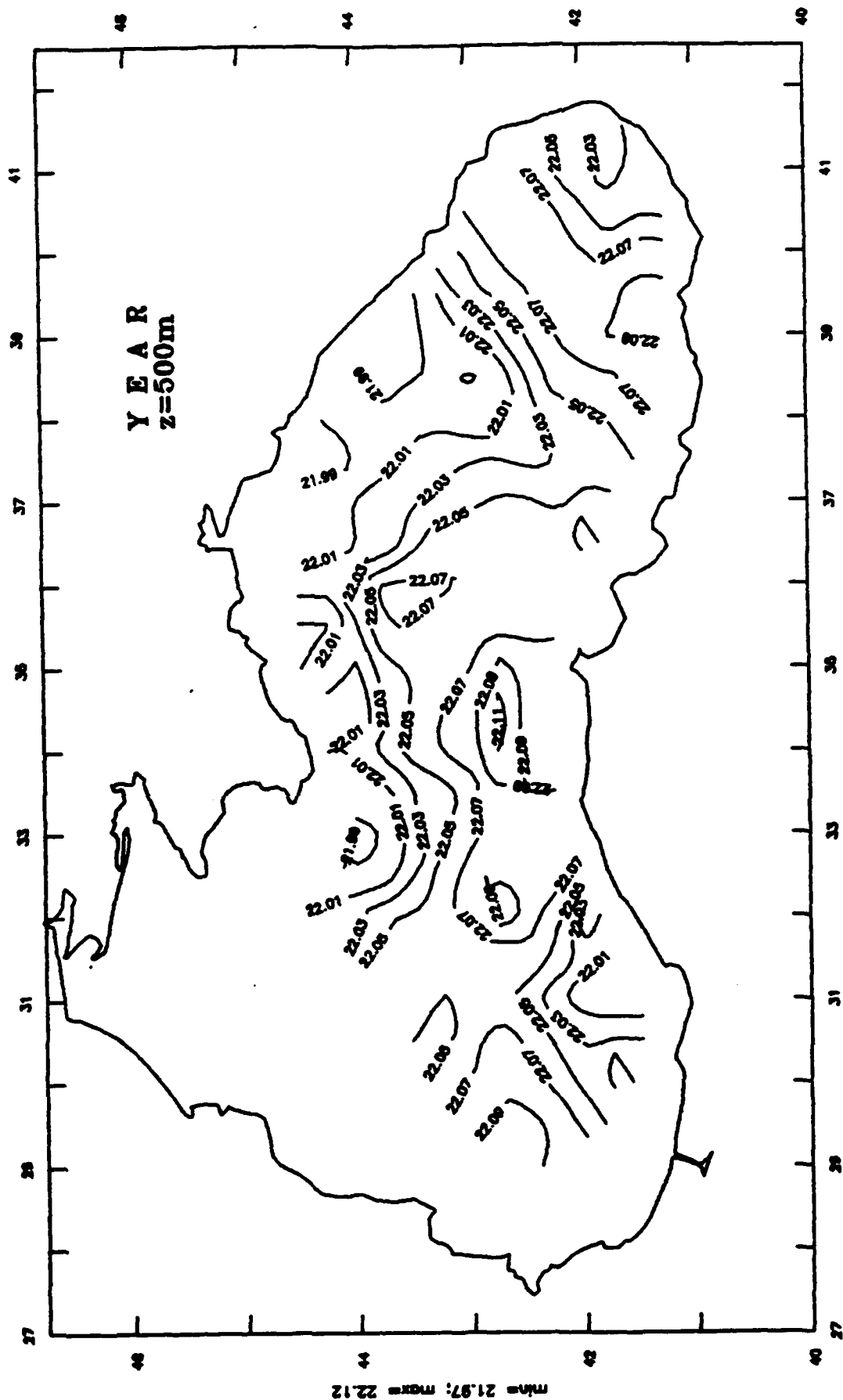
The Black Sea Climate Salinity



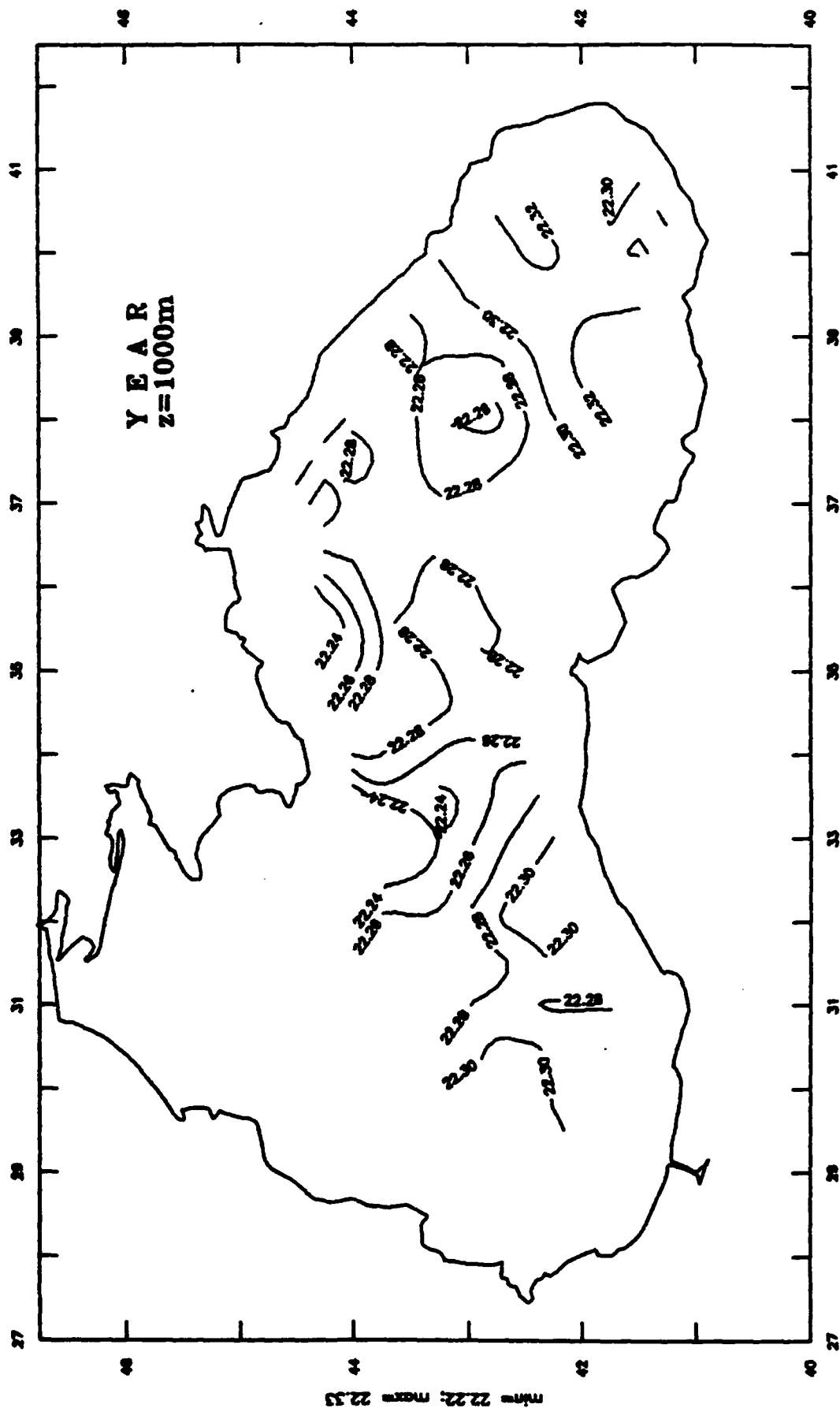
The Black Sea Climate Salinity



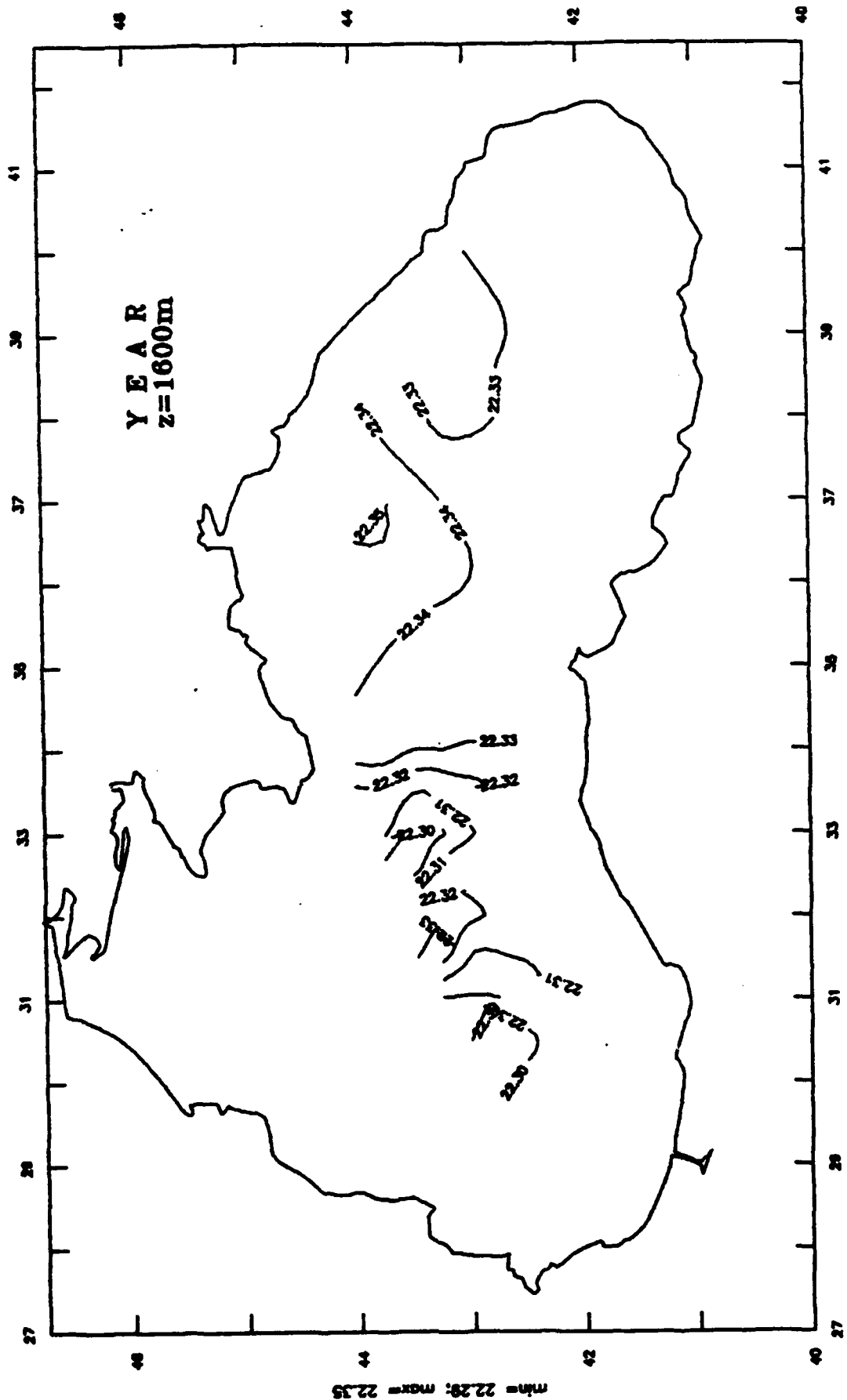
The Black Sea Climate Salinity



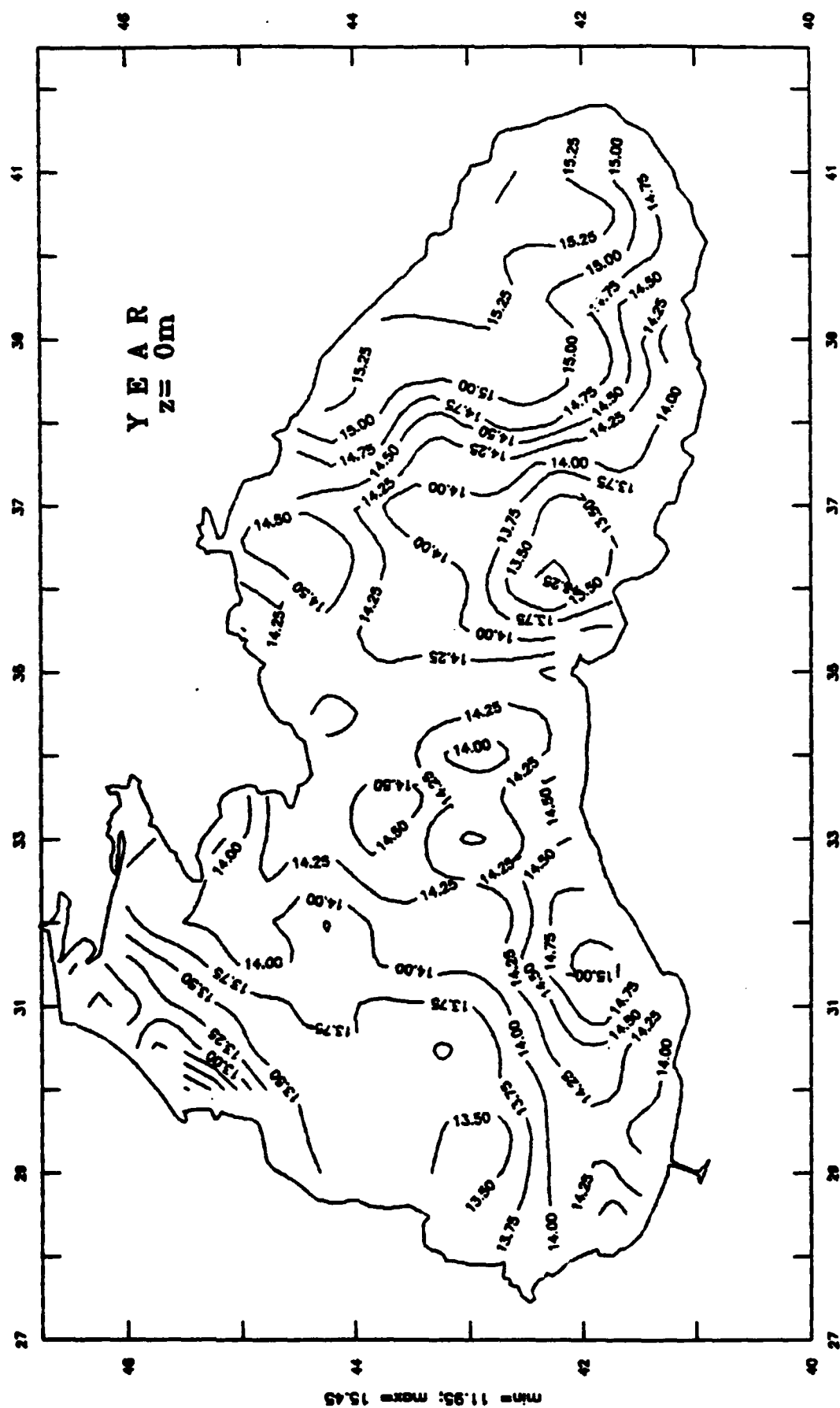
The Black Sea Climate Salinity



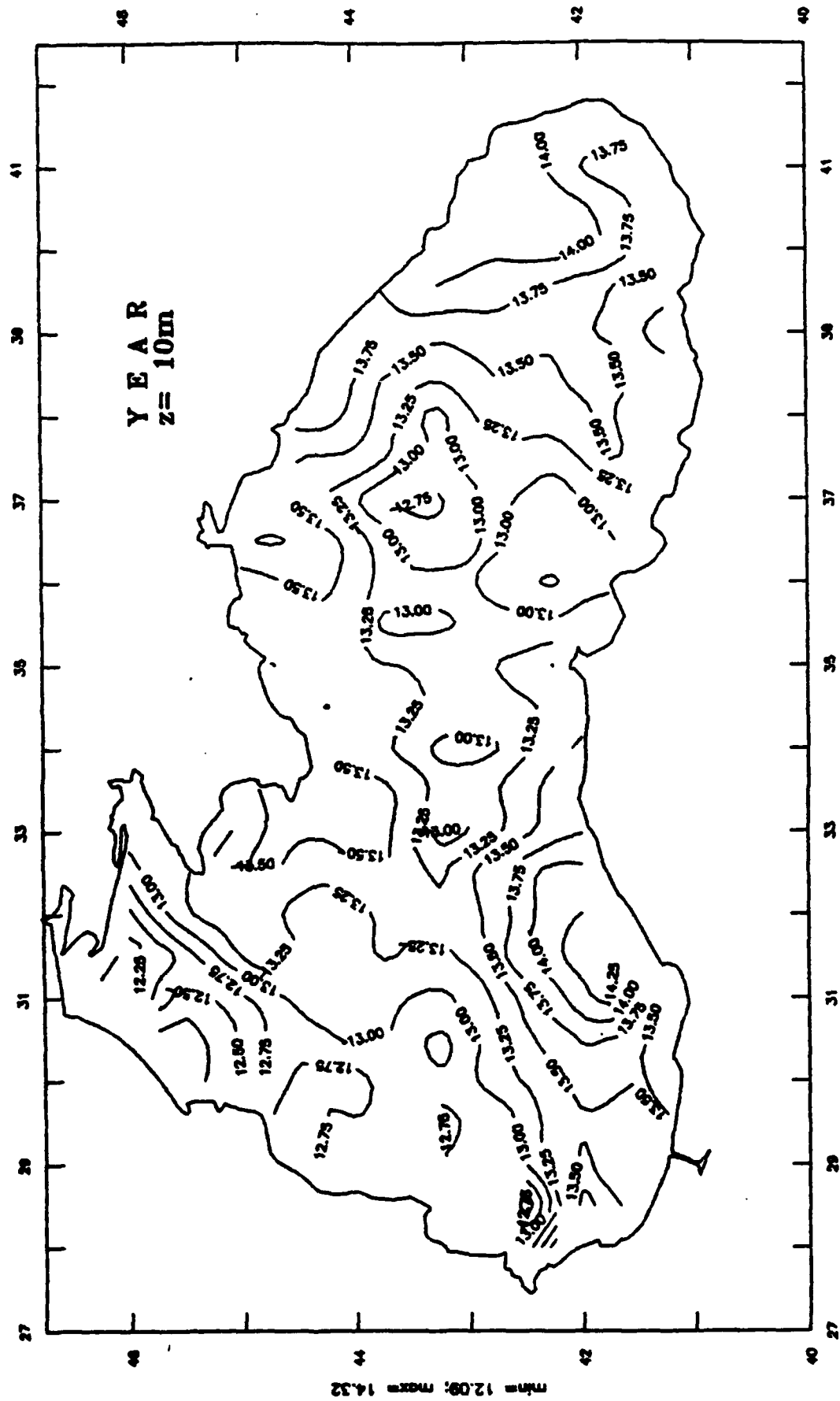
The Black Sea Climate Salinity



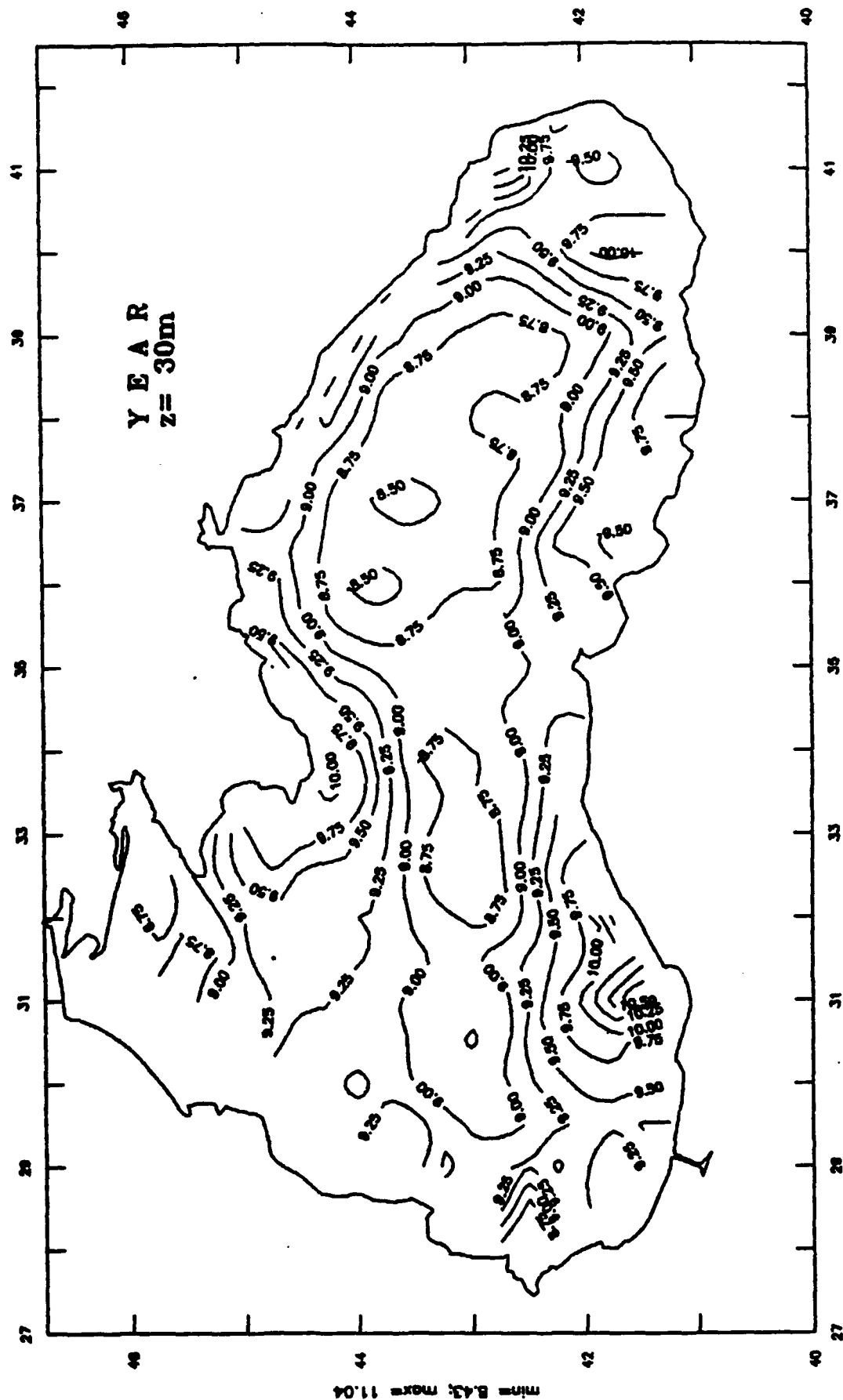
The Black Sea Climate Temperature



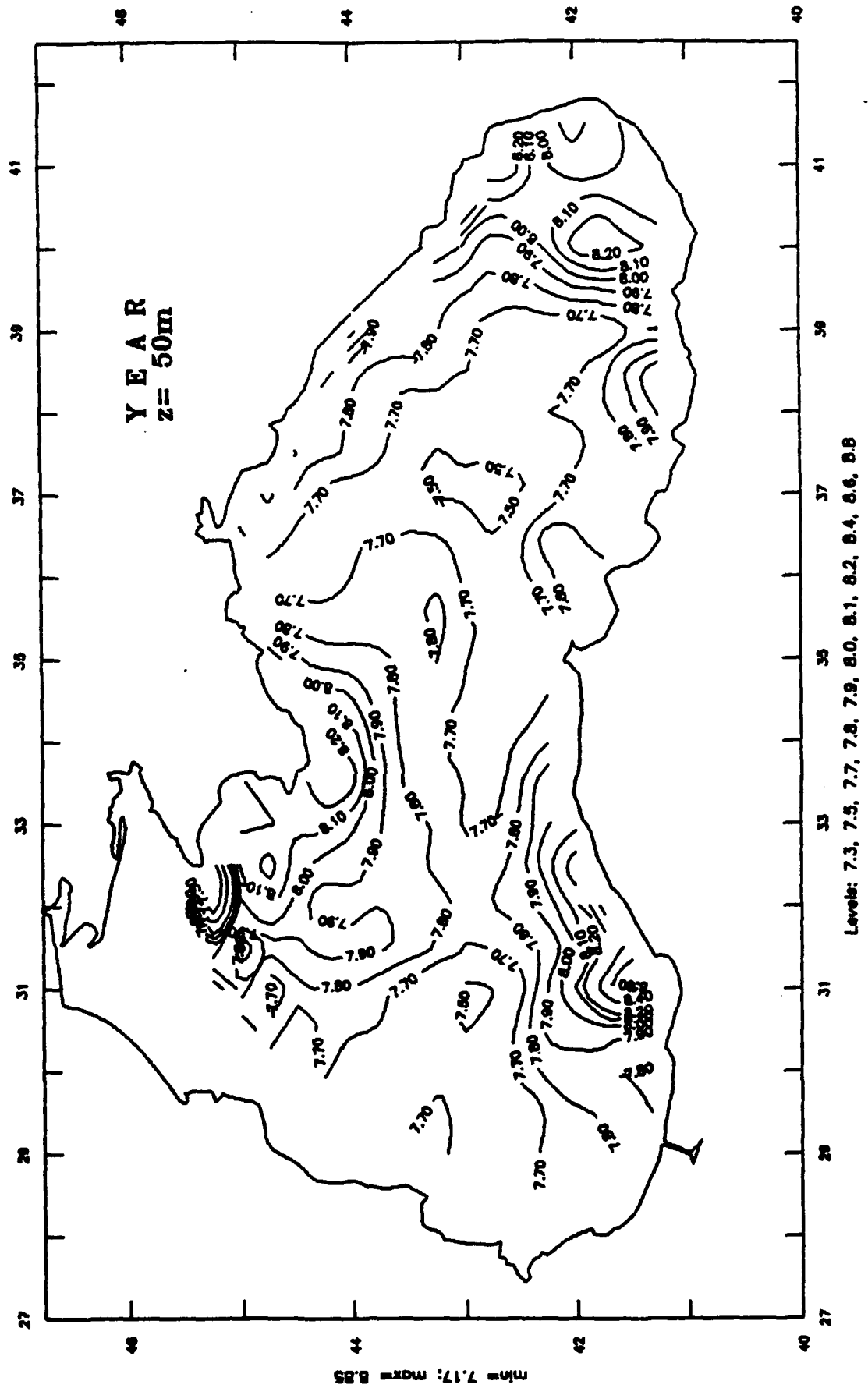
The Black Sea Climate Temperature



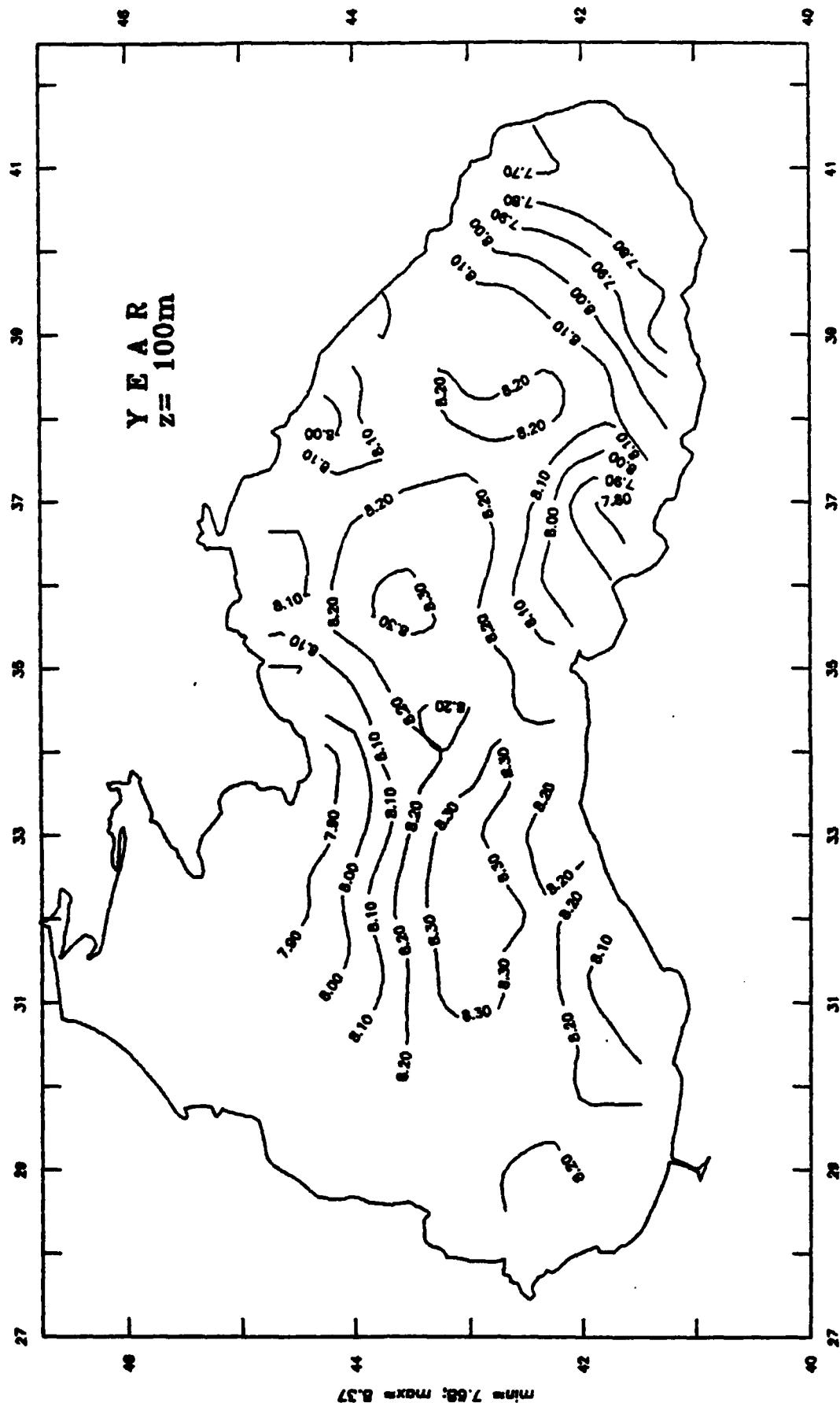
The Black Sea Climate Temperature



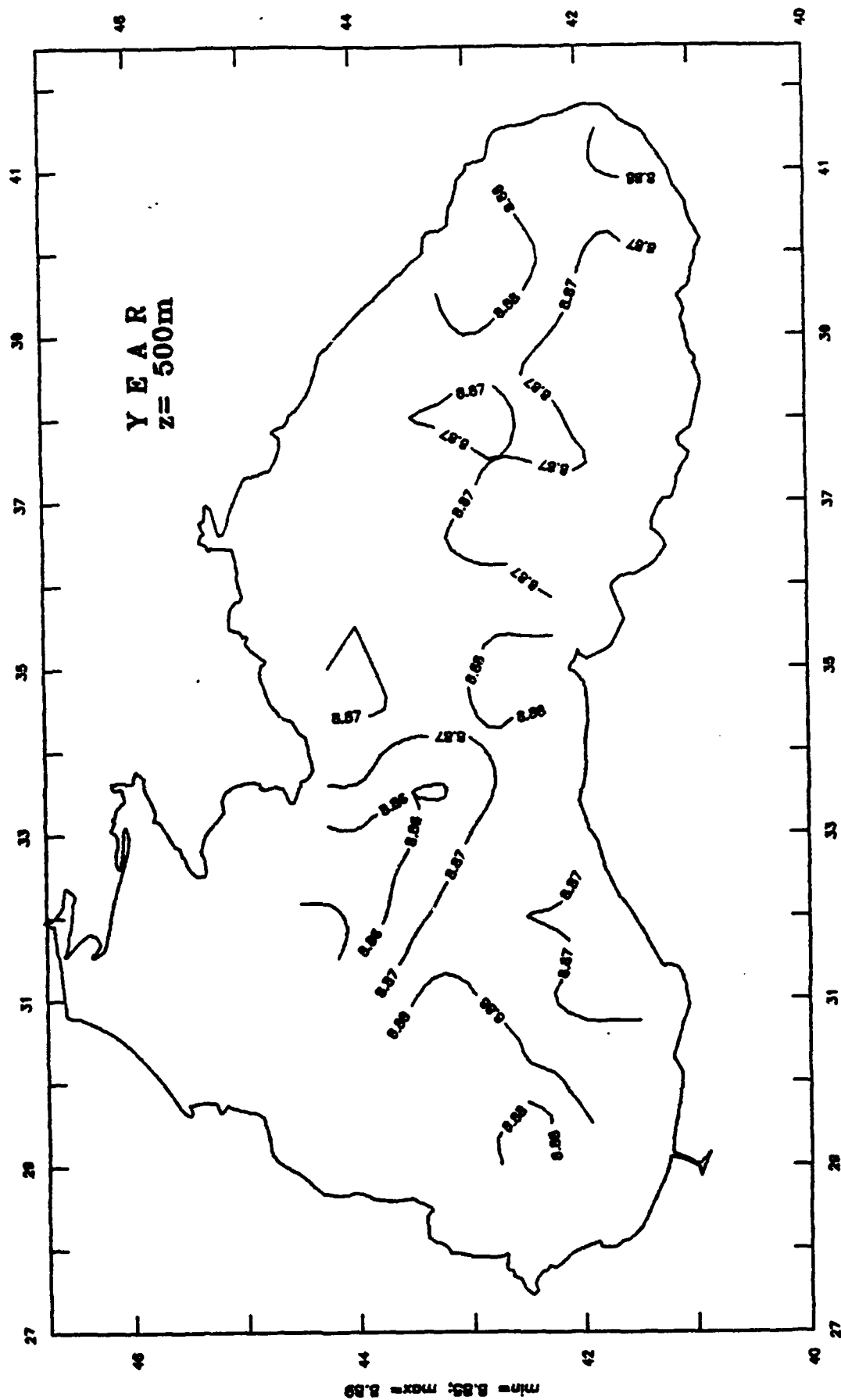
The Black Sea Climate Temperature



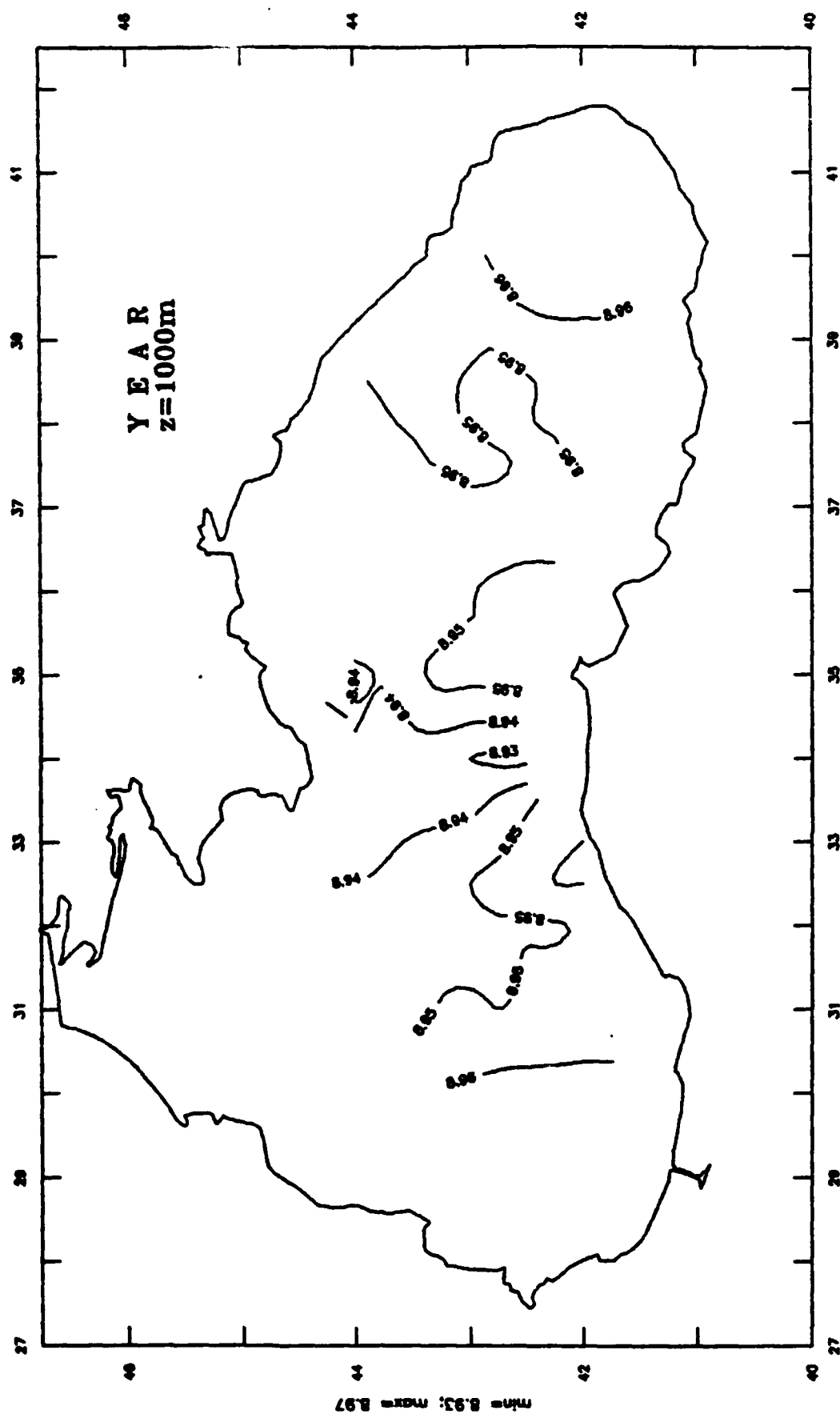
The Black Sea Climate Temperature



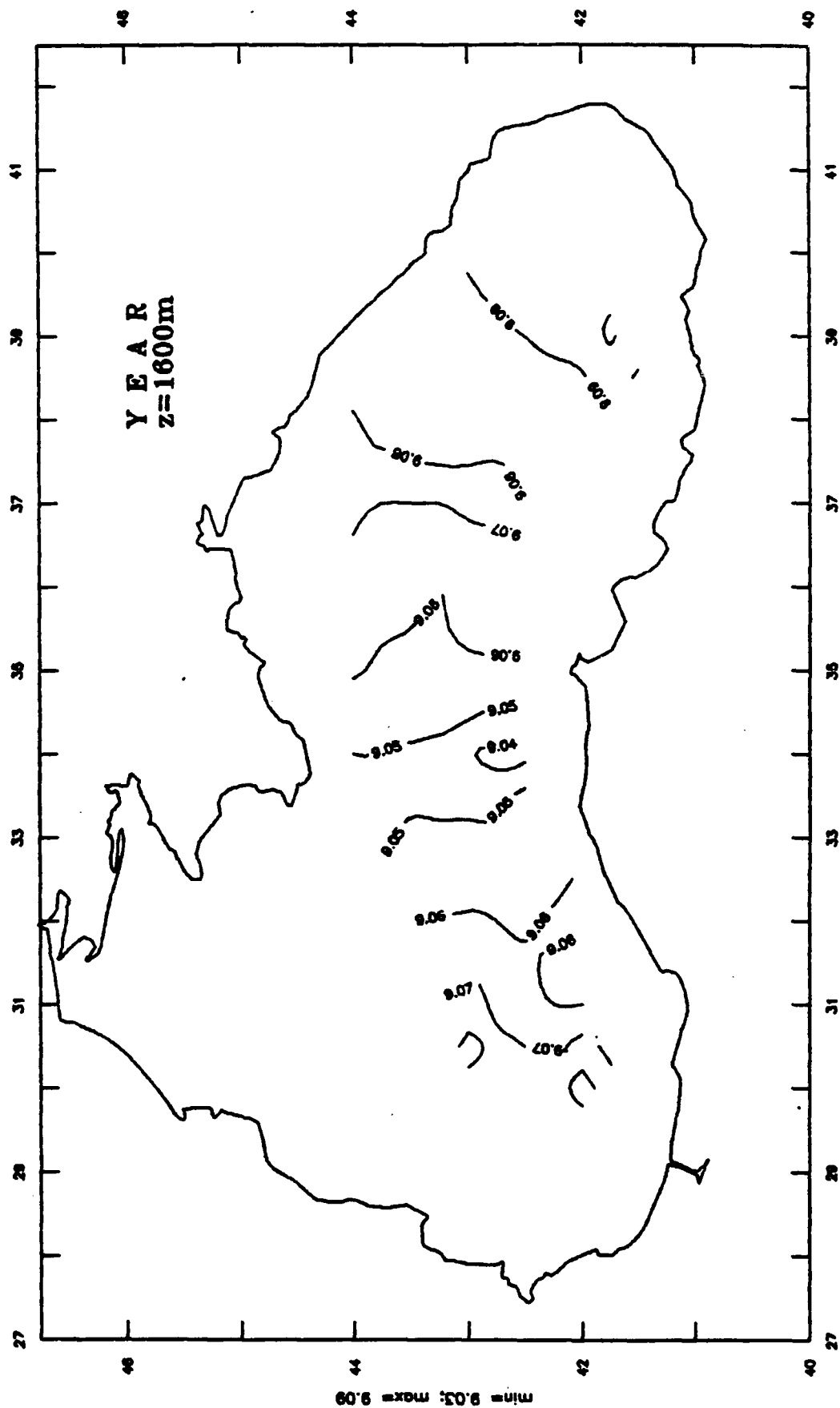
The Black Sea Climate Temperature



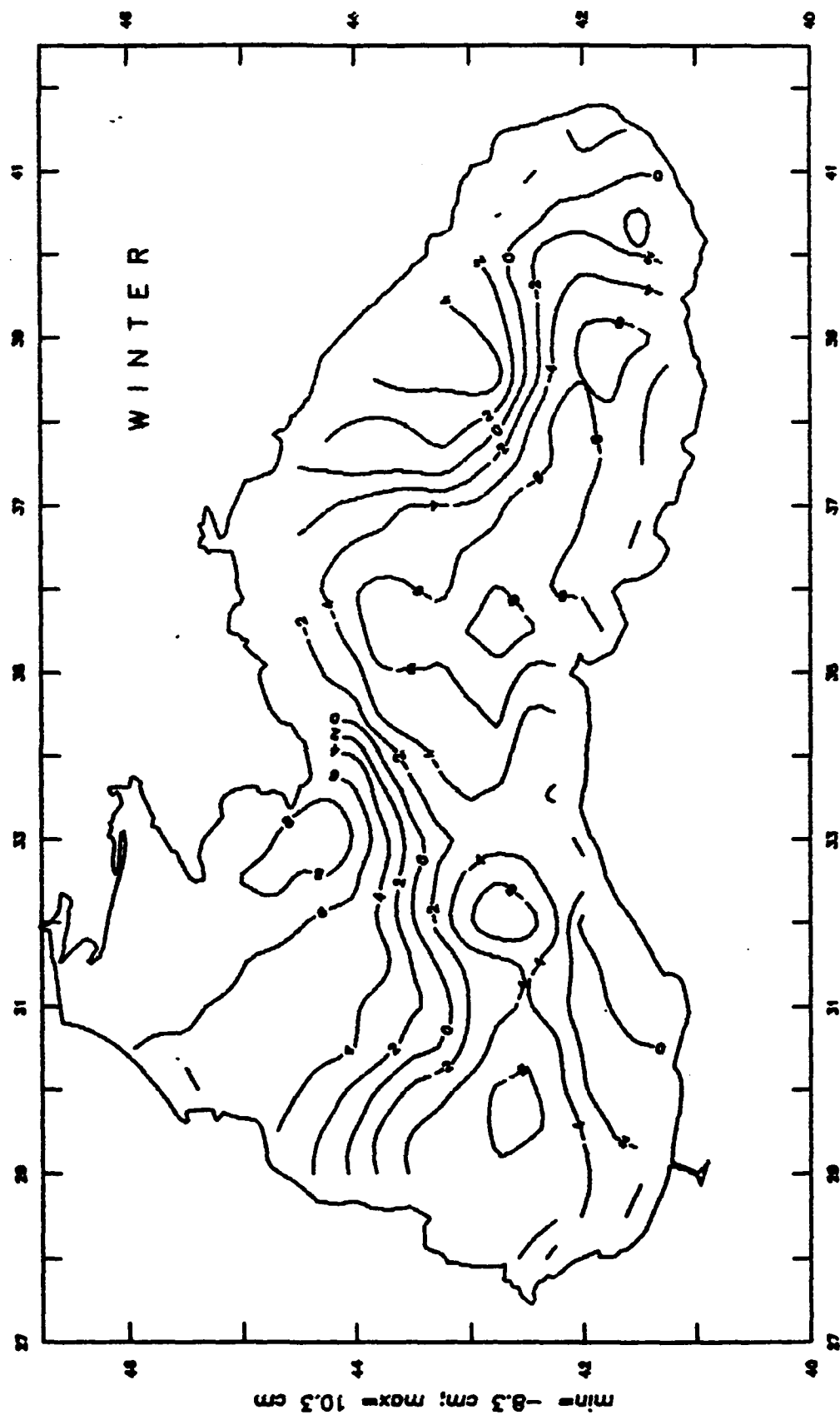
The Black Sea Climate Temperature



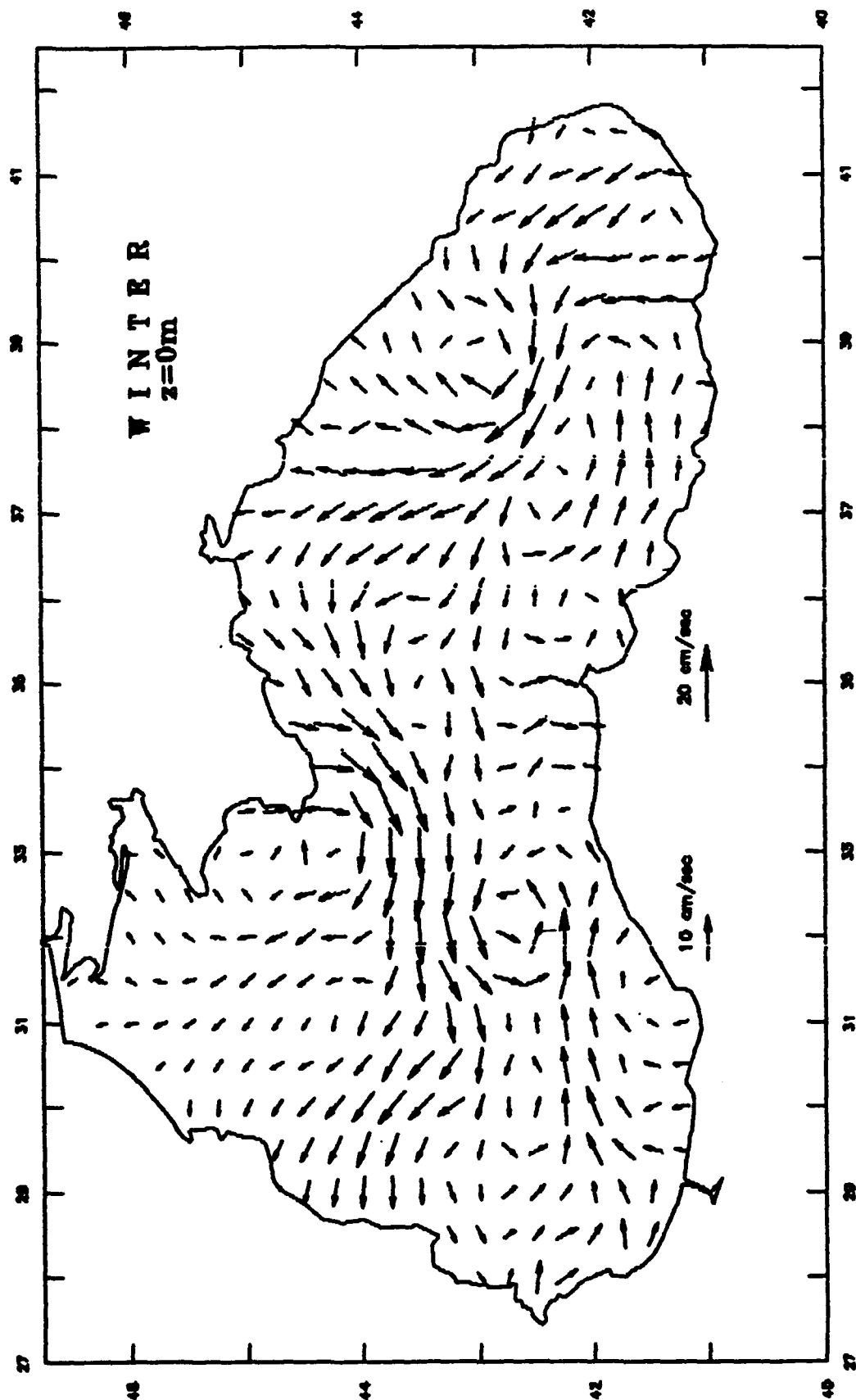
The Black Sea Climate Temperature



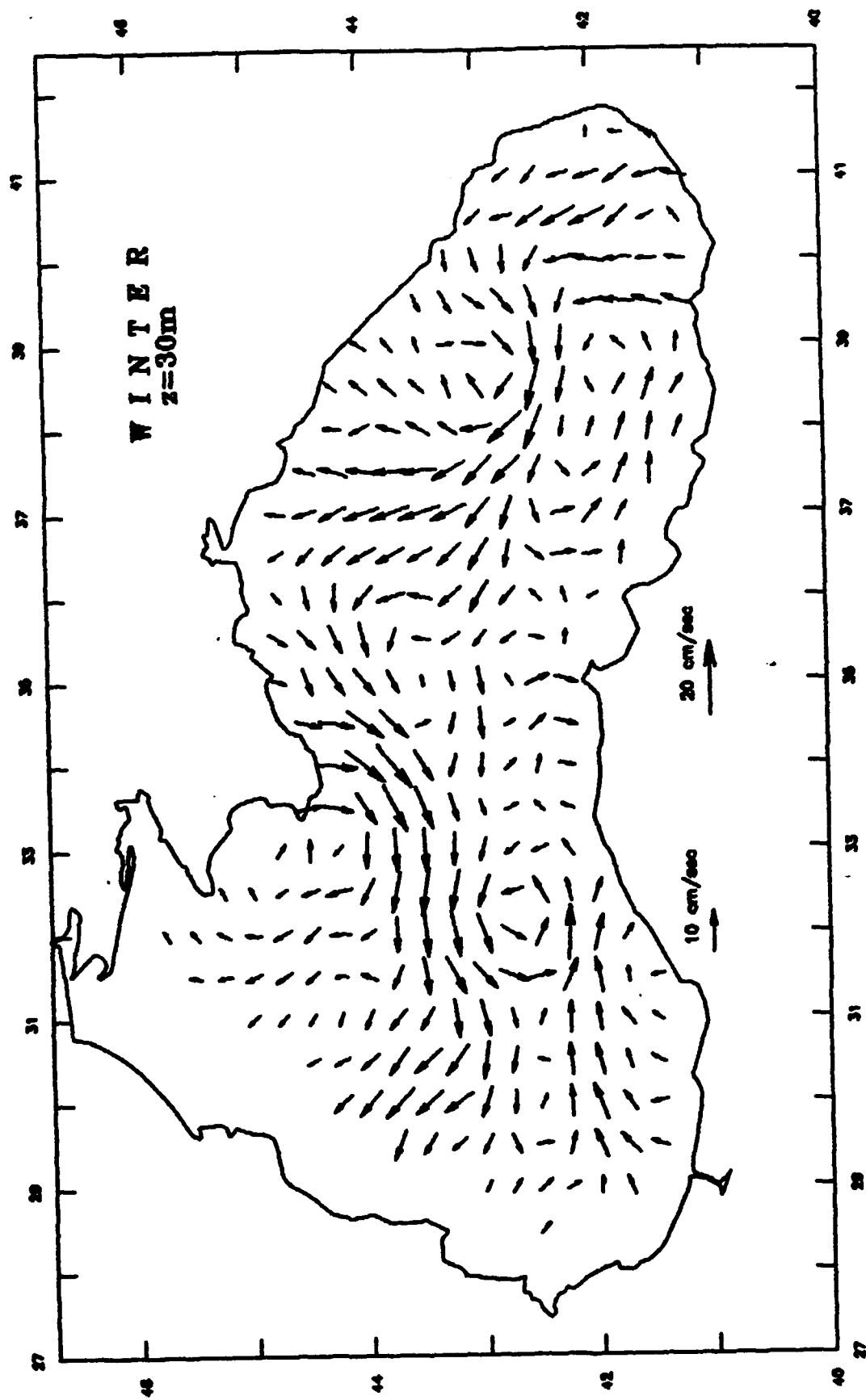
The Black Sea Climate Surface



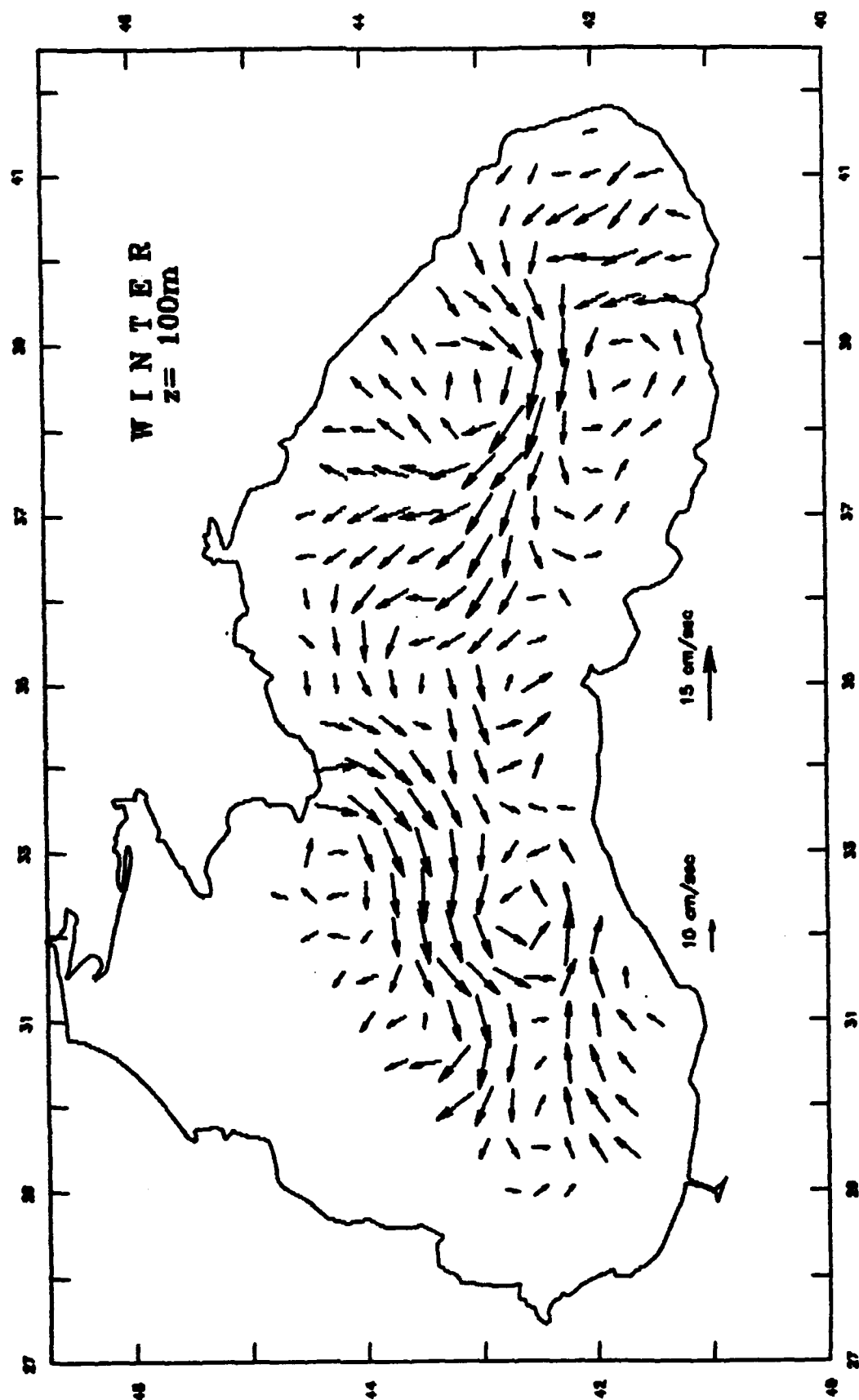
The Black Sea Climate Velocity



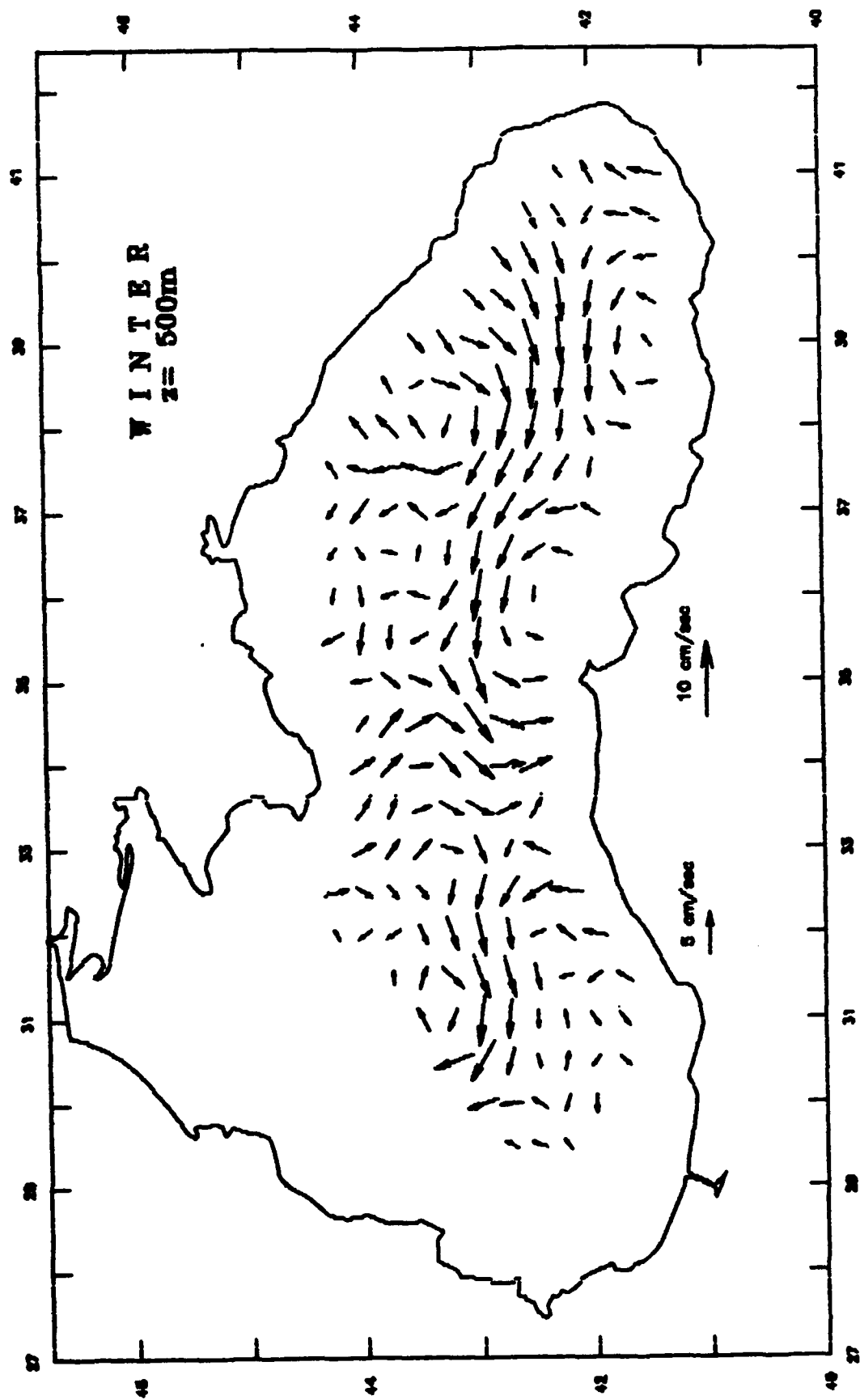
The Black Sea Climate Velocity



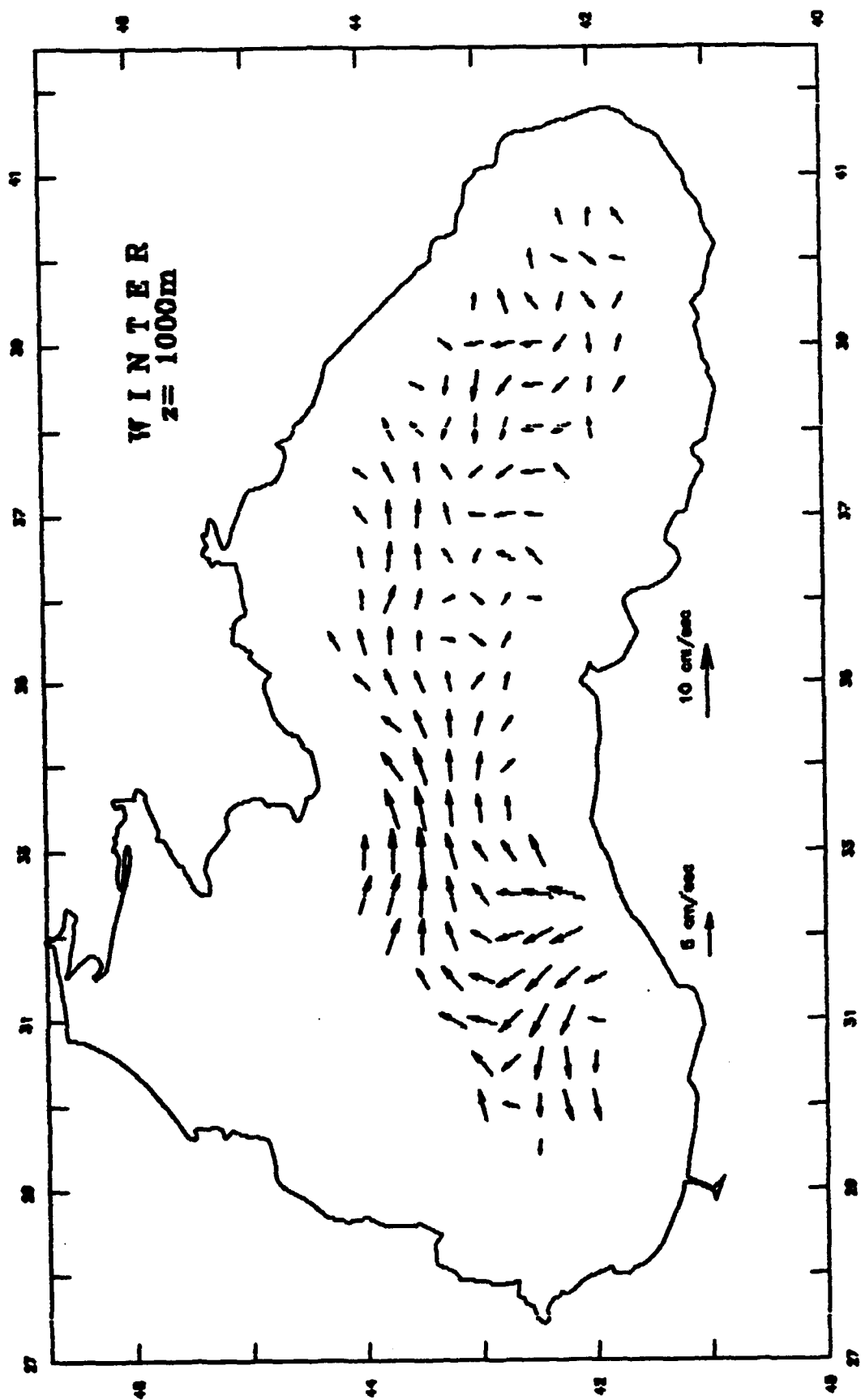
The Black Sea Climate Velocity



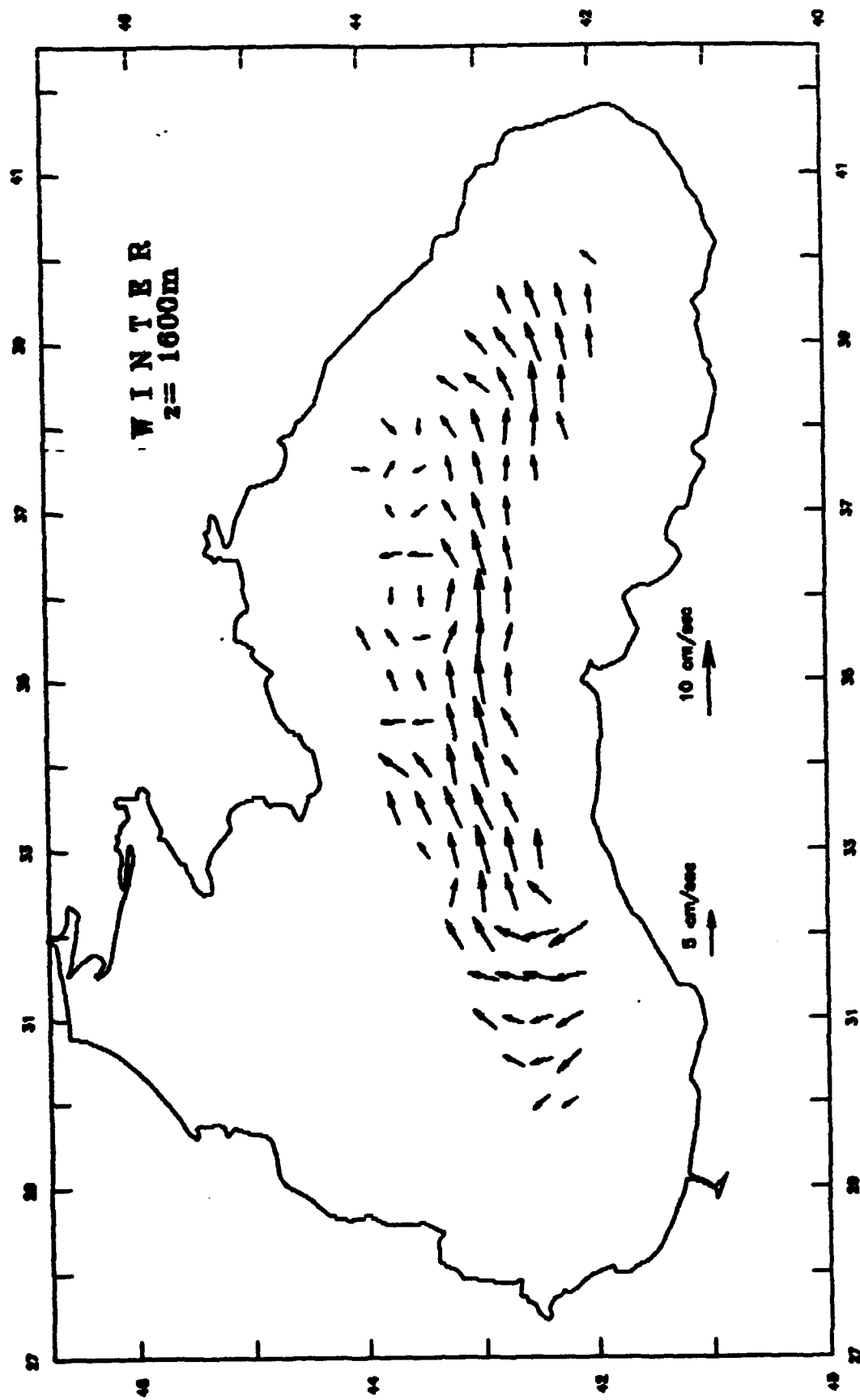
The Black Sea Climate Velocity



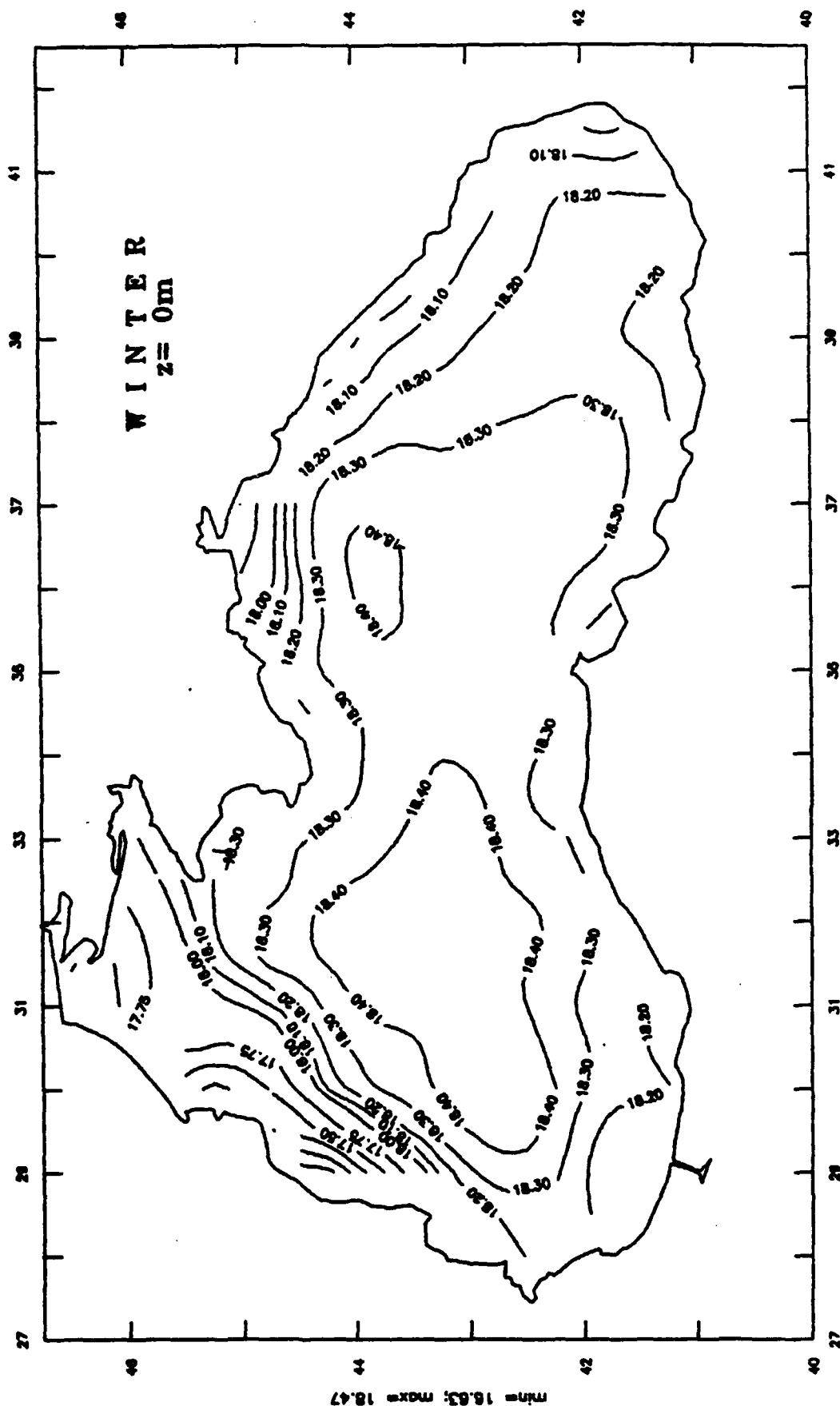
The Black Sea Climate Velocity



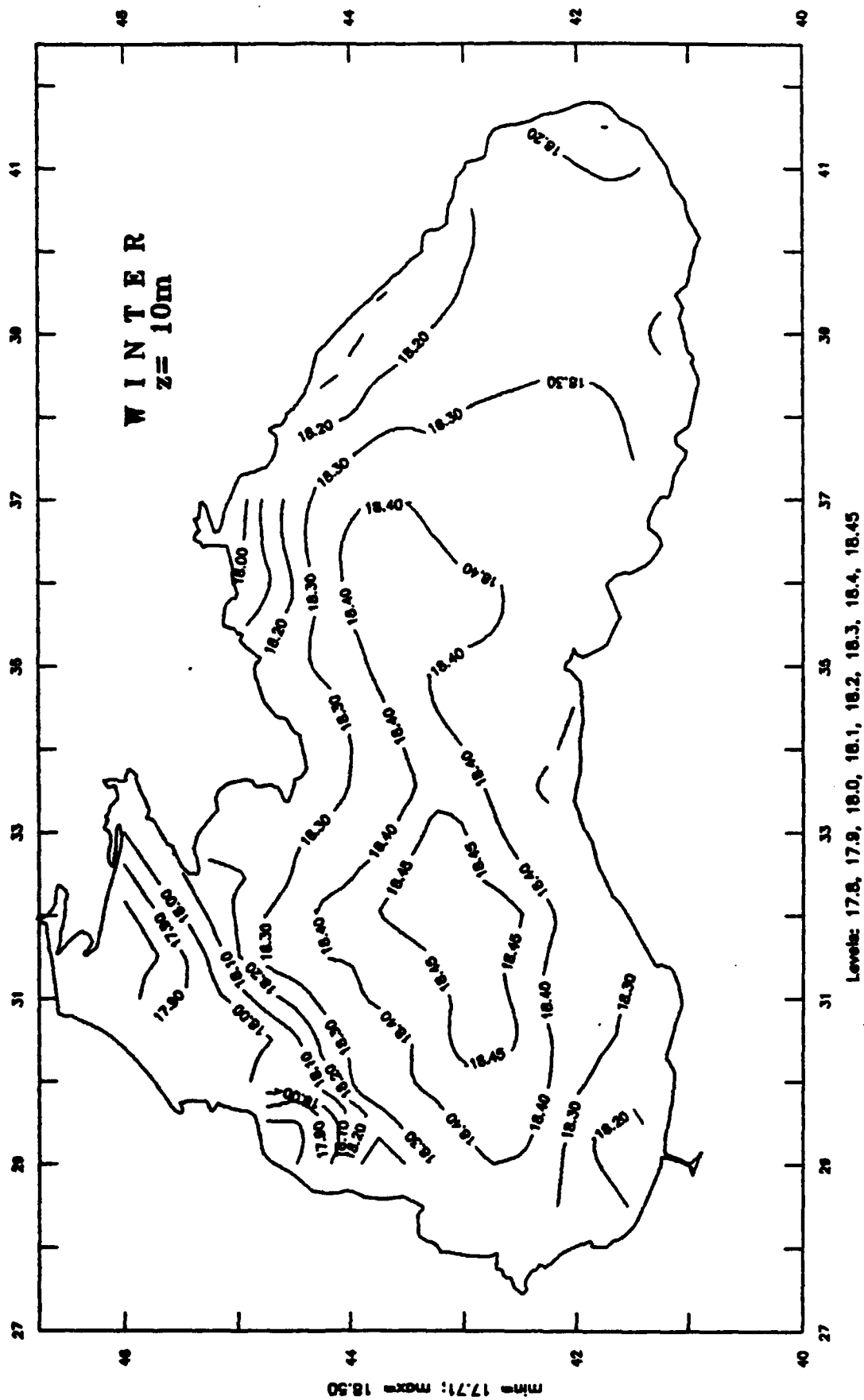
The Black Sea Climate Velocity



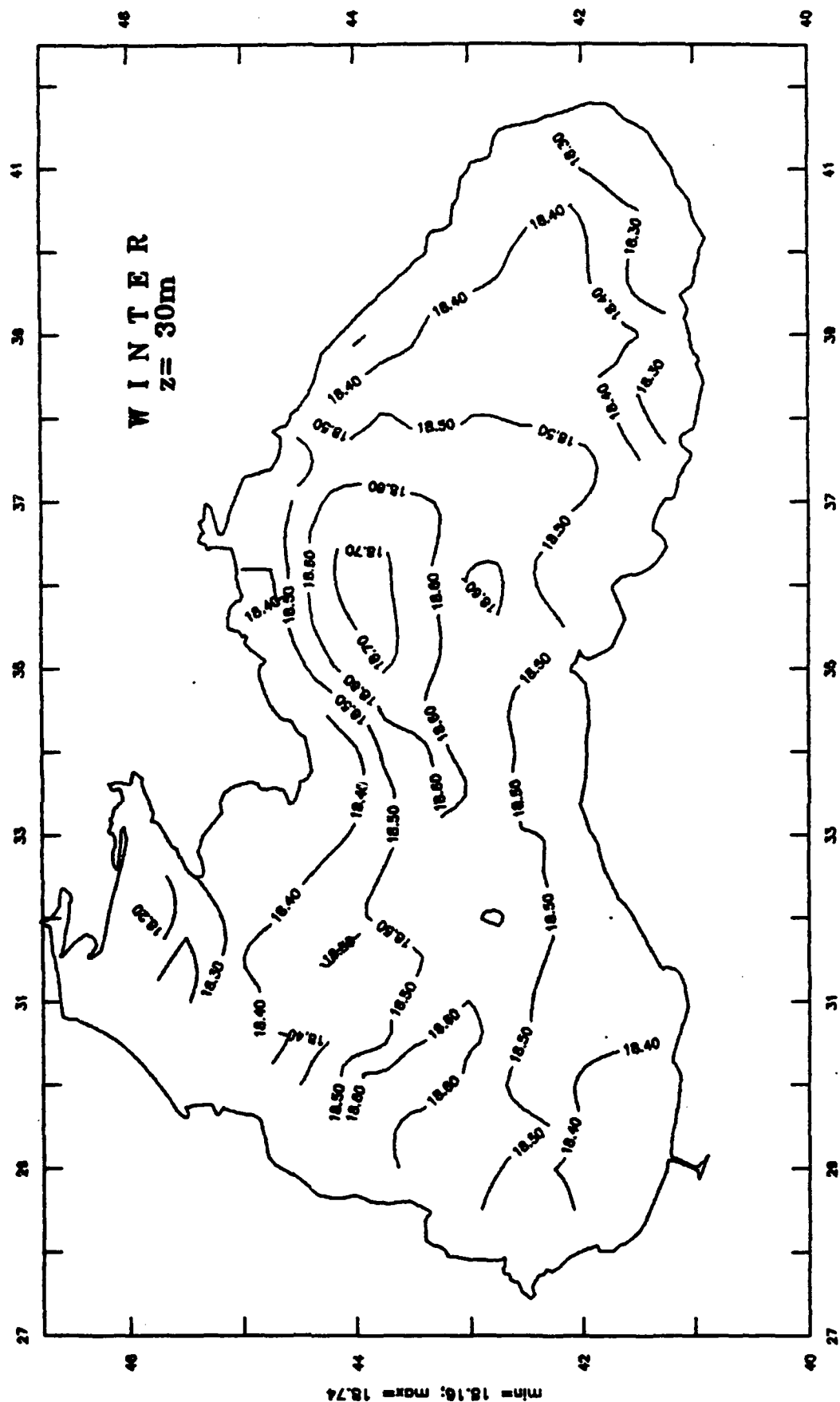
The Black Sea Climate Salinity



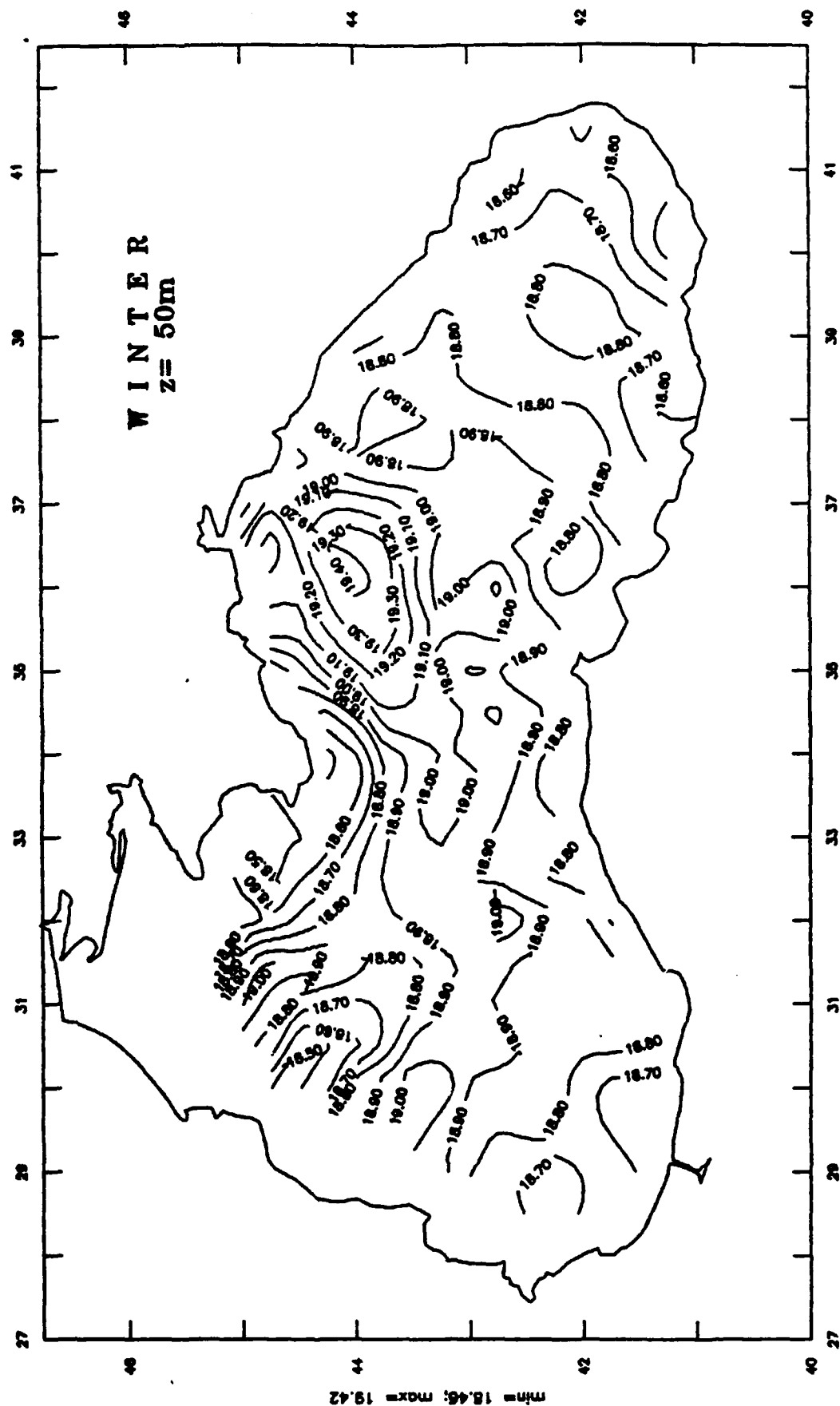
The Black Sea Climate Salinity



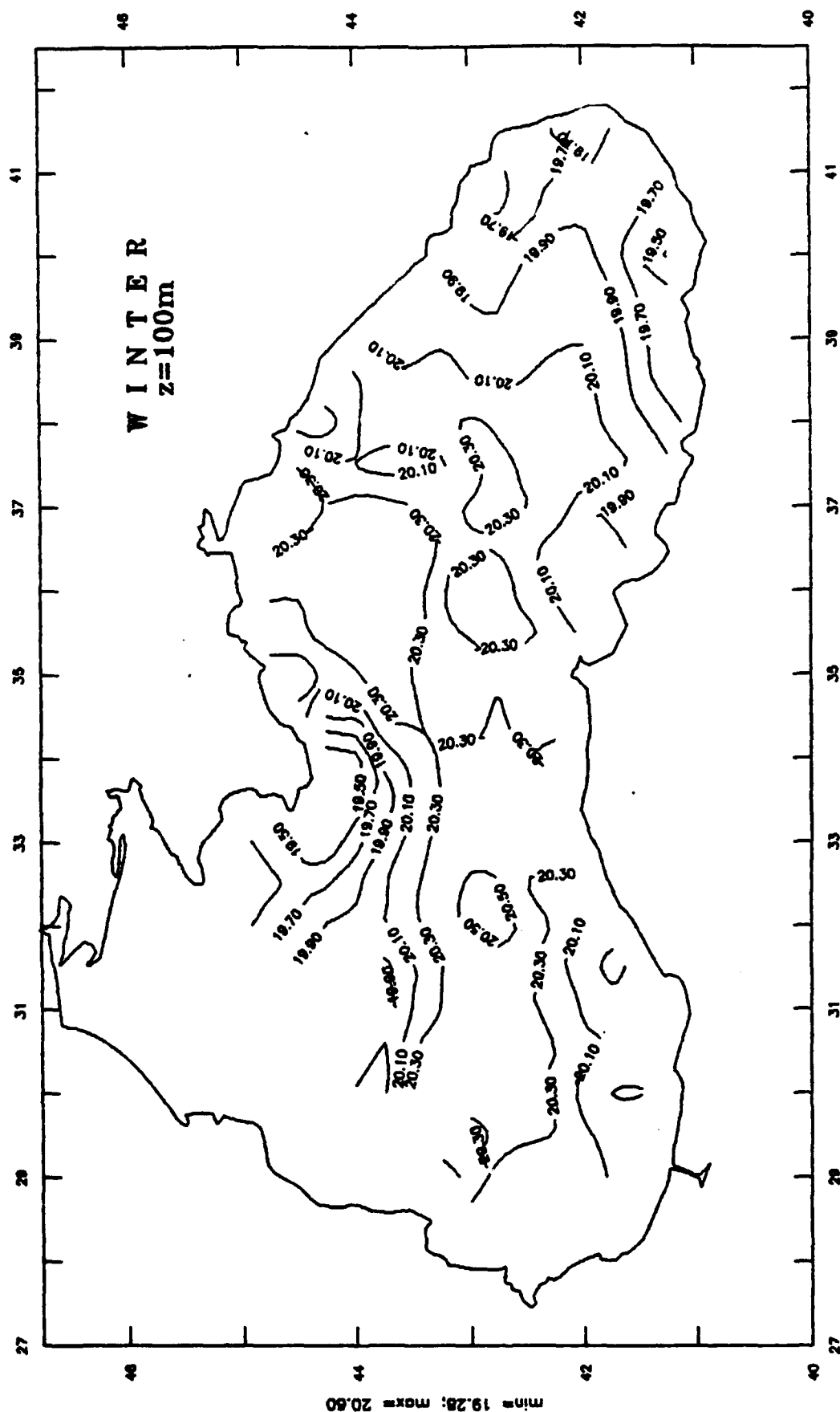
The Black Sea Climate Salinity



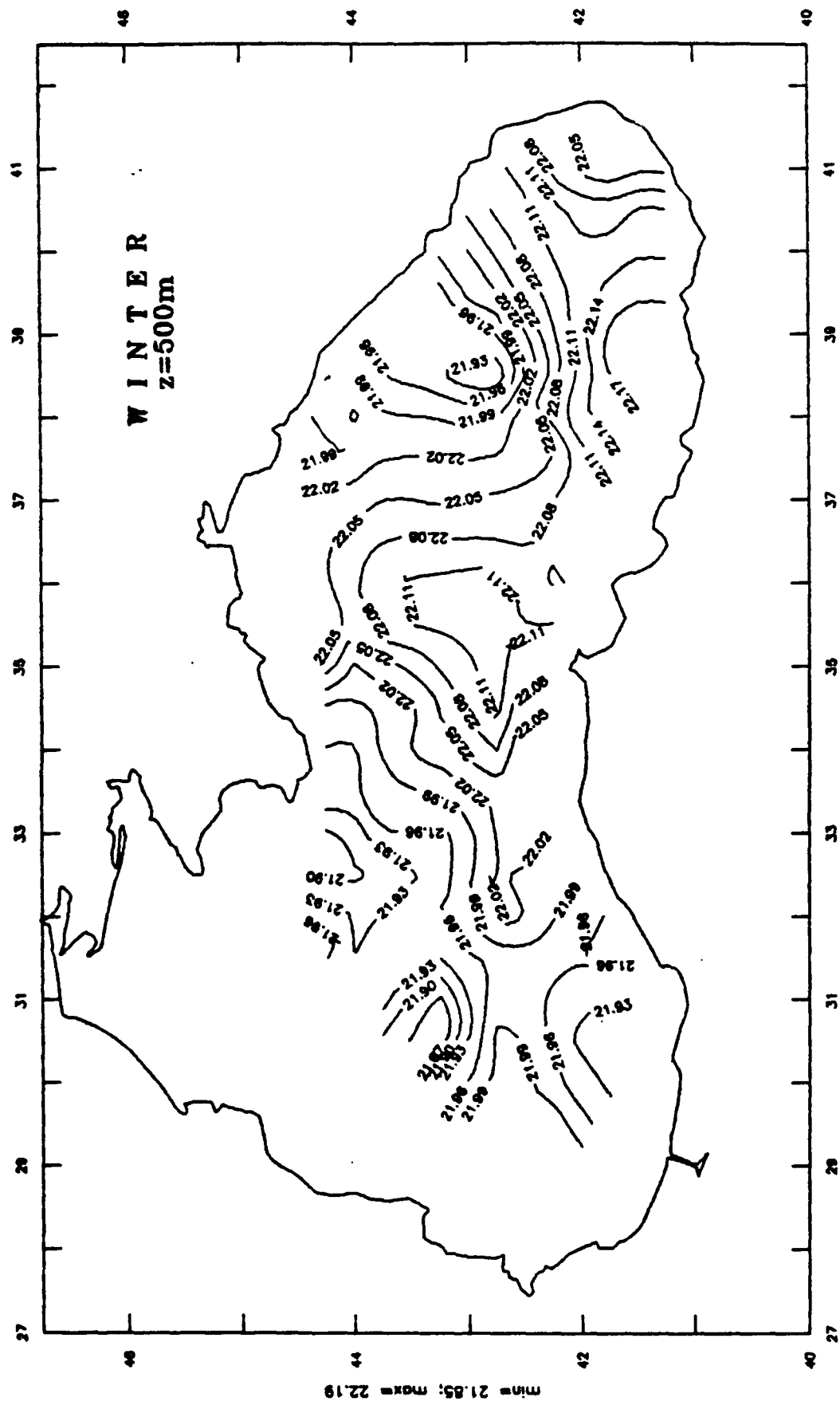
The Black Sea Climate Salinity



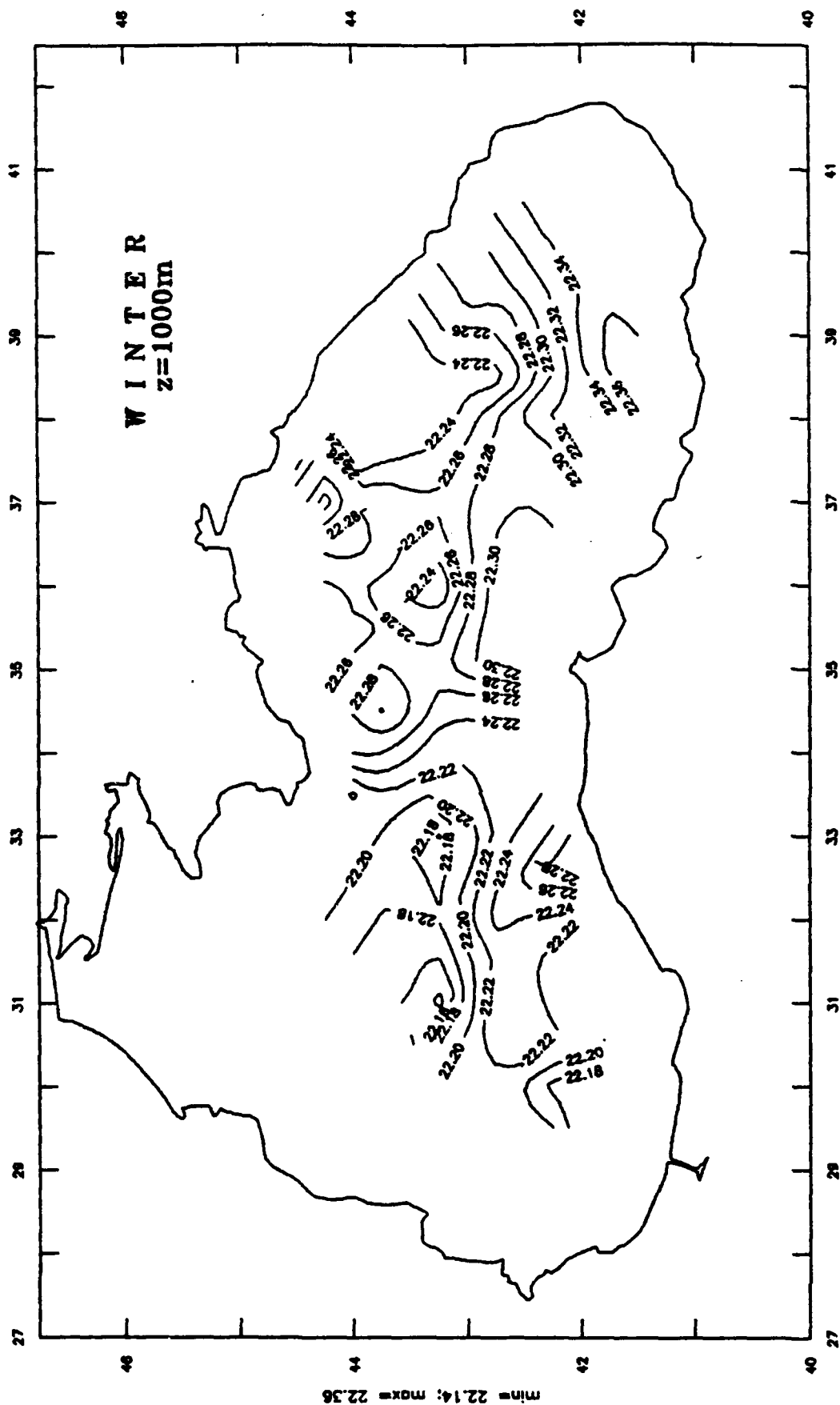
The Black Sea Climate Salinity



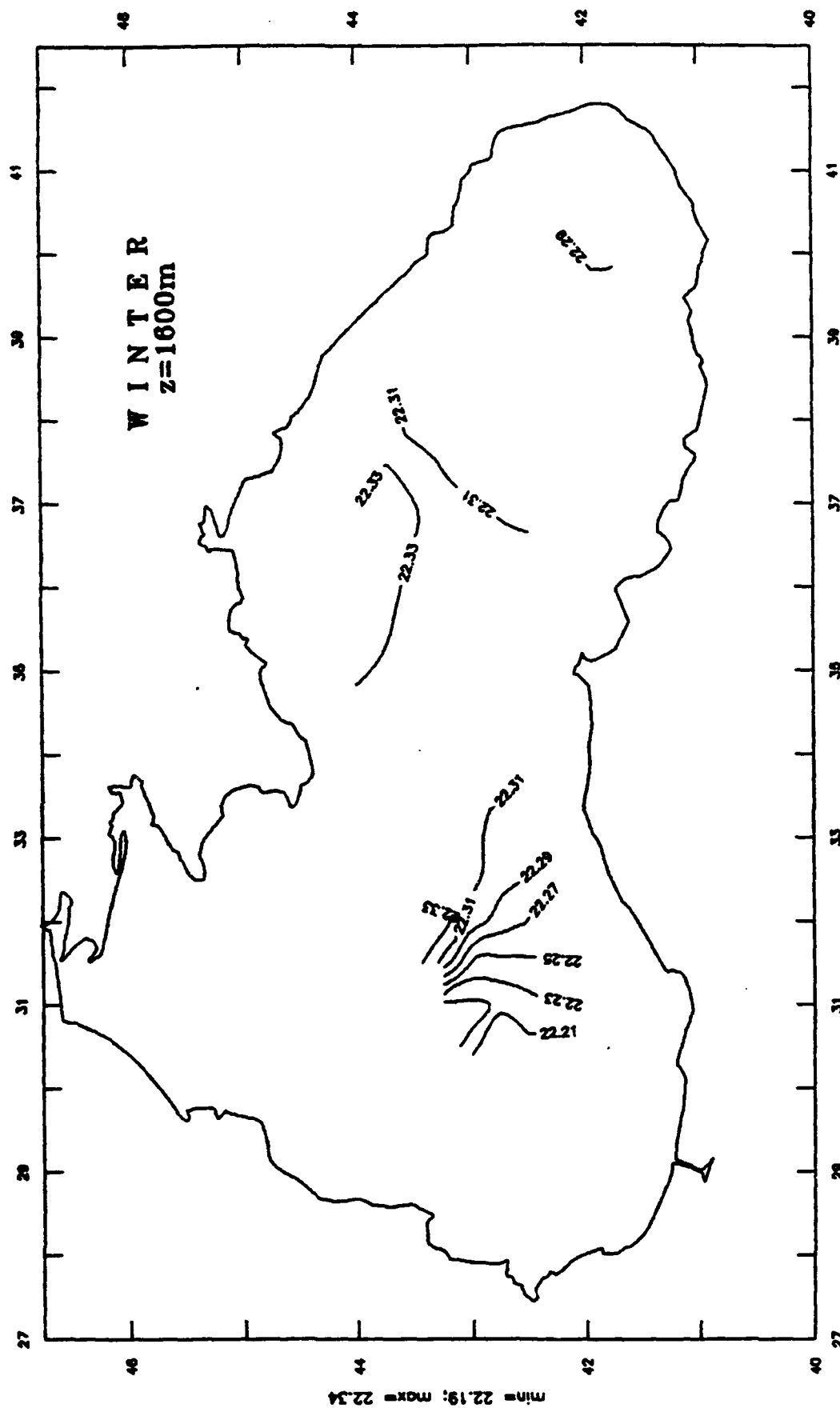
The Black Sea Climate Salinity



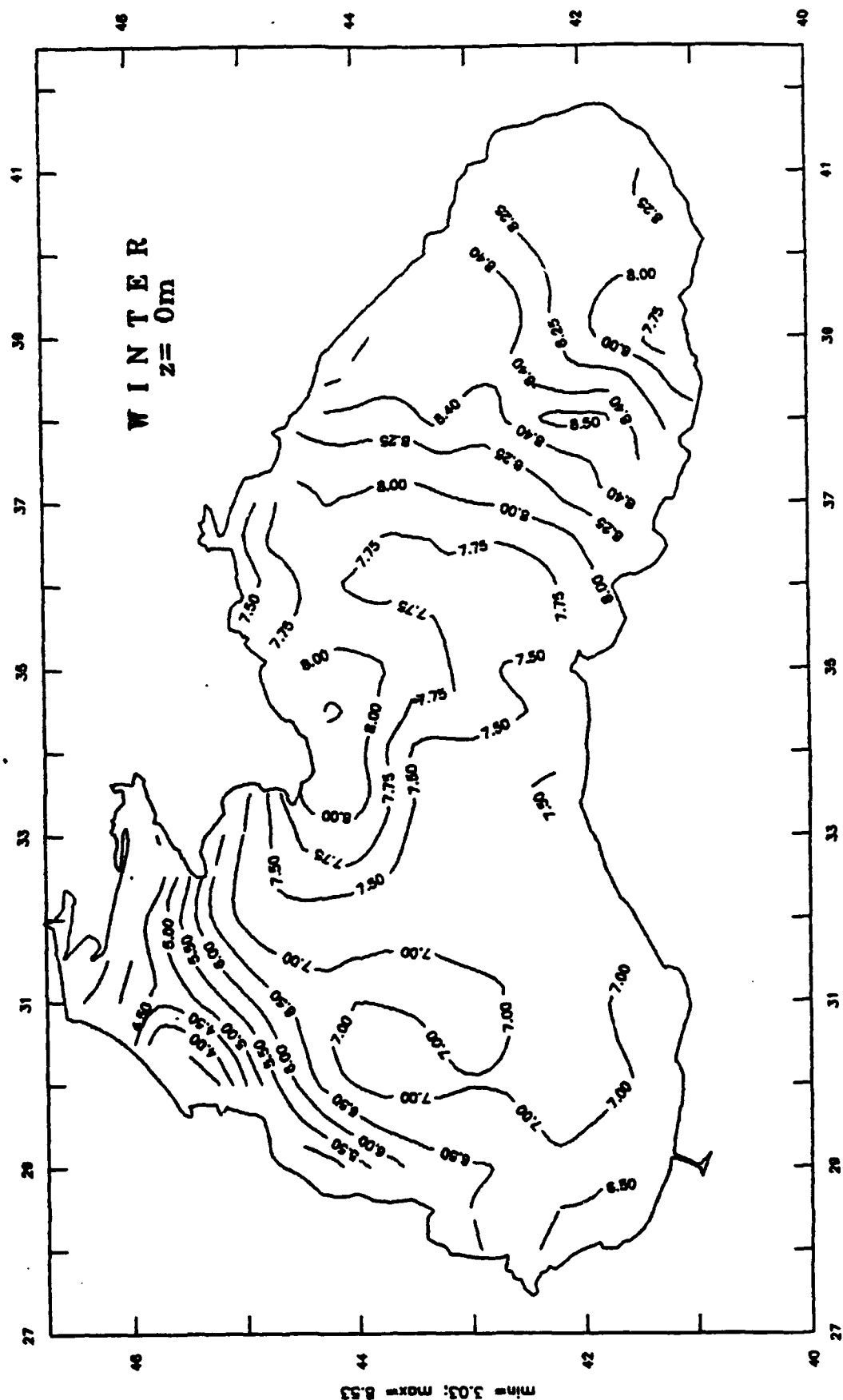
The Black Sea Climate Salinity



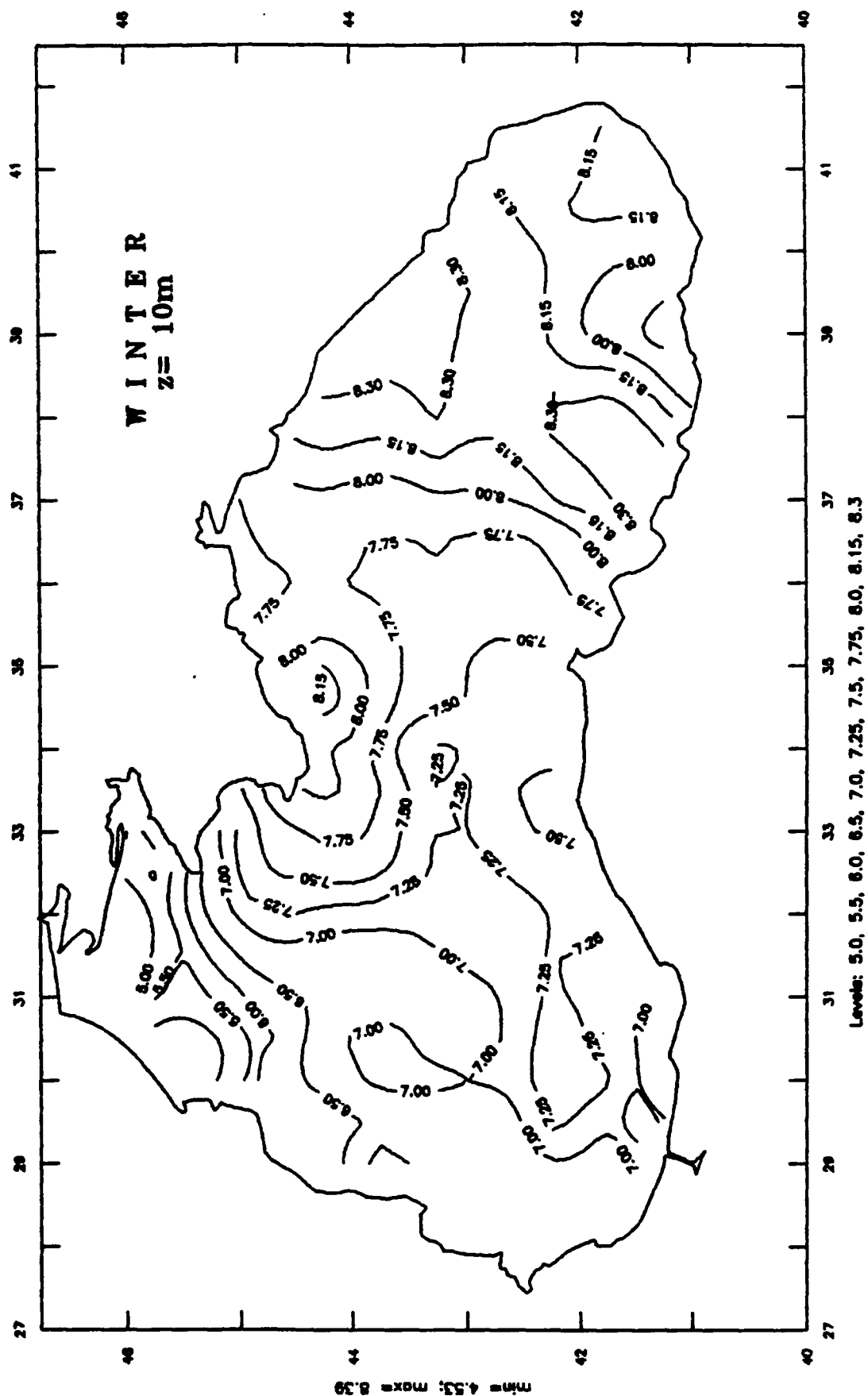
The Black Sea Climate Salinity



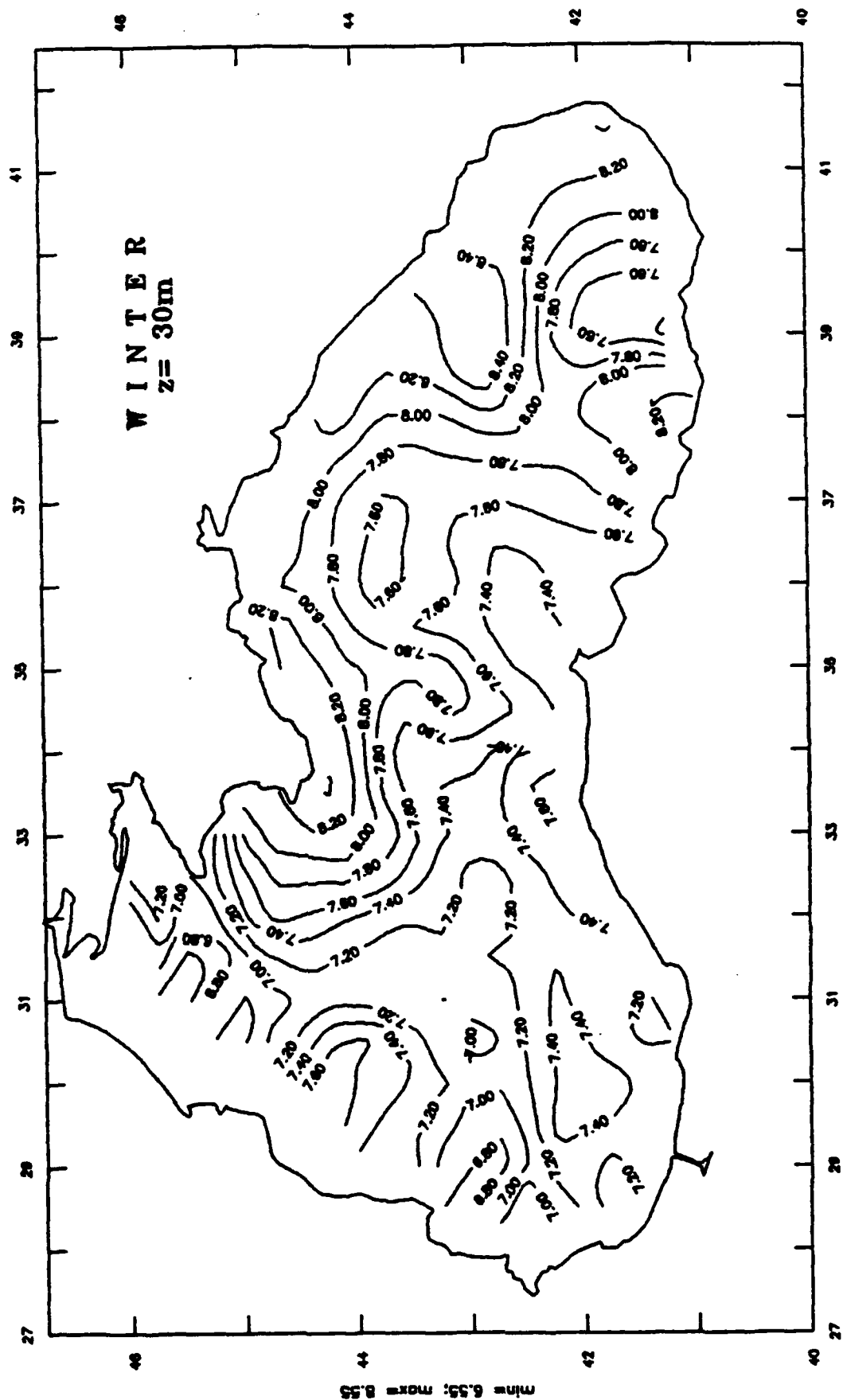
The Black Sea Climate Temperature



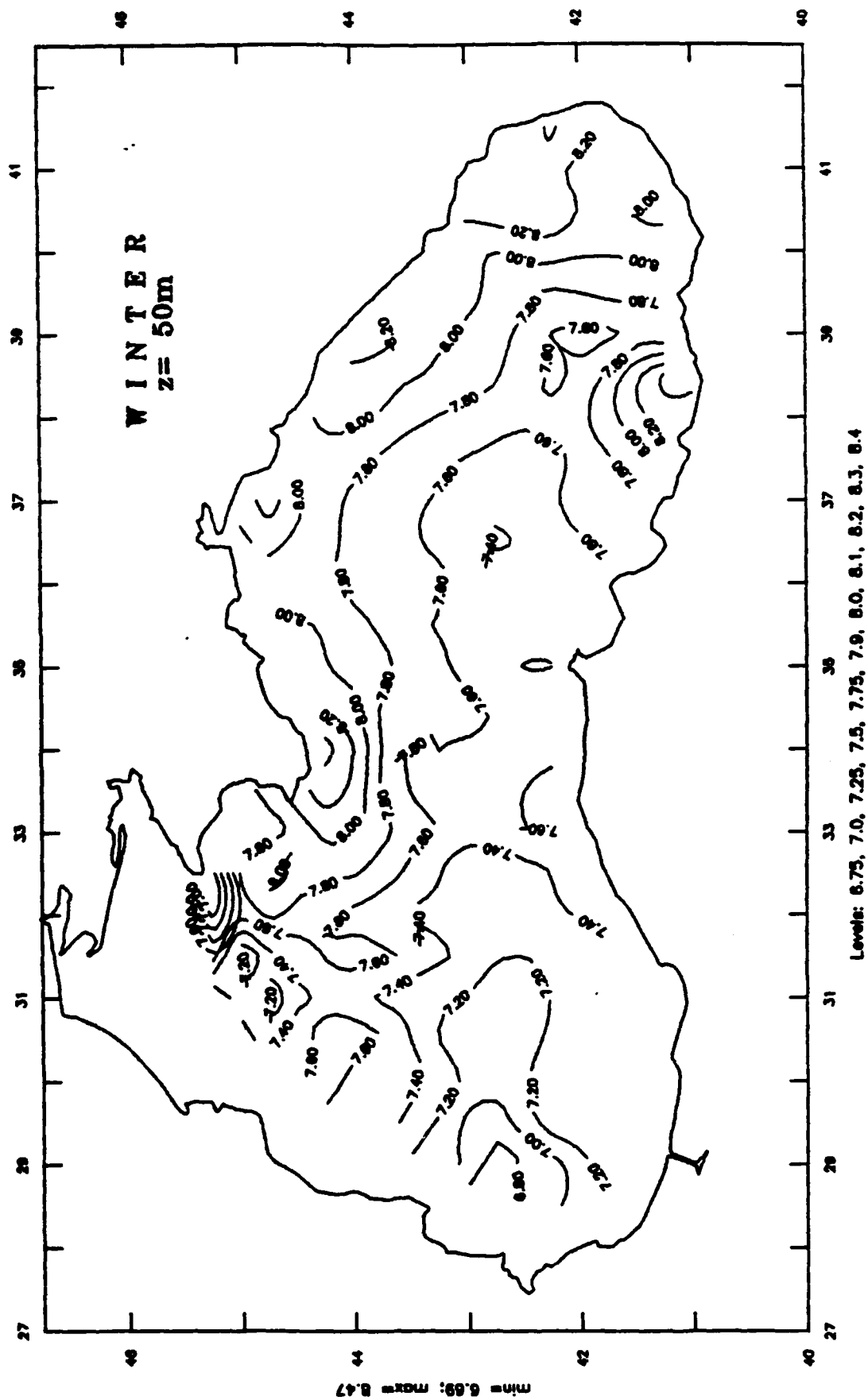
The Black Sea Climate Temperature



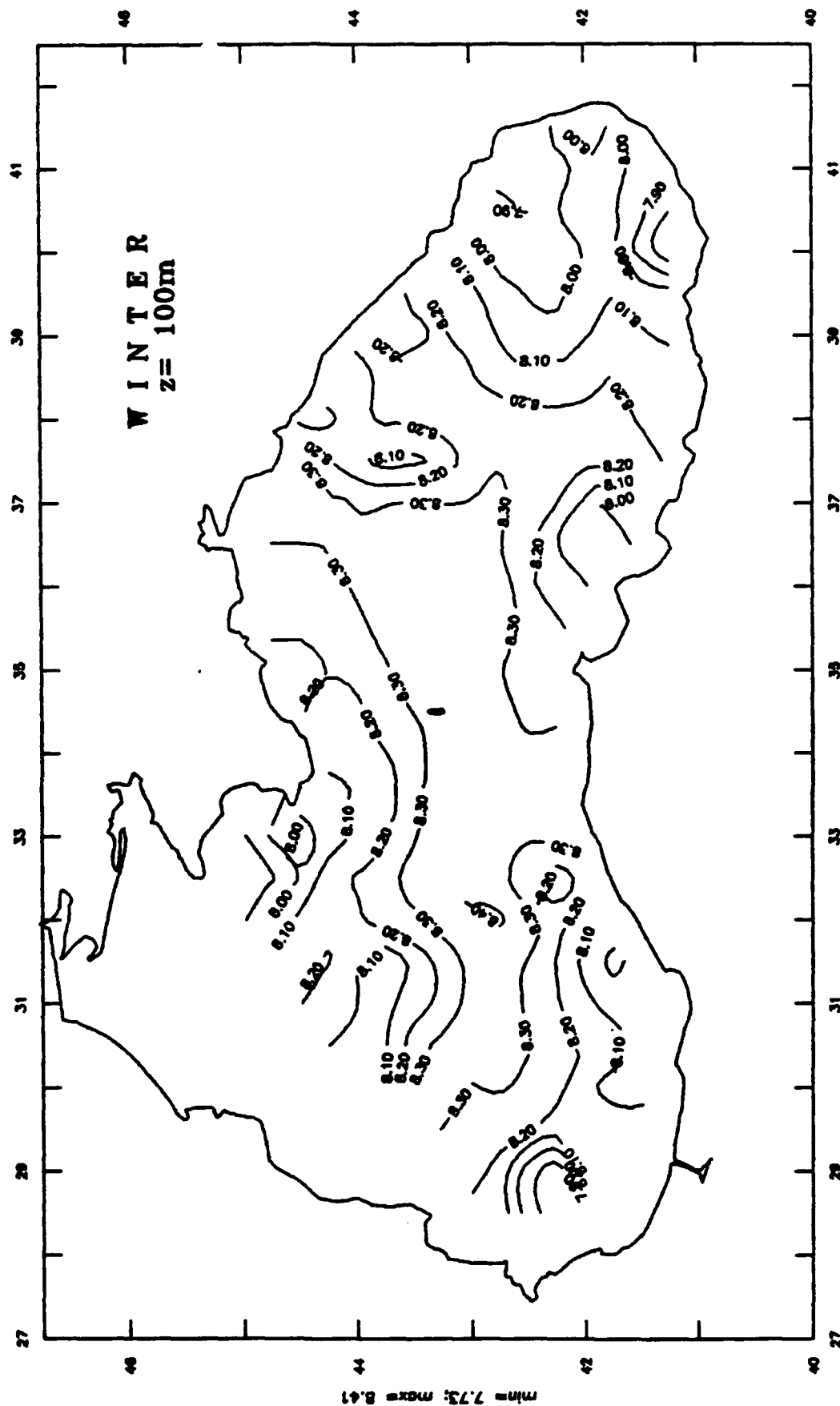
The Black Sea Climate Temperature



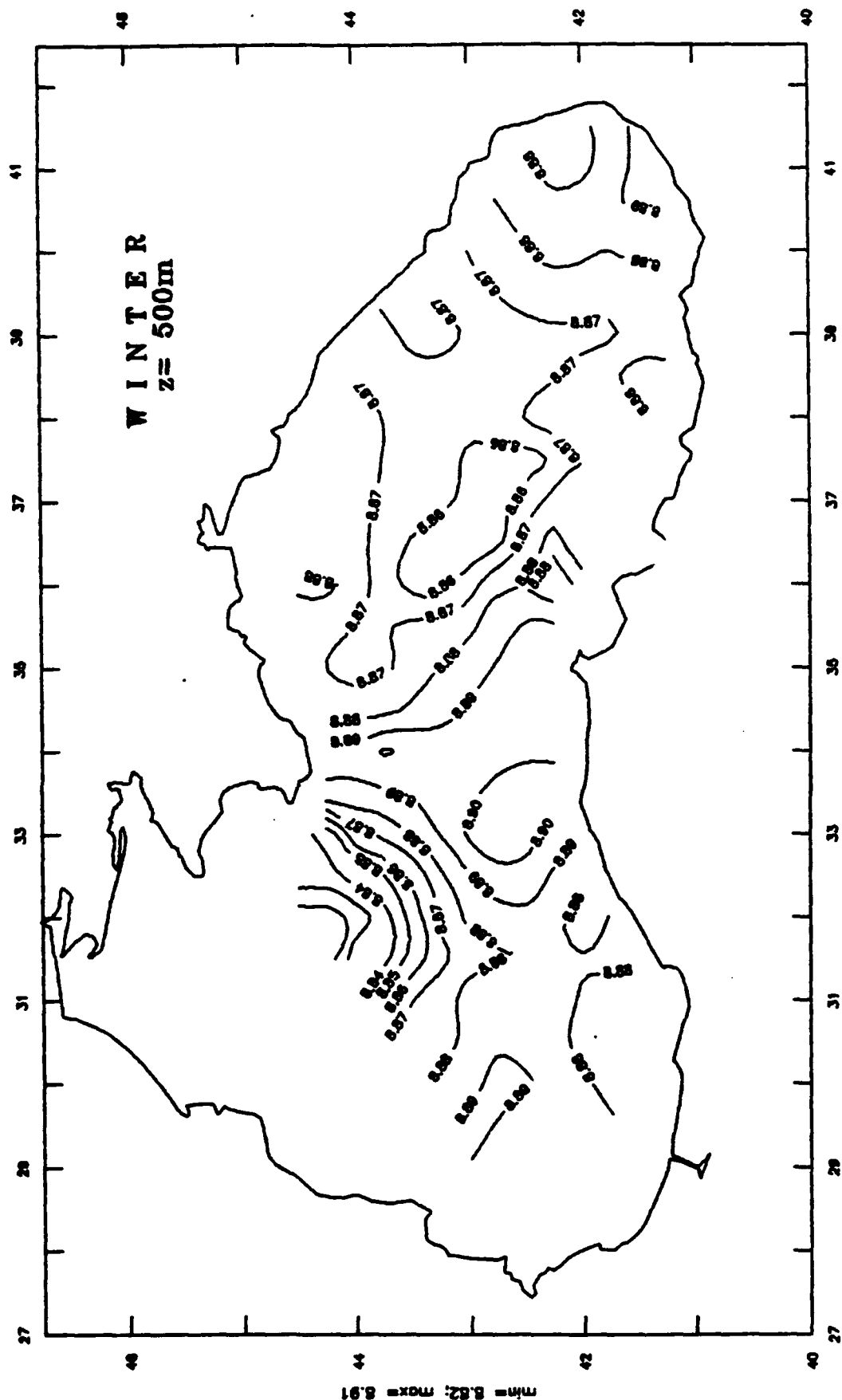
The Black Sea Climate Temperature



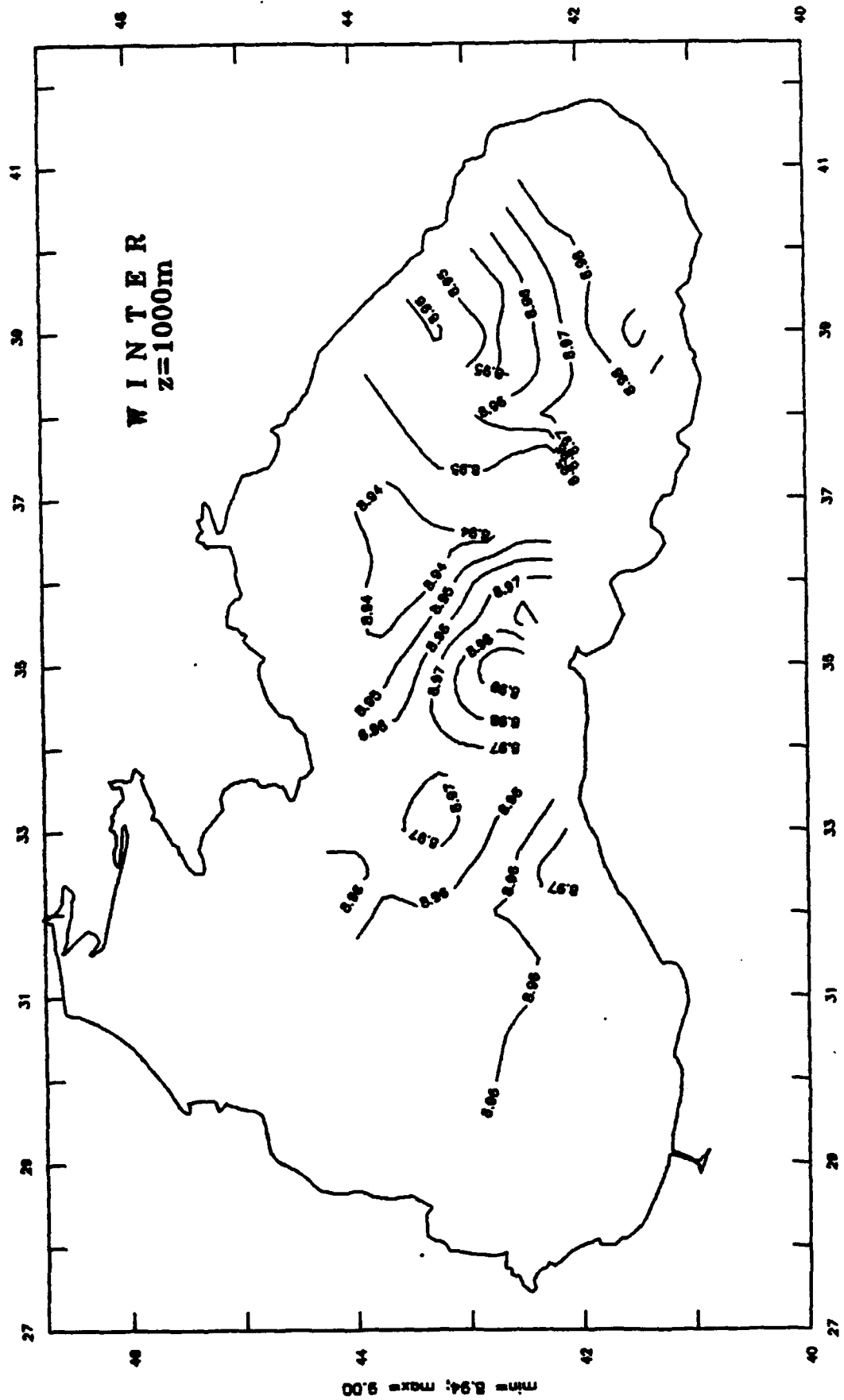
The Black Sea Climate Temperature



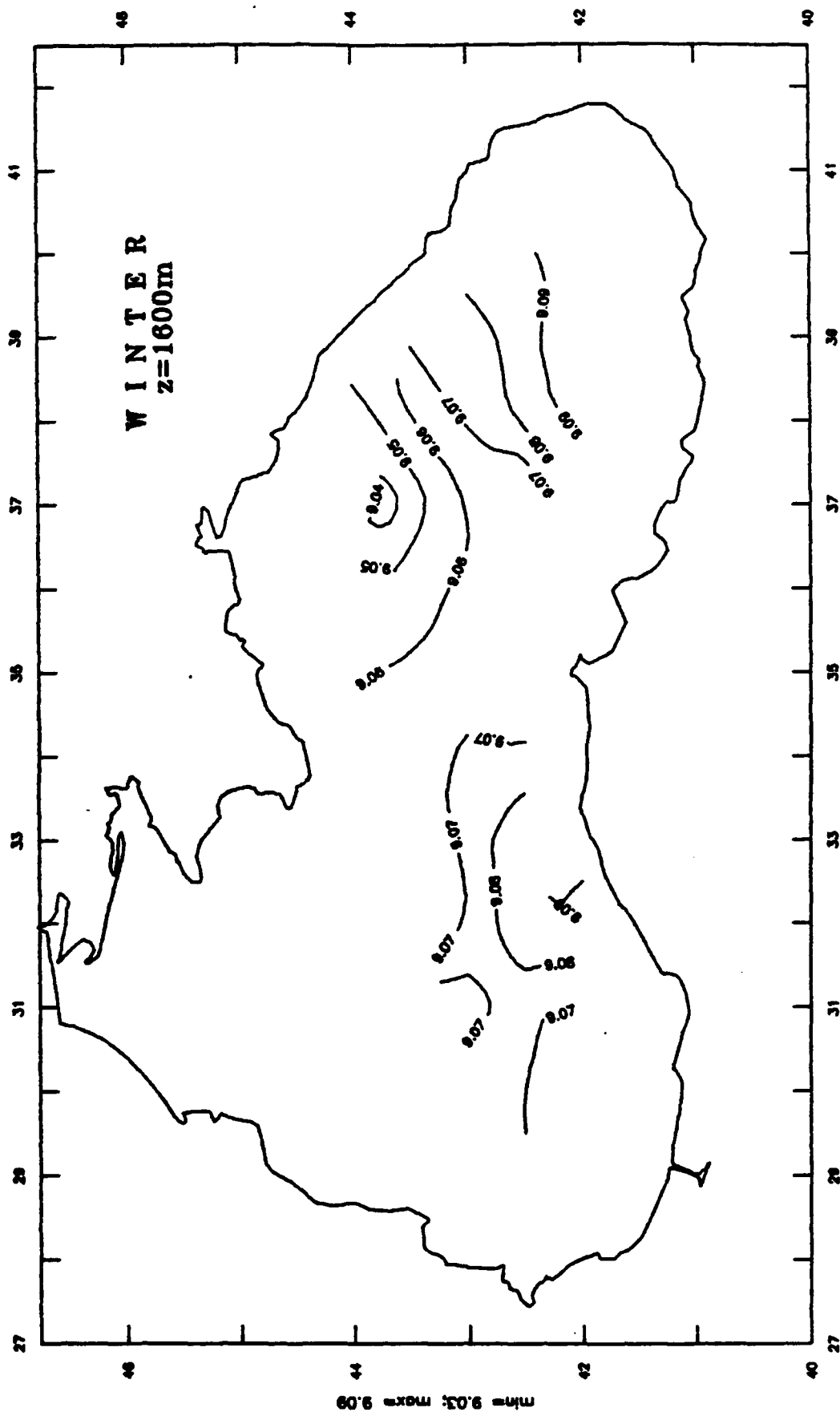
The Black Sea Climate Temperature



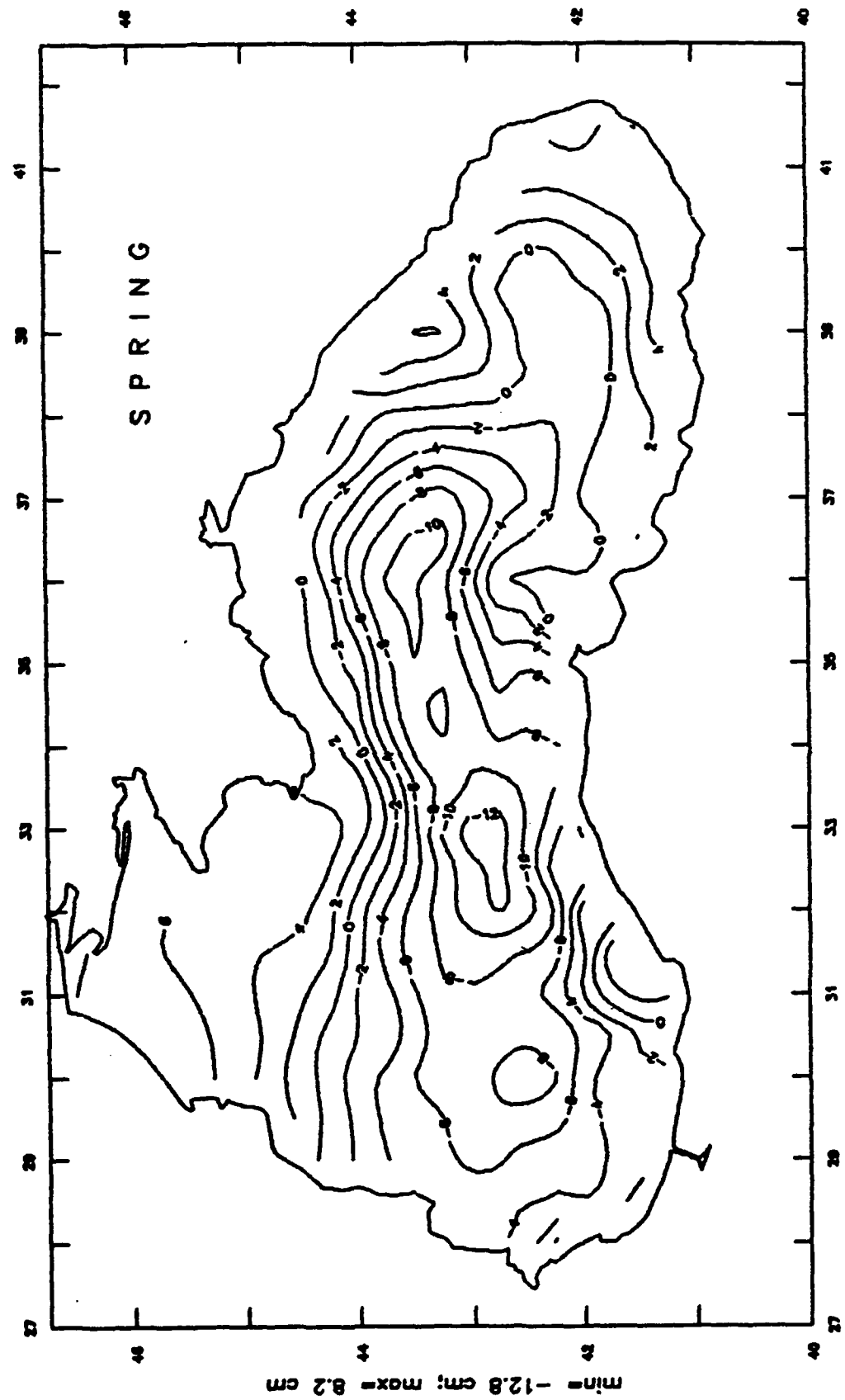
The Black Sea Climate Temperature



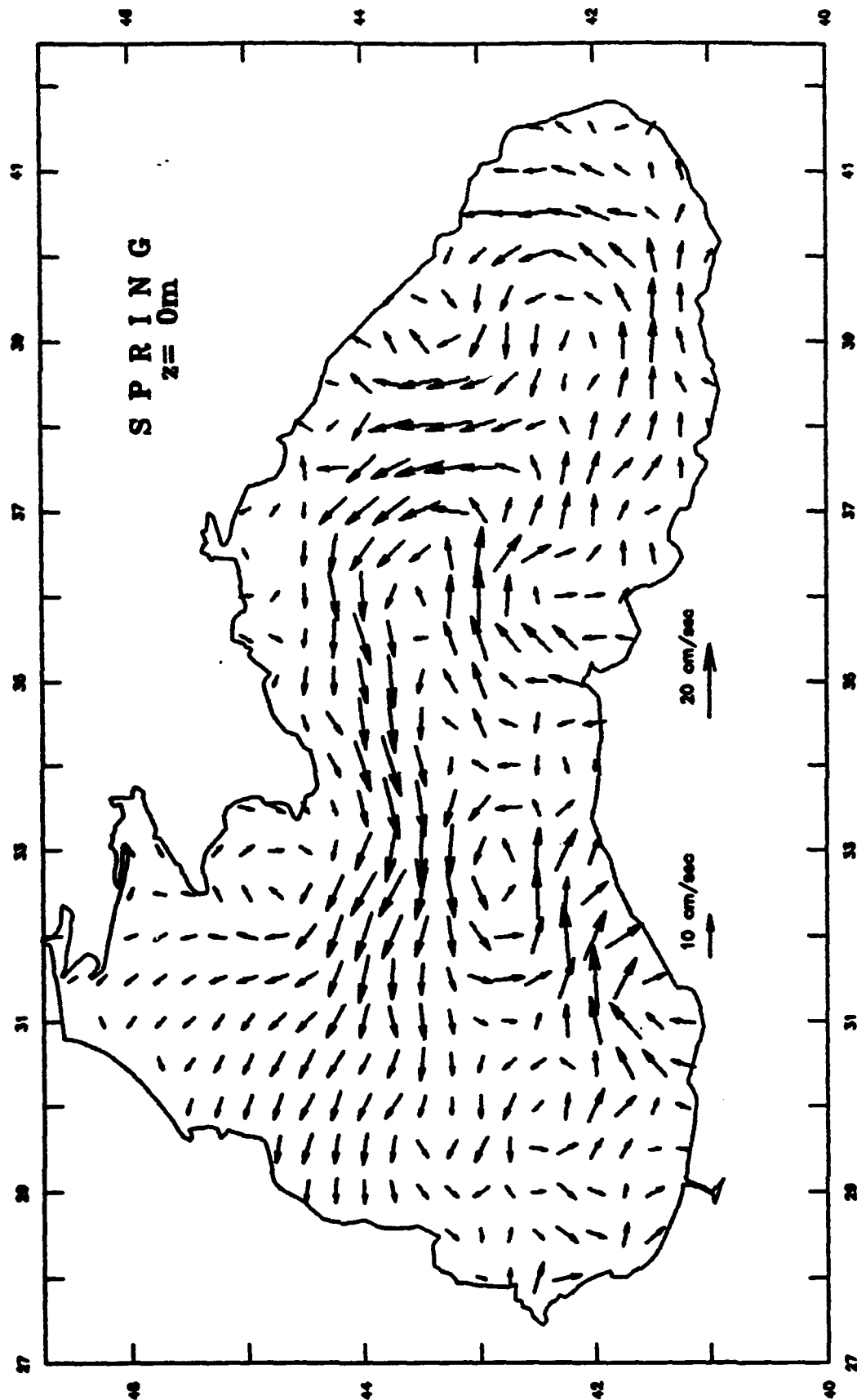
The Black Sea Climate Temperature



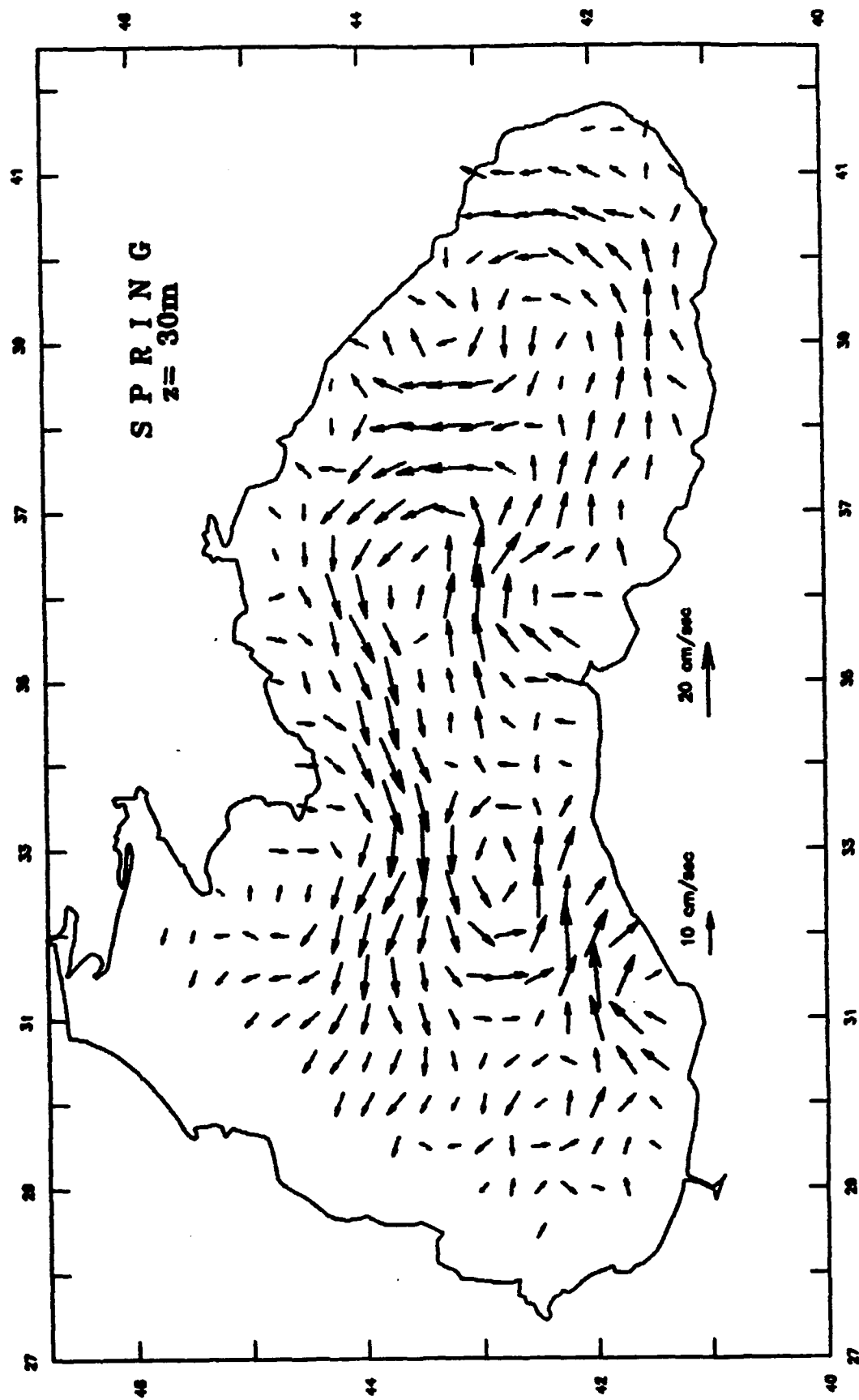
The Black Sea Climate Surface



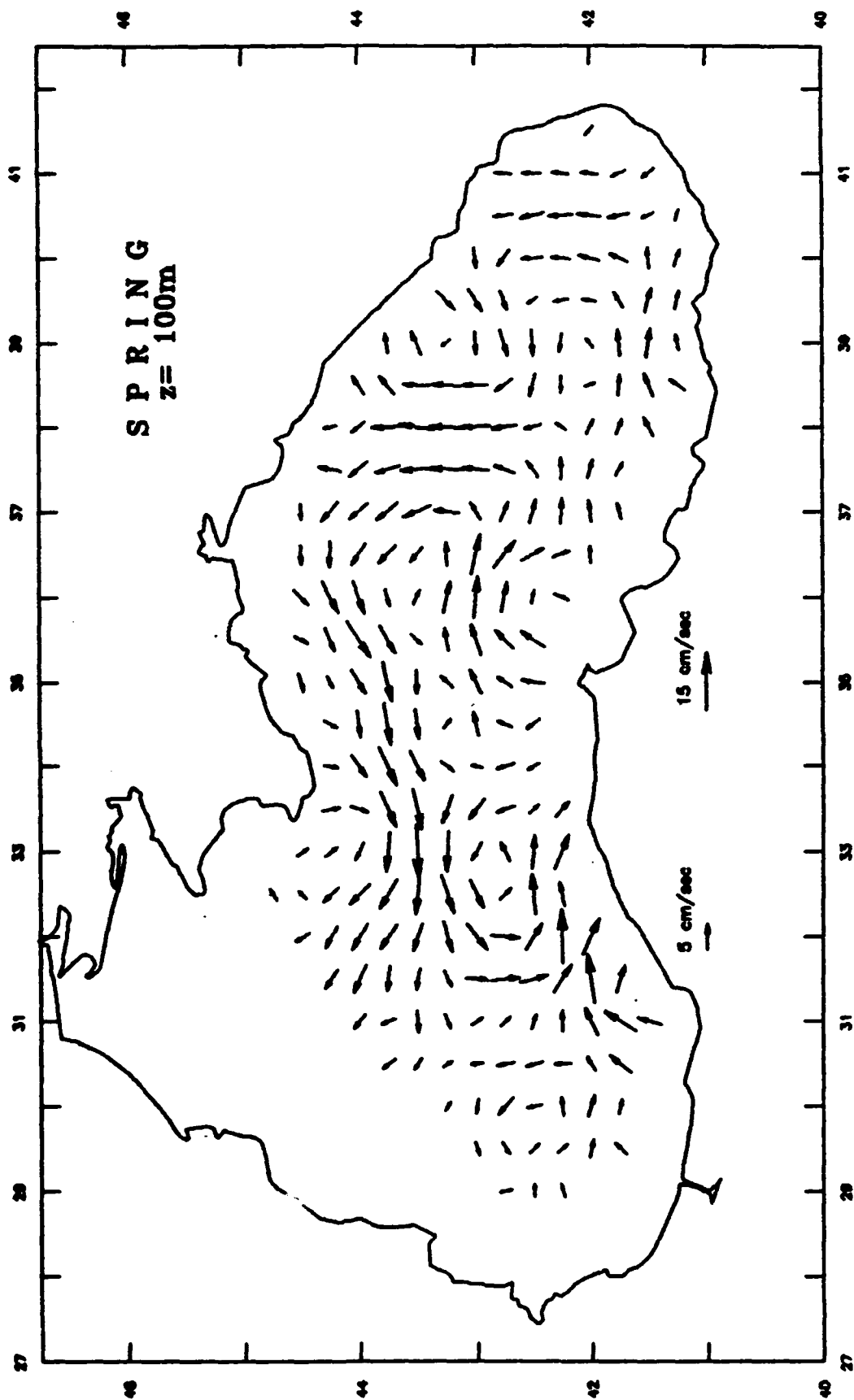
The Black Sea Climate Velocity



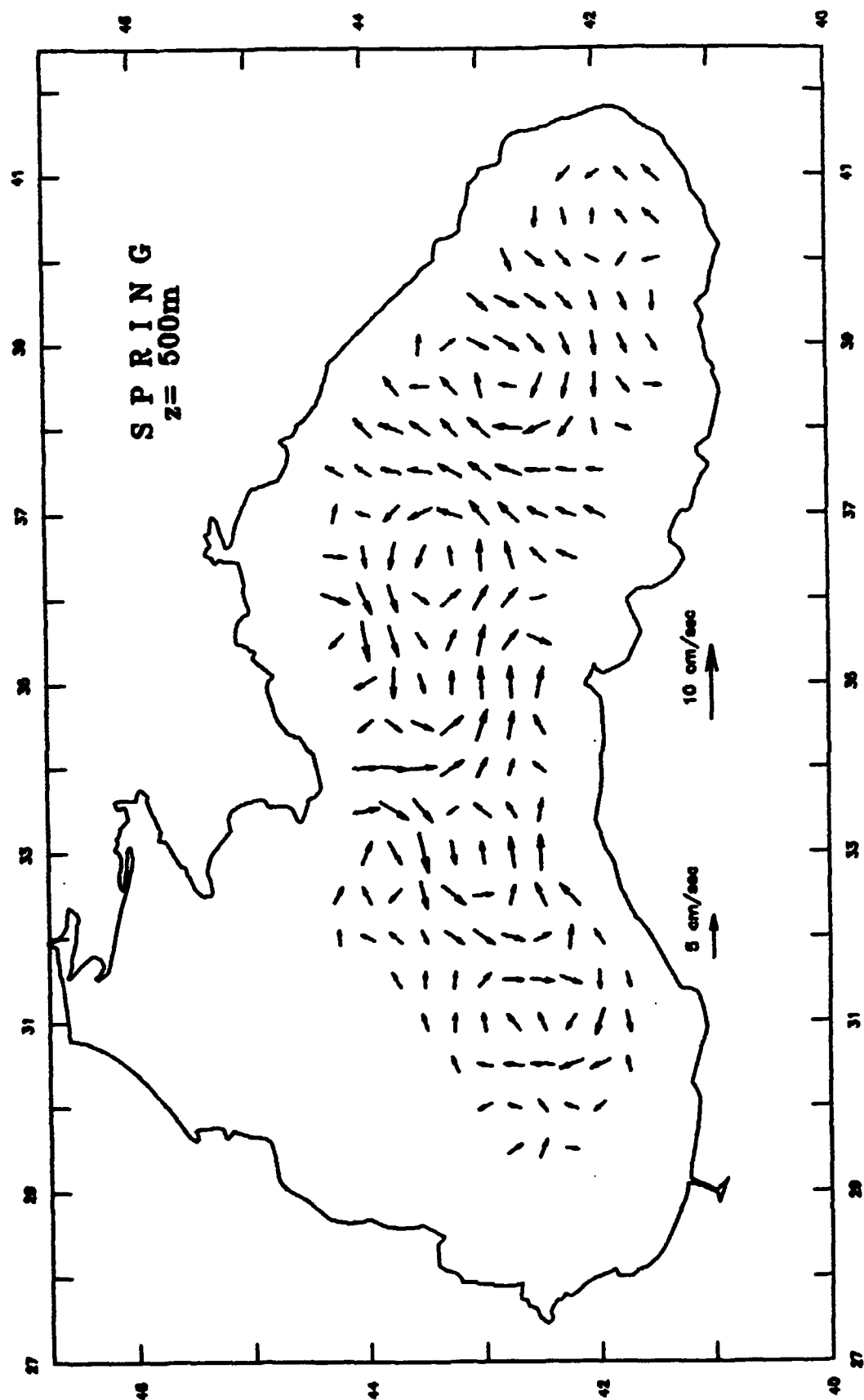
The Black Sea Climate Velocity



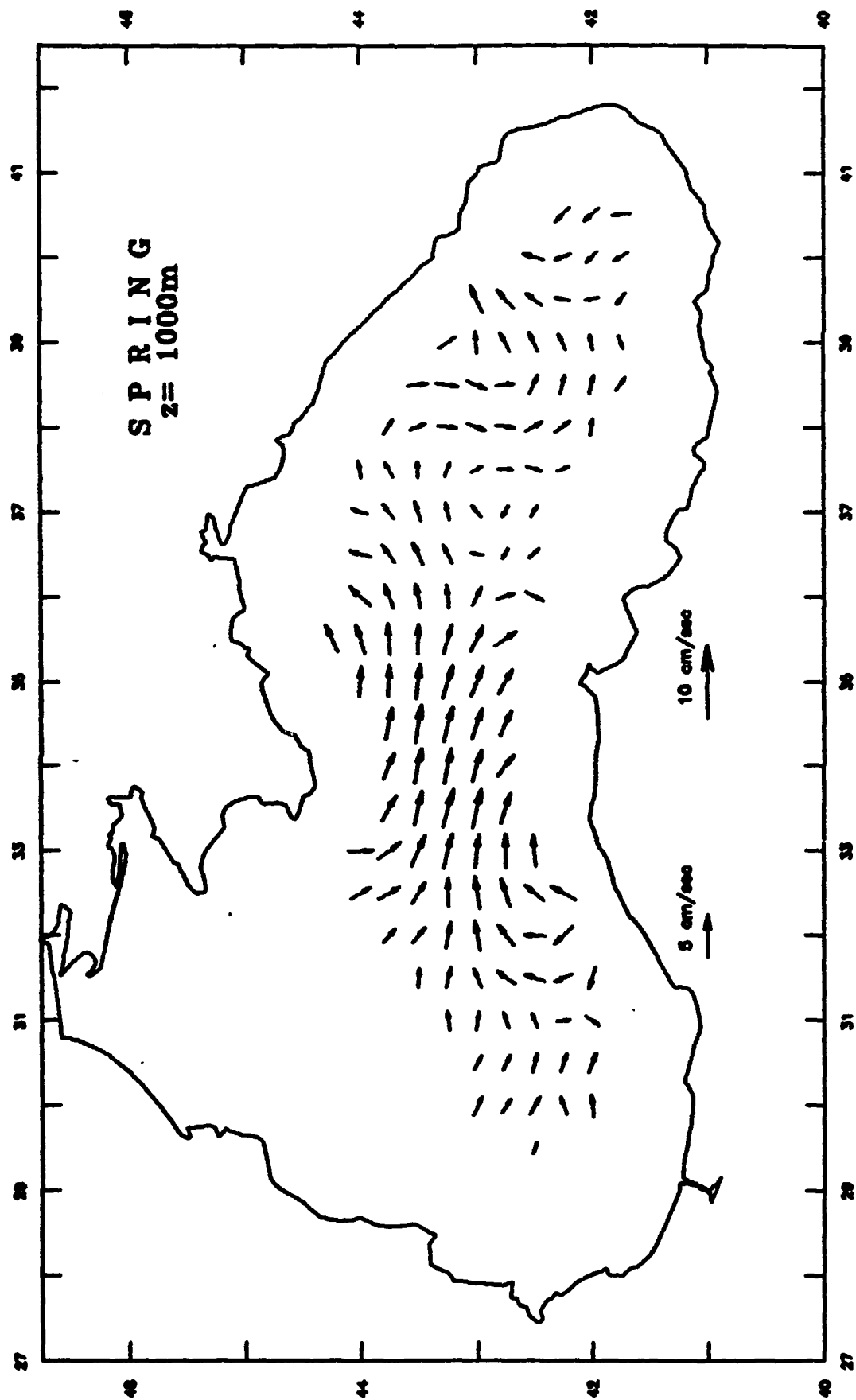
The Black Sea Climate Velocity



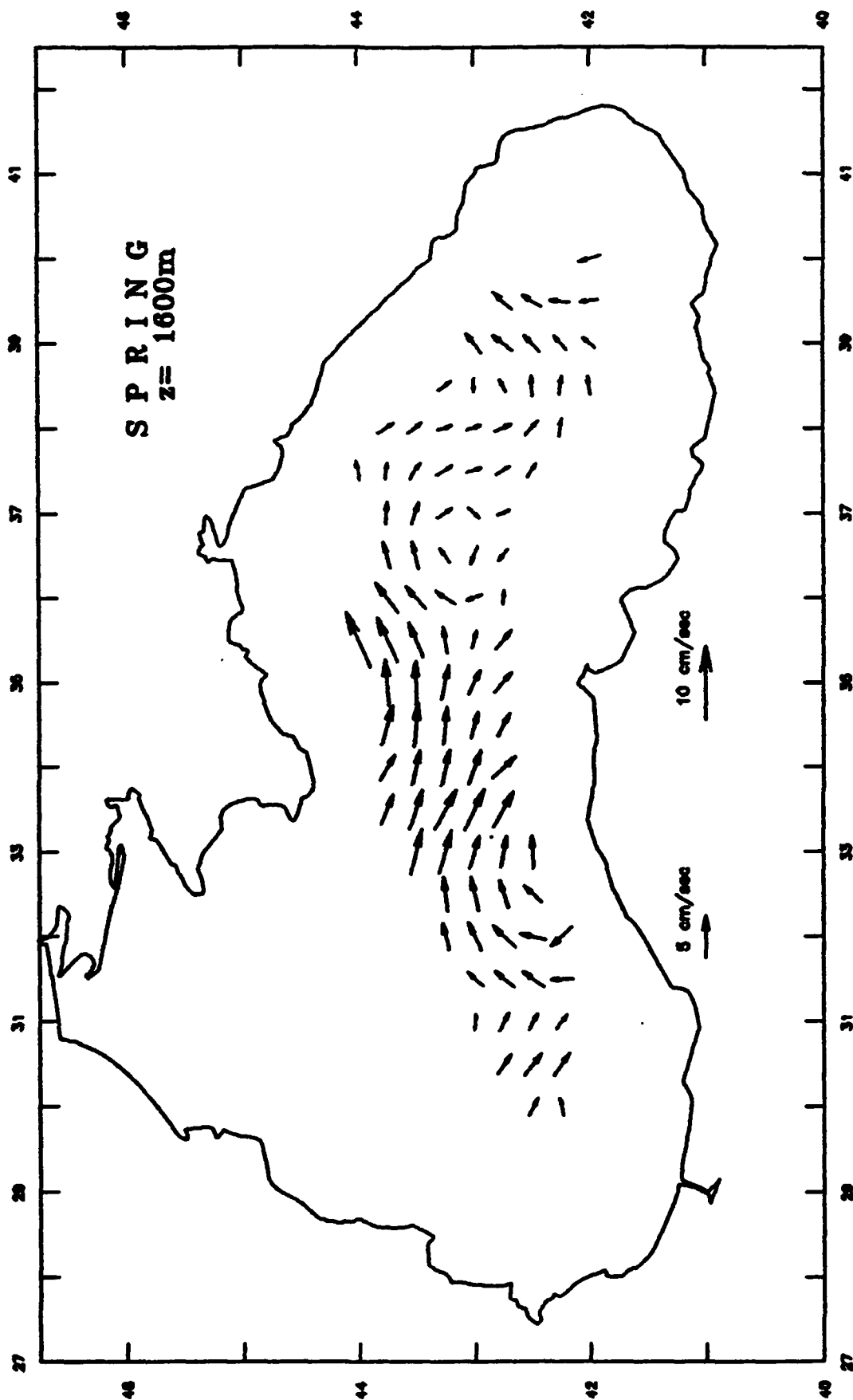
The Black Sea Climate Velocity



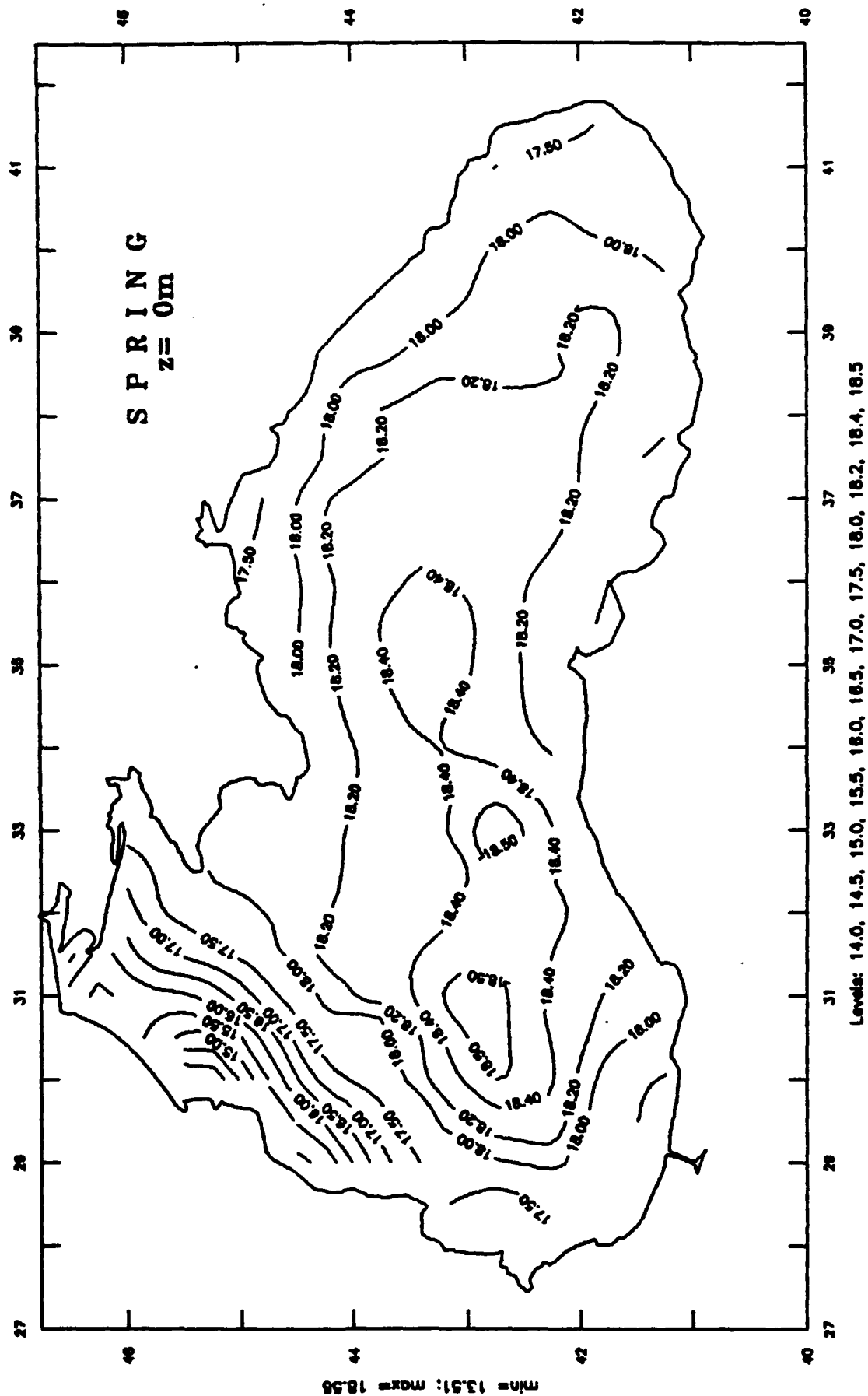
The Black Sea Climate Velocity



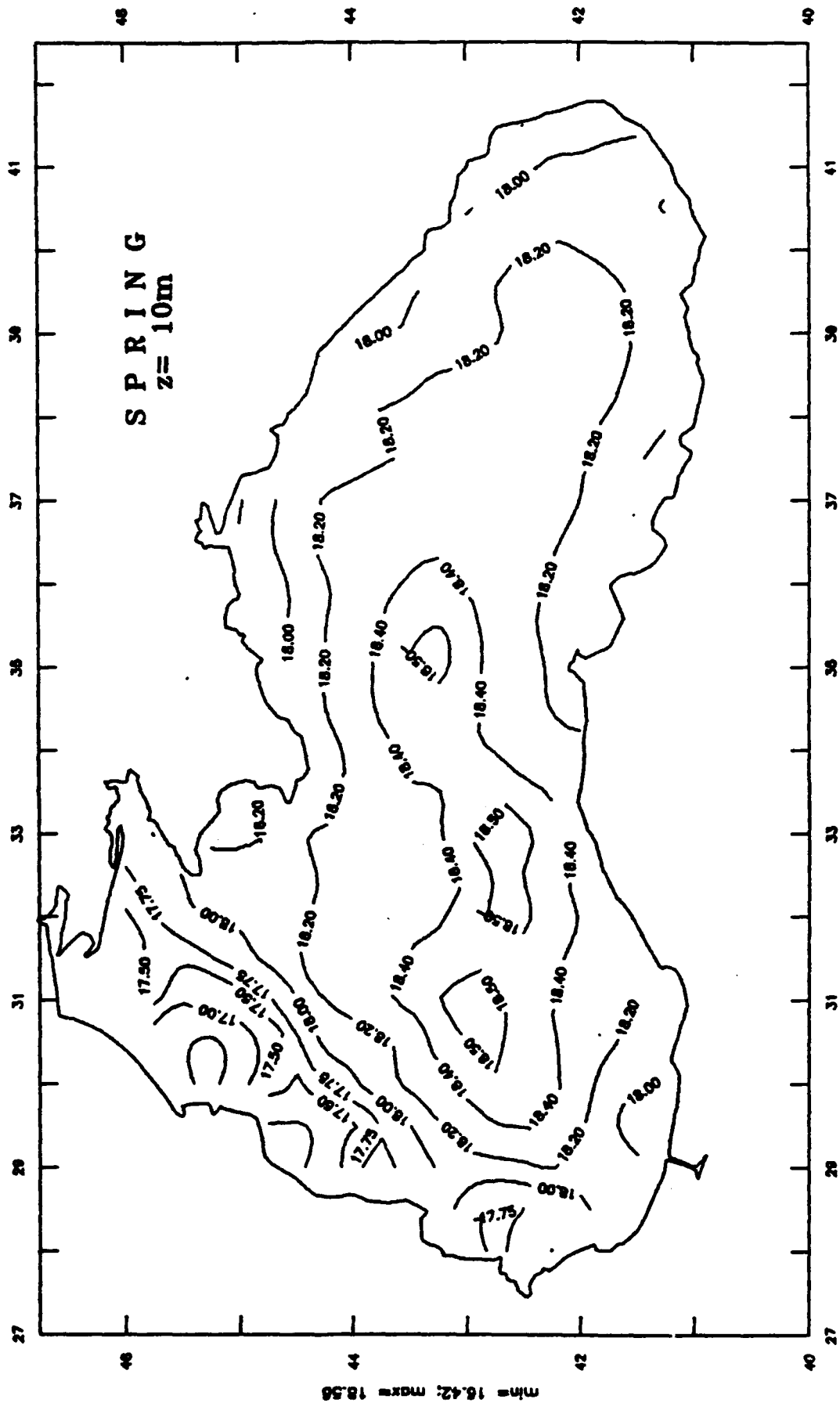
The Black Sea Climate Velocity



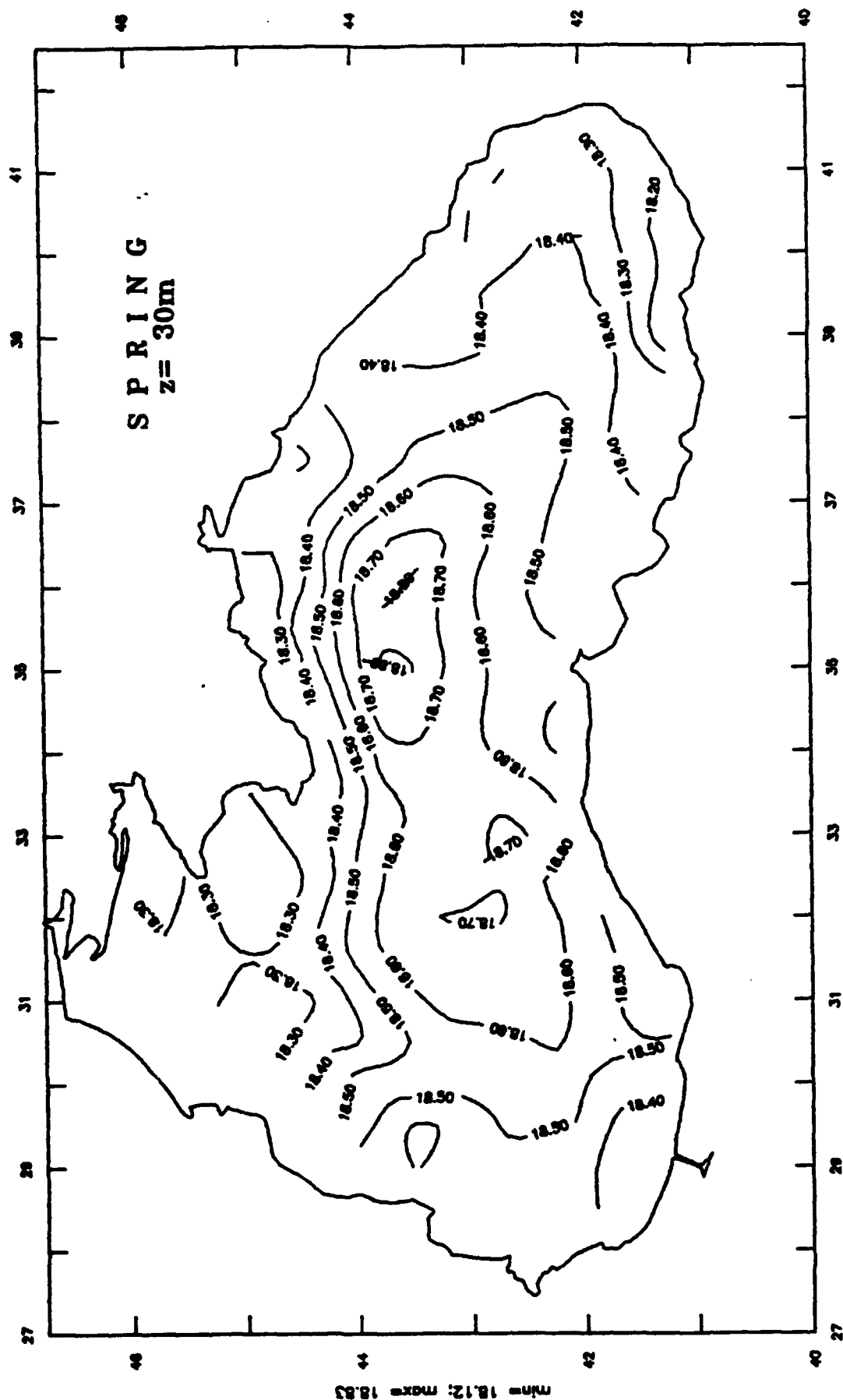
The Black Sea Climate Salinity



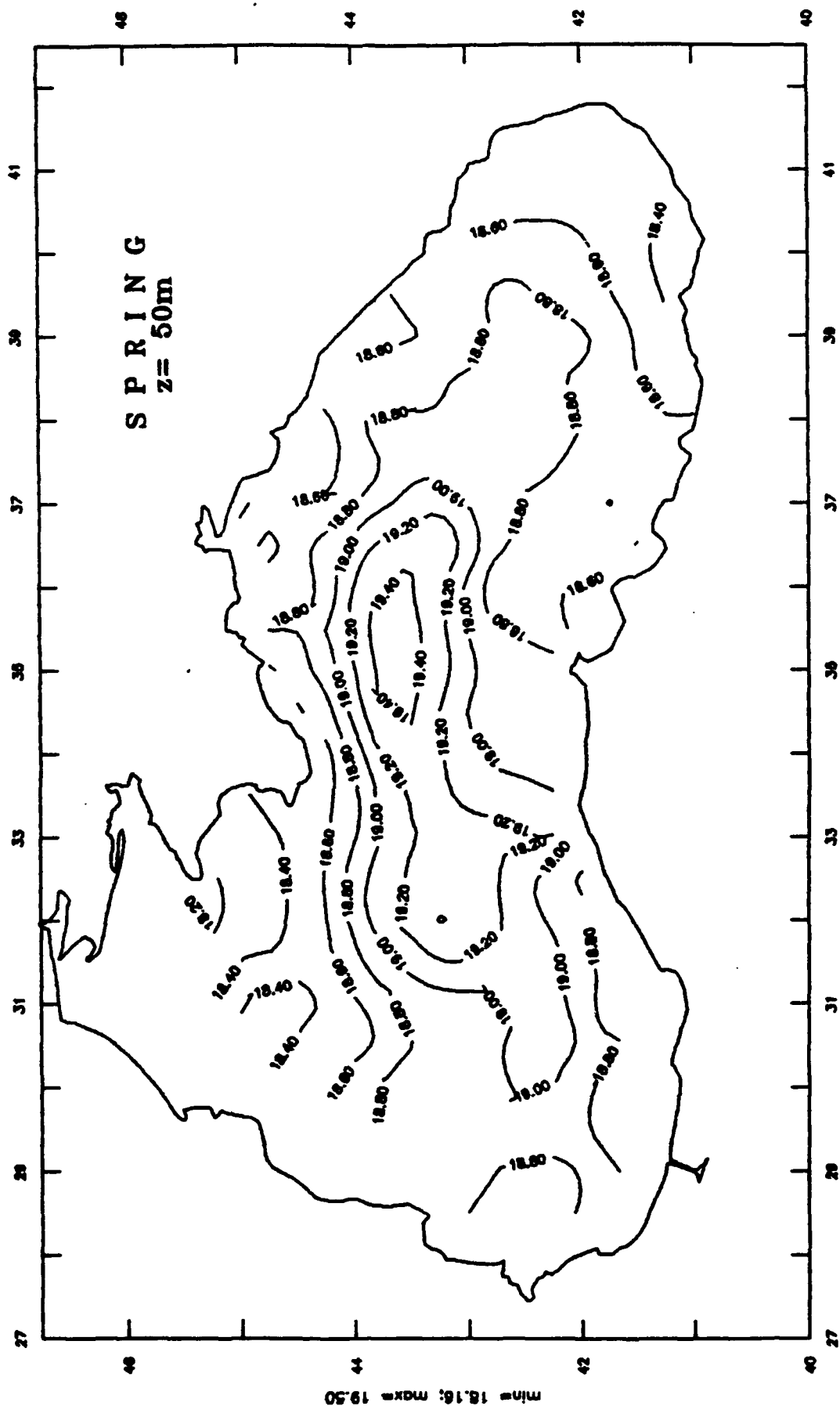
The Black Sea Climate Salinity



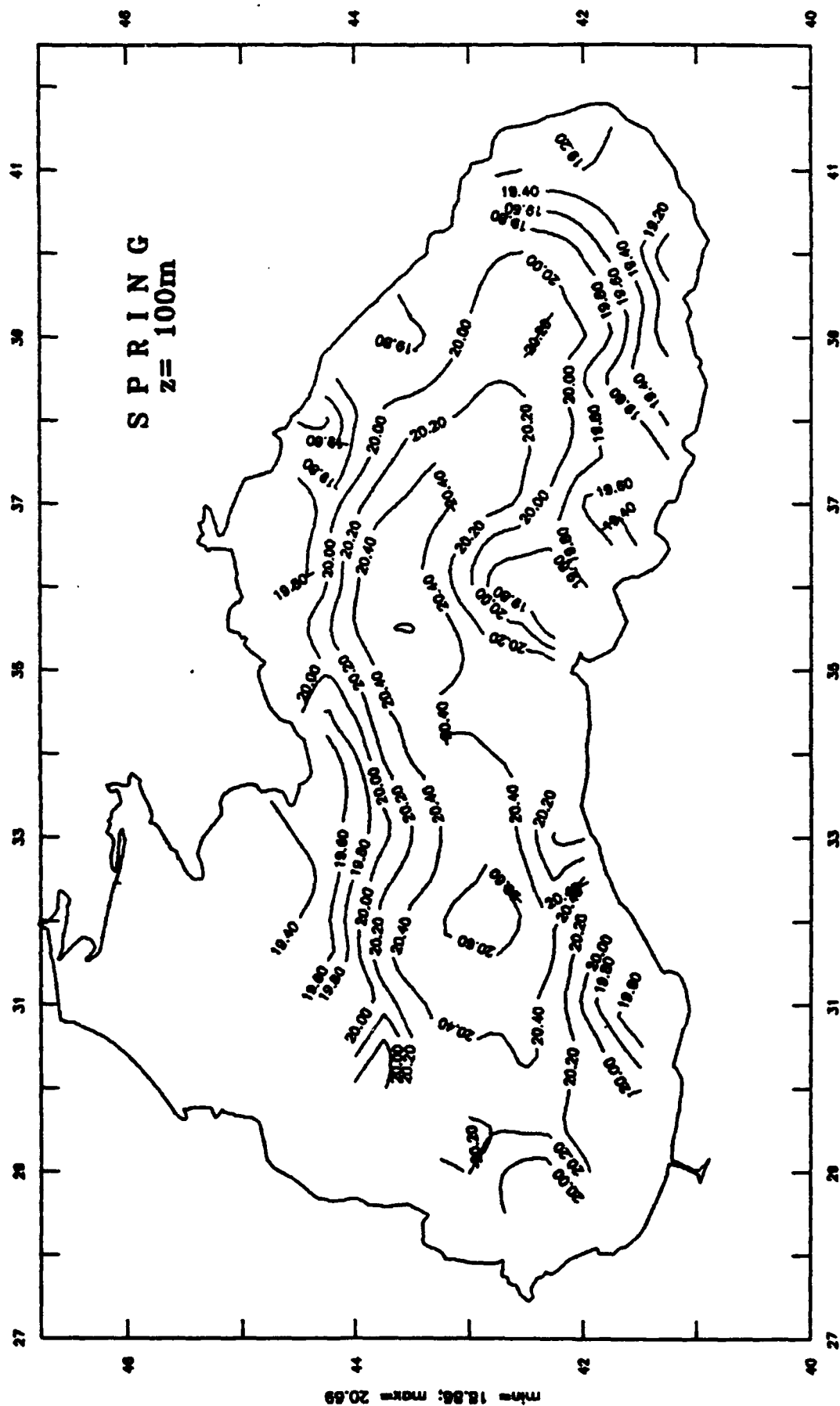
The Black Sea Climate Salinity



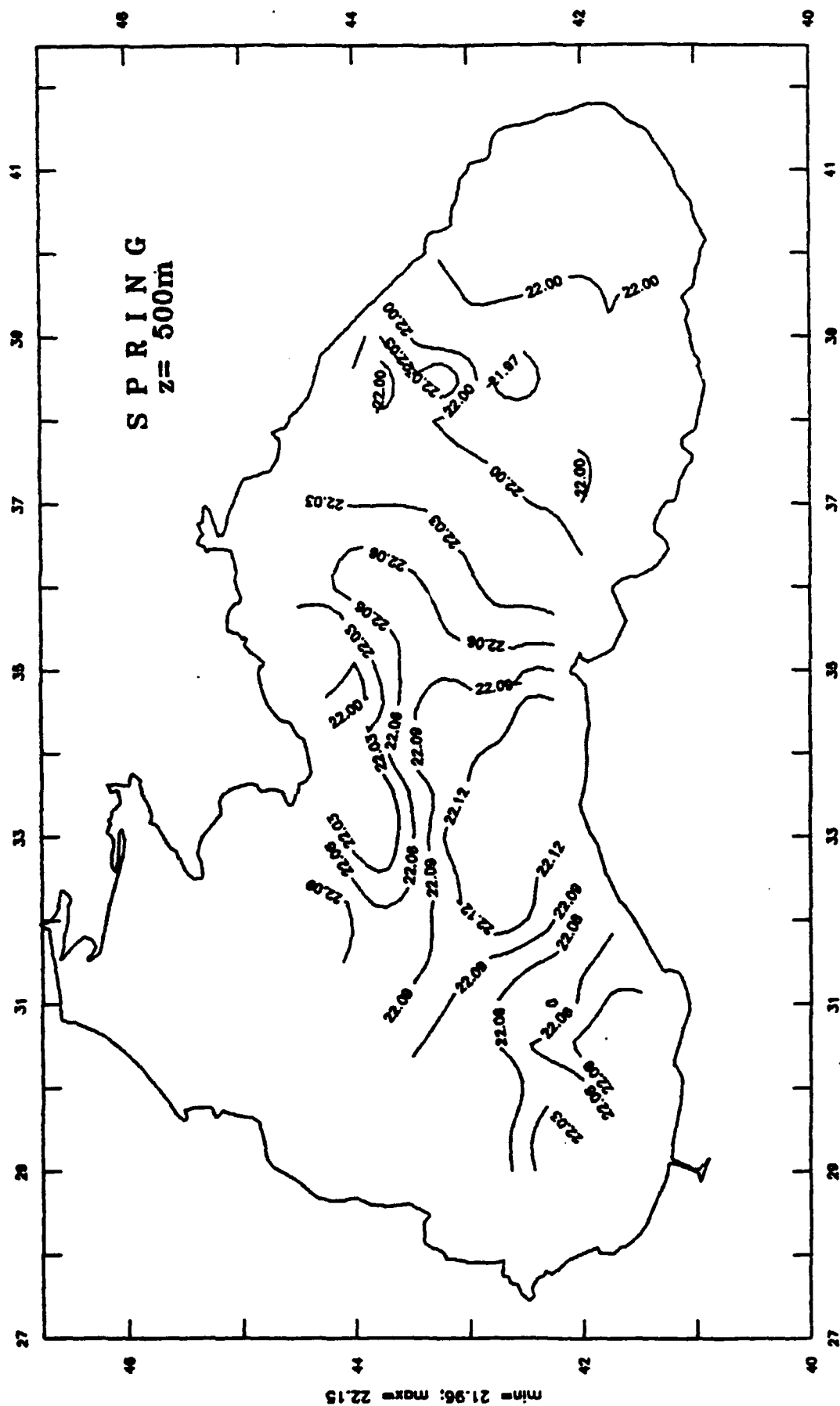
The Black Sea Climate Salinity



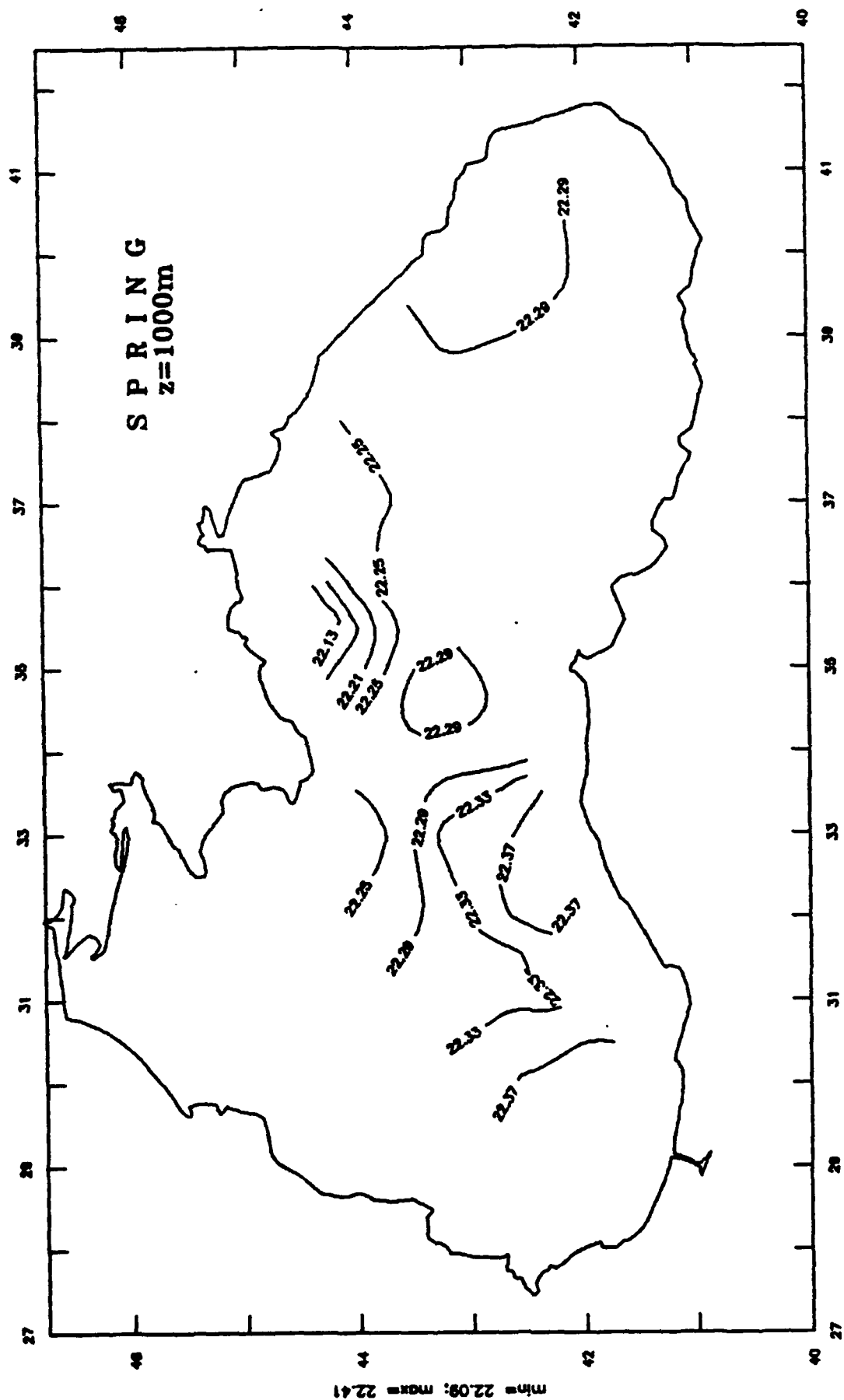
The Black Sea Climate Salinity



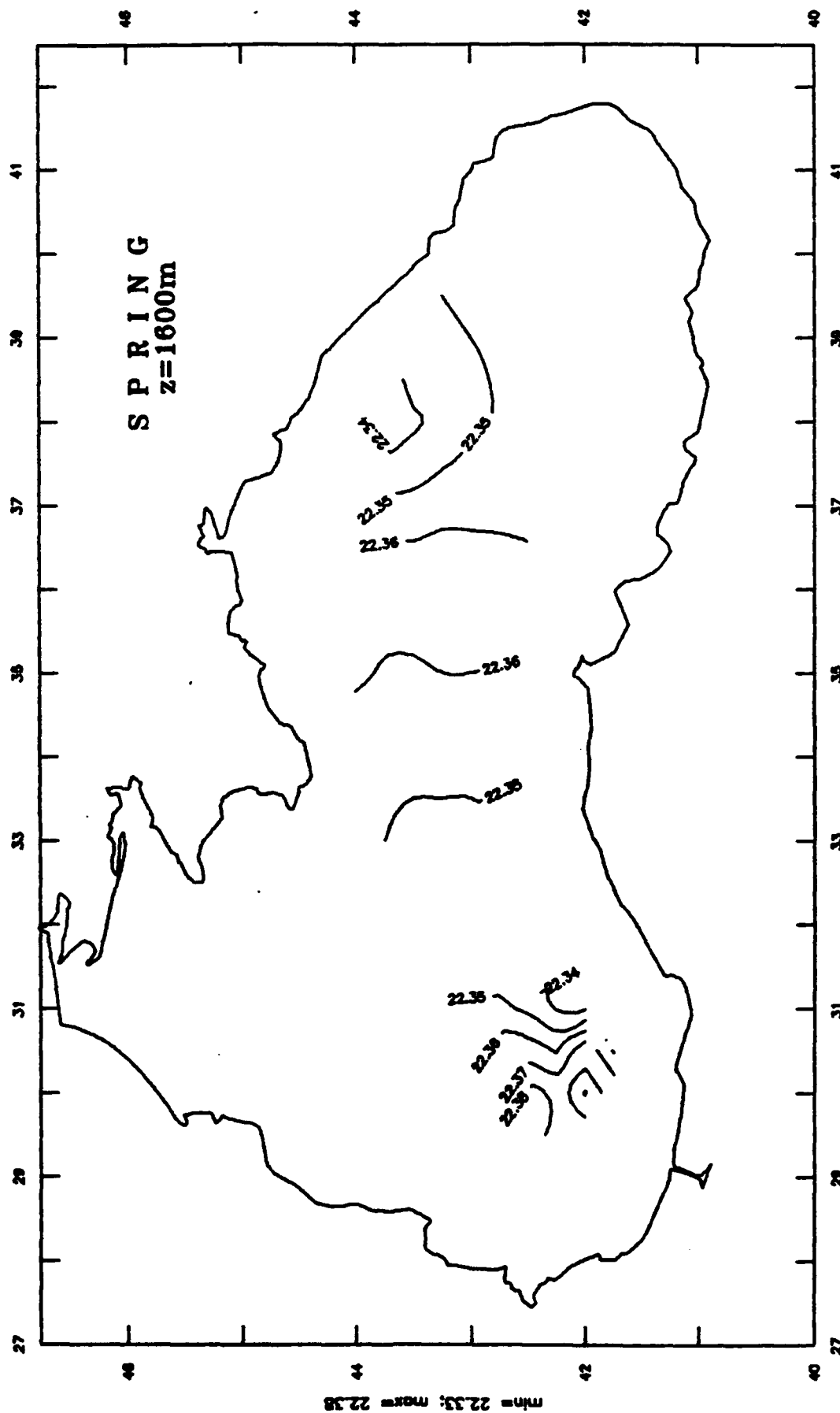
The Black Sea Climate Salinity



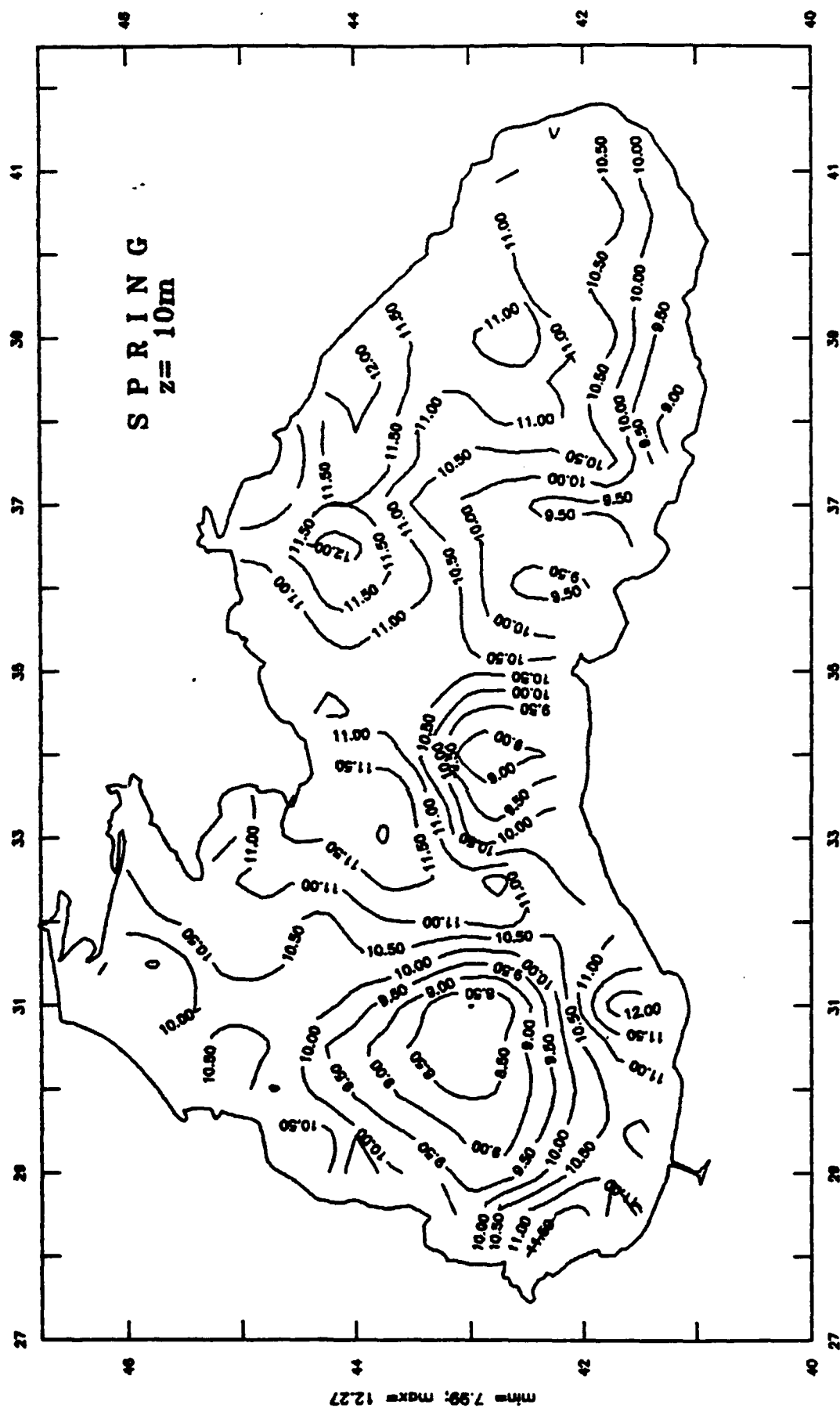
The Black Sea Climate Salinity



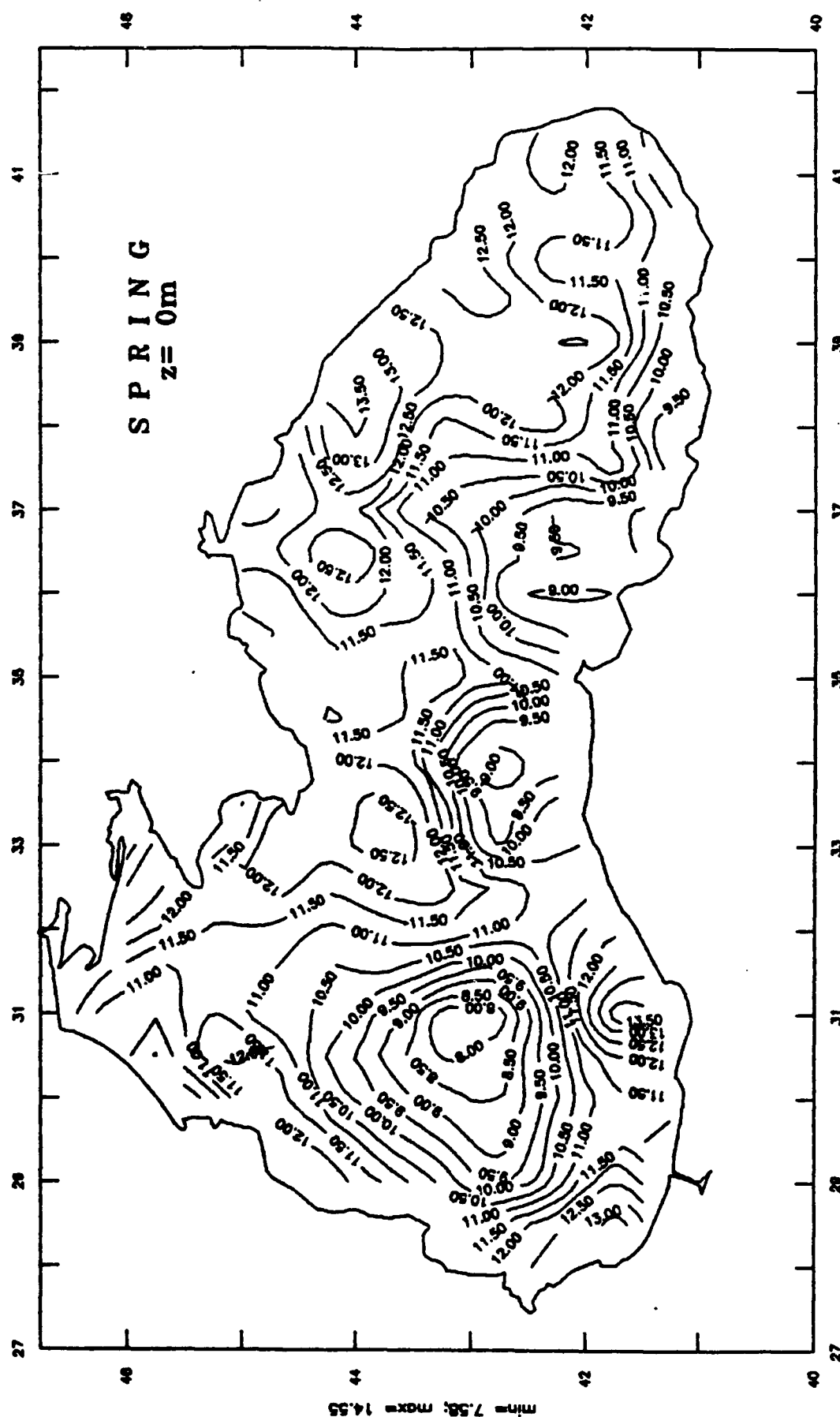
The Black Sea Climate Salinity



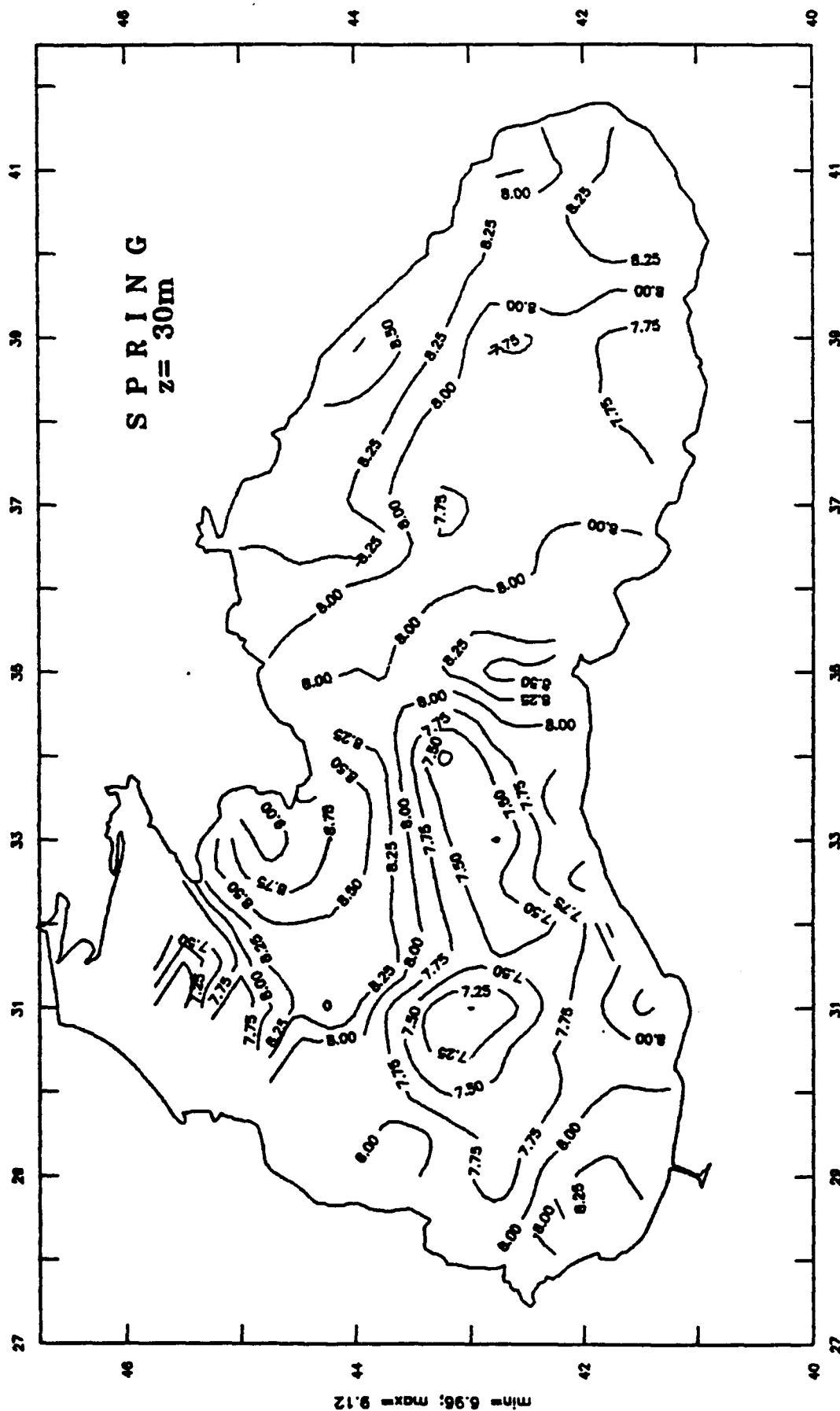
The Black Sea Climate Temperature



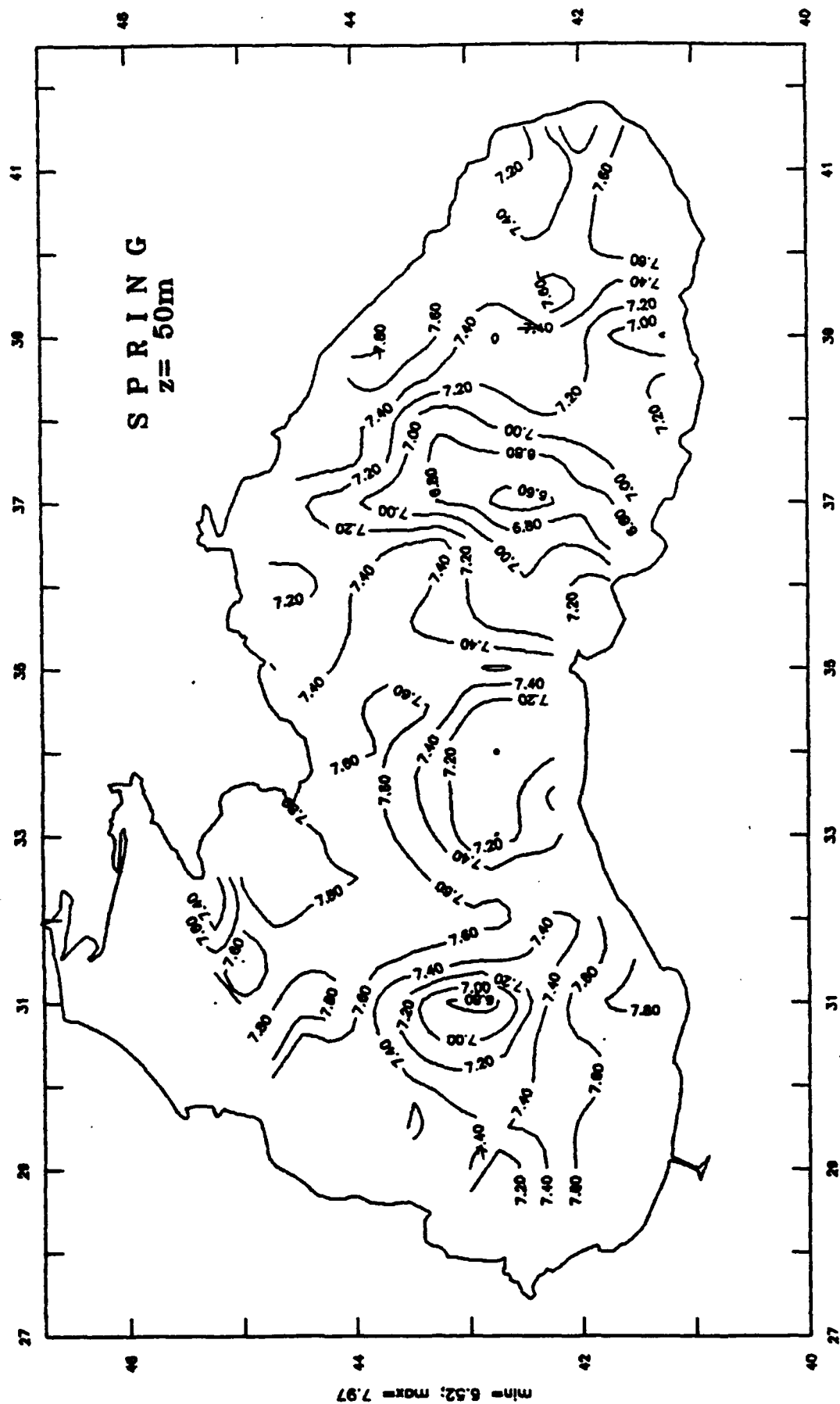
The Black Sea Climate Temperature



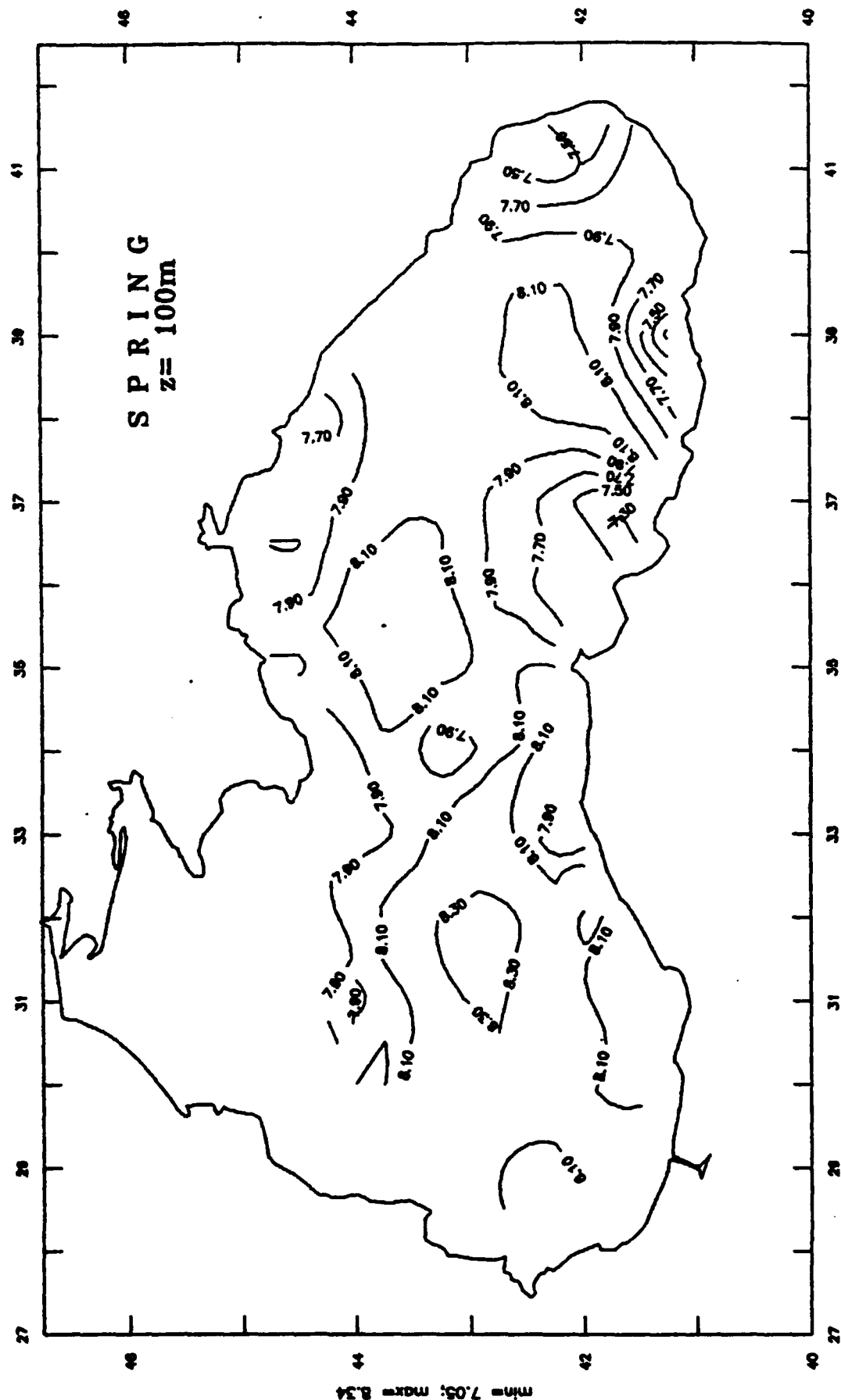
The Black Sea Climate Temperature



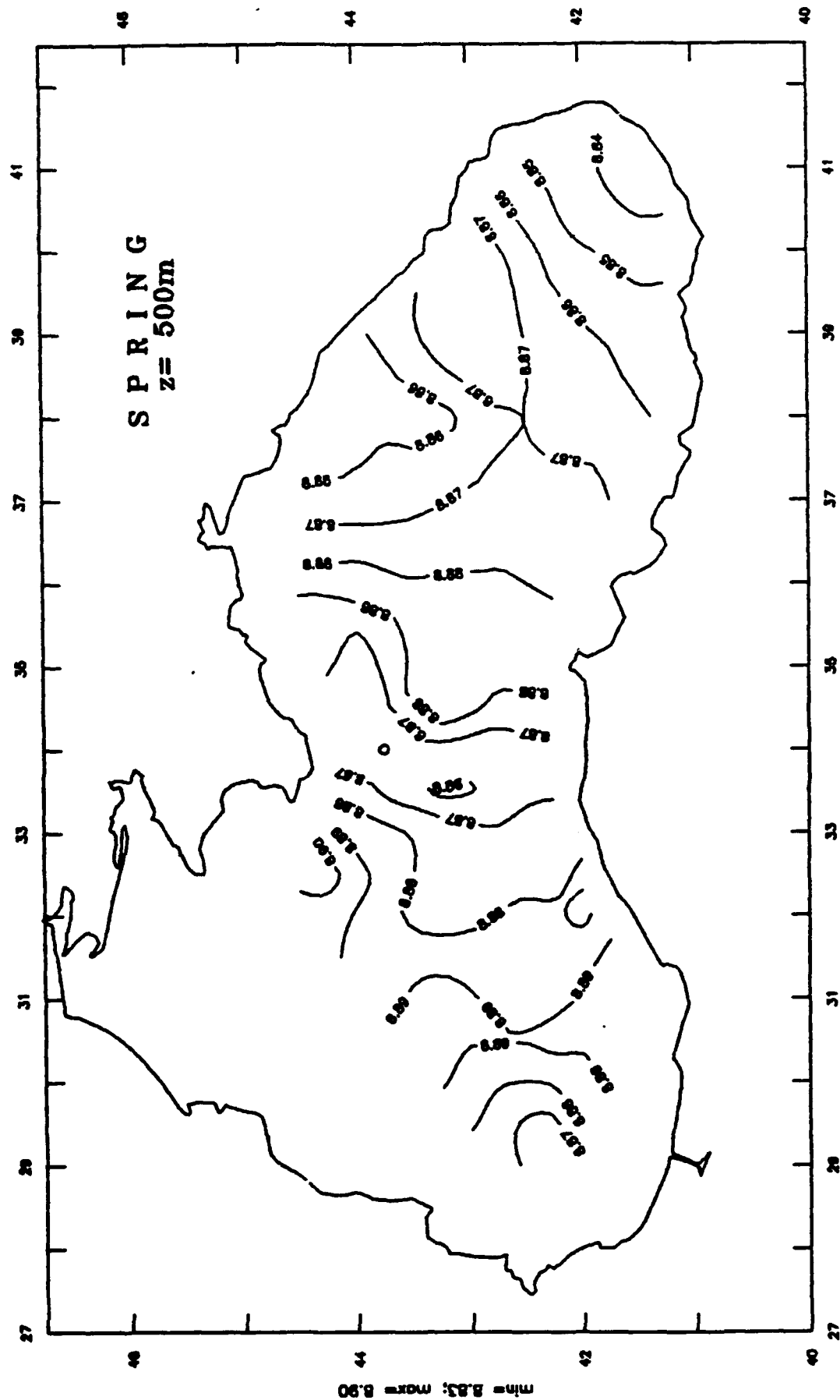
The Black Sea Climate Temperature



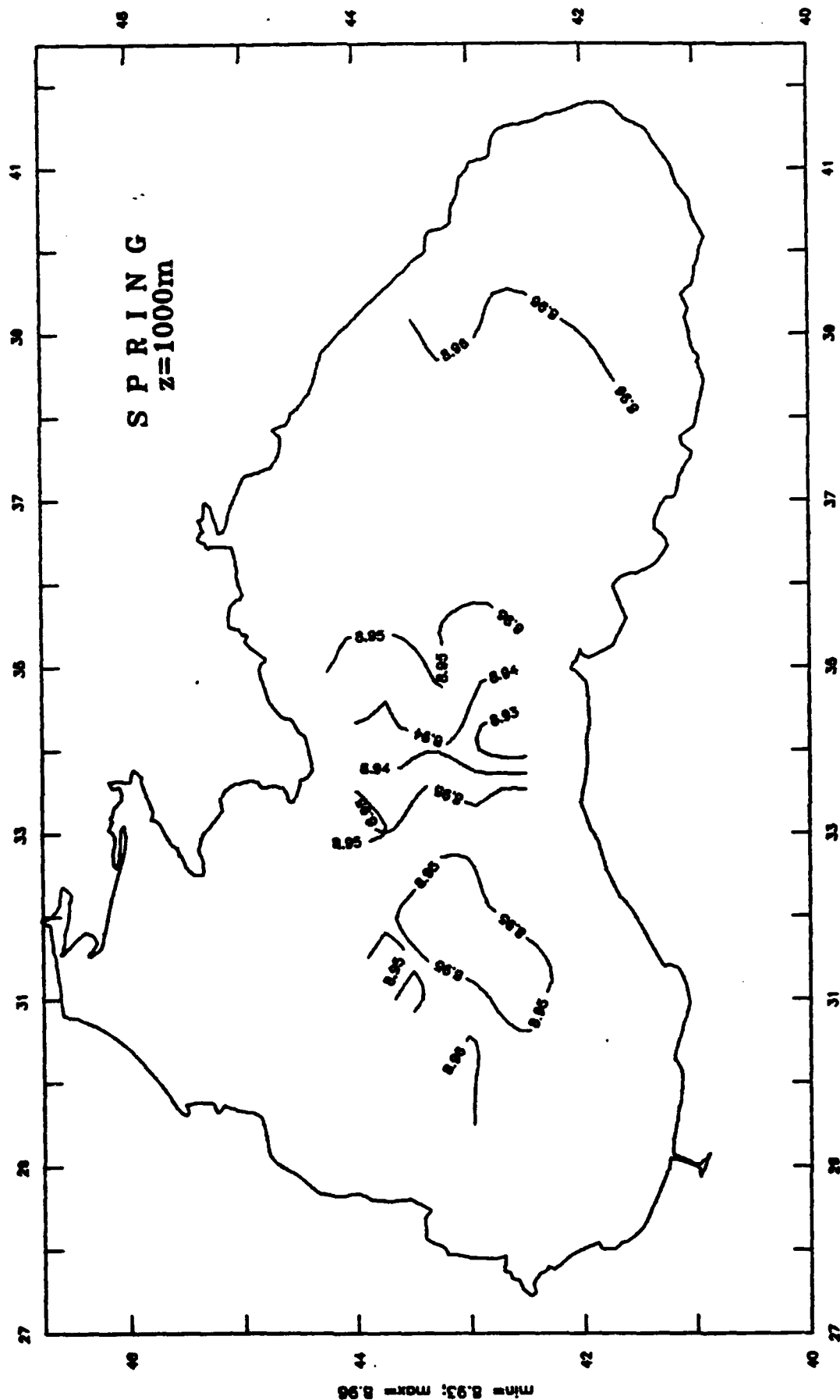
The Black Sea Climate Temperature



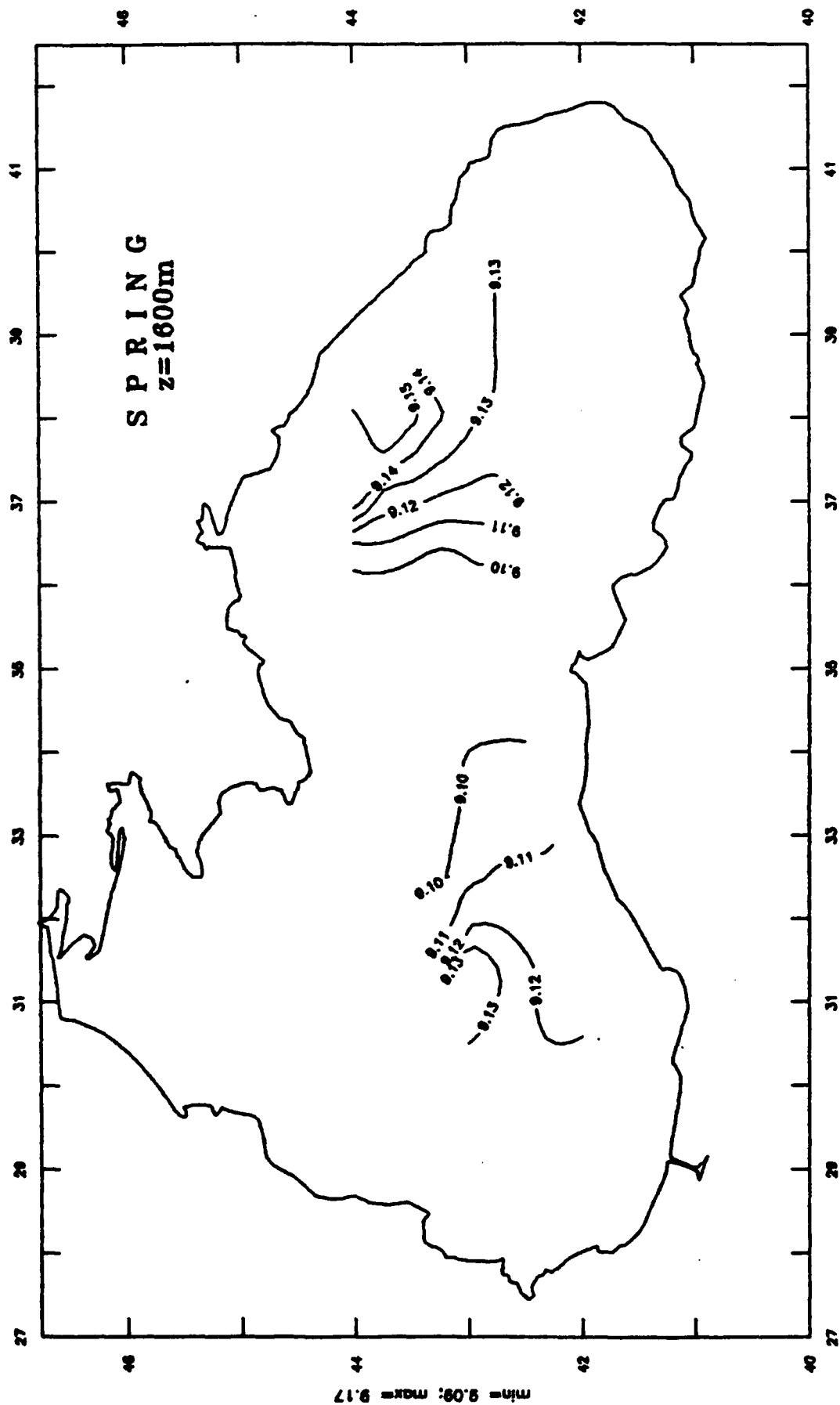
The Black Sea Climate Temperature



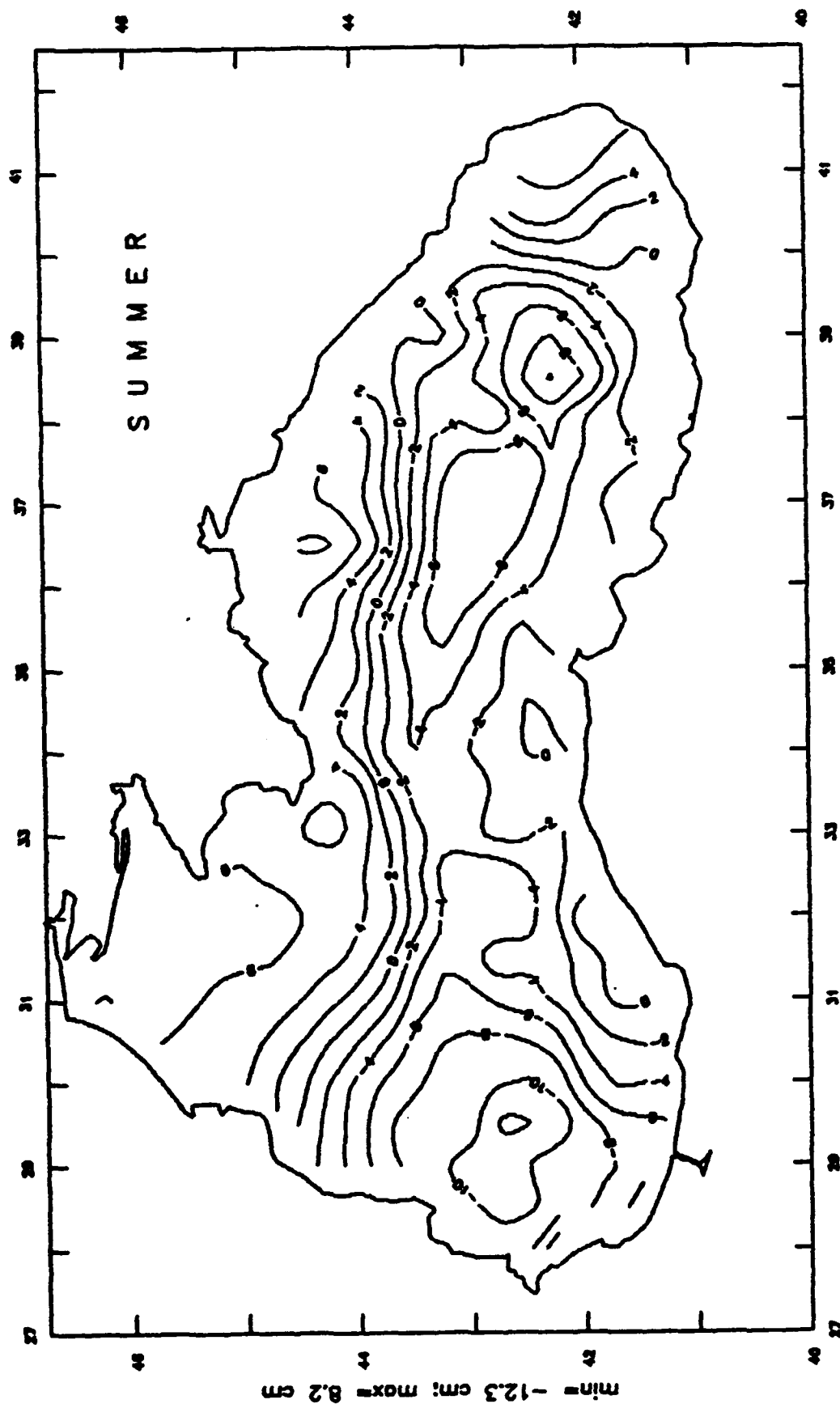
The Black Sea Climate Temperature



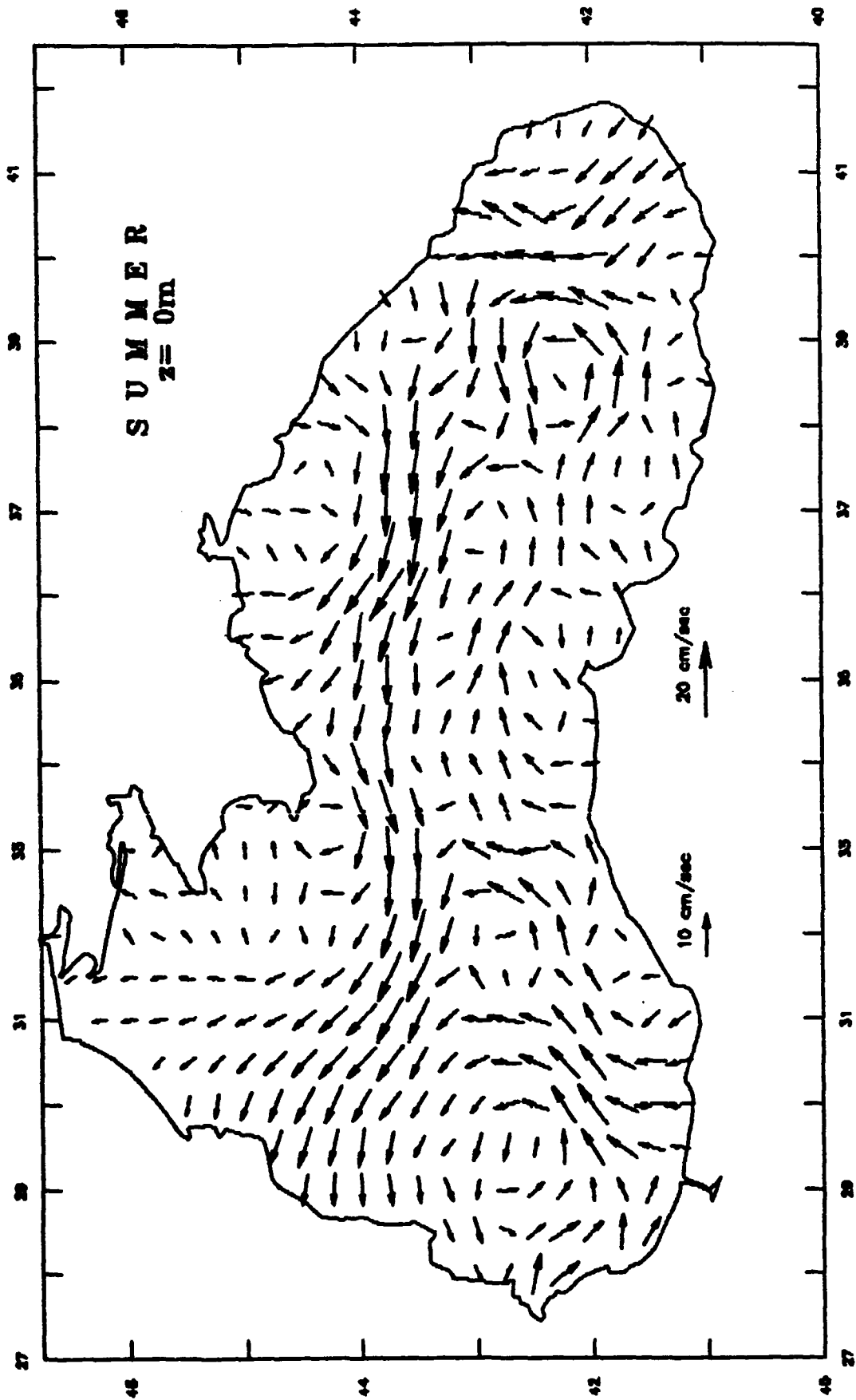
The Black Sea Climate Temperature



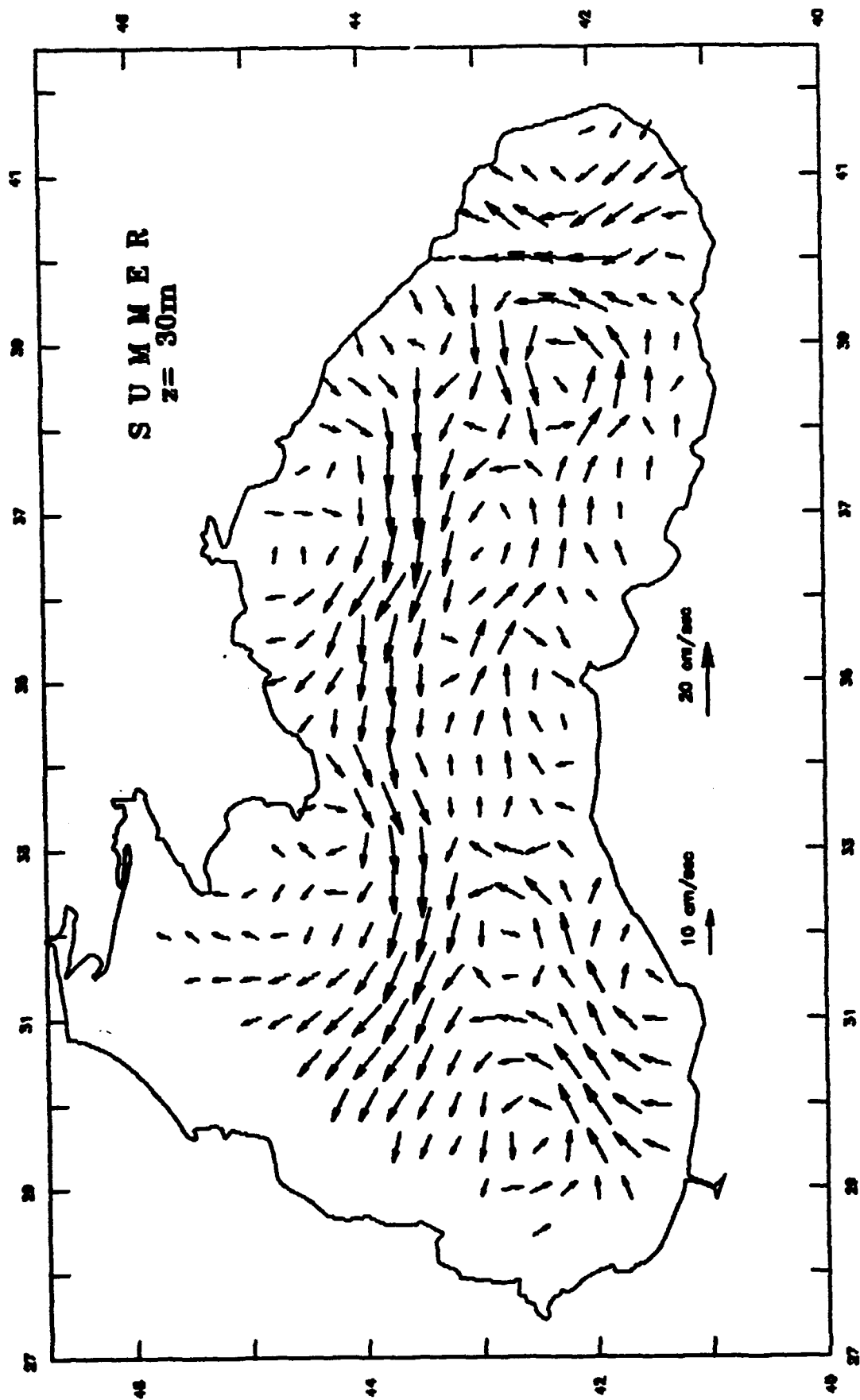
The Black Sea Climate Surface



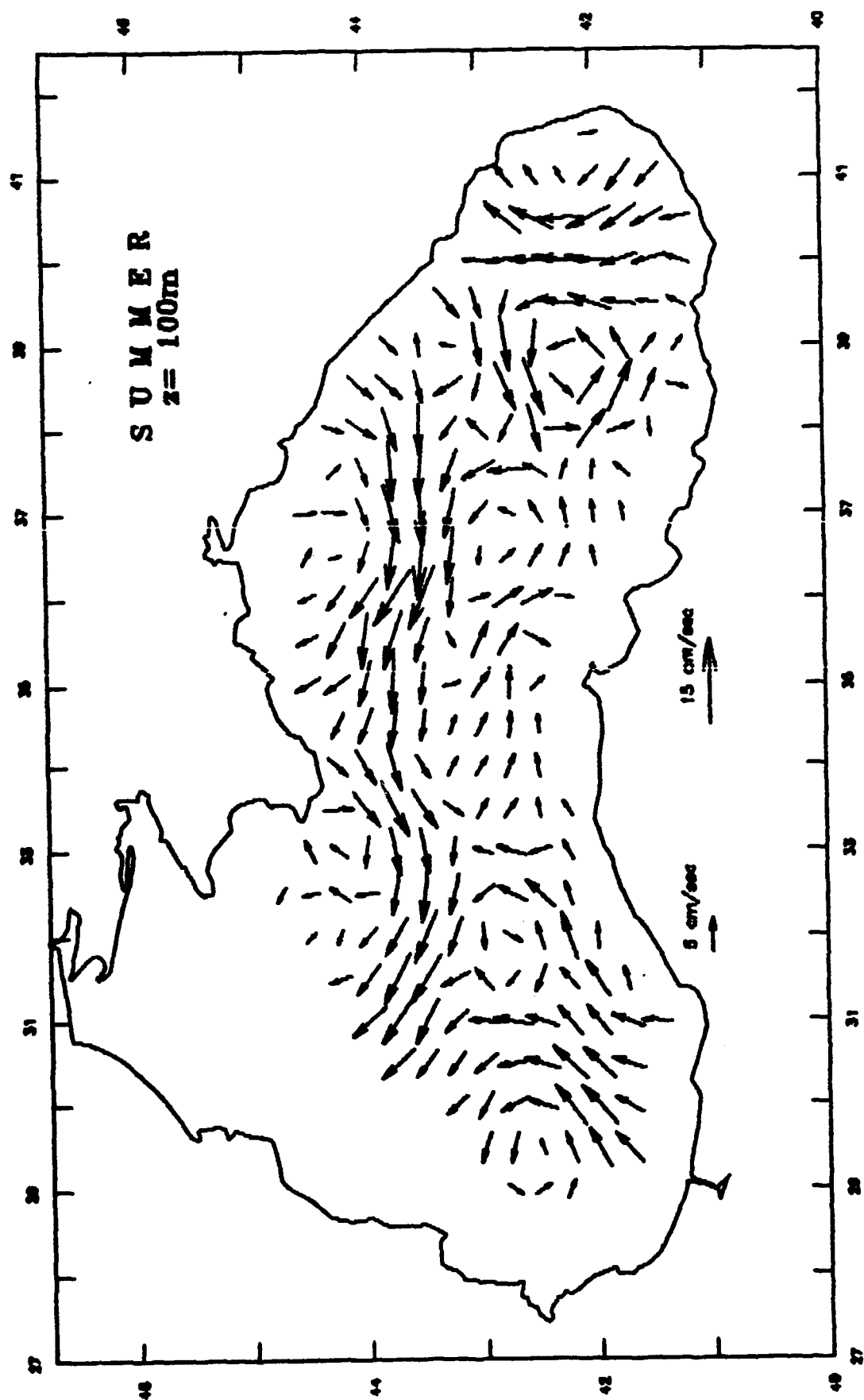
The Black Sea Climate Velocity



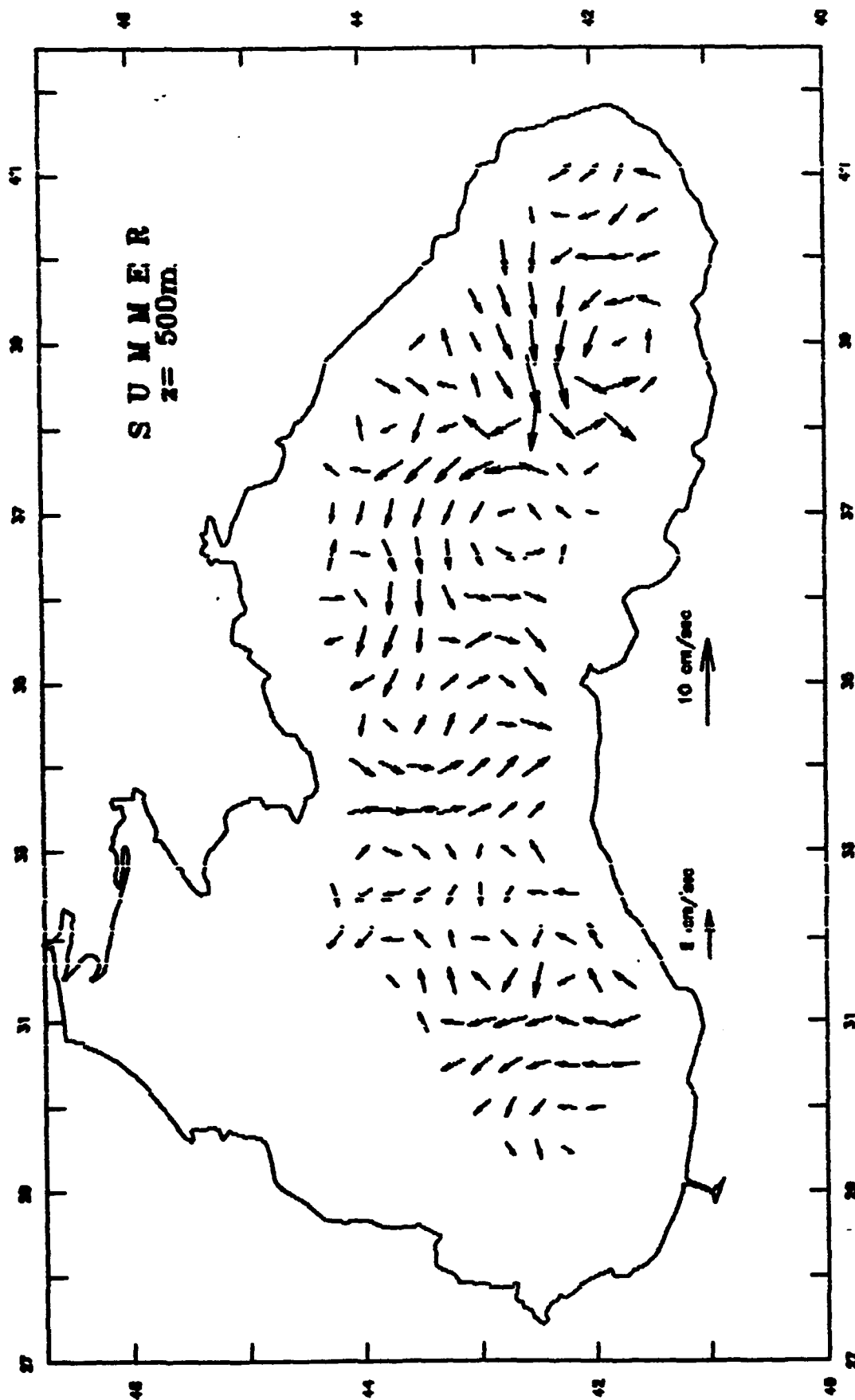
The Black Sea Climate Velocity



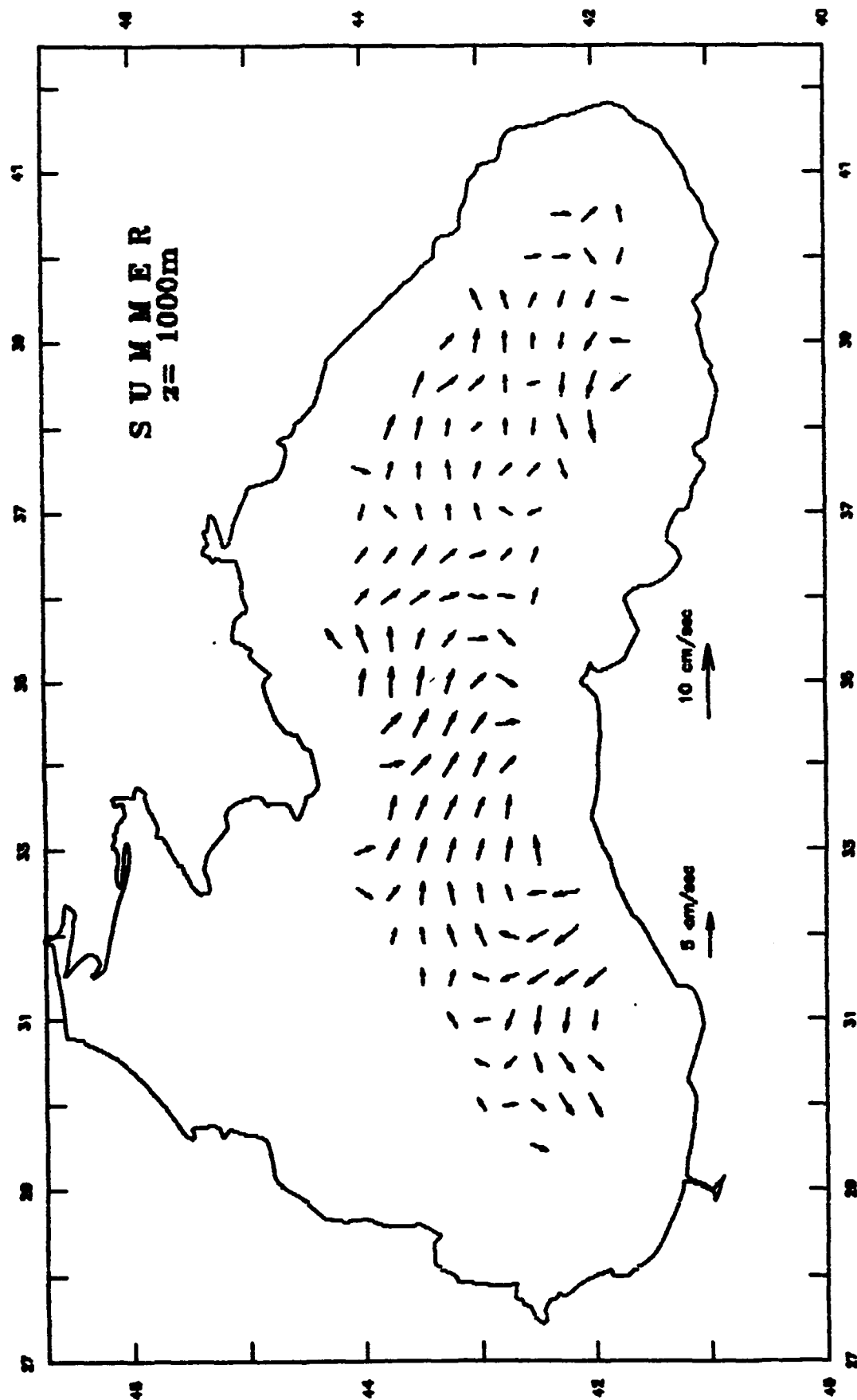
The Black Sea Climate Velocity



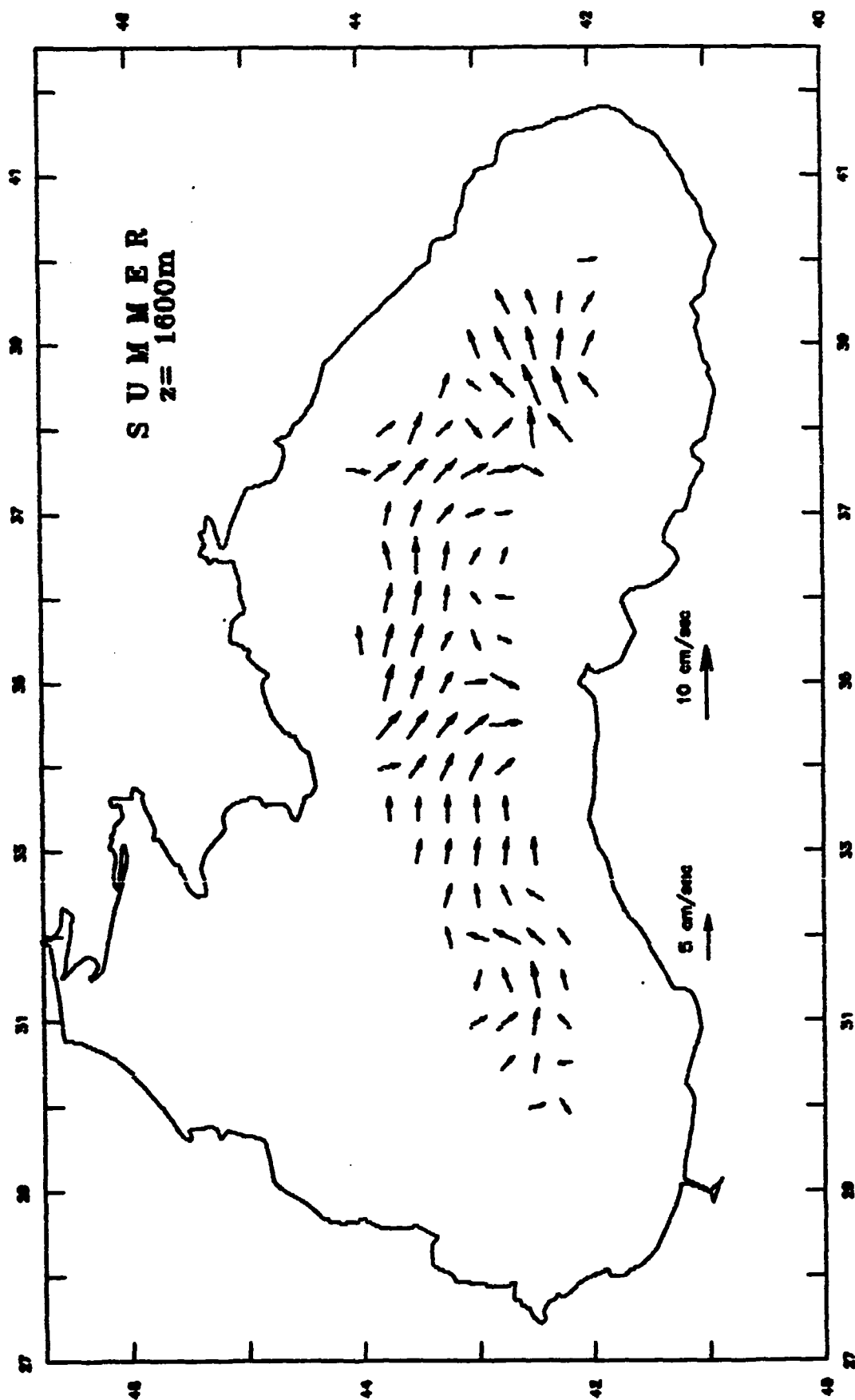
The Black Sea Climate Velocity



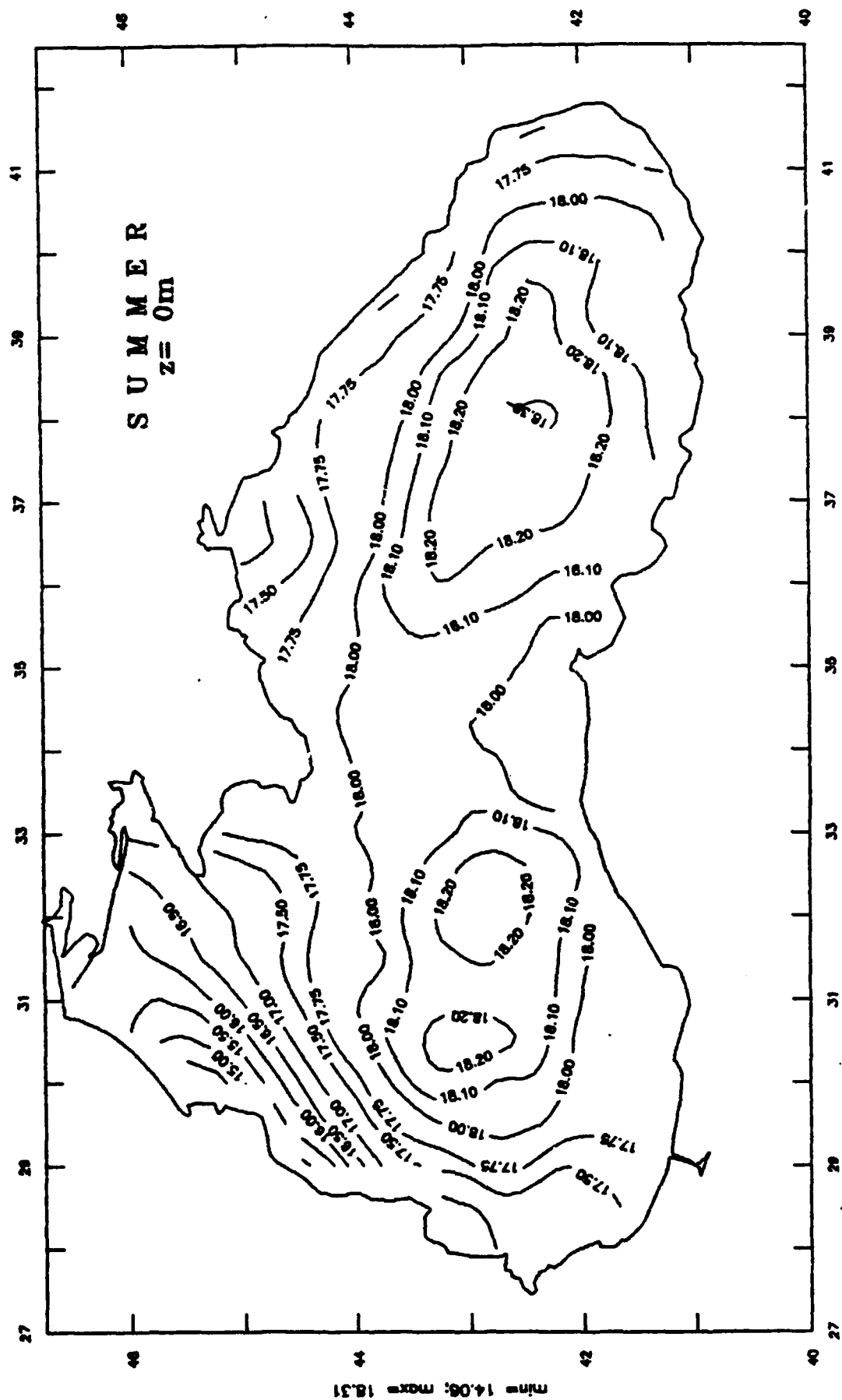
The Black Sea Climate Velocity



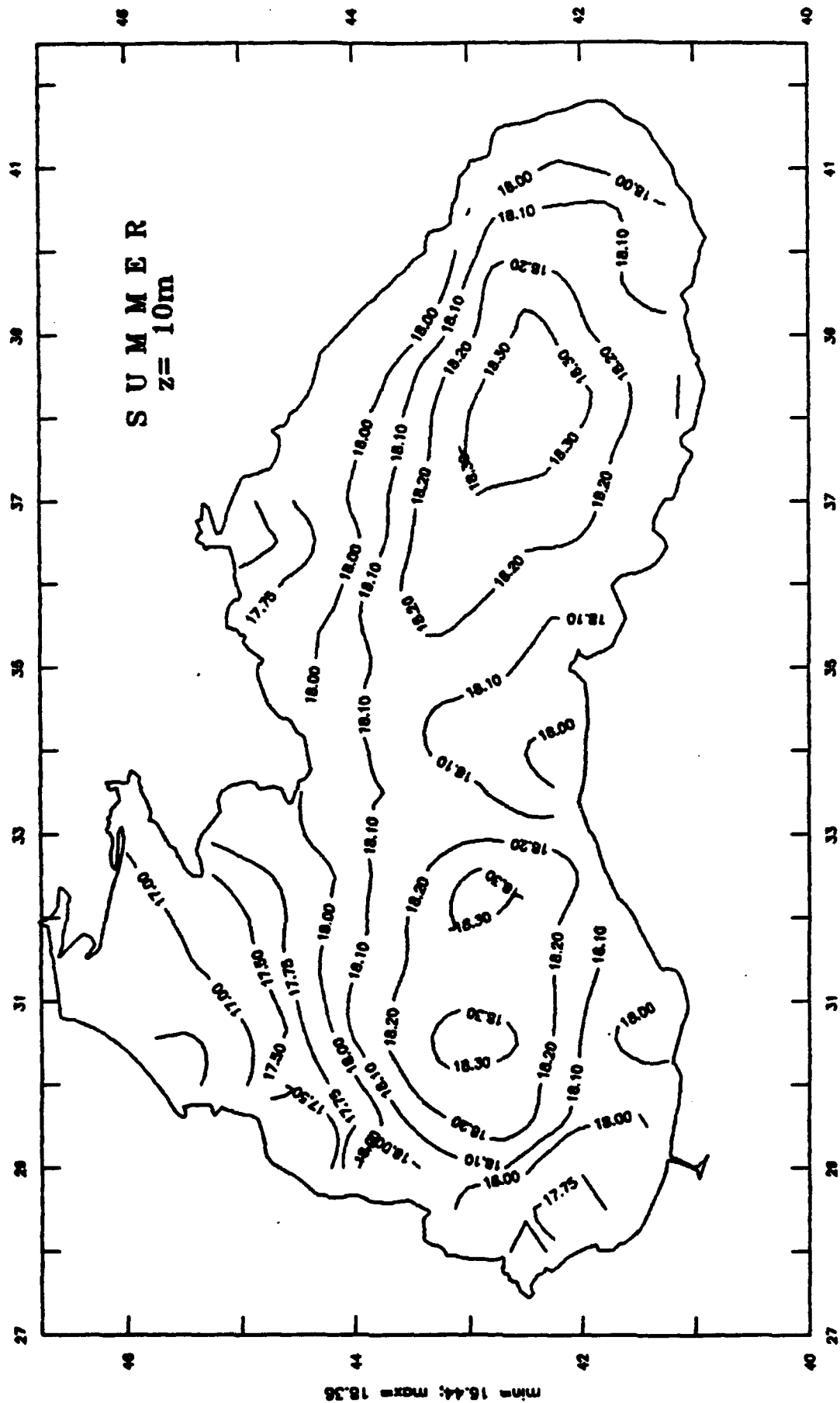
The Black Sea Climate Velocity



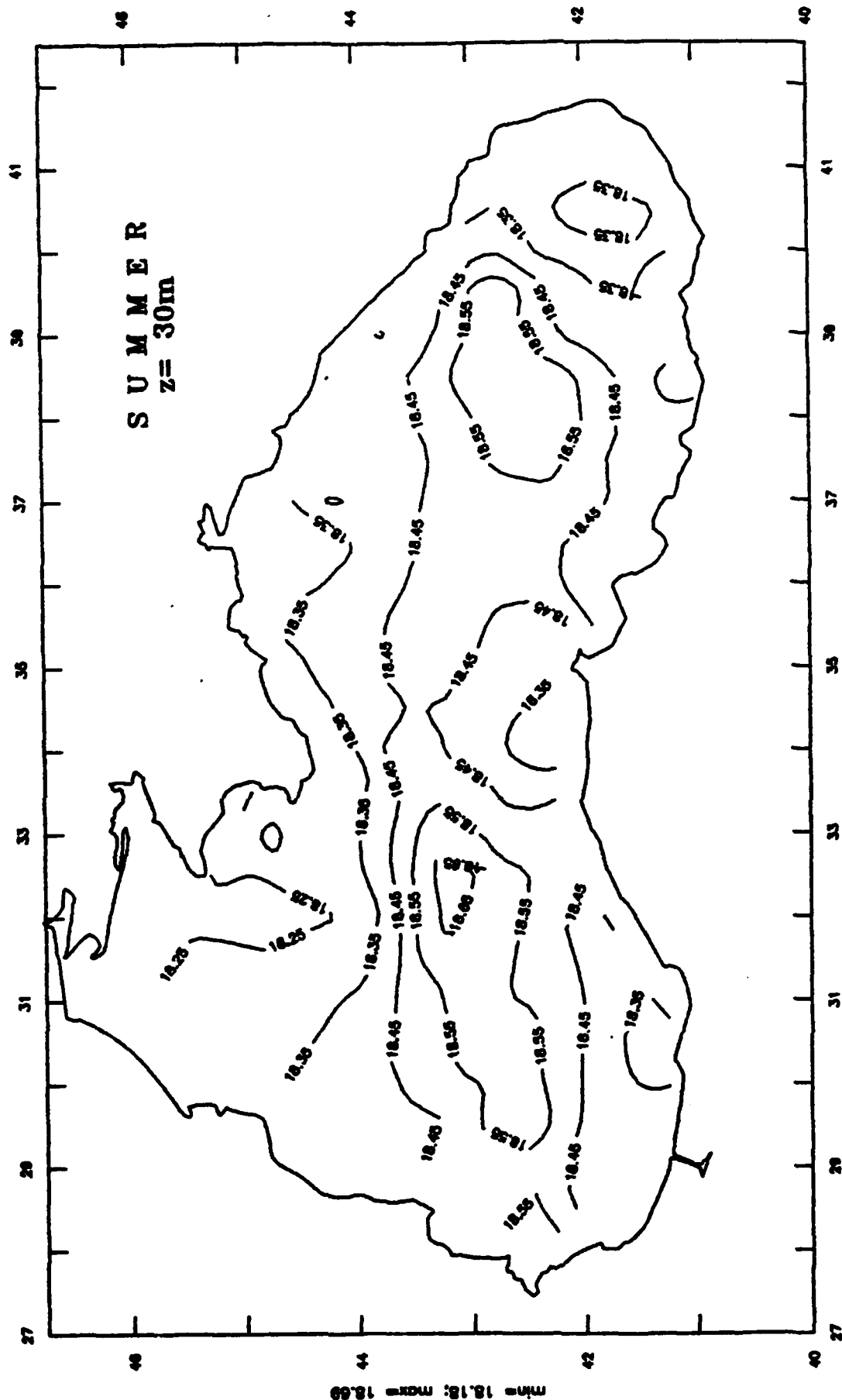
The Black Sea Climate Salinity



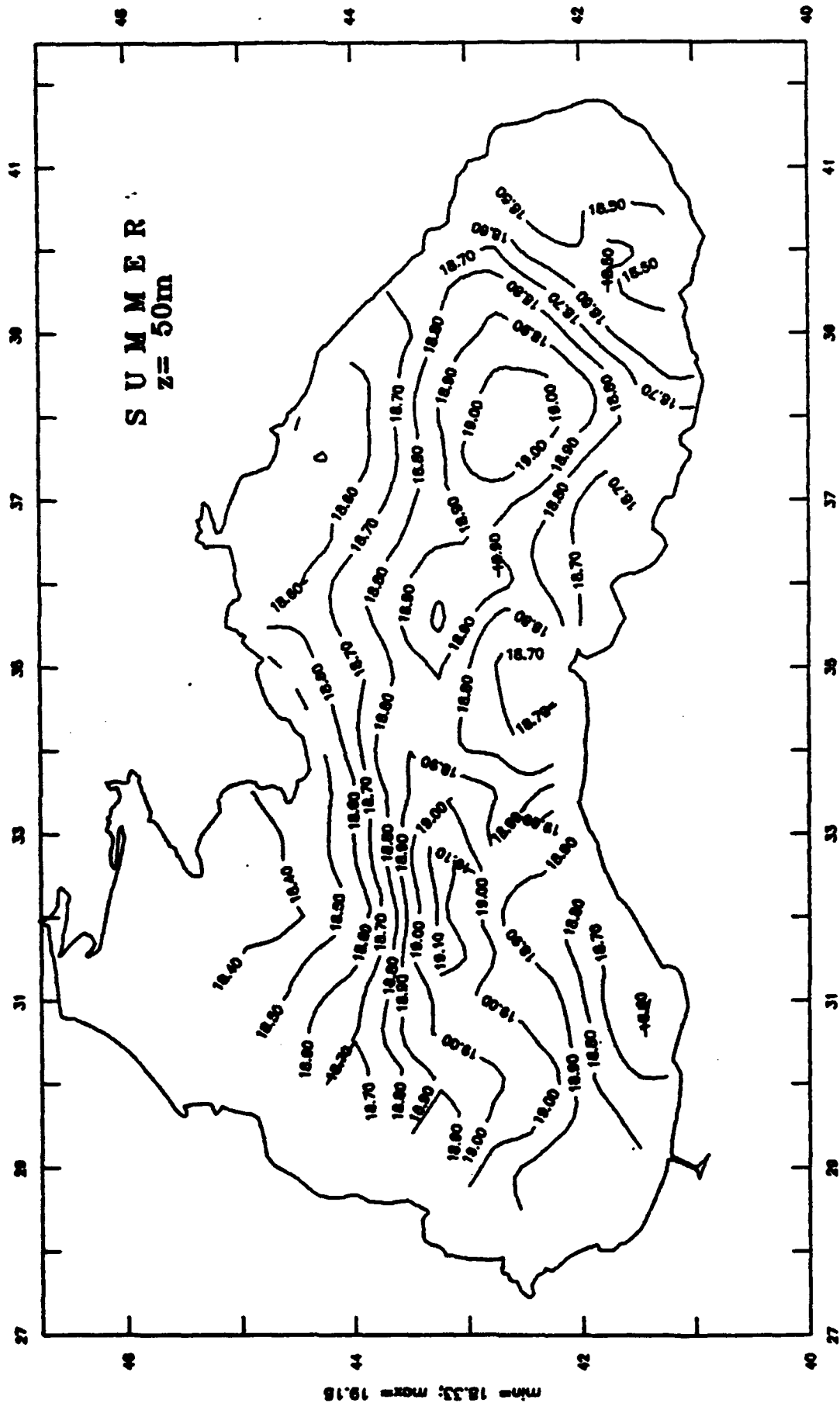
The Black Sea Climate Salinity



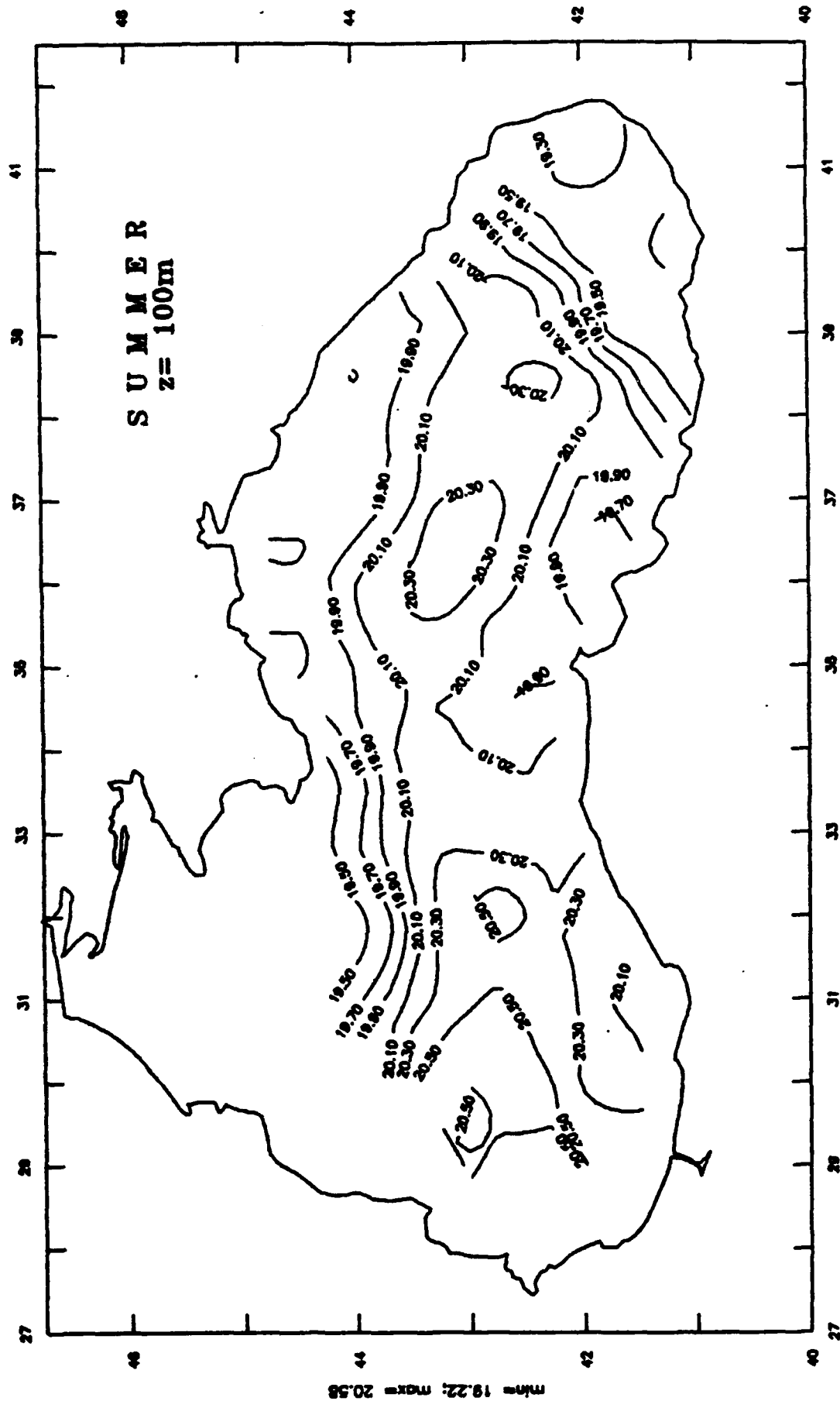
The Black Sea Climate Salinity



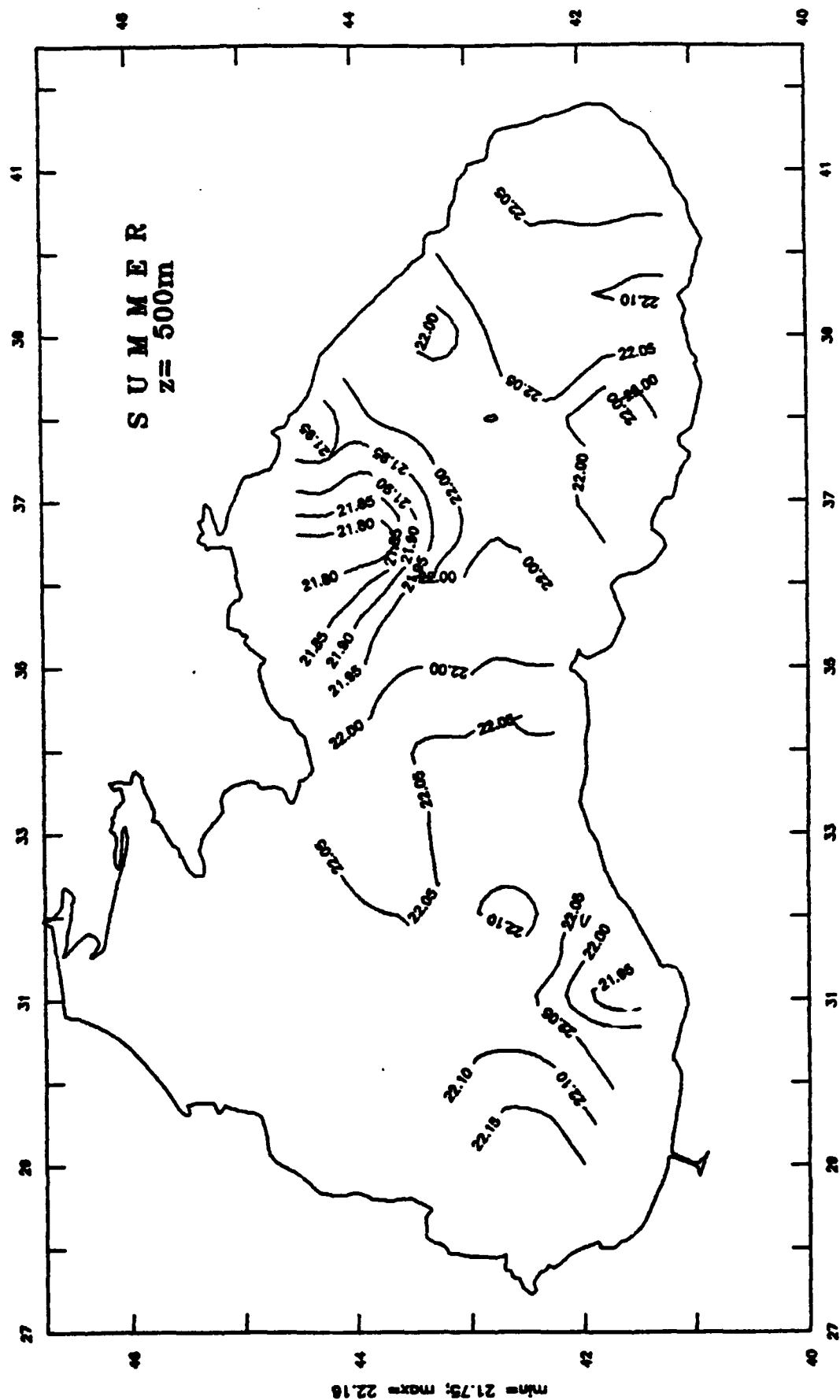
The Black Sea Climate Salinity



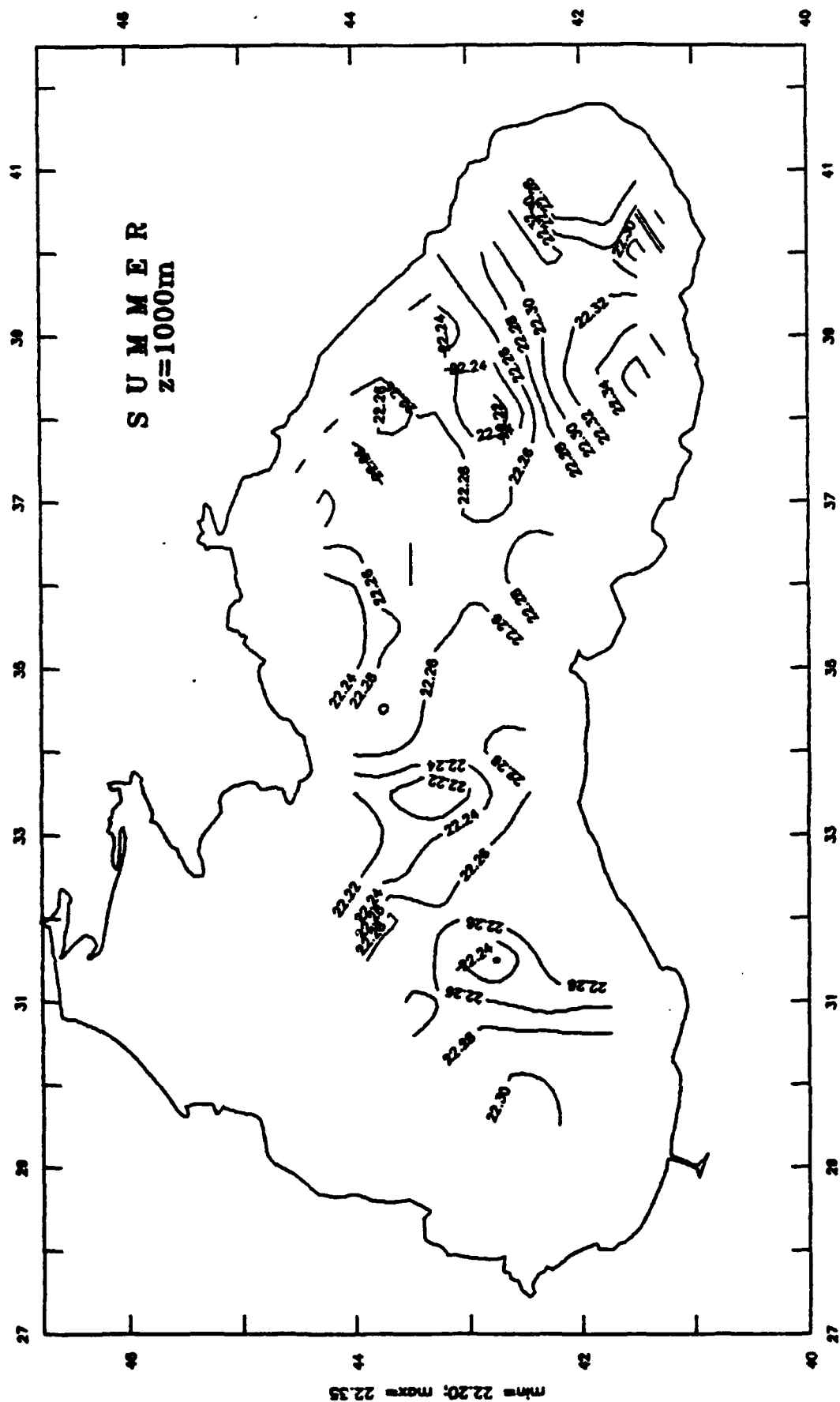
The Black Sea Climate Salinity



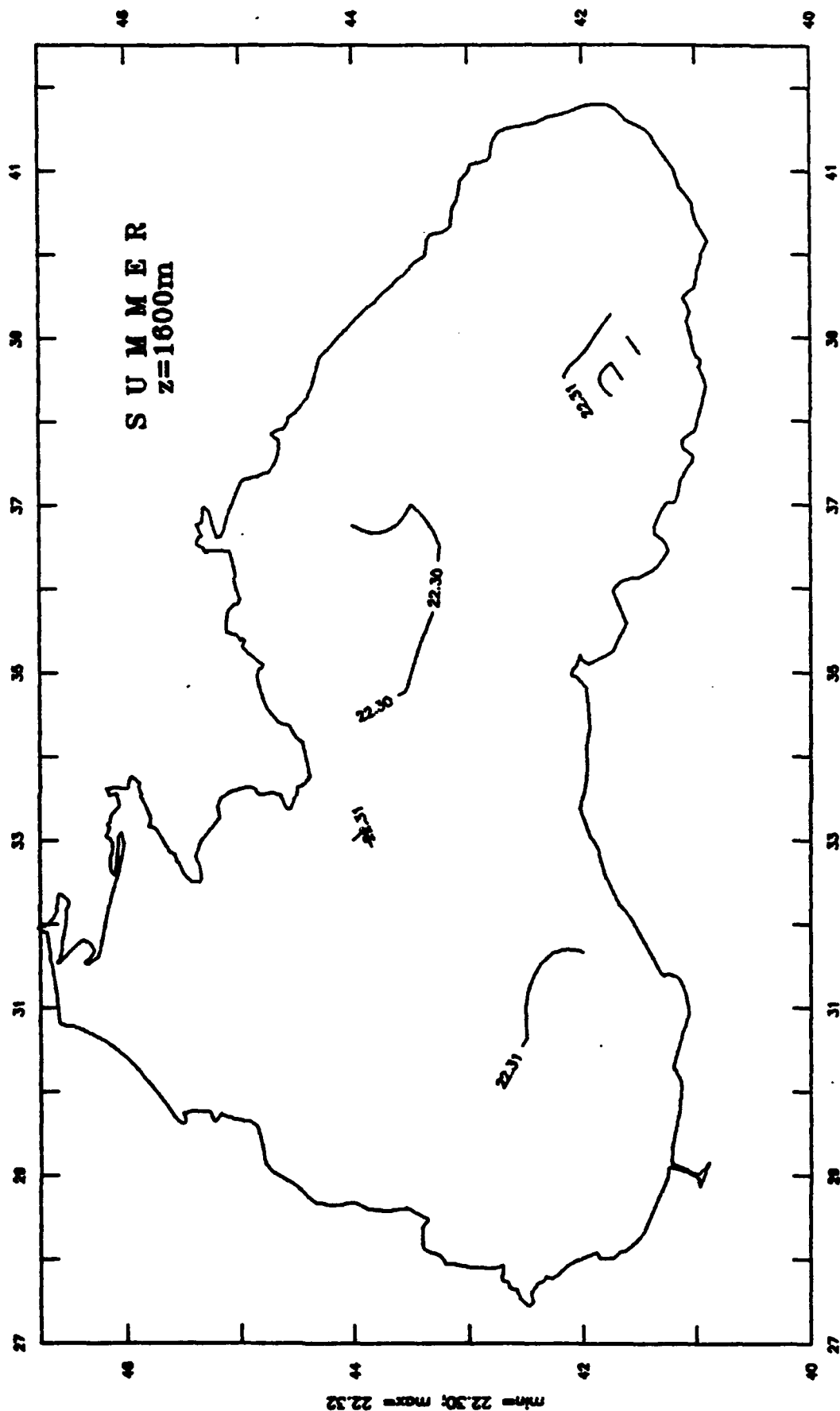
The Black Sea Climate Salinity



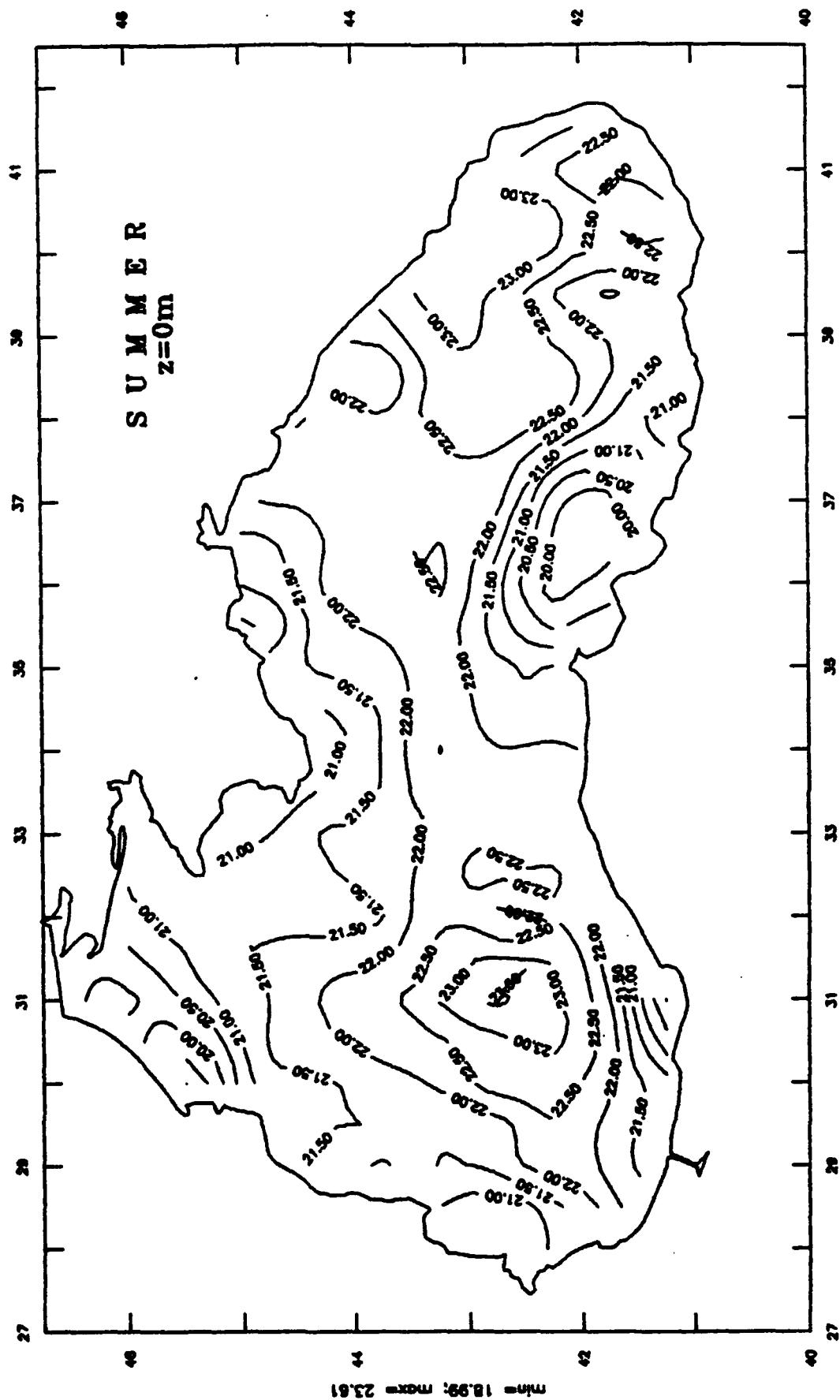
The Black Sea Climate Salinity



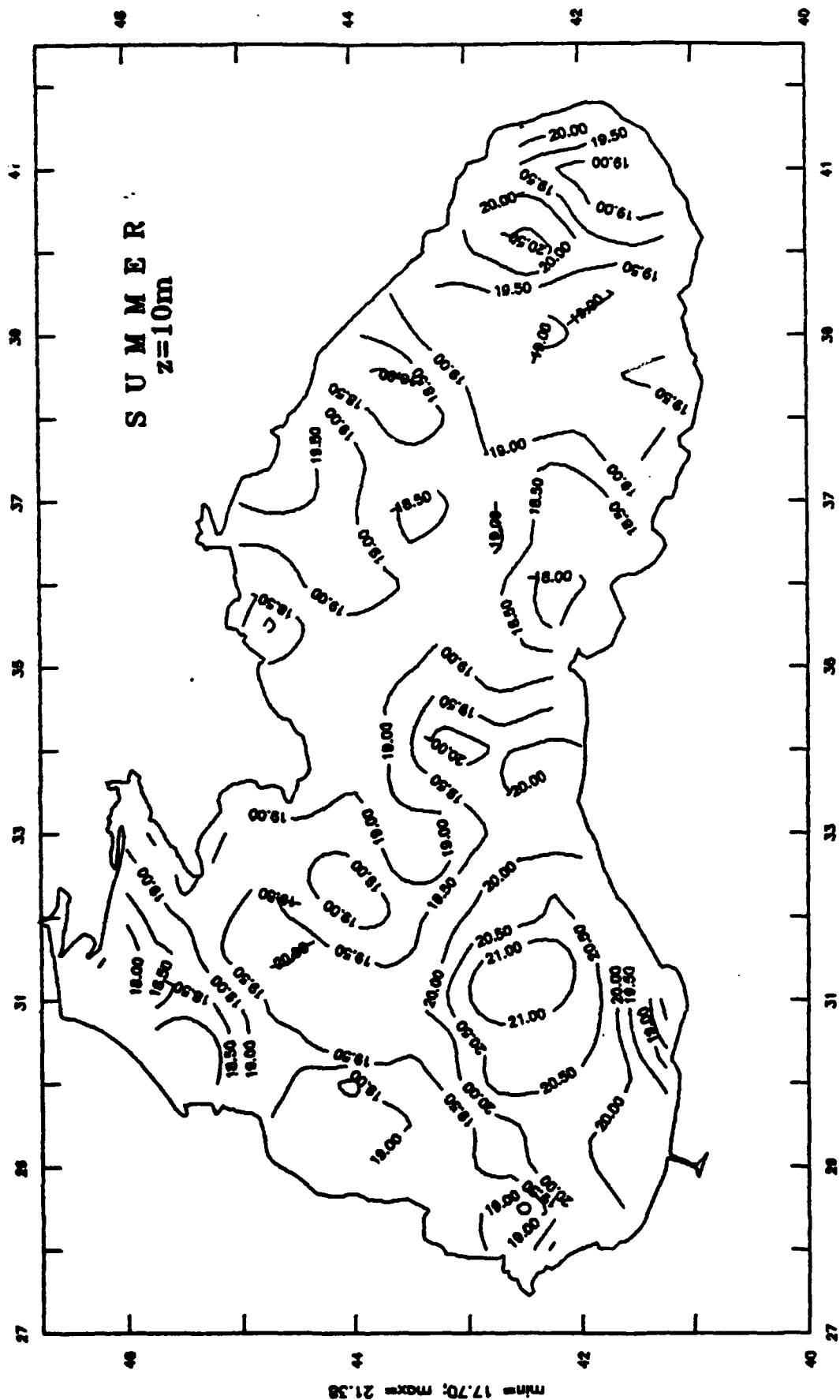
The Black Sea Climate Salinity



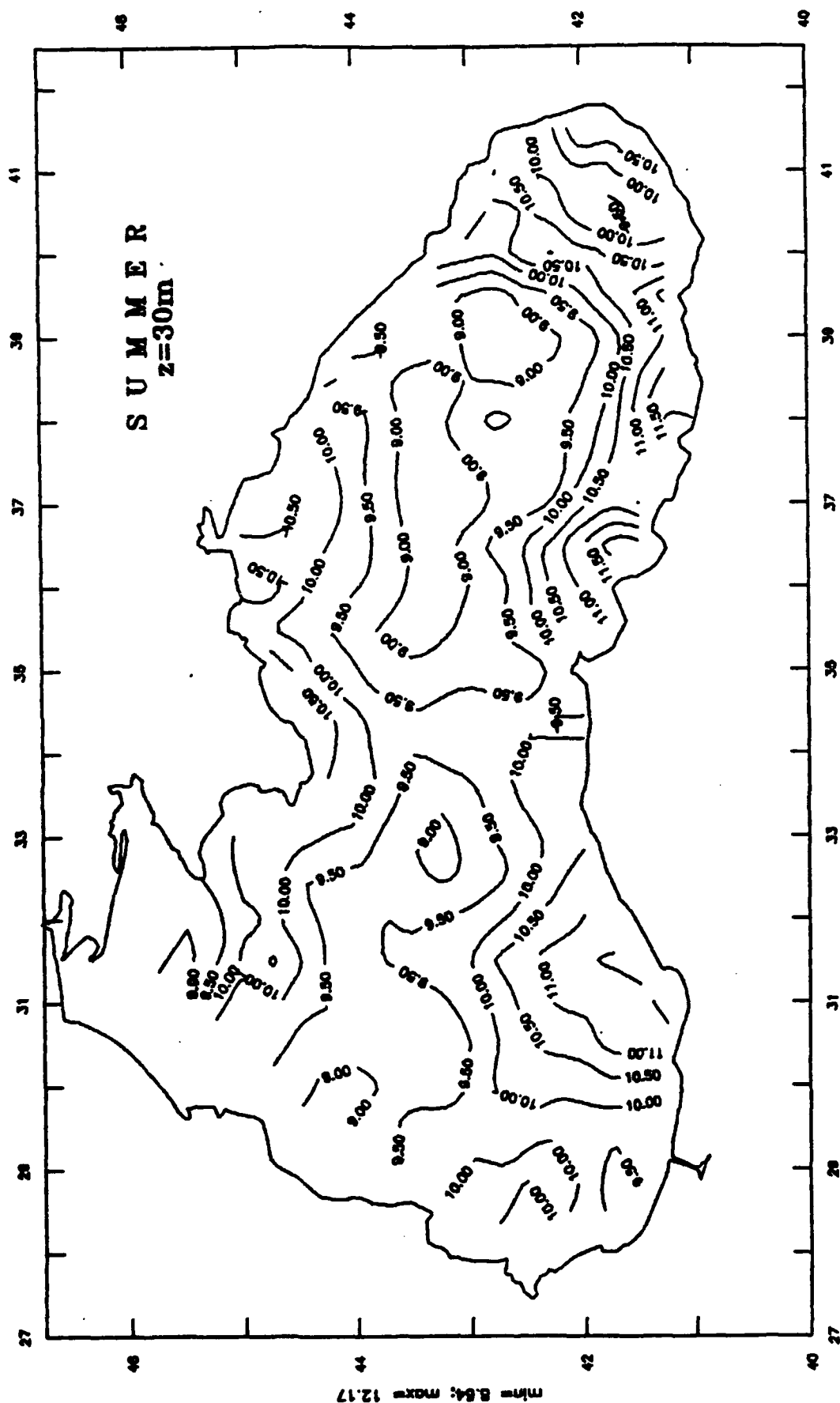
The Black Sea Climate Temperature



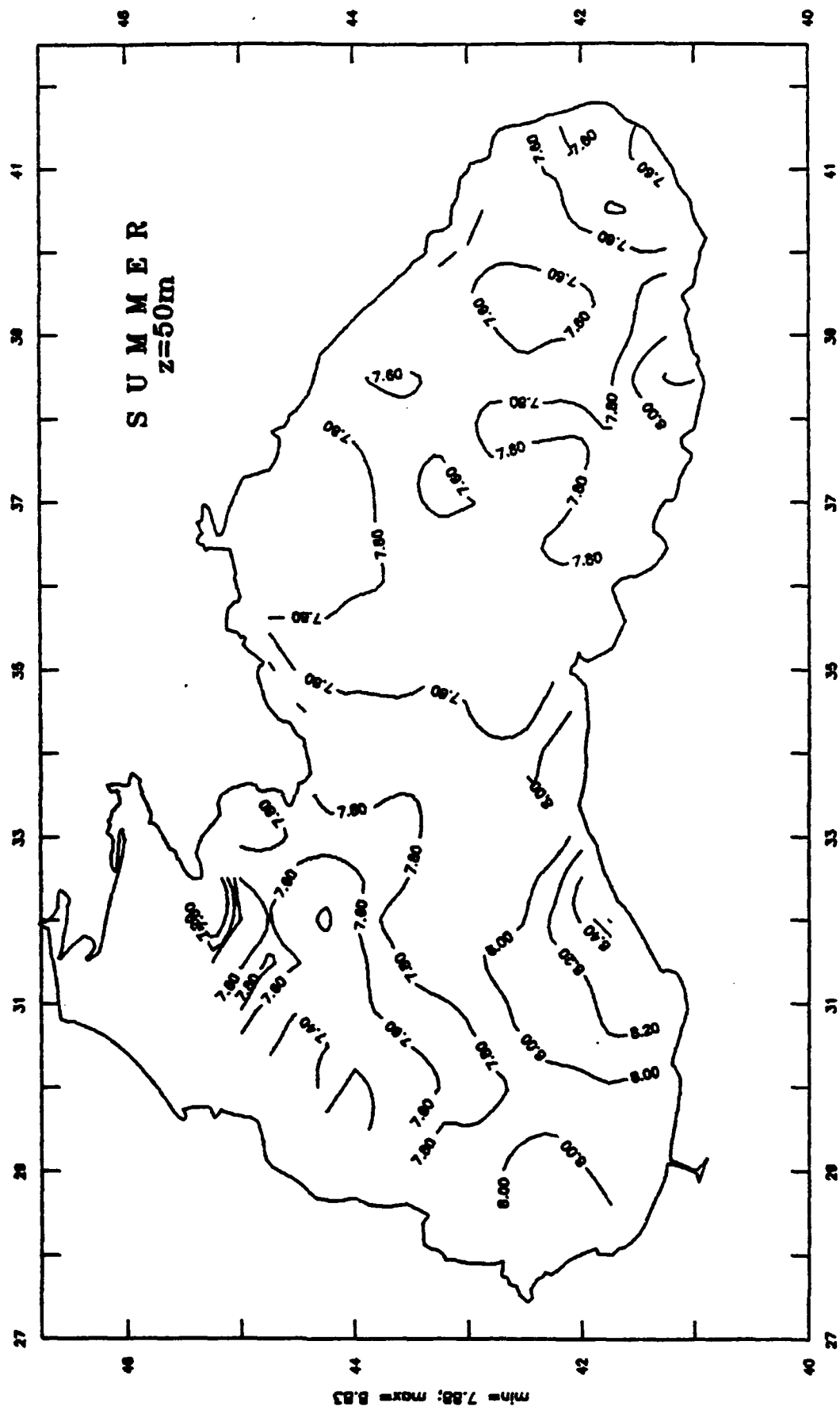
The Black Sea Climate Temperature



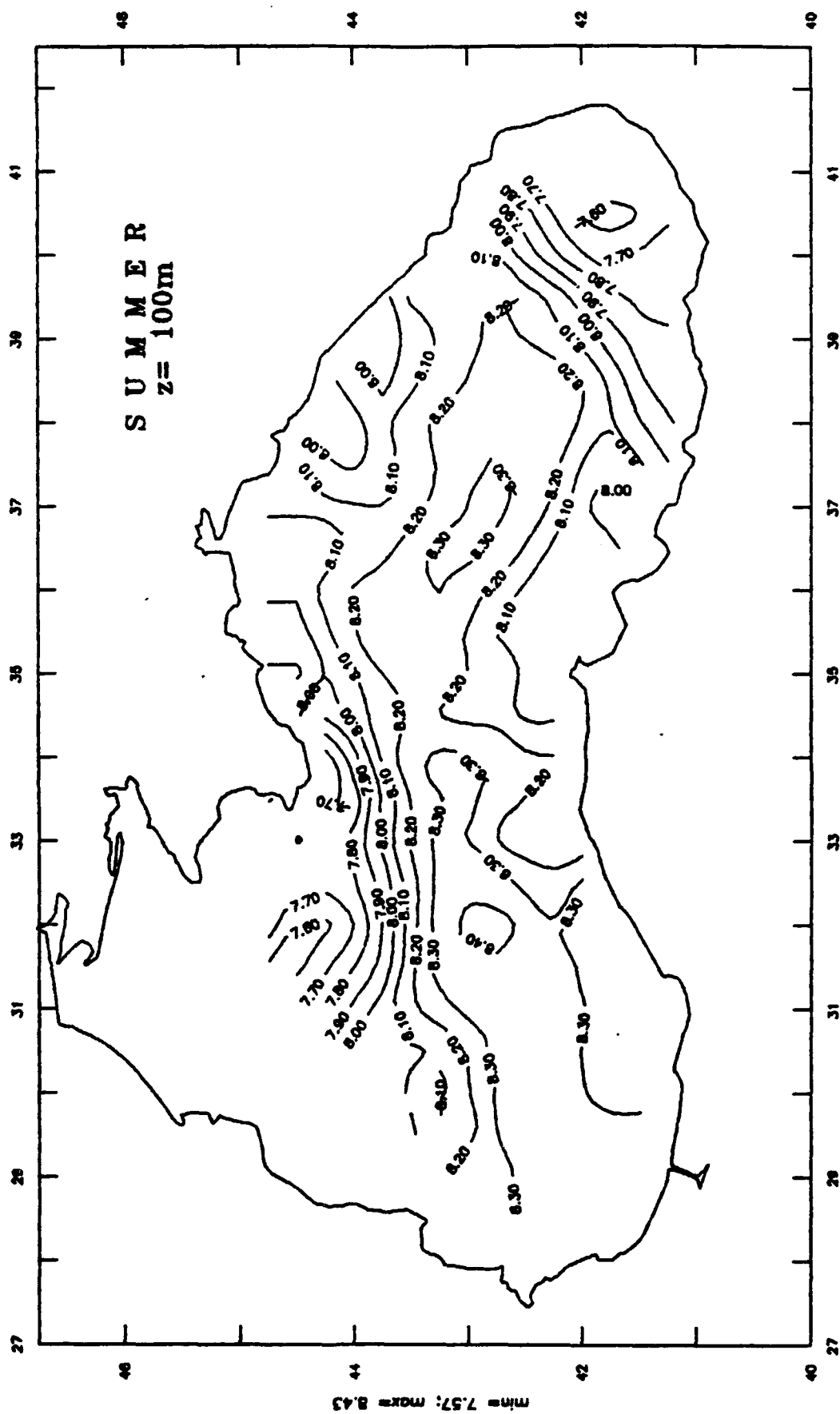
The Black Sea Climate Temperature



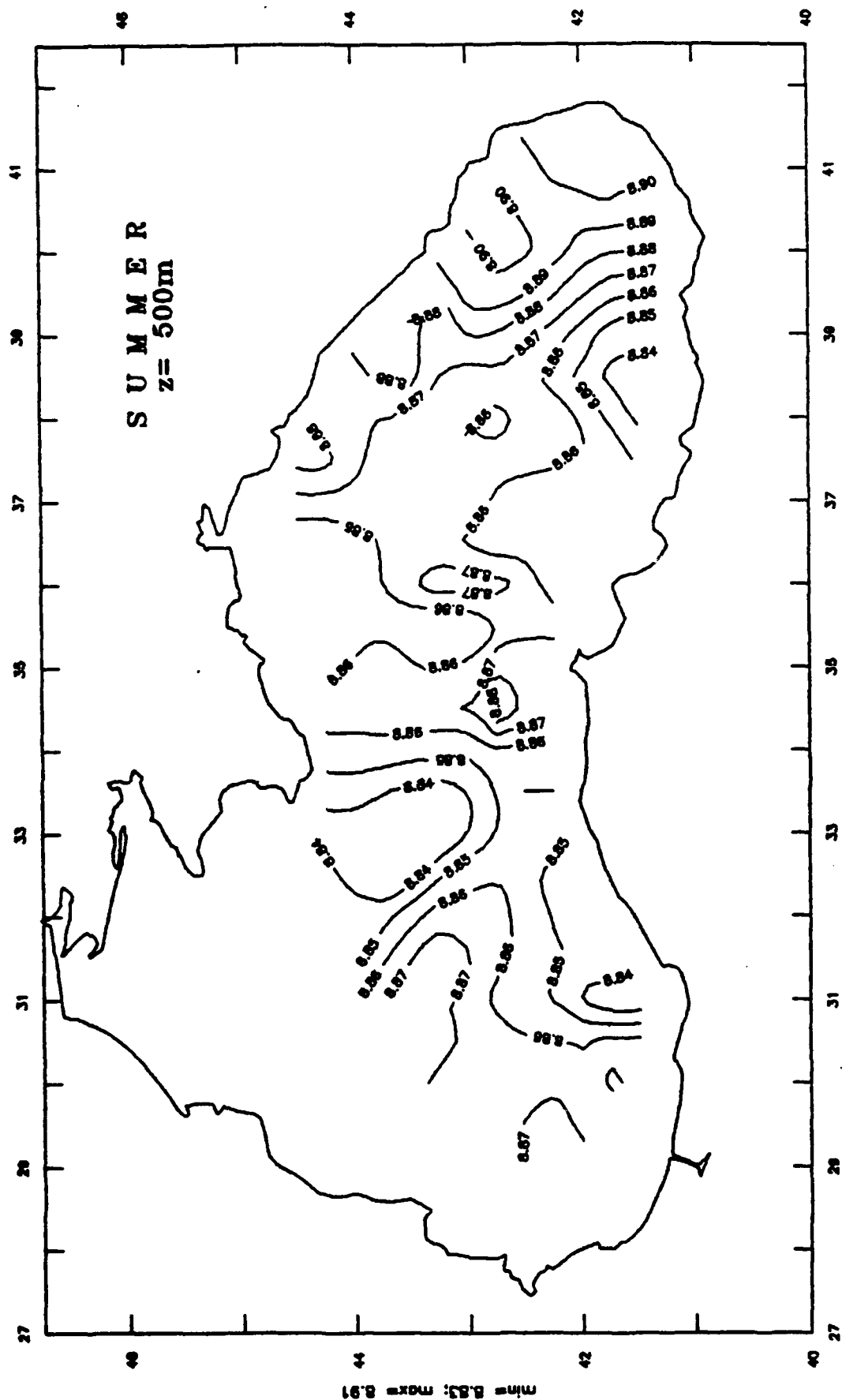
The Black Sea Climate Temperature



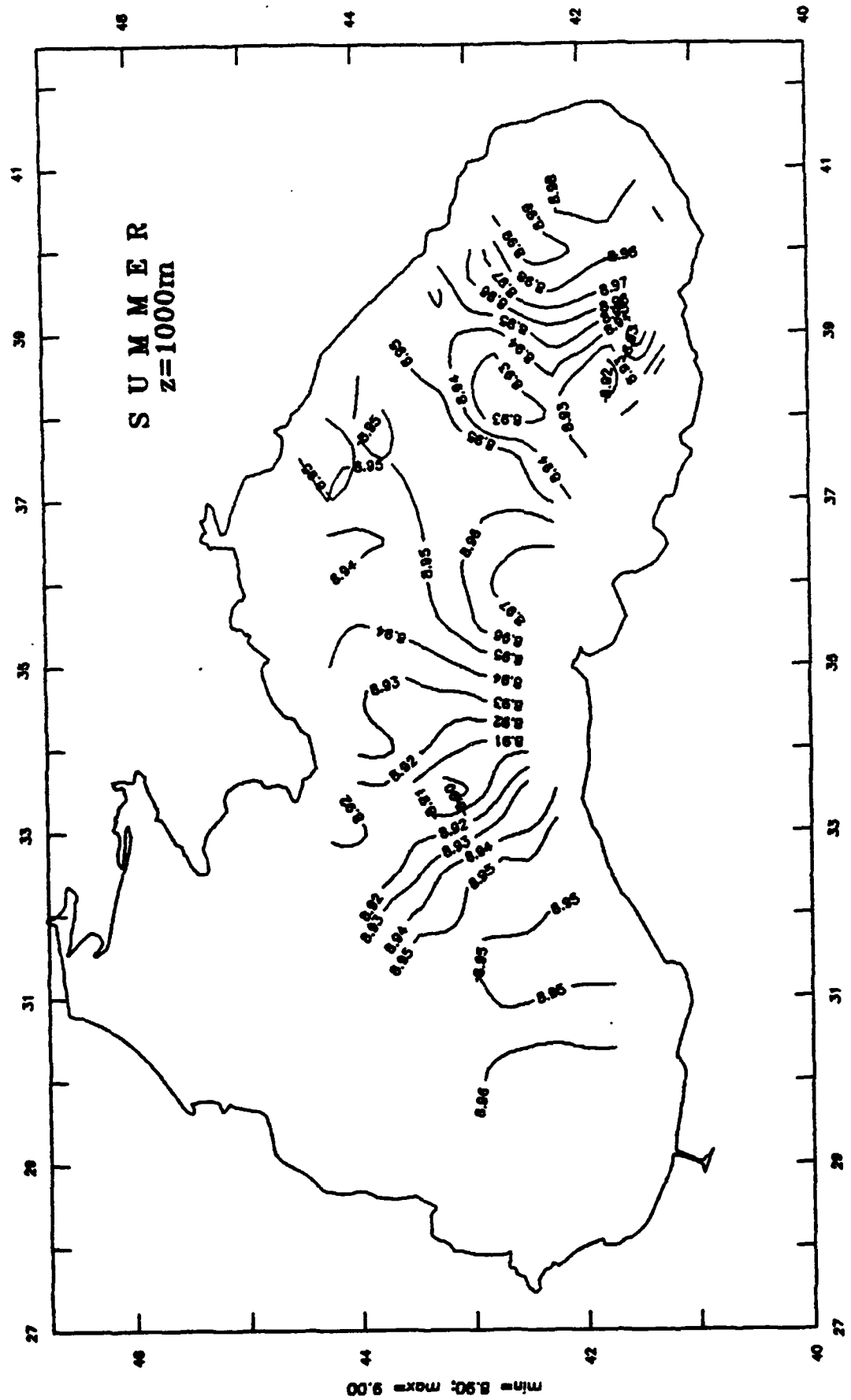
The Black Sea Climate Temperature



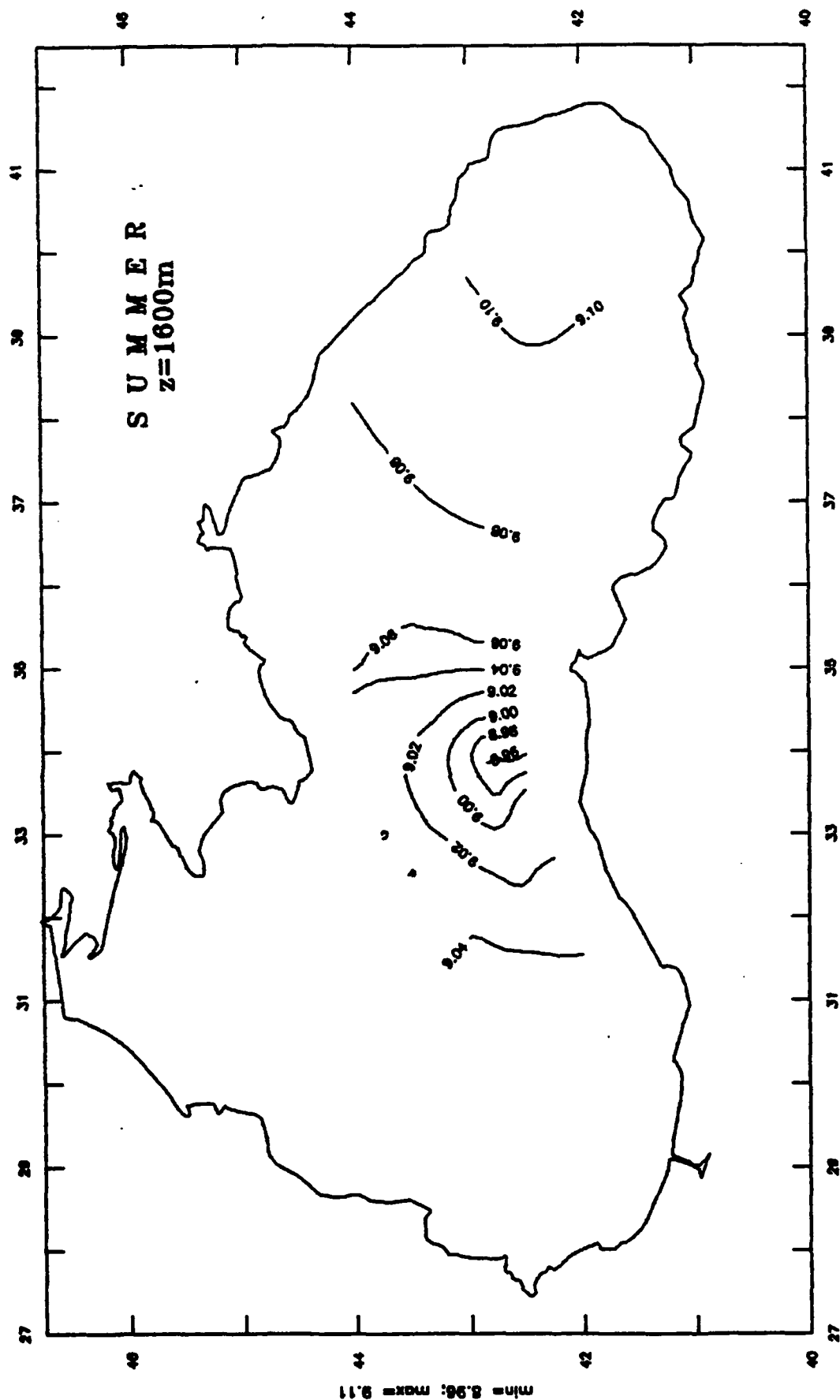
The Black Sea Climate Temperature



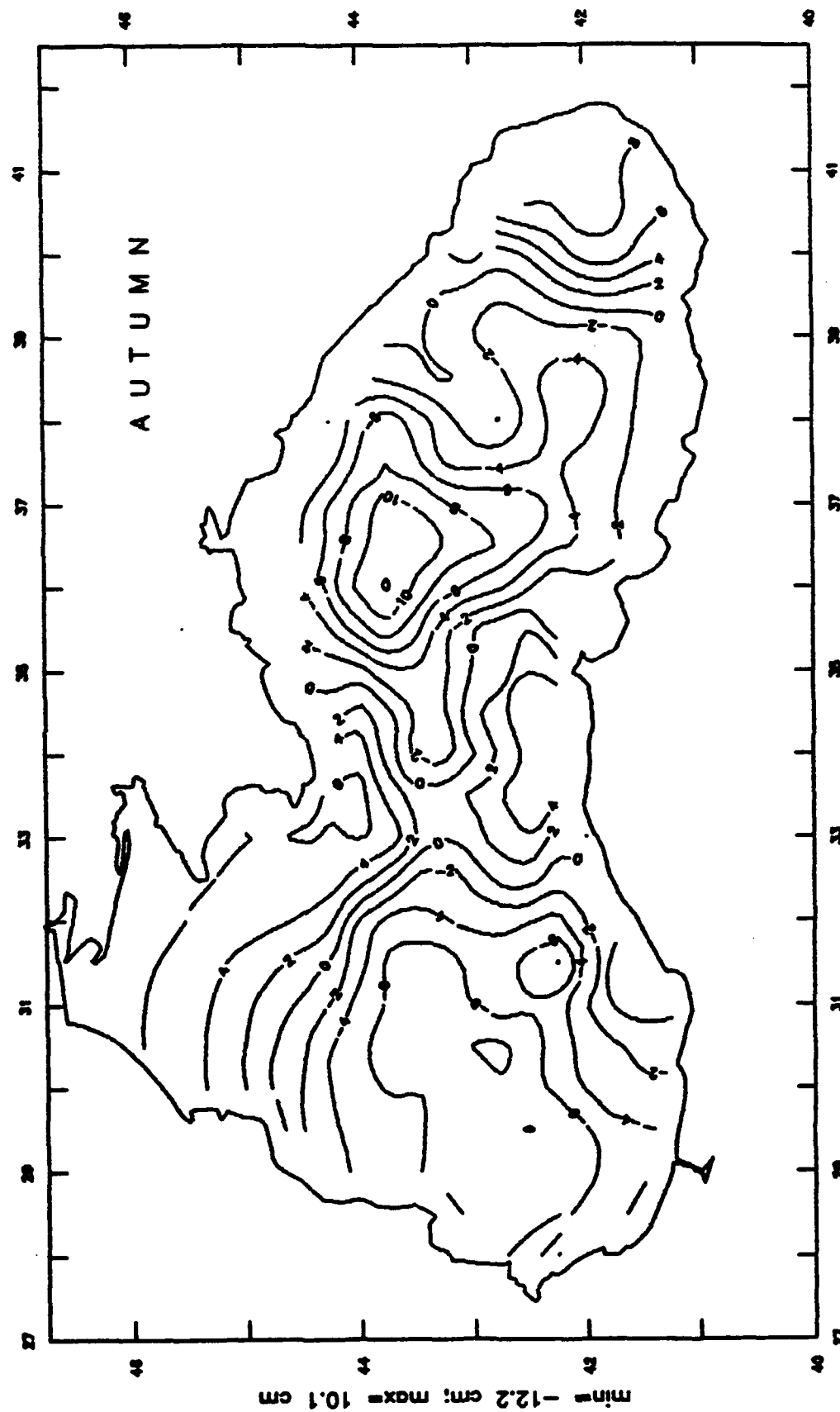
The Black Sea Climate Temperature



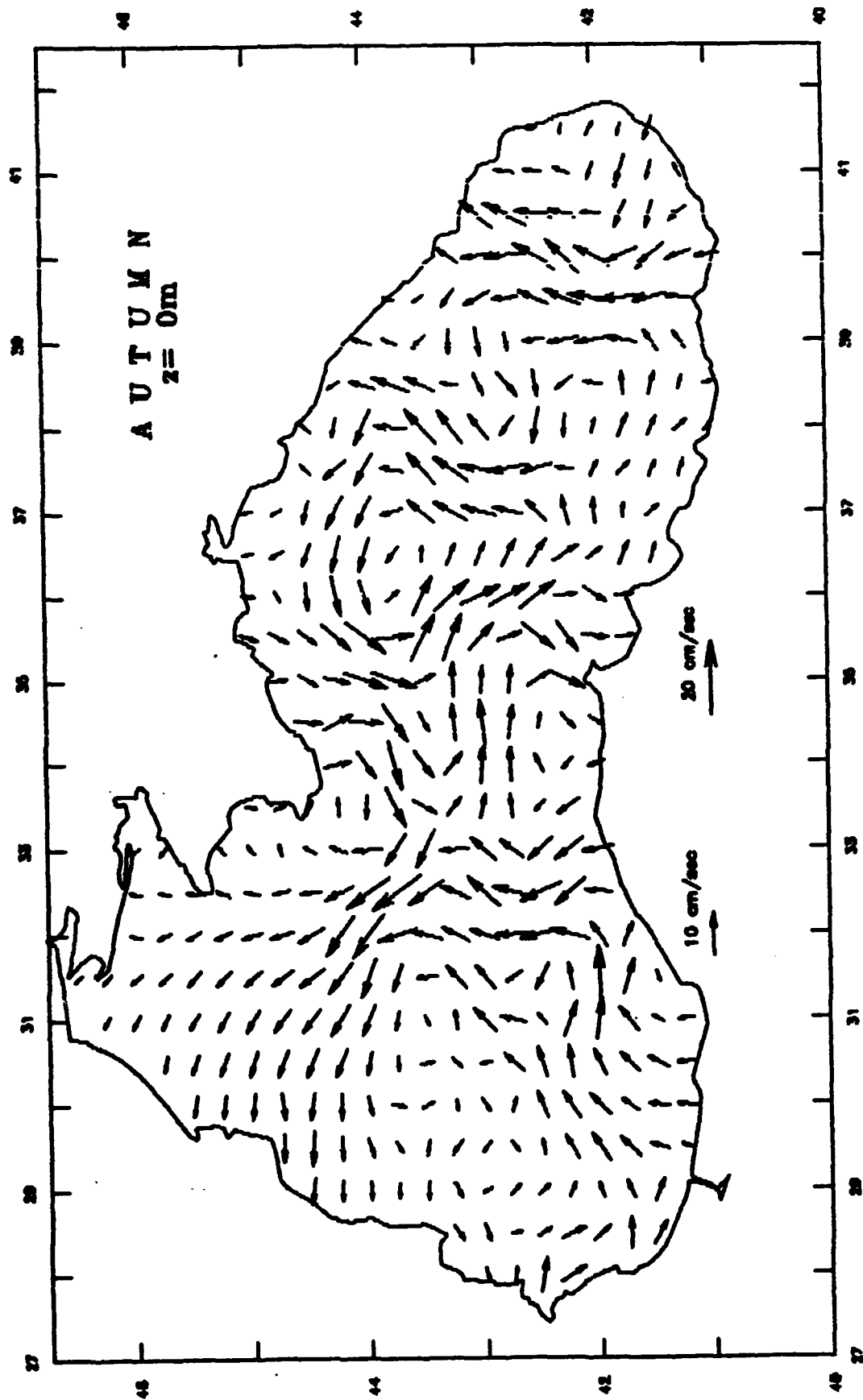
The Black Sea Climate Temperature



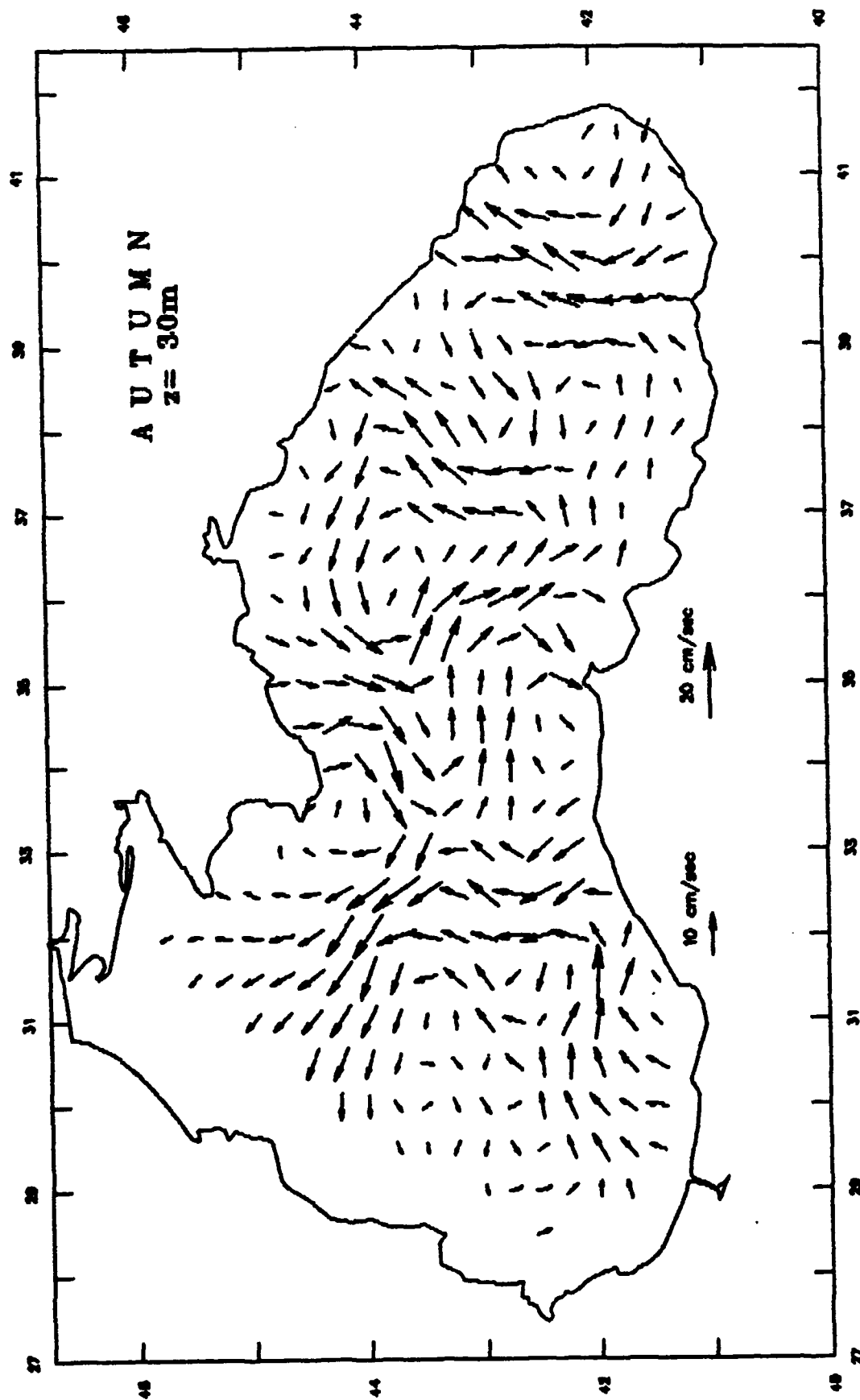
The Black Sea Climate Surface



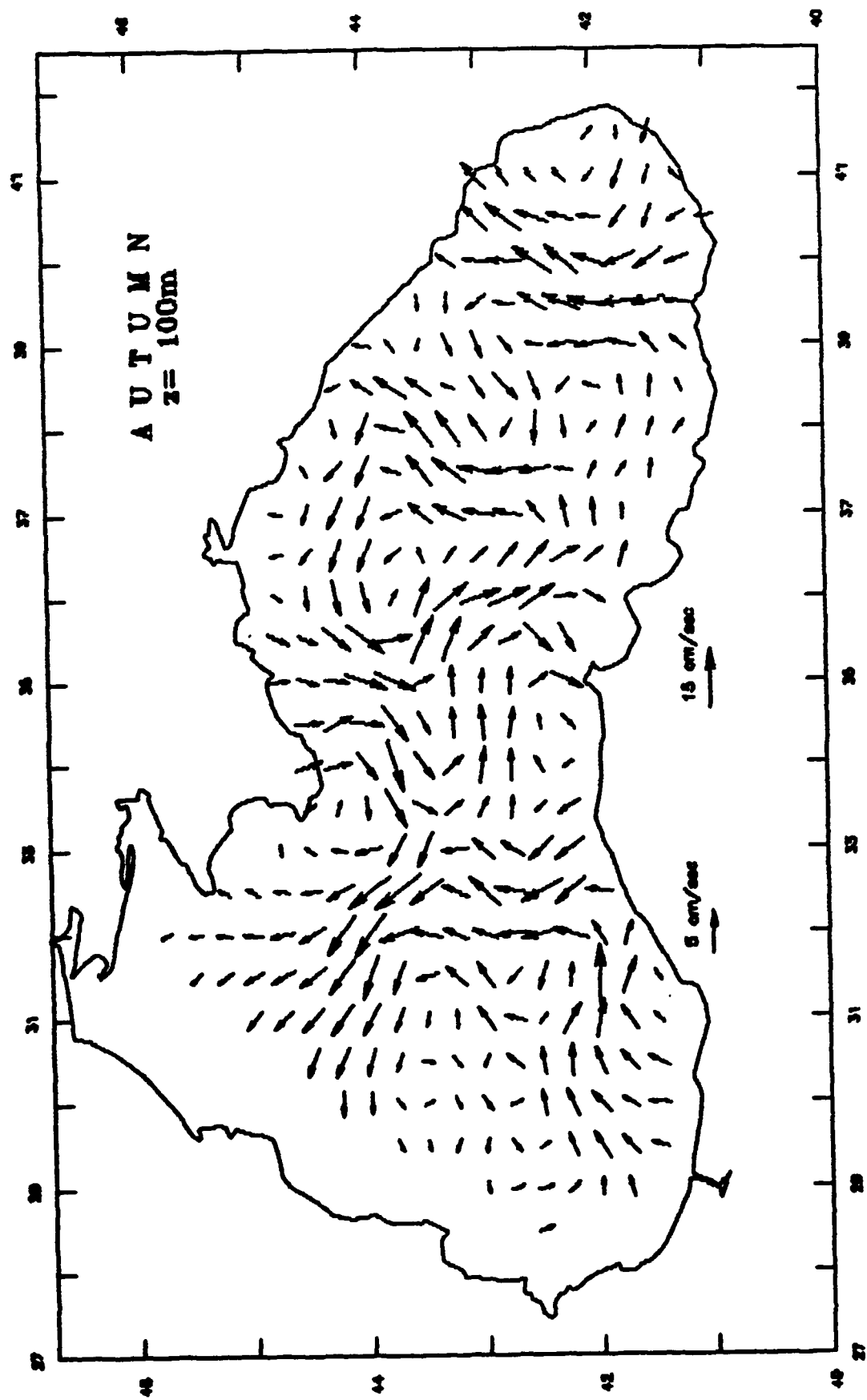
The Black Sea Climate Velocity



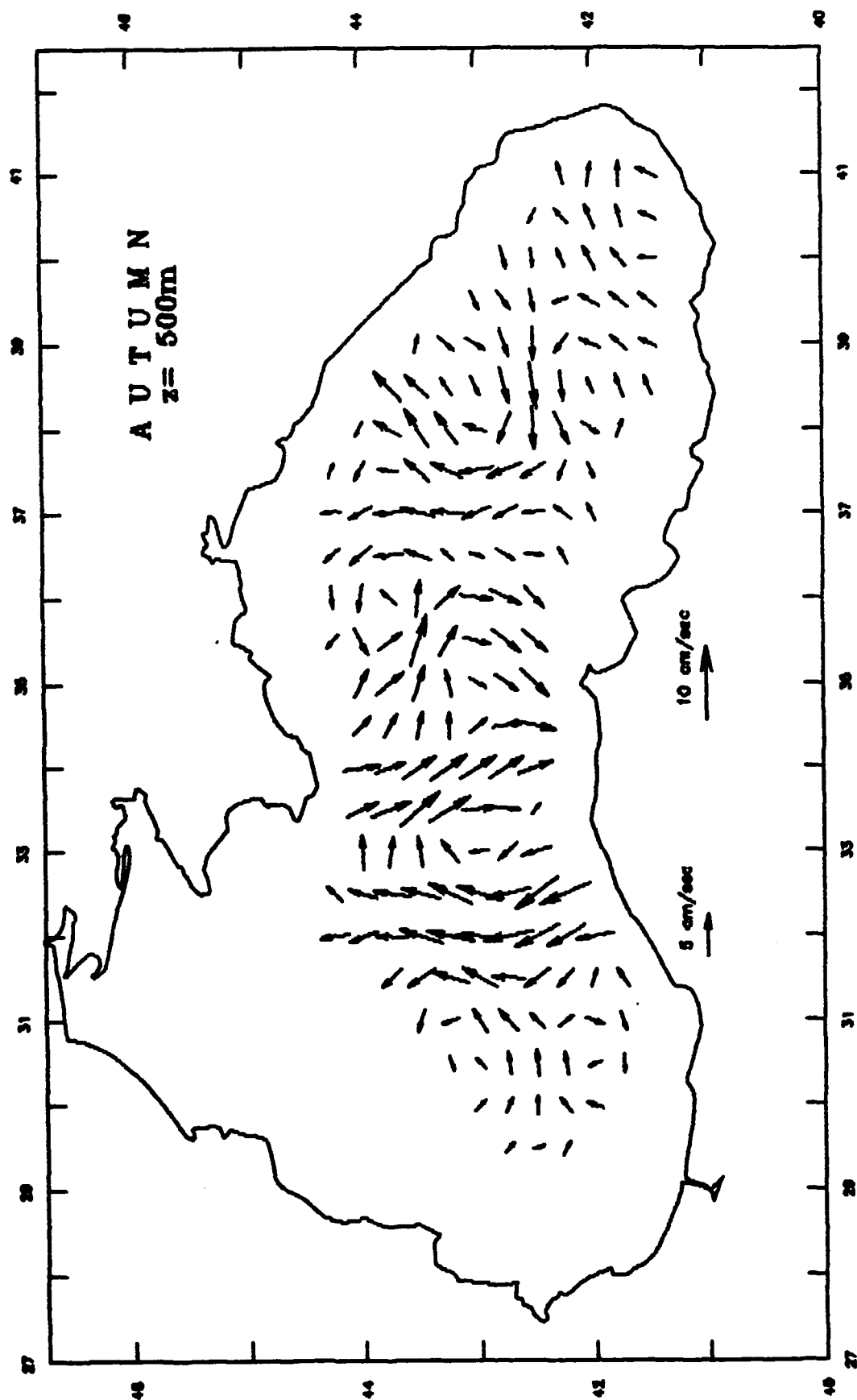
The Black Sea Climate Velocity



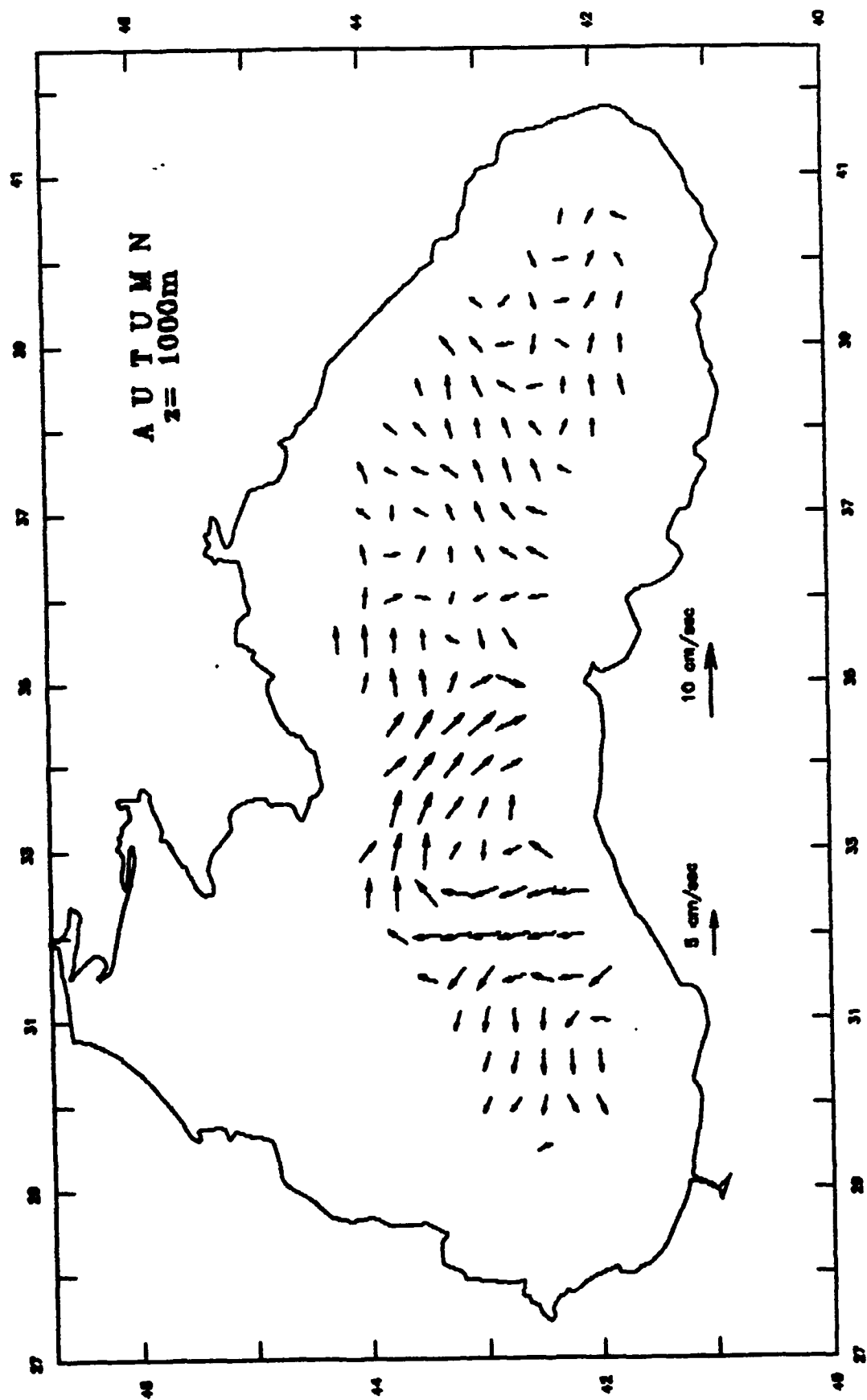
The Black Sea Climate Velocity



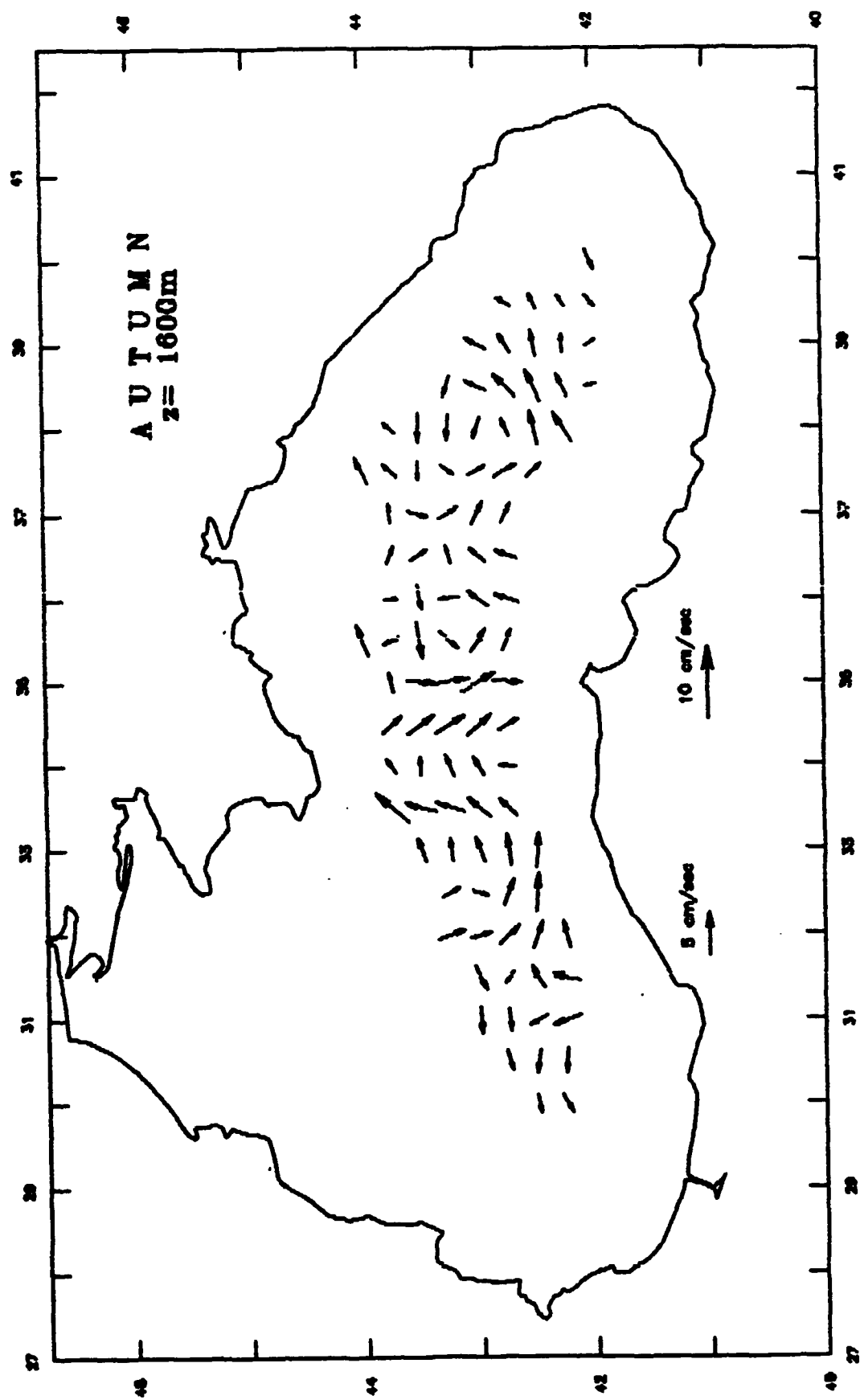
The Black Sea Climate Velocity



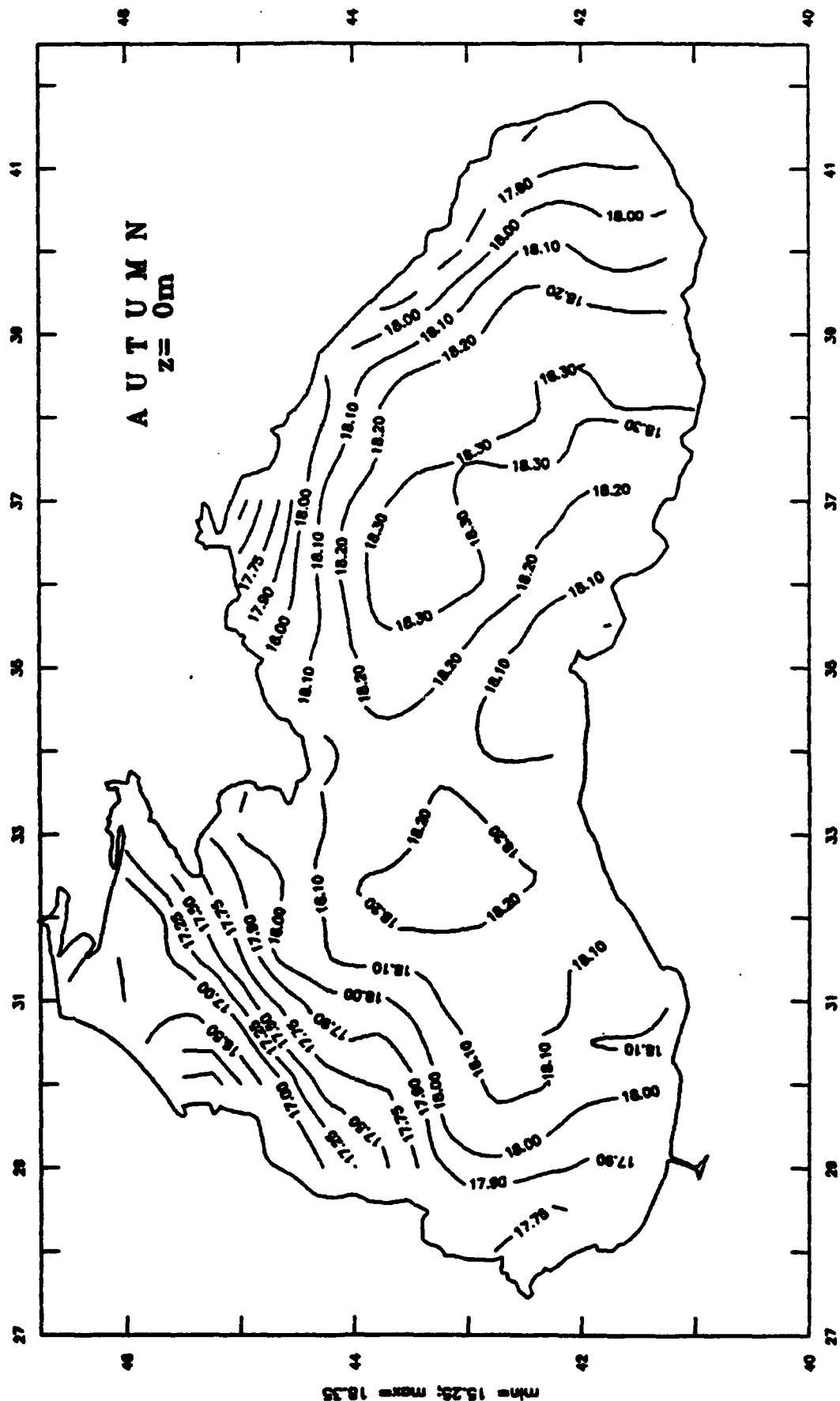
The Black Sea Climate Velocity



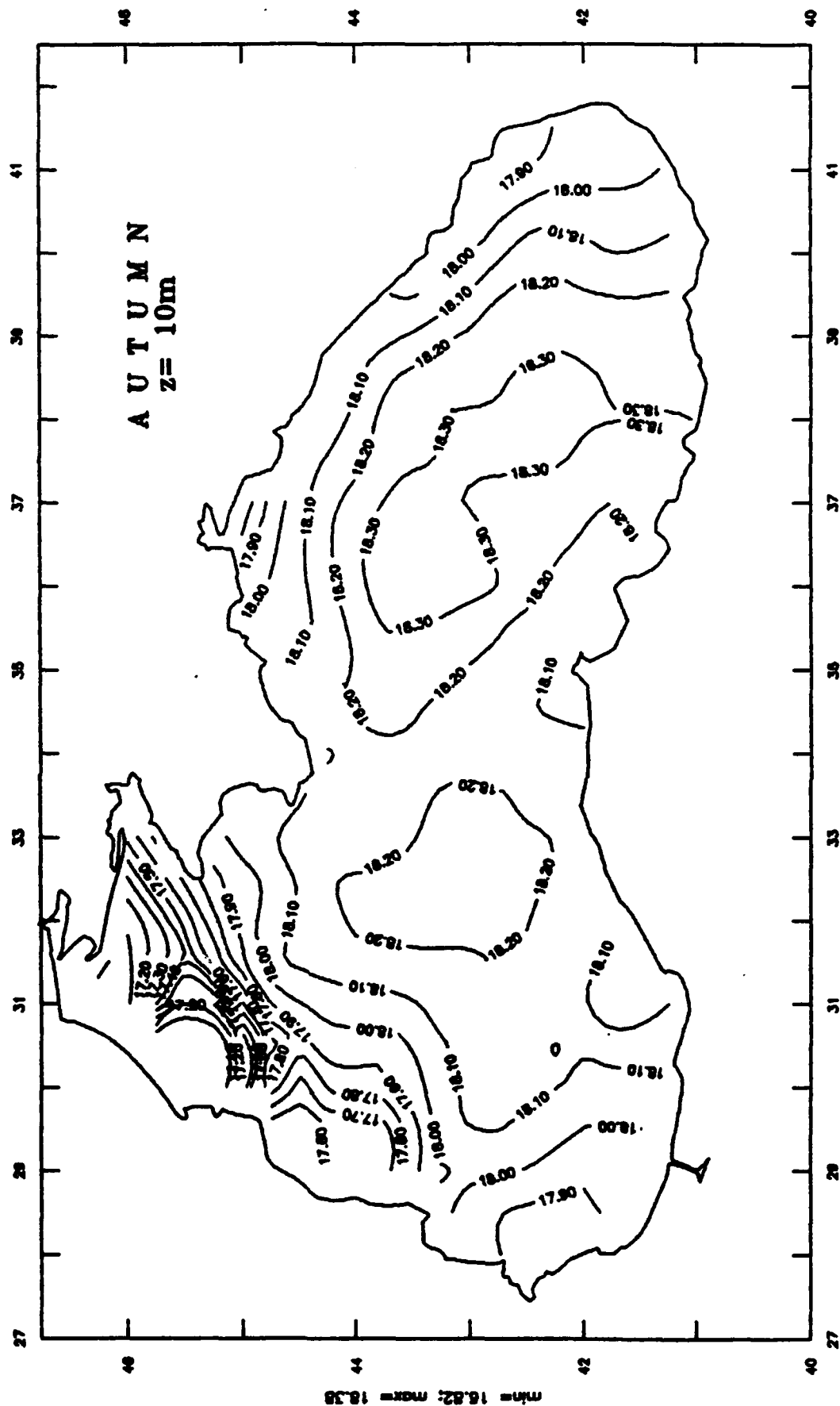
The Black Sea Climate Velocity



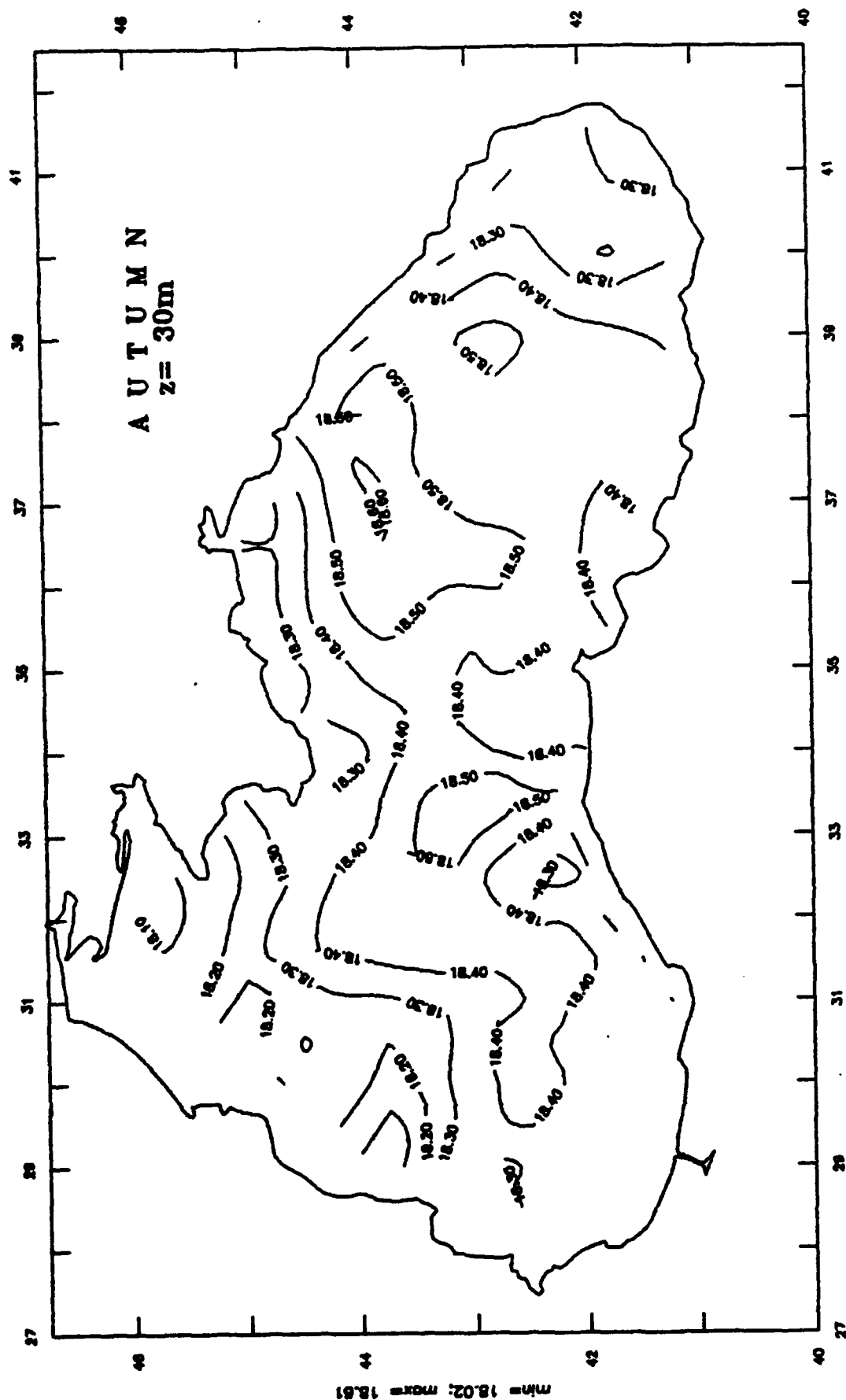
The Black Sea Climate Salinity



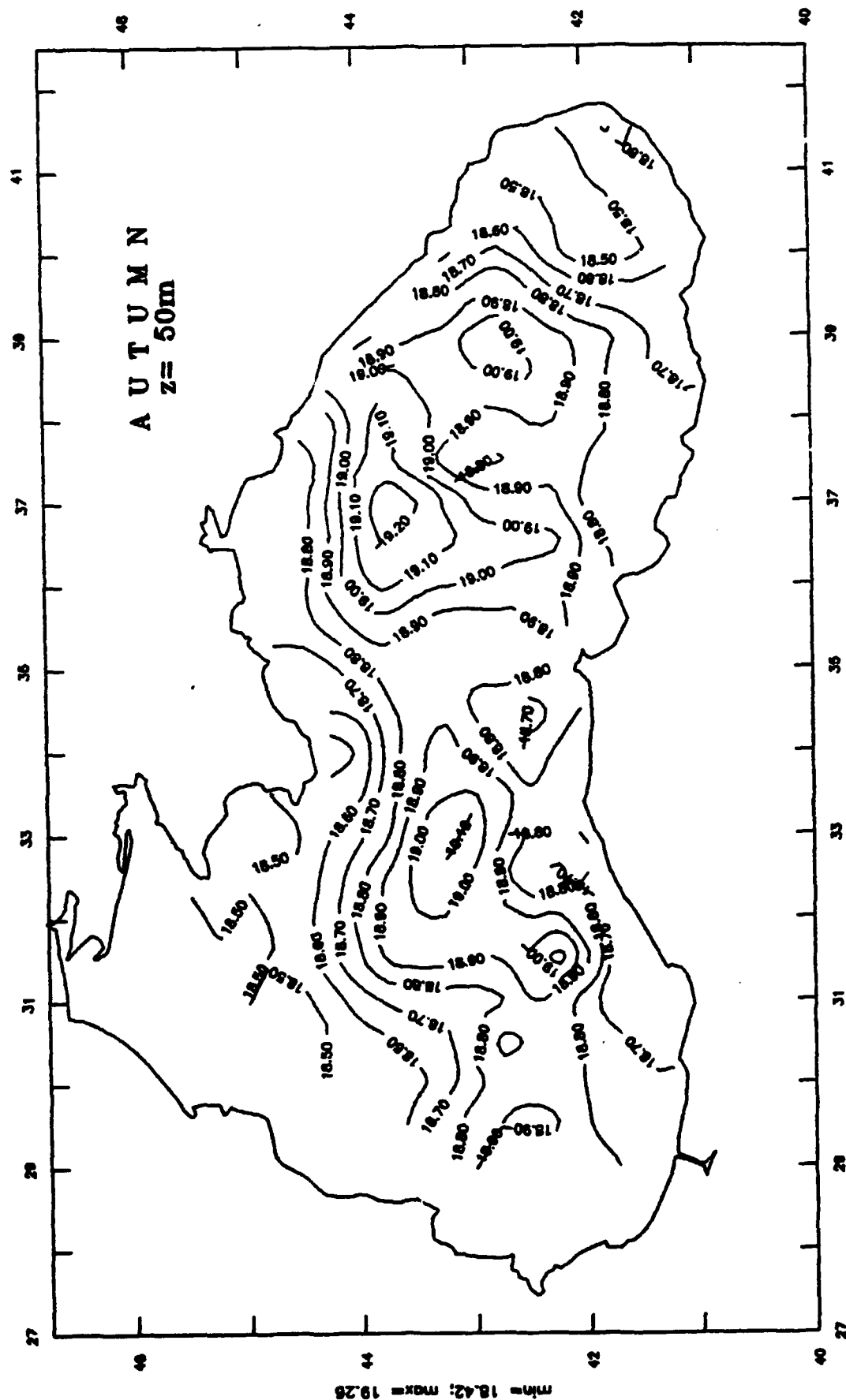
The Black Sea Climate Salinity



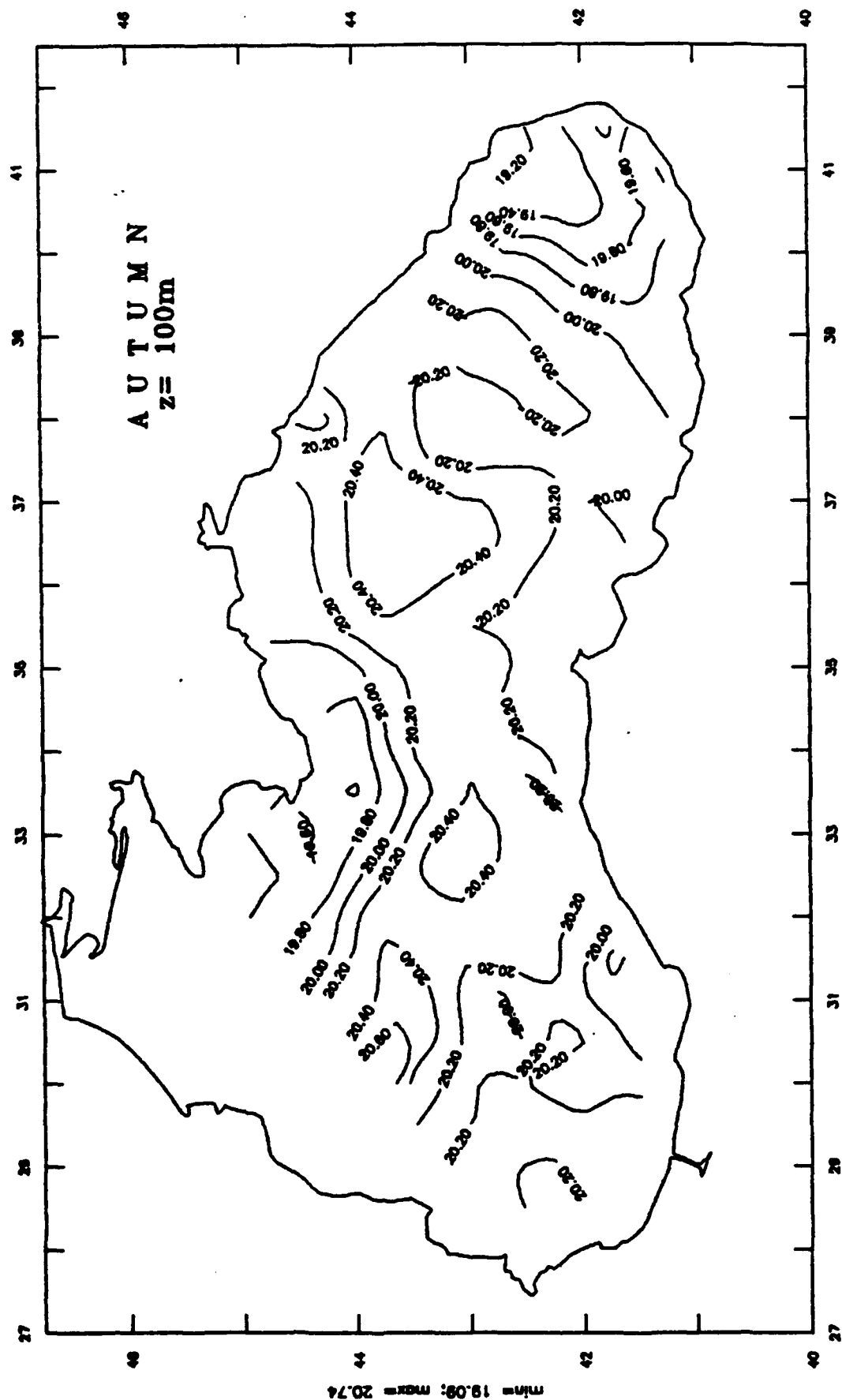
The Black Sea Climate Salinity



The Black Sea Climate Salinity



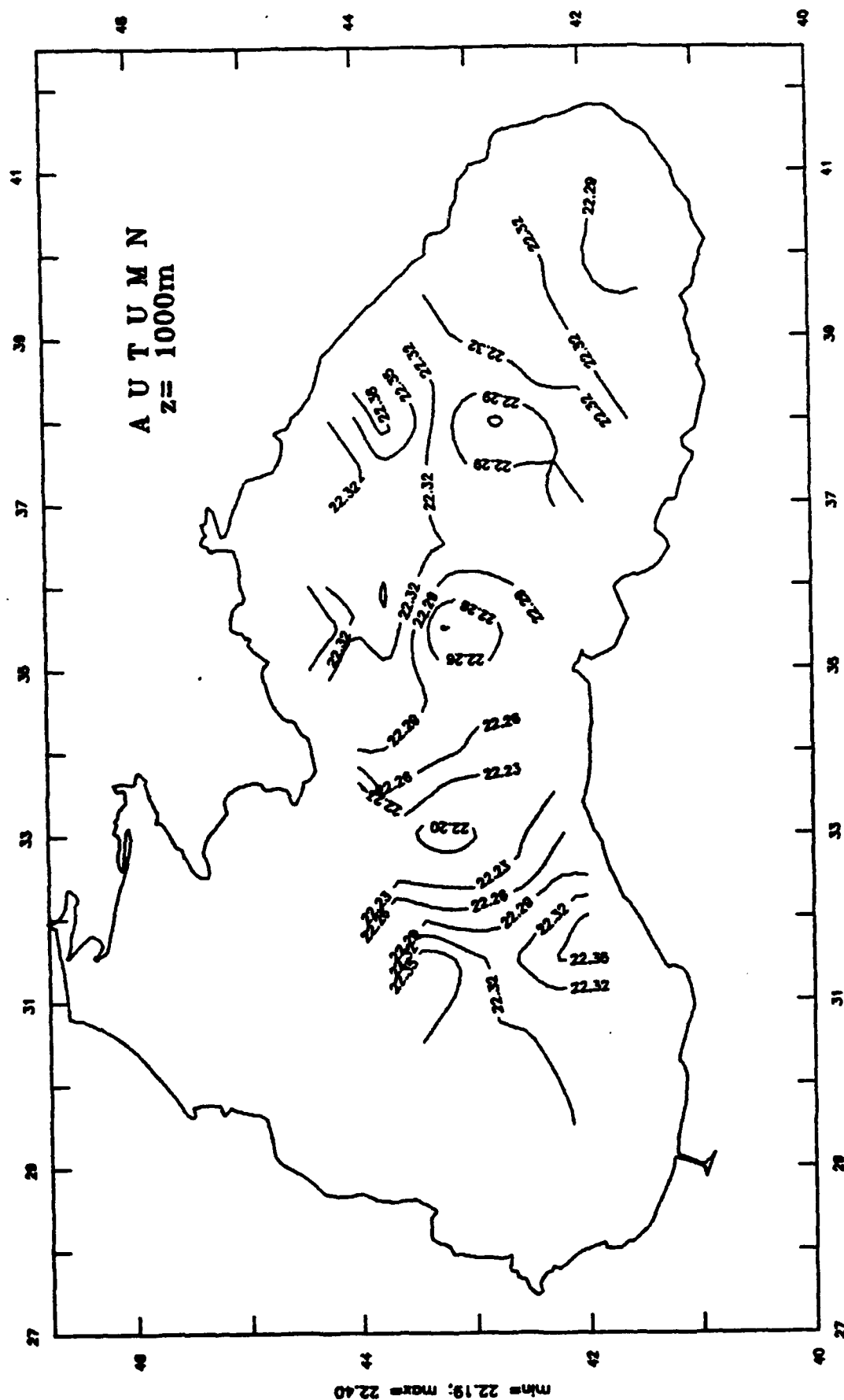
The Black Sea Climate Salinity



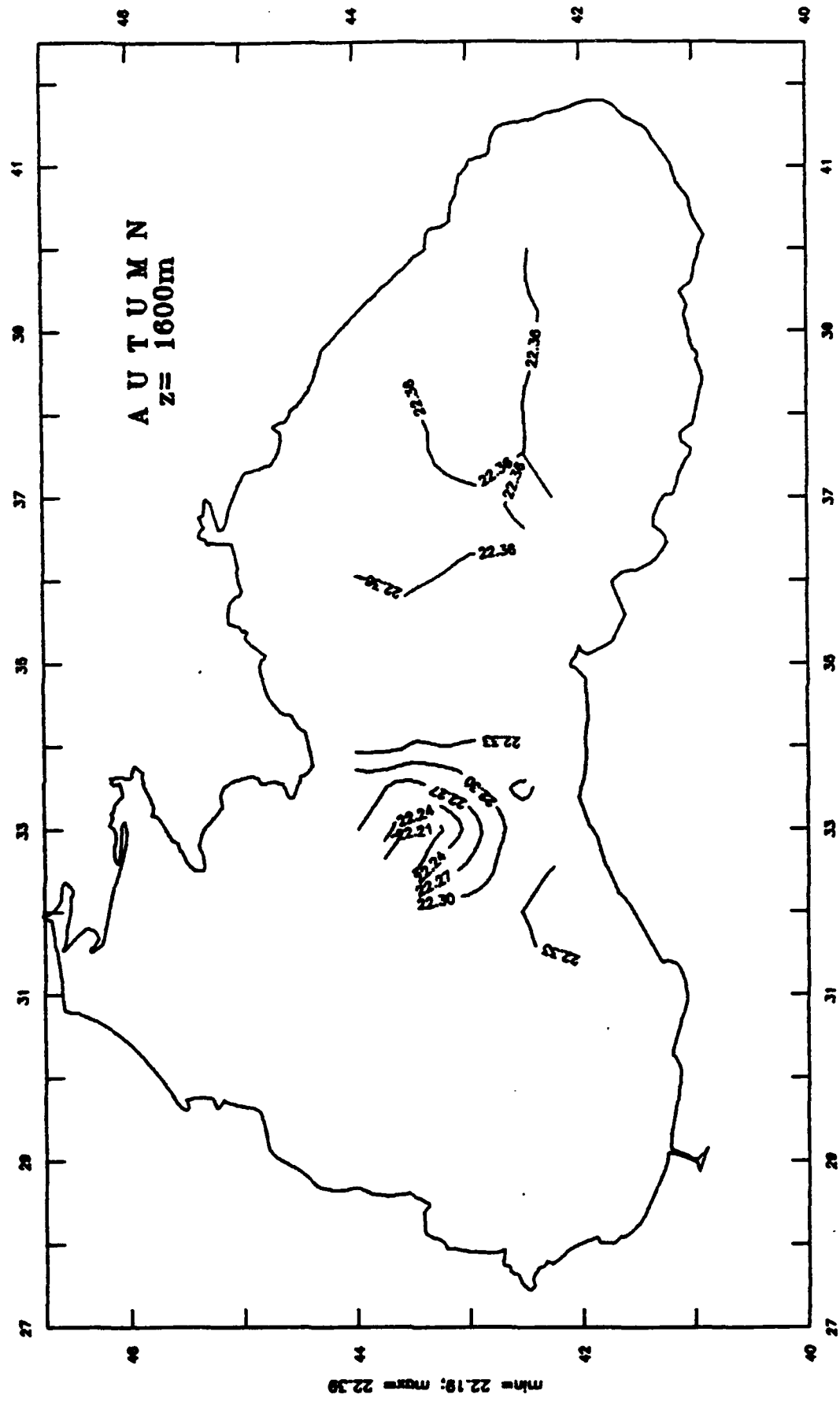
A U T U M N
Z = 500m

min = 21.90; max = 21.16

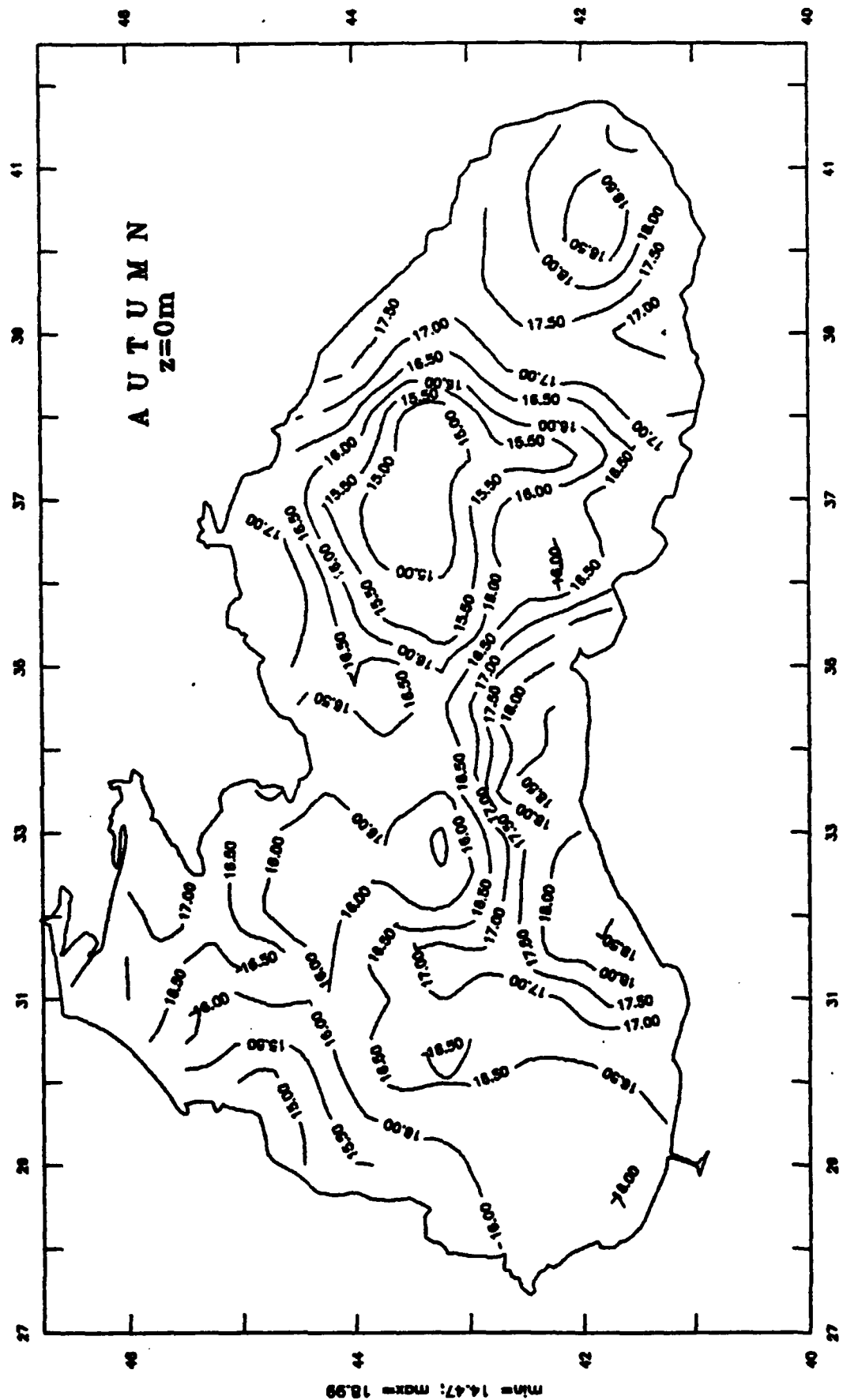
The Black Sea Climate Salinity



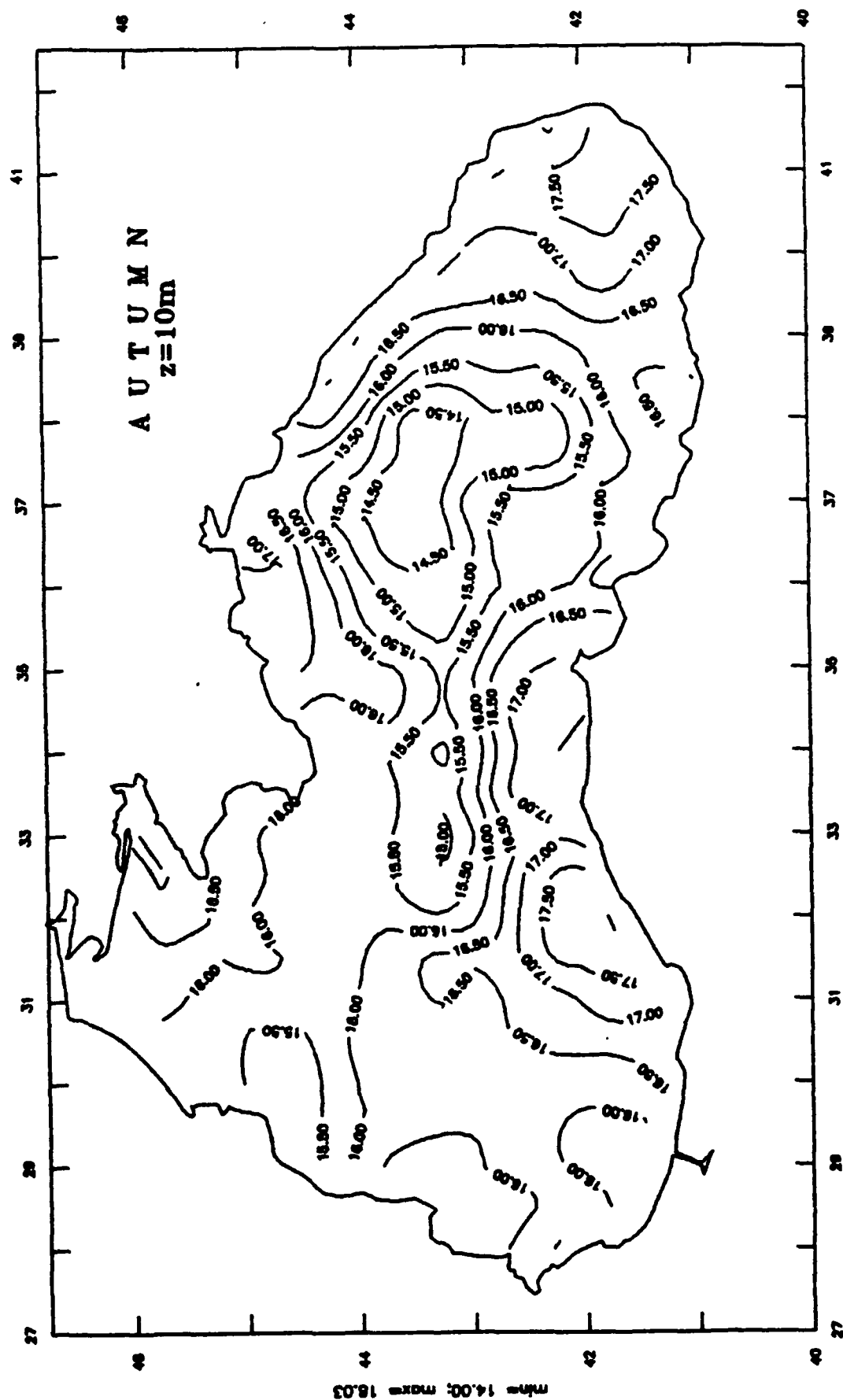
The Black Sea Climate Salinity



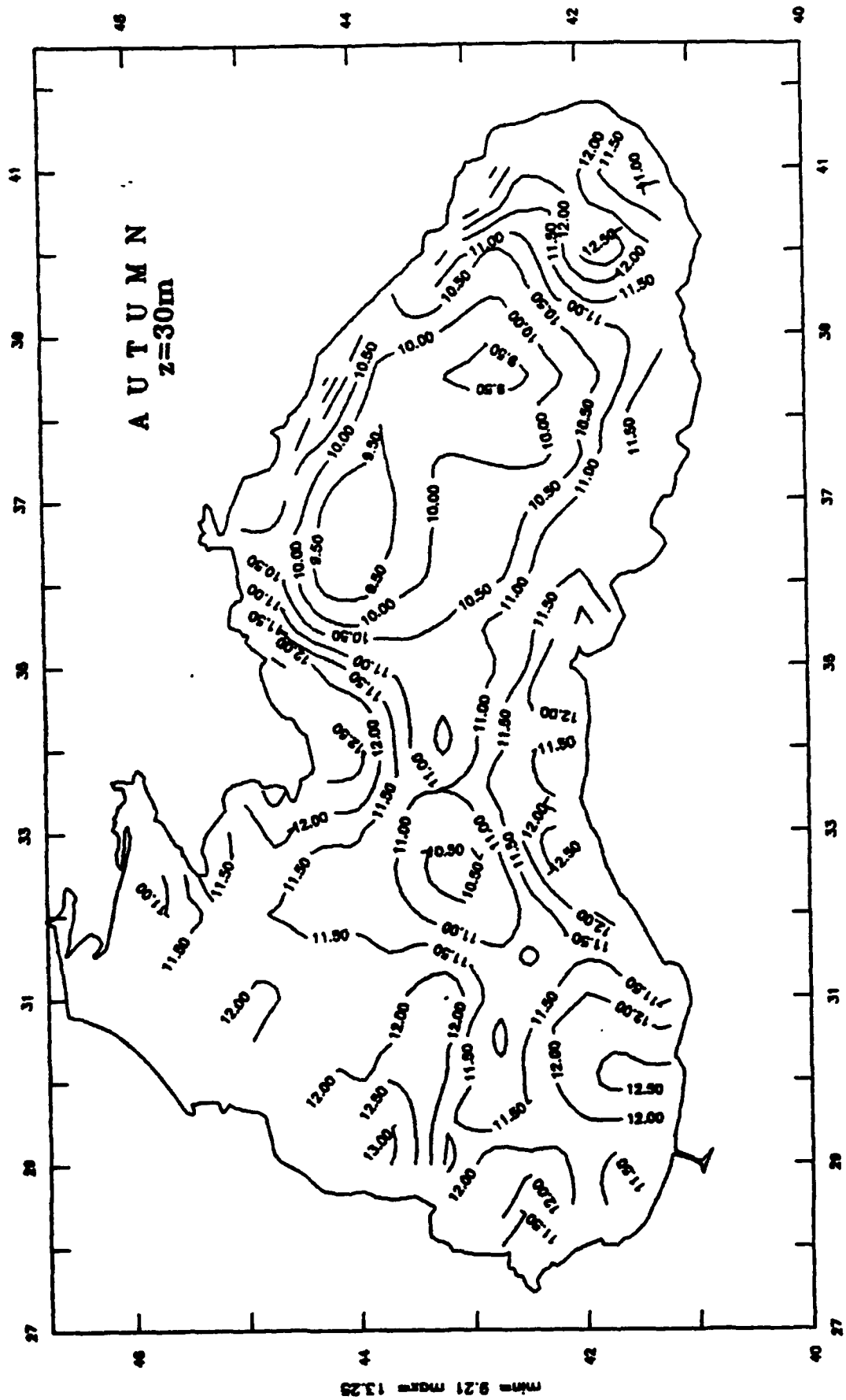
The Black Sea Climate Temperature



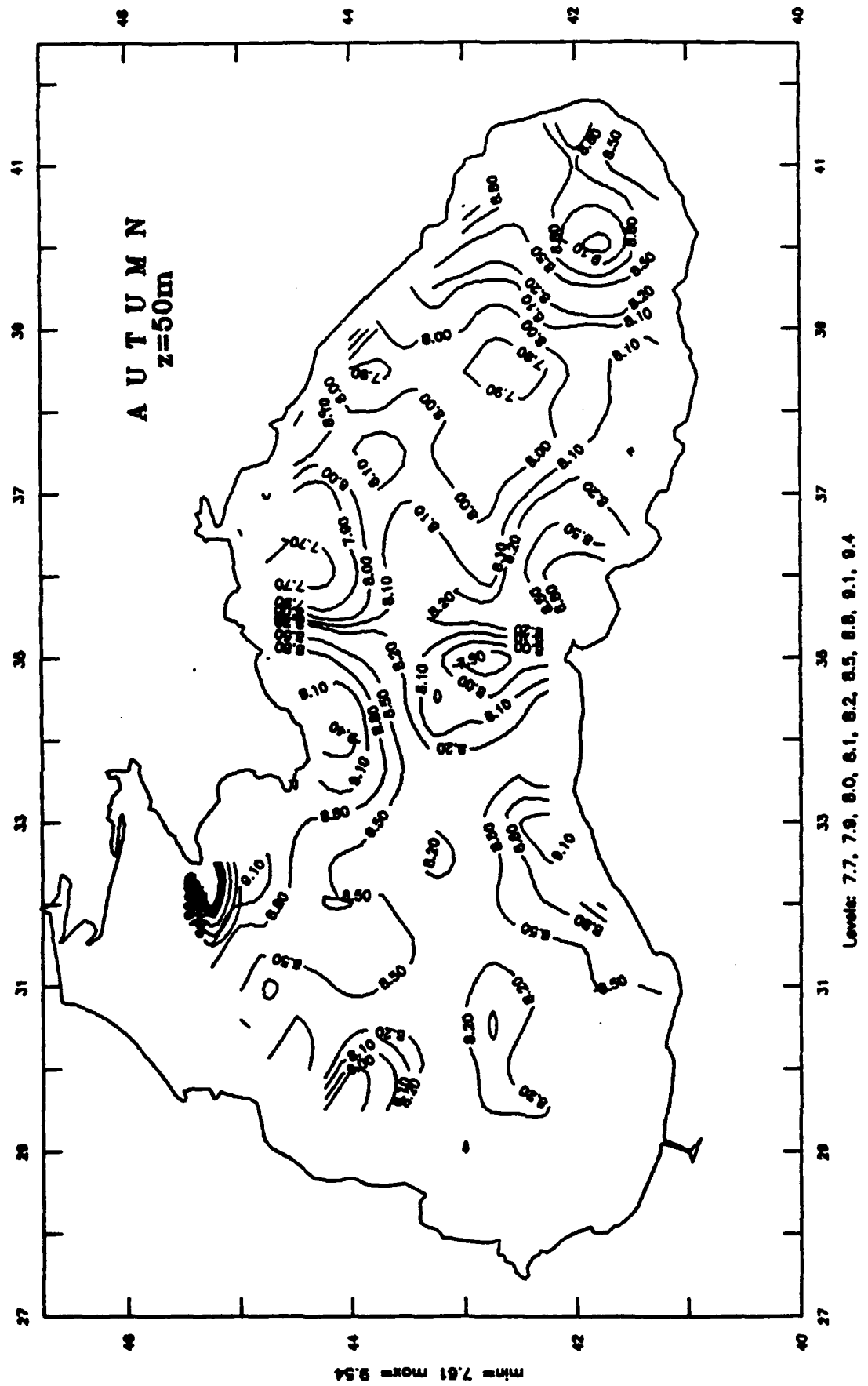
The Black Sea Climate Temperature



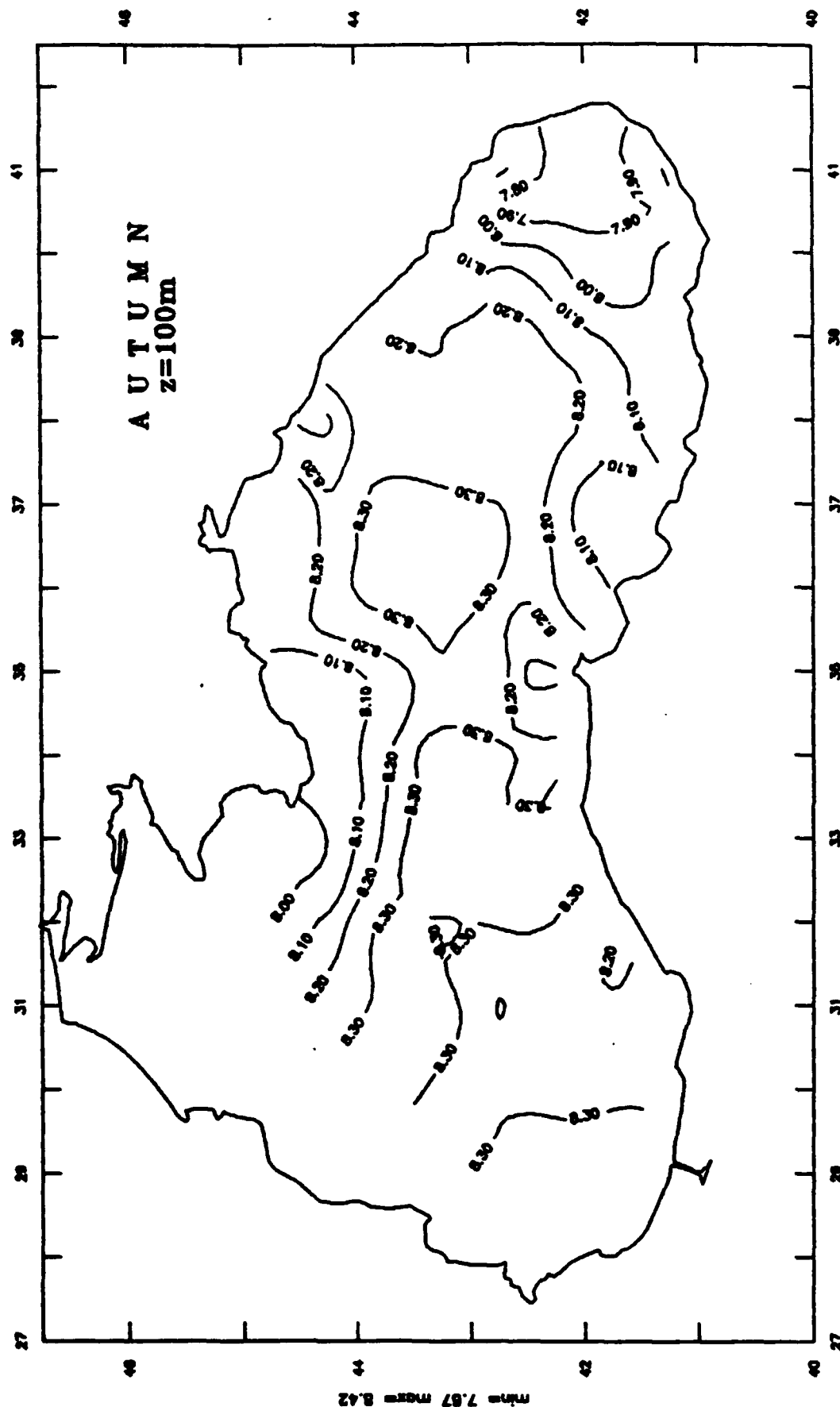
The Black Sea Climate Temperature



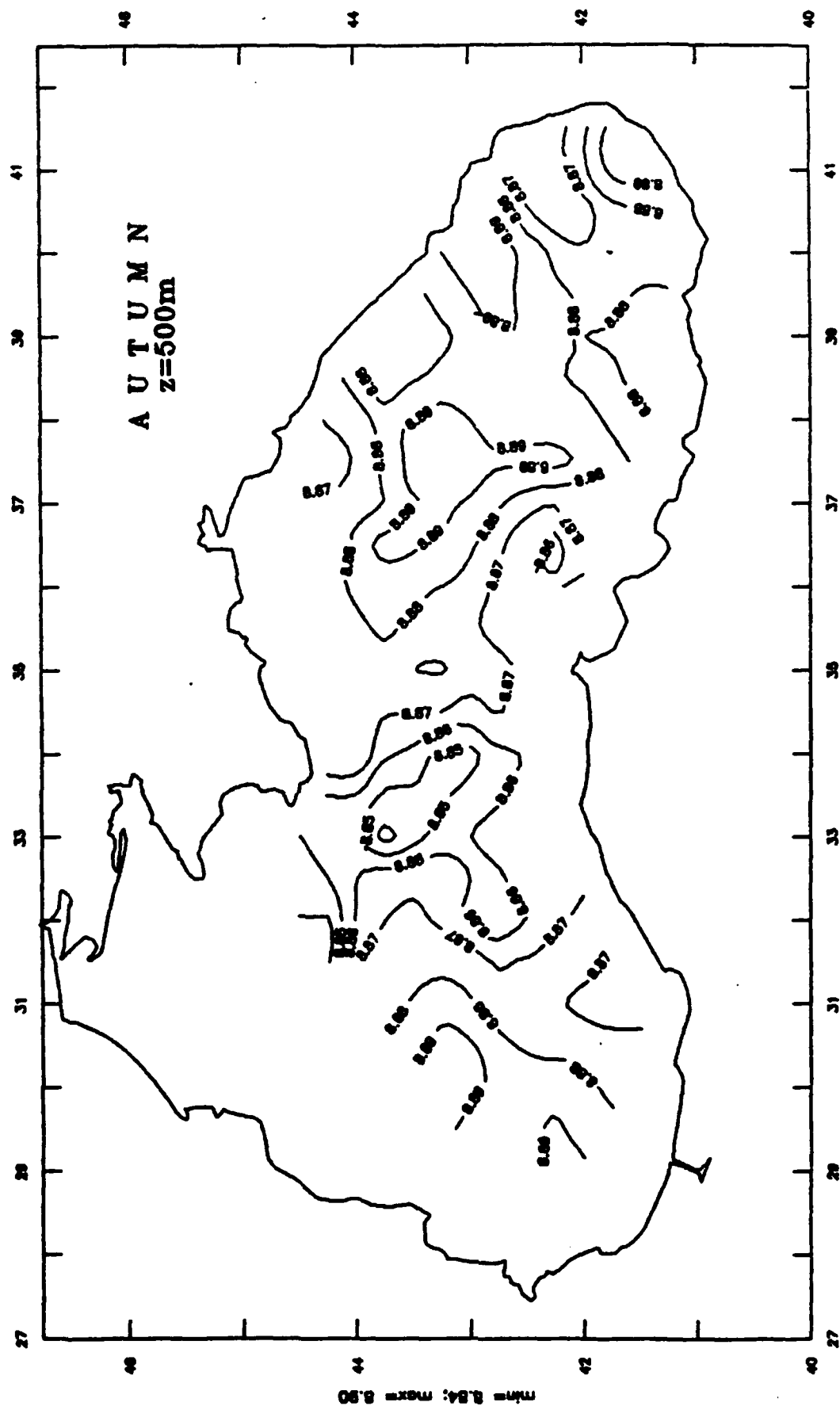
The Black Sea Climate Temperature



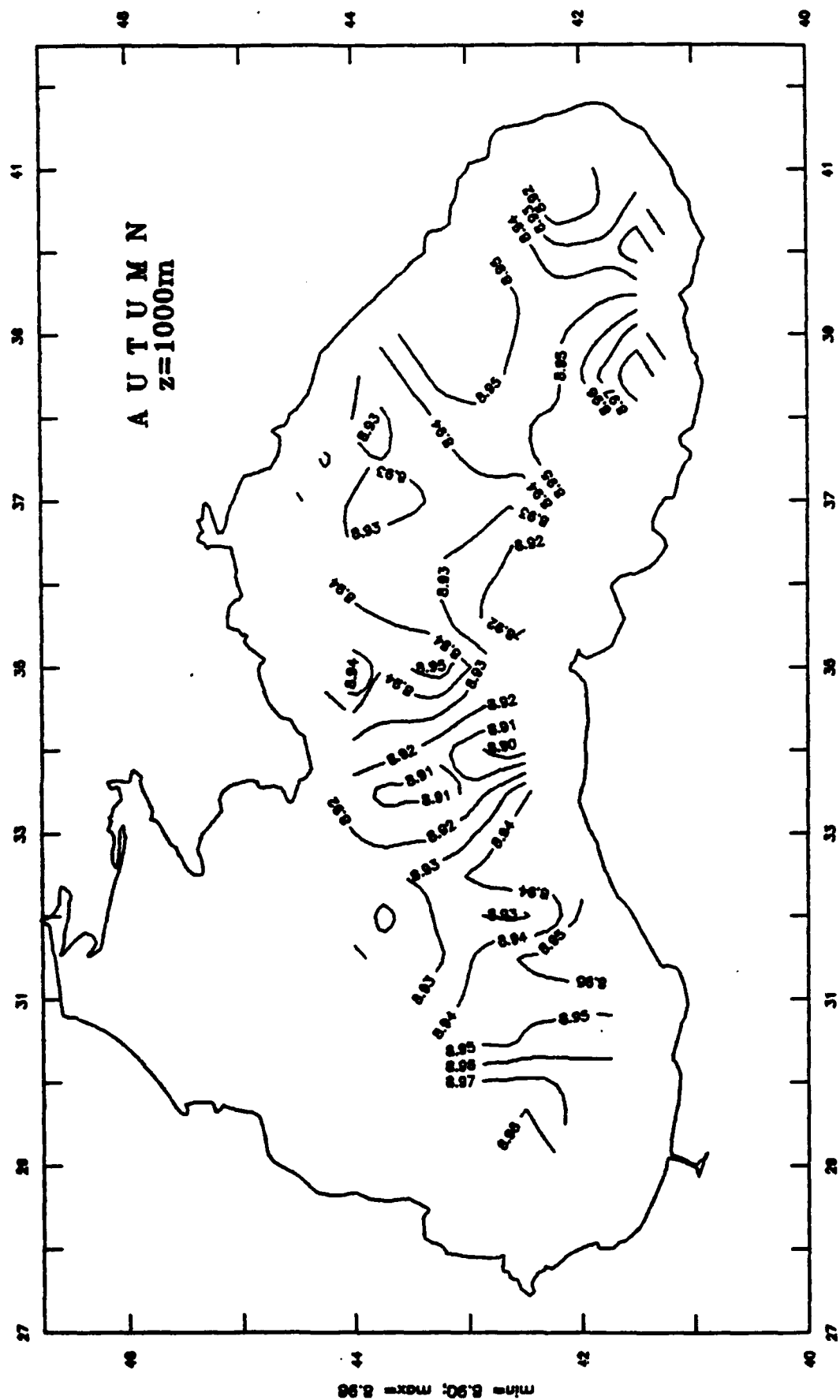
The Black Sea Climate Temperature



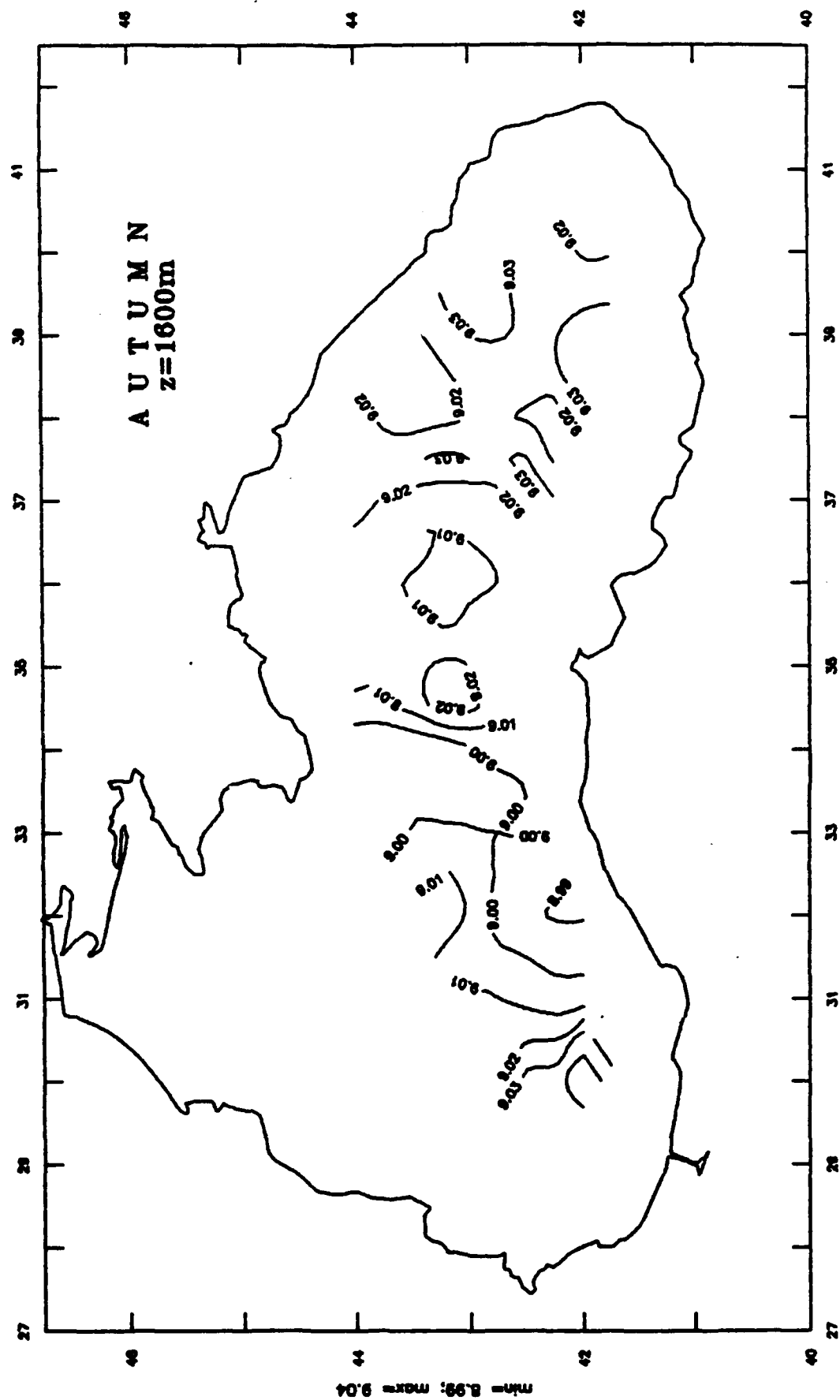
The Black Sea Climate Temperature



The Black Sea Climate Temperature



The Black Sea Climate Temperature



DOCUMENT LIBRARY

March 11, 1991

Distribution List for Technical Report Exchange

Attn: Stella Sanchez-Wade
Documents Section
Scripps Institution of Oceanography
Library, Mail Code C-075C
La Jolla, CA 92093

Hancock Library of Biology &
Oceanography
Alan Hancock Laboratory
University of Southern California
University Park
Los Angeles, CA 90089-0371

Gifts & Exchanges
Library
Bedford Institute of Oceanography
P.O. Box 1006
Dartmouth, NS, B2Y 4A2, CANADA

Office of the International
Ice Patrol
c/o Coast Guard R & D Center
Avery Point
Groton, CT 06340

NOAA/EDIS Miami Library Center
4301 Rickenbacker Causeway
Miami, FL 33149

Library
Skidaway Institute of Oceanography
P.O. Box 13687
Savannah, GA 31416

Institute of Geophysics
University of Hawaii
Library Room 252
2525 Correa Road
Honolulu, HI 96822

Marine Resources Information Center
Building E38-320
MIT
Cambridge, MA 02139

Library
Lamont-Doherty Geological
Observatory
Columbia University
Palisades, NY 10964

Library
Serials Department
Oregon State University
Corvallis, OR 97331

Pell Marine Science Library
University of Rhode Island
Narragansett Bay Campus
Narragansett, RI 02882

Working Collection
Texas A&M University
Dept. of Oceanography
College Station, TX 77843

Library
Virginia Institute of Marine Science
Gloucester Point, VA 23062

Fisheries-Oceanography Library
151 Oceanography Teaching Bldg.
University of Washington
Seattle, WA 98195

Library
R.S.M.A.S.
University of Miami
4600 Rickenbacker Causeway
Miami, FL 33149

Maury Oceanographic Library
Naval Oceanographic Office
Stennis Space Center
NSTL, MS 39522-5001

Marine Sciences Collection
Mayaguez Campus Library
University of Puerto Rico
Mayaguez, Puerto Rico 00708

Library
Institute of Oceanographic Sciences
Deacon Laboratory
Wormley, Godalming
Surrey GU8 5UB
UNITED KINGDOM

The Librarian
CSIRO Marine Laboratories
G.P.O. Box 1538
Hobart, Tasmania
AUSTRALIA 7001

Library
Proudman Oceanographic Laboratory
Bidston Observatory
Birkenhead
Merseyside L43 7 RA
UNITED KINGDOM

REPORT DOCUMENTATION PAGE	1. REPORT NO. WHOI-92-34	2.	3. Recipient's Accession No.
4. Title and Subtitle The Black Sea General Circulation and Climatic Temperature and Salinity Fields			5. Report Date September, 1992
			6.
7. Author(s) Dimitar Ivanov Trukhchev, Ph.D. and Yurii Leonidovich Demin, Prof., Sc.D.			8. Performing Organization Rept. No. WHOI 92-34
9. Performing Organization Name and Address The Woods Hole Oceanographic Institution Woods Hole, Massachusetts 02543			10. Project/Task/Work Unit No.
			11. Contract(C) or Grant(G) No. (C) (G)
12. Sponsoring Organization Name and Address			13. Type of Report & Period Covered Technical Report
			14.
15. Supplementary Notes This report should be cited as: Woods Hole Oceanog. Inst. Tech. Rept., WHOI-92-34, CRC-92-02.			
16. Abstract (Limit: 200 words) The Black Sea is a nearly enclosed ocean basin, exhibiting many features common with larger ocean basins. Lacking an open boundary and having a limited exchange with sources of fresh and salt water, this basin is an ideal laboratory for developing and evaluating numerical circulation models. The present report describes one numerical model of the Black Sea, developed by Bulgarian and Russian scientists. The new approach has the advantages of both diagnostic models (incorporation of experimental data) and prognostic models (producing hydrodynamical adjustment and filtered fields). Successive application of diagnostic and prognostic models is used. The temperature and salinity fields obtained from observations, and currents obtained from diagnostic models, are used as the initial approximation to the prognostic model. Judicious selection of an integration time prevents over-smoothing of the results while preserving the stability of the solution. Using this model, calculations have been made at 25 levels over a grid interval of 0.25° (latitude) by 0.5°. Input data consist of nearly 50,000 observations taken over nearly 100 years, averaged over 0.5° by 0.5° cells. Seasonal fields of temperature, salinity, and velocity form the output of these experiments. The results provide the basis for various hypotheses that must be tested using future field observations and more sophisticated models.			
17. Document Analysis a. Descriptors 1. numerical modeling 2. general circulation 3. Black Sea 4. data assimilation b. Identifiers/Open-Ended Terms c. COSATI Field/Group			
18. Availability Statement Approved for publication; distribution unlimited.		19. Security Class (This Report) UNCLASSIFIED	21. No. of Pages 132
		20. Security Class (This Page)	22. Price